



International Agreement Report

Nuclear Regulatory Authority Experimental Program to Characterize and Understand High Energy Arcing Fault (HEAF) Phenomena

Prepared by:

S. Tsuchino*, H. Kabashima*, S. Turner**, S. Mehta, D. Stroup, N. Melly, G. Taylor, F. Gonzalez

*Regulatory Standard and Development Department
Secretariat of Nuclear Regulatory Authority (S/NRA/R)
Tokyo, Japan 106-8450

**Leidos, Inc.
301 Laboratory Road
Oak Ridge, TN 37830

M. H. Salley, NRC Project Manager

**Division of Risk Analysis
Office of Nuclear Regulatory Research
U.S. Nuclear Regulatory Commission
Washington, DC 20555-0001**

Manuscript Completed: August 2016

Date Published: August 2016

Prepared as part of
the Agreement between NRC and NRA in the Area of Fire-Related Research

**Published by
U.S. Nuclear Regulatory Commission**

AVAILABILITY OF REFERENCE MATERIALS IN NRC PUBLICATIONS

NRC Reference Material

As of November 1999, you may electronically access NUREG-series publications and other NRC records at NRC's Library at www.nrc.gov/reading-rm.html. Publicly released records include, to name a few, NUREG-series publications; *Federal Register* notices; applicant, licensee, and vendor documents and correspondence; NRC correspondence and internal memoranda; bulletins and information notices; inspection and investigative reports; licensee event reports; and Commission papers and their attachments.

NRC publications in the NUREG series, NRC regulations, and Title 10, "Energy," in the *Code of Federal Regulations* may also be purchased from one of these two sources.

1. The Superintendent of Documents

U.S. Government Publishing Office
Mail Stop IDCC
Washington, DC 20402-0001
Internet: bookstore.gpo.gov
Telephone: (202) 512-1800
Fax: (202) 512-2104

2. The National Technical Information Service

5301 Shawnee Rd., Alexandria, VA 22312-0002
www.ntis.gov
1-800-553-6847 or, locally, (703) 605-6000

A single copy of each NRC draft report for comment is available free, to the extent of supply, upon written request as follows:

Address: **U.S. Nuclear Regulatory Commission**
Office of Administration
Publications Branch
Washington, DC 20555-0001
E-mail: distribution.resource@nrc.gov
Facsimile: (301) 415-2289

Some publications in the NUREG series that are posted at NRC's Web site address www.nrc.gov/reading-rm/doc-collections/nuregs are updated periodically and may differ from the last printed version. Although references to material found on a Web site bear the date the material was accessed, the material available on the date cited may subsequently be removed from the site.

Non-NRC Reference Material

Documents available from public and special technical libraries include all open literature items, such as books, journal articles, transactions, *Federal Register* notices, Federal and State legislation, and congressional reports. Such documents as theses, dissertations, foreign reports and translations, and non-NRC conference proceedings may be purchased from their sponsoring organization.

Copies of industry codes and standards used in a substantive manner in the NRC regulatory process are maintained at—

The NRC Technical Library

Two White Flint North
11545 Rockville Pike
Rockville, MD 20852-2738

These standards are available in the library for reference use by the public. Codes and standards are usually copyrighted and may be purchased from the originating organization or, if they are American National Standards, from—

American National Standards Institute

11 West 42nd Street
New York, NY 10036-8002
www.ansi.org
(212) 642-4900

Legally binding regulatory requirements are stated only in laws; NRC regulations; licenses, including technical specifications; or orders, not in NUREG-series publications. The views expressed in contractor prepared publications in this series are not necessarily those of the NRC.

The NUREG series comprises (1) technical and administrative reports and books prepared by the staff (NUREG-XXXX) or agency contractors (NUREG/CR-XXXX), (2) proceedings of conferences (NUREG/CP-XXXX), (3) reports resulting from international agreements (NUREG/IA-XXXX), (4) brochures (NUREG/BR-XXXX), and (5) compilations of legal decisions and orders of the Commission and Atomic and Safety Licensing Boards and of Directors' decisions under Section 2.206 of NRC's regulations (NUREG-0750).

DISCLAIMER: This report was prepared under an international cooperative agreement for the exchange of technical information. Neither the U.S. Government nor any agency thereof, nor any employee, makes any warranty, expressed or implied, or assumes any legal liability or responsibility for any third party's use, or the results of such use, of any information, apparatus, product or process disclosed in this publication, or represents that its use by such third party would not infringe privately owned rights.



International Agreement Report

Nuclear Regulatory Authority Experimental Program to Characterize and Understand High Energy Arcing Fault (HEAF) Phenomena

Prepared by:

S. Tsuchino*, H. Kabashima*, S. Turner**, S. Mehta, D. Stroup, N. Melly, G. Taylor, F. Gonzalez

*Regulatory Standard and Development Department
Secretariat of Nuclear Regulatory Authority (S/NRA/R)
Tokyo, Japan 106-8450

**Leidos, Inc.
301 Laboratory Road
Oak Ridge, TN 37830

M. H. Salley, NRC Project Manager

**Division of Risk Analysis
Office of Nuclear Regulatory Research
U.S. Nuclear Regulatory Commission
Washington, DC 20555-0001**

Manuscript Completed: August 2016

Date Published: August 2016

Prepared as part of
the Agreement between NRC and NRA in the Area of Fire-Related Research

**Published by
U.S. Nuclear Regulatory Commission**

ABSTRACT

A High Energy Arcing Fault (HEAF) occurred in a high-voltage (6.9 kV) switchgear (SWGR) in Unit 1 of the Onagawa Nuclear Power Plant of the Tohoku Electric Power Company on March 11, 2011 during the Great East Earthquake in Japan. HEAF events are not common and have occurred in nuclear power plants (NPP) worldwide. The operating experience seen from the Onagawa event illustrate that HEAFs can present a potential threat to the safe operation of NPPs. As a result, the nuclear power industry has placed a new emphasis on understanding and developing evaluation methods for these events.

To investigate the HEAF event sequence and to understand the phenomena, the Regulatory Standard and Research Department, Secretariat of the Nuclear Regulation Authority (S/NRA/R) (Japan) conducted HEAF tests by simulating the design and operating conditions of the SWGR HEAF at Onagawa NPP in addition to simulating the HEAF energy effects using a "Rocket Fuel Arc Simulator" (RFAS). Tests of 480 V Motor Control Center (MCC) and Distribution Panel (DP) cabinets were also conducted to understand HEAF characteristics.

The results of the HEAF tests simulating the SWGR at Onagawa NPP showed similar damage to the actual HEAF with respect to the duration time, energy level, and ensuing cable fires. However, the overall structural damage and extent of the internal fire damage was much less severe than Onagawa. The tests for the MCC and the DP provide insight on HEAF behavior and ensuing fires in low voltage systems. Data such as temperature, heat flux, heat release rate during the arc and ensuing fires due to HEAF conditions were successfully simulated by the RFAS test.

The results were generally consistent with the previously observed behavior. However, the tests also provided a new appreciation for and recognition of the high thermal energy from the oxidation of aluminum bus bars, such as those used in the SWGR tests. Since aluminum is sometimes used in bus bars, the energetic effects of an arc involving this material should be considered when analyzing HEAF effects.

This report provides the results of the S/NRA/R tests that, in combination with operating experience and other HEAF test data, will be used by international teams to develop consensus conclusions on HEAF behavior, understand the potential for HEAF damage including ensuing fires, establish HEAF evaluation criteria to support Fire Hazards Analyses (FHA), and recommend protection measures.

FOREWARD

This work was completed under the “Implementing Agreement between the United States Nuclear Regulatory Commission and the Japan Nuclear Energy Safety Organization” in the Area of Fire-Related Research,” as amended to change the Japan party to the Nuclear Regulation Authority (NRA).

The Regulatory Standard and Research Department, Secretariat of the Nuclear Regulation Authority (S/NRA/R) (Japan) was the lead organization for the tests and prepared the analysis and results. The Nuclear Regulatory Commission (NRC) attended all tests and provided support for specialized instrumentation, technical advice, and general testing support. The NRC also completed the final preparation of this report for publication.

The contents of this report should not be viewed as an official NRC endorsement of the results or observations in this report. Nor should this report be viewed as binding the NRC in its rulemaking, licensing or adjudicatory process.

TABLE OF CONTENTS

	Page
ABSTRACT	iii
FOREWARD	v
TABLE OF CONTENTS	vii
FIGURES	xi
TABLES	xvii
EXECUTIVE SUMMARY	xix
CITATIONS	xxv
ACKNOWLEDGMENTS	xxvii
ACRONYMS AND ABBREVIATIONS	xxix
1 INTRODUCTION	1-1
1.1 Background	1-1
1.2 Onagawa HEAF Event	1-1
1.3 Test Approach and Electrical Test Conditions	1-3
1.3.1 Arc Current	1-4
1.3.2 Arc Duration	1-4
1.4 Measurements and Instrumentation	1-7
2 Distribution Panel HEAF TEST – KEMA (January 2014 and March 2015)	2-1
2.1 DP Test Overview (2014 and 2015)	2-1
2.2 DP Tests Summary of Results	2-1
2.3 DP Test Configuration	2-2
2.4 DP Test Configuration	2-4
2.5 DP Test Cable Combustible Loading	2-5
2.5.1 Internal Combustible Loading	2-5
2.6 DP Test Temperature and Heat Flux Instrumentation	2-6
2.6.1 Cable Tray Combustible Loading	2-9
2.7 DP Test Pressure Instrumentation	2-9
2.8 DP Test 1 Key Observations (January 2013)	2-10
2.8.1 DP Test 1 Calorimetry Data	2-14
2.8.2 DP Test 1 Temperature Data	2-15
2.8.3 DP Test 1 Pressure Data	2-16
2.8.4 DP Test 1 Arc Energy	2-17
2.9 DP Test 2 Key Observations (January 2013)	2-18
2.9.1 DP Test 2 Calorimetry Data	2-21
2.9.2 DP Test 2 Temperature Data	2-22
2.9.3 DP Test 2 Pressure Data	2-23
2.9.4 DP Test 2 Arc Energy	2-24
2.10 DP Test 3 Key Observations (January 2013)	2-25
2.10.1 DP Test 3 Calorimetry Data	2-29
2.10.2 DP Test 3 Temperature Data	2-30
2.10.3 DP Test 3 Pressure Data	2-31
2.10.4 DP Test 3 Arc Energy	2-32
2.11 DP Test 4 Key Observations (March 2015)	2-33
2.11.1 DP Test 4 Calorimetry Data	2-37
2.11.2 DP Test 4 Temperature Data	2-39
2.11.3 DP Test 4 Pressure Data	2-40
2.11.4 DP Test 4 Arc Energy	2-41
2.12 DP Test 5 Key Observations (March 2015)	2-42
2.12.1 DP Test 5 Calorimetry Data	2-47

	2.12.2	DP Test 5 Temperature Data	2-48
	2.12.3	DP Test 5 Pressure Data	2-49
	2.12.4	DP Test 5 Arc Energy	2-50
2.13		DP Test 6 Key Observations (March 2015)	2-51
	2.13.1	DP Test 6 Calorimetry Data	2-55
	2.13.2	DP Test 6 Temperature Data	2-56
	2.13.3	DP Test 6 Pressure Data	2-58
	2.13.4	DP Test 6 Arc Energy	2-59
2.14		DP Tests 1 through 6: Summary of Electrical Conditions	2-60
2.15		DP Tests 1 through 6 Qualitative Summary	2-61
3		Motor Control Center HEAF TEST – KEMA (May 2013).....	3-1
	3.1	MCC Test Overview.....	3-1
	3.2	MCC Summary of Results.....	3-1
	3.3	MCC Test Configuration.....	3-3
	3.4	MCC Cable Combustible Loading.....	3-5
	3.5	MCC Temperature and Heat Flux Instrumentation.....	3-6
	3.6	MCC Test Pressure Instrumentation	3-8
	3.7	MCC Test 1 Key Observations.....	3-9
	3.7.1	MCC Test 1 Calorimetry Data	3-12
	3.7.2	MCC Test 1 Temperature Data	3-13
	3.7.3	MCC Test 1 Pressure Data	3-14
	3.7.4	MCC Test 1 Arc Energy	3-15
3.8		MCC Test 2 Key Observations.....	3-16
	3.8.1	MCC Test 2 Calorimetry Data	3-21
	3.8.2	MCC Test 2 Temperature Data	3-22
	3.8.3	MCC Test 2 Pressure Data	3-23
	3.8.4	MCC Test 2 Arc Energy	3-24
3.9		MCC Test 3 Key Observations.....	3-25
	3.9.1	MCC Test 3 Calorimetry Data	3-27
	3.9.2	MCC Test 3 Temperature Data	3-28
	3.9.3	MCC Test 3 Pressure Data	3-29
	3.9.4	MCC Test 3 Arc Energy	3-30
3.10		MCC Test 4 Key Observations.....	3-31
	3.10.1	MCC Test 4 Calorimetry Data	3-33
	3.10.2	MCC Test 4 Temperature Data	3-34
	3.10.3	MCC Test 4 Pressure Data	3-35
	3.10.4	MCC Test 4 Arc Energy	3-36
3.11		MCC Tests 1 through 4: Electrical Conditions	3-37
3.12		MCC Tests 1 through 4 Qualitative Summary	3-38
4		Switchgear HEAF Tests 1 through 3, Single Arc Tests – KEMA (June 2013).....	4-1
	4.1	SWGR Tests 1 through 3 Overview	4-1
	4.2	SWGR Tests 1 through 3 Summary of Results	4-1
	4.3	SWGR Tests 1 through 3 Cabinet Configuration.....	4-2
	4.4	SWGR Tests 1 through 3 Cable Combustible Loading.....	4-6
	4.5	SWGR Tests 1 through 3 Temperature and Heat Flux Instrumentation.....	4-9
	4.6	SWGR Tests 1 through 3 Pressure Instrumentation.....	4-11
	4.7	SWGR Test 1 Key Observations.....	4-11
	4.7.1	SWGR Test 1 Calorimetry Data	4-17
	4.7.2	SWGR Test 1 Temperature Data	4-18
	4.7.3	SWGR Test 1 Pressure Data	4-19
	4.7.4	SWGR Test 1 Arc Energy	4-20

4.8	SWGR Test 2 Changes.....	4-21
4.9	SWGR Test 2 Key Observations.....	4-23
4.9.1	SWGR Test 2 Calorimetry Data	4-38
4.9.2	SWGR Test 2 Temperature Data	4-39
4.9.3	SWGR Test 2 Pressure Data	4-41
4.9.4	SWGR Test 2 Arc Energy	4-42
4.10	SWGR Test 3 Key Observations.....	4-43
4.10.1	SWGR Test 3 Calorimetry Data	4-48
4.10.2	SWGR Test 3 Temperature Data	4-49
4.10.3	SWGR Test 3 Pressure Data	4-50
4.10.4	SWGR Test 3 Arc Energy	4-51
4.11	SWGR Tests 1 through 3: Summary of Electrical Conditions	4-52
4.12	SWGR Tests 1 through 3 Qualitative Summary	4-52
5	Switchgear HEAF Tests 4 through 6, Two Arcs Tests - KEMA (March 2014, March 2015).....	5-1
5.1	SWGR Tests 4 through 6 Overview	5-1
5.2	SWGR Tests 4 through 6 Summary of Results	5-1
5.3	SWGR Tests 4 through 6 Cabinet Lineup and Combustible Load	5-2
5.3.1	Internal Combustible Load	5-6
5.3.2	External Combustible Load	5-6
5.4	SWGR Tests 4 through 6 Temperature, Heat Flux and Pressure Instrumentation	5-6
5.5	SWGR Test 4 Key Observations (March 2014).....	5-10
5.5.1	SWGR Test 4 Calorimetry Data	5-17
5.5.2	SWGR Test 4 Temperature Data	5-19
5.5.3	SWGR Test 4 Pressure Data	5-21
5.5.4	SWGR Test 4 Arc Energy	5-23
5.6	SWGR Test 5 Key Observations (March 2014).....	5-24
5.6.1	SWGR Test 5 Calorimetry Data	5-31
5.6.2	SWGR Test 5 Temperature Data	5-33
5.6.3	SWGR Test 5 Pressure Data	5-35
5.6.4	SWGR Test 5 Arc Energy	5-37
5.7	SWGR Test 6 Key Observations (March 2015).....	5-38
5.7.1	SWGR Test 6 Calorimetry Data	5-48
5.7.2	SWGR Test 6 Temperature Data	5-49
5.7.3	SWGR Test 6 Pressure Data	5-51
5.7.4	SWGR Test 6 Arc Energy	5-53
5.8	SWGR Tests 4 through 6 Summary of Electrical Conditions	5-54
5.9	SWGR Tests 4 through 6 Qualitative Summary	5-55
6	Switchgear with Rocket Fuel Arc Simulator Fire Test - SwRI (July 2013)	6-1
6.1	RFAS Test Overview	6-1
6.2	RFAS Test Summary of Results	6-1
6.3	RFAS 5-Cabinet Test Configuration.....	6-3
6.4	RFAS Test Heat Flux Instrumentation.....	6-6
6.5	RFAS Test Temperature Instrumentation.....	6-6
6.6	RFAS Test Pressure Instrumentation.....	6-8
6.7	RFAS Test Heat Release Rate and Smoke Production Instrumentation	6-8
6.8	RFAS Test Oxygen Measurement	6-9
6.9	RFAS Test 1 Key Observations	6-9
6.9.1	RFAS Heat Test 1 Flux Data.....	6-12
6.9.2	Test 1 Temperature Data	6-13

6.9.3	RFAS Test 1 Heat Release Rate/Smoke Production Data	6-13
6.10	RFAS Test 2 Key Observations	6-14
6.10.1	RFAS Test 2 Flux Data	6-17
6.10.2	RFAS Test 2 Temperature Data.....	6-19
6.10.3	RFAS Test 2 Heat Release Rate/Smoke Production Rate Data	6-21
6.10.4	RFAS Test 2 Oxygen Data.....	6-22
6.10.5	RFAS Summary	6-23
7	Switchgear Tests Results Discussion	7-1
7.1	Onagawa Comparison	7-1
7.1.1	Exterior Damage	7-1
7.1.2	Horizontal Bus Bar Arc.....	7-1
7.1.3	Secondary Side Arc and Damage	7-1
7.2	Aluminum Bus Bar Oxidation	7-3
7.2.1	Case 1: Onagawa Bus Bar Oxidation in Cabinet 7	7-3
7.2.2	Case 2: KEMA 5-Cabinet Lineup June 2013 Test 3	7-4
7.2.3	Case 3: KEMA 5-Cabinet Lineup March 2014 Test 4	7-4
7.2.4	Case 4: KEMA 5-Babinet Lineup March 2014 Test 5	7-5
7.2.5	Case 5: KEMA 3-Cabinet Lineup March 2015, Test 6	7-6
7.2.6	Aluminum Oxidation Effects Summary	7-7
8	REFERENCES.....	8-1
APPENDIX A.	MEASUREMENTS	A-1
APPENDIX B.	KEMA TEST LABORATORY.....	B-1
APPENDIX C.	CABLE PROPERTIES	C-1
APPENDIX D.	SHORT CIRCUIT CURRENT CALCULATIONS	D-1

FIGURES

	Page
Figure 1.2-1.	Damage in Onagawa HEAF Event1-2
Figure 1.2-2.	Onagawa Arching Scenario.....1-3
Figure 2.3-1.	DP Test Configuration2-3
Figure 2.4-1.	DP Used in Tests2-4
Figure 2.5-1.	DP Test Cable Combustible Load2-5
Figure 2.6-1.	DP Tests 1 through 3 Calorimeter Locations2-6
Figure 2.6-2.	DP Tests 1 through 3 TC Locations.....2-7
Figure 2.6-3.	DP Tests 4 through 6 Calorimeter Hood and PT Locations2-8
Figure 2.7-1.	DP Tests 1 through 6 Pressure Transducer and Locations (Rear View)2-9
Figure 2.8-1.	DP Test 1 Arc.....2-10
Figure 2.8-2.	DP Test 1 Ensuing Fire, 12 Minutes After Arc2-11
Figure 2.8-3.	DP Test 1 Exterior Damage2-11
Figure 2.8-4.	DP Test 1 HEAF and Fire Interior Damage2-13
Figure 2.8-5.	DP Test 1 Slug Calorimeter Data: Temperature2-14
Figure 2.8-6.	DP Test 1 Thermocouple Data2-15
Figure 2.8-7.	DP Test 1 Pressure.....2-16
Figure 2.8-8.	DP Test 1 Arc Energy2-17
Figure 2.9-1.	DP Test 2 Arc.....2-18
Figure 2.9-2.	DP Test 2 HEAF Exterior Damage2-19
Figure 2.9-3.	DP Test 2 Cabinet Top Deformation.....2-19
Figure 2.9-4.	DP Test 2 Interior Cabinet Damage.....2-20
Figure 2.9-5.	DP Test 2 Calorimetry Temperature Data: Temperature2-21
Figure 2.9-6.	DP Test 2 Thermocouple Data2-22
Figure 2.9-7.	DP Test 2 Pressure.....2-23
Figure 2.9-8.	DP Test 2 Arc Energy2-24
Figure 2.10-1.	DP Test 3 Arc.....2-25
Figure 2.10-2.	DP Test 3 Ensuing Fire2-26
Figure 2.10-3.	DP Test 3 Exterior Cabinet Damage2-27
Figure 2.10-4.	DP Test 3 Cabinet Top Deformation.....2-27
Figure 2.10-5.	DP Test 3 Interior Damage.....2-28
Figure 2.10-6.	DP Test 3 Calorimetry Data: Temperature2-29
Figure 2.10-7.	DP Test 3 Thermocouple Data2-30
Figure 2.10-8.	DP Test 3 Pressure.....2-31
Figure 2.10-9.	DP Test 3 Arc Energy2-32
Figure 2.11-1.	DP Test 4 Arc.....2-33
Figure 2.11-2.	DP Test 4 Arc Flames2-34
Figure 2.11-3.	DP Test 4 Thermal Images2-34
Figure 2.11-4.	DP Test 4 Exterior Cabinet Damage2-35
Figure 2.11-5.	DP Test 4 External Cable Tray Damage2-36
Figure 2.11-6.	DP Test 4 Interior Cable Damage2-36
Figure 2.11-7.	DP Test 4 Ground Fault during the Arc2-36
Figure 2.11-8.	DP Test 4 Bus Bar Damage at Arc Location.....2-36
Figure 2.11-9.	DP Test 4 Calorimetry Data: Temperature2-37
Figure 2.11-10.	DP Test 4 Cable Tray Plate Thermometer Data2-39
Figure 2.11-11.	DP Test 4 Pressure.....2-40
Figure 2.11-12.	DP Test 4 Arc Energy2-41
Figure 2.12-1.	DP Test 5 Arc.....2-42
Figure 2.12-2.	DP Test 5 Arc Flames2-43

Figure 2.12-3.	DP Test 5 Thermal Images	2-44
Figure 2.12-4.	DP Test 5 Exterior Damage	2-45
Figure 2.12-5.	DP Test 5 Interior and Cable Damage.....	2-46
Figure 2.12-6.	DP Test 5 Bus Bar Damage at Arc Location.....	2-46
Figure 2.12-7.	DP Test 5 Calorimetry Data: Temperature	2-47
Figure 2.12-8.	DP Test 5 Cable Tray Plate Thermometer Data	2-48
Figure 2.12-9.	DP Test 5 Pressure.....	2-49
Figure 2.12-10.	DP Test 5 Arc Energy	2-50
Figure 2.13-1.	DP Test 6 Arc.....	2-51
Figure 2.13-2.	DP Test 6 Arc Flames	2-52
Figure 2.13-3.	DP Test 6 Thermal Images	2-52
Figure 2.13-4.	DP Test 6 Exterior Damage	2-53
Figure 2.13-5.	DP Test 6 Interior Cable Damage	2-54
Figure 2.13-6.	DP Test 6 Bus Bar Damage at Arc Location.....	2-54
Figure 2.13-7.	DP Test 6 Calorimetry Data: Temperature	2-55
Figure 2.13-8.	DP Test 6 Cable Tray Plate Thermometer Data	2-56
Figure 2.13-9.	DP Test 6 Pressure.....	2-58
Figure 2.13-10.	DP Test 6 Arc Energy	2-59
Figure 3.3-1.	MCC Test Configuration.....	3-3
Figure 3.3-2.	MCC for Test.....	3-4
Figure 3.4-1.	MCC Cable Combustible Load	3-5
Figure 3.5-1.	MCC Calorimeter and TC Location.....	3-6
Figure 3.6-1.	MCC Pressure Measurement Locations	3-8
Figure 3.7-1.	MCC Test 1 Arc.....	3-9
Figure 3.7-2.	MCC Test 1 Thermal Image	3-9
Figure 3.7-3.	MCC Test 1 Exterior Damage	3-10
Figure 3.7-4.	Test 1 Exterior and Interior Damage.....	3-11
Figure 3.7-5.	MCC Test 1 Calorimetry Temperature Data	3-12
Figure 3.7-6.	MCC Test 1 Thermocouple Data	3-13
Figure 3.7-7.	MCC Test 1 Pressure Data	3-14
Figure 3.7-8.	MCC Test 1 Arc Energy	3-15
Figure 3.8-1.	MCC Test 2 Arcs at Bottom and Top.....	3-16
Figure 3.8-2.	MCC Test 2 Sequence for 2 Arcs	3-17
Figure 3.8-3.	MCC Test 2 Thermal Images	3-18
Figure 3.8-4.	MCC Test 2 Exterior Damage	3-19
Figure 3.8-5.	MCC Test 2 Interior Damage.....	3-20
Figure 3.8-6.	MCC Test 2 Calorimetry Temperature Data	3-21
Figure 3.8-7.	MCC Test 2 Thermocouple Data	3-22
Figure 3.8-8.	MCC Test 2 Pressure Data	3-23
Figure 3.8-9.	MCC Test 2 Arc Energy	3-24
Figure 3.9-1.	MCC Test 3 Arc.....	3-25
Figure 3.9-2.	MCC Test 3 Thermal Images (Rear View).....	3-25
Figure 3.9-3.	MCC Test 3 Exterior Damage	3-26
Figure 3.9-4.	MCC Test 3 Interior Damage.....	3-26
Figure 3.9-5.	MCC Test 3 Calorimetry Data	3-27
Figure 3.9-6.	MCC Test 3 Thermocouple Data	3-28
Figure 3.9-7.	MCC Test 3 Pressure Data	3-29
Figure 3.9-8.	MCC Test 3 Arc Energy	3-30
Figure 3.10-1.	MCC Test 4 Arc.....	3-31
Figure 3.10-2.	MCC Test 4 Thermal Images (Rear View).....	3-31
Figure 3.10-3.	MCC Test 4 Exterior Damage	3-32

Figure 3.10-4.	MCC Test 4 Interior Damage.....	3-33
Figure 3.10-5.	MCC Test 4 Calorimetry Data	3-33
Figure 3.10-6.	MCC Test 4 Thermocouple Data.....	3-34
Figure 3.10-7.	MCC Test 4 Pressure Data	3-35
Figure 3.10-8.	MCC Test 4 Arc Energy	3-36
Figure 4.3-1.	SWGR 5-Cabinet Test Configuration.....	4-3
Figure 4.3-2.	Onagawa SWGR and GE Magneblast SWGR	4-4
Figure 4.3-3.	Modified GE Magneblast Dimensions (in cm).....	4-4
Figure 4.3-4.	SWGR Cabinet Configuration Cabinets 7 and 8.....	4-5
Figure 4.3-5.	SWGR Bus Bar Configuration	4-5
Figure 4.4-1.	SWGR Cabinet Combustible Load	4-6
Figure 4.4-2.	SWGR Test Cable Combustible Load	4-8
Figure 4.5-1.	SWGR Tests 1 through 3 Instrument Locations	4-10
Figure 4.7-1.	SWGR Test 1 Arc.....	4-11
Figure 4.7-2.	SWGR Test 1 Thermal Image at Arc Extinction.....	4-12
Figure 4.7-3.	SWGR Test 1 Exterior Damage	4-12
Figure 4.7-4.	SWGR Test 1 Interior Damage.....	4-13
Figure 4.7-5.	SWGR Test 1 Interior Damage, Detailed.....	4-14
Figure 4.7-6.	SWGR Test 1 Insulator and Bus Bar Damage.....	4-15
Figure 4.7-7.	SWGR Test 1 Breaker Damage	4-16
Figure 4.7-8.	SWGR Test 1 Calorimetry Temperature Data	4-17
Figure 4.7-9.	SWGR Test 1 Thermocouple Data.....	4-18
Figure 4.7-10.	SWGR Test 1 Pressure Data	4-19
Figure 4.7-11.	SWGR Test 1 Arc Energy	4-20
Figure 4.8-1.	SWGR Test 2 Shorting Wire Changes	4-21
Figure 4.8-2.	SWGR Test 2 Breaker Changes	4-22
Figure 4.8-3.	SWGR Test 2 Wiring Changes.....	4-22
Figure 4.8-4.	SWGR Test 2 Front Door Meter Changes.....	4-23
Figure 4.9-1.	SWGR Test 2 Exterior Damage	4-35
Figure 4.9-2.	SWGR Test 2 Interior Damage, Continued.....	4-36
Figure 4.9-3.	SWGR Test 2 Insulator and Bus Bar Damage.....	4-37
Figure 4.9-4.	SWGR Test 2 Breaker 7 and 8 Damage	4-38
Figure 4.9-5.	SWGR Test 2 Slug Calorimeter Temperature Data	4-39
Figure 4.9-6.	SWGR Test 2 Thermocouple Data	4-40
Figure 4.9-7.	SWGR Test 2 Pressure Data	4-41
Figure 4.9-8.	SWGR Test 2 Arc Energy	4-42
Figure 4.10-1.	SWGR Test 3 Arc.....	4-43
Figure 4.10-2.	SWGR Test 3 Ensuing Fire	4-44
Figure 4.10-3.	SWGR Test 3 Exterior Damage	4-45
Figure 4.10-4.	SWGR Test 3 Interior Damage.....	4-45
Figure 4.10-5.	SWGR Test 3 Interior Damage, Detailed.....	4-46
Figure 4.10-6.	SWGR Test 3 Insulator and Bus Bar Damage.....	4-47
Figure 4.10-7.	SWGR Test 3 Breaker Damage	4-47
Figure 4.10-8.	SWGR Test 3 Calorimetry Temperature Data	4-48
Figure 4.10-9.	SWGR Test 3 Thermocouple Data.....	4-49
Figure 4.10-10.	SWGR Test 3 Pressure Data	4-50
Figure 4.10-11.	SWGR Test 3 Arc Energy	4-51
Figure 5.3-1.	SWGR Tests 4 through 6: Cabinet 7	5-3
Figure 5.3-2.	SWGR Tests 4 through 6: Cabinet 8.....	5-4
Figure 5.3-3.	SWGR Tests 4 through 6: Schematic of Cabinets 6, 9, and 10	5-5
Figure 5.3-4.	SWGR Tests 4 through 6 Cabinets 7 and 8 Shorting Wire Locations	5-5

Figure 5.4-1.	SWGR Tests 4 and 5, Instrument Locations.....	5-7
Figure 5.4-2.	SWGR Test 6 Instrument Locations	5-9
Figure 5.5-1.	SWGR Test 4 Arcs.....	5-10
Figure 5.5-2.	SWGR Test 4 Thermal Image Ensuing Fire	5-11
Figure 5.5-3.	SWGR Test 4 Exterior Damage	5-12
Figure 5.5-4.	SWGR Test 4 Interior Damage.....	5-13
Figure 5.5-5.	SWGR Test 4 Interior Damage, Detailed.....	5-14
Figure 5.5-6.	SWGR Test 4 Insulator and Bus Bar Damage.....	5-16
Figure 5.5-7.	SWGR Test 4 Breaker Damage	5-17
Figure 5.5-8.	SWGR Test 4 Calorimetry Data: Temperature	5-18
Figure 5.5-9.	SWGR Test 4 Thermocouple Data.....	5-20
Figure 5.5-10.	SWGR Test 4 Pressure Data, Arc 1	5-21
Figure 5.5-11.	SWGR Test 4 Pressure Data, Arc 2	5-22
Figure 5.5-12.	SWGR Test 4 Arc Energy (both arcs).....	5-23
Figure 5.6-1.	SWGR Test 5 Arcs.....	5-24
Figure 5.6-2.	SWGR Test 5 Thermal Image Ensuing Fire	5-25
Figure 5.6-3.	SWGR Test 5 Exterior Damage	5-26
Figure 5.6-4.	SWGR Test 5 Interior Damage.....	5-27
Figure 5.6-5.	SWGR Test 5 Interior Damage, Detailed.....	5-28
Figure 5.6-6.	SWGR Test 5 Insulator and Bus Bar Damage.....	5-29
Figure 5.6-7.	SWGR Test 5 Breaker Damage	5-30
Figure 5.6-8.	SWGR Test 5 Slug Calorimeter Temperature Data	5-31
Figure 5.6-9.	SWGR Test 5 Thermocouple Data.....	5-33
Figure 5.6-10.	SWGR Test 5 Pressure Data, Arc 1	5-35
Figure 5.6-11.	SWGR Test 5 Pressure Data, Arc 2	5-36
Figure 5.6-12.	SWGR Test 5 Arc Energy (both arcs).....	5-37
Figure 5.7-1.	SWGR Test 6 Arc 1.....	5-38
Figure 5.7-2.	SWGR Test Arc 2.....	5-39
Figure 5.7-3.	SWGR Test 6 Thermal Image, Arc 1	5-39
Figure 5.7-4.	SWGR Test 6 Thermal Image, Arc 2.....	5-40
Figure 5.7-5.	SWGR Test 6 Breaker Opened in Arc 2	5-41
Figure 5.7-6.	SWGR Test 6 Cabinet Exterior Damage	5-42
Figure 5.7-7.	SWGR Test 6 Cabinet Interior Damage	5-43
Figure 5.7-8.	SWGR Test 6 Cabinet Interior Damage, Detailed.....	5-44
Figure 5.7-9.	SWGR Test 6 Cabinet 8 Breaker Control Interior Wire Fire.....	5-45
Figure 5.7-10.	SWGR Test 6 Arc 1, Cabinet 7 Bus Bar Damage.....	5-45
Figure 5.7-11.	SWGR Test 6 Arc 2 on Cabinet 8 Damage.	5-46
Figure 5.7-12.	SWGR Test 6 Arc 2, Breaker Secondary Side Damage	5-47
Figure 5.7-13.	SWGR Test 6 Breaker 8 Damage	5-47
Figure 5.7-14.	SWGR Test 6 Calorimetry Data: Temperature	5-48
Figure 5.7-15.	SWGR Test 6 Cable Tray Plate Thermometer Data	5-50
Figure 5.7-16.	SWGR Test 6 Pressure Data, Arc 1	5-51
Figure 5.7-17.	SWGR Test 6 Pressure Data, Arc 2	5-52
Figure 5.7-18.	SWGR Test 6 Arc Energy (both arcs).....	5-53
Figure 6.3-1.	SwRI 5-Cabinet RFAS Test Setup	6-3
Figure 6.3-2.	RFAS Arrangement.....	6-5
Figure 6.5-1.	Heat Flux and Pressure Sensors: Stations 1, 2, and 3	6-7
Figure 6.9-1.	Test 1: RFAS Event	6-9
Figure 6.9-2.	Test 1 Ensuing Fire	6-10
Figure 6.9-3.	Test 1 Interior Cabinet Damage	6-11
Figure 6.9-4.	Test 1 Exterior Cabinet Damage	6-11

Figure 6.9-5.	RFAS Test 1 Heat Flux	6-12
Figure 6.9-6.	RFAS Test 1 TC Measurements	6-13
Figure 6.9-7.	Test 1 Heat Release Rates and Smoke Production.....	6-14
Figure 6.10-1.	RFAS Test 2 Events.....	6-14
Figure 6.10-2.	RFAS Test 2 Ensuing Cable Fire	6-15
Figure 6.10-3.	Test 2 Interior Cabinet Damage	6-16
Figure 6.10-4.	Test 2 Exterior Cabinets Damage	6-17
Figure 6.10-5.	RFAS Test 2 Heat Flux	6-18
Figure 6.10-6.	RFAS Test 1 TC Measurements, Cable Bundles for Cabinets 7 and 8.....	6-20
Figure 6.10-7.	RFAS Test 1 TC Measurements, Cable Bundles for Cabinets 6, 9 and 10 ..	6-20
Figure 6.10-8.	Test 1 Heat Release Rates and Smoke Production.....	6-22
Figure 6.10-9.	RFAS Test 2 Oxygen Concentration in Cabinet 8.....	6-22
Figure 7.1-1.	SWGR Test Comparisons to Onagawa Damage.....	7-2
Figure 7.2-1.	Onagawa Cabinet 7 Bus Bar Damage.....	7-3
Figure 7.2-2.	SWGR Test 3 Bus Bar Damage	7-4
Figure 7.2-3.	SWGR Test 4 Arc 1, Cabinet 7 Bus Bar Damage.....	7-4
Figure 7.2-4.	SWGR Test 4 Arc 2, Cabinet 7 Bus Bar Damage.....	7-5
Figure 7.2-5.	SWGR Test 5 Arc 1, Cabinet 7 Bus Bar Damage.....	7-5
Figure 7.2-6.	SWGR Test 5 Arc 2, Cabinet 8 Rear Bus Bar Damage	7-6
Figure 7.2-7.	SWGR Test 6 Arc 1, Cabinet 7 Bus Bar Damage.....	7-6
Figure 7.2-8.	SWGR Test 6 Arc 2, Cabinet 8 Bus Bar Damage.....	7-7
Figure 7.2-9.	SWGR Test and Onagawa Front Panel Damage	7-8

TABLES

	Page
Table 1-1. Summary of NRA HEAF Tests.	1-1
Table 1-2. Measurements and Instrumentation.	1-7
Table 2-1. DP Test Summary of Results.	2-2
Table 2-2. DP Tests 1 through 3 Calorimeter and TC Locations.....	2-7
Table 2-3. DP Tests 4 through 6 Calorimeter Locations.	2-8
Table 2-4. DP Test 1 Flux Results.....	2-14
Table 2-5. DP Test 1 TC Results.....	2-15
Table 2-6. DP Test 2 Flux Results.....	2-21
Table 2-7. DP Test 2 TC Results.....	2-22
Table 2-8. DP Test 3 Flux Results.....	2-29
Table 2-9. DP Test 3 TC Results.....	2-30
Table 2-10. DP Test 4 Flux Results.....	2-38
Table 2-11. DP Test 4 Plate Thermometer Results.	2-39
Table 2-12. DP Test 5 Flux Results.....	2-48
Table 2-13. DP Test 5 Plate Thermometer Results.	2-49
Table 2-14. DP Test 6 Flux Results.....	2-56
Table 2-15. DP Test 6 Plate Thermometer Results.	2-57
Table 2-15. DP Tests Electrical Results.	2-60
Table 2-16. Acronyms and Abbreviations for Electrical Test Results.....	2-61
Table 3-1. MCC Test Summary of Results.	3-2
Table 3-2. MCC Calorimeter and TC Locations.....	3-7
Table 3-3. MCC Test 1 Flux Results.	3-12
Table 3-4. MCC Test 1 TC Results.	3-13
Table 3-5. MCC Test 2 Flux Results.	3-22
Table 3-6. MCC Test 2 TC Results.	3-22
Table 3-7. MCC Test 3 Flux Results.	3-27
Table 3-8. MCC Test 3 TC Results.	3-28
Table 3-9. MCC Test 4 Flux Results.	3-34
Table 3-10. MCC Test 4 TC Results.	3-34
Table 3-11. MCC Test 1 through 4 Electrical Results (1).....	3-37
Table 4-1. SWGR Tests 1 through 3 Summary of Results.....	4-1
Table 4-2. Calorimeter and TC Locations SWGR Tests 1 through 3.	4-9
Table 4-3. SWGR Test 1 Flux Results.....	4-17
Table 4-4. SWGR Test 1 TC Results.	4-18
Table 4-5. Arc Sequence SWGR Test 2.....	4-24
Table 4-6. Ensuing Fire Sequence SWGR Test 2.	4-28
Table 4-7. Thermal Image of Ensuing Fire SWGR Test 2.....	4-31
Table 4-8. SWGR Test 2 Flux Results.....	4-39
Table 4-9. SWGR Test 2 TC Results.	4-40
Table 4-10. SWGR Test 3 Flux Results.....	4-48
Table 4-11. SWGR Test 3 TC Results.	4-49
Table 4-12. SWGR Tests 1 through 3 Electrical Results (1).....	4-52
Table 5-1. SWGR Tests 4 through 6 Summary of Results.....	5-1
Table 5-2. SWGR Test 4 and 5 Calorimeter and TC Locations.	5-8
Table 5-3. SWGR Test 6 Calorimeter Locations.....	5-8
Table 5-4. SWGR Test 4 Flux Results.....	5-19
Table 5-5. SWGR Test 4 TC Results.	5-20
Table 5-6. SWGR Test 5 Flux Results.....	5-32

Table 5-7.	SWGR Test 5 TC Results.	5-34
Table 5-8.	SWGR Test 6 Flux Results.....	5-49
Table 5-9.	SWGR Test 6 Plate Thermometer Results.....	5-50
Table 5-10.	SWGR Test 4 through 6 Electrical Results (1).....	5-54
Table 6-1.	SWGR RFAS Summary of Results.....	6-2
Table 7-1.	Comparison of Arcs in Front Bus Bars of Cabinets.....	7-9

EXECUTIVE SUMMARY

A High Energy Arcing Fault (HEAF) occurred in a high-voltage (6.9 kV) switchgear (SWGR) at Unit 1 of the Onagawa Nuclear Power Plant of the Tohoku Electric Power Company on March 11, 2011 during the Great East Earthquake in Japan. The Onagawa nuclear power plant (NPP) was the closest plant to the epicenter of the 2011 Great Eastern Earthquake. (To learn more about the effects of the earthquake and tsunami on the Onagawa NPP please see reference [1].) This type of HEAF event has occurred in electric equipment in NPPs worldwide and HEAF events have gained high interest in the safe operation of NPPs with an emphasis on developing evaluation methods.

To investigate the HEAF event sequence and to understand the phenomena, the Regulatory Standard and Research Department, Secretariat of the Nuclear Regulation Authority (S/NRA/R) (Japan) conducted HEAF tests by simulating the design and operating conditions of the SWGR HEAF at Onagawa in addition to simulating the HEAF energy effects using a Rocket Fuel Arc Simulator (RFAS). Tests of 480 V Motor Control Center (MCC) and Distribution Panel (DP) cabinets were also conducted to understand HEAF characteristics.

The objectives were not only to understand the Onagawa event but also to obtain measurements of HEAF phenomenon such as pressures, temperatures, heat fluxes, electrical characteristics, and ability to cause ensuing (secondary) fires within the equipment and of external cables. The objectives also included making observations to assess current HEAF evaluation guidance, including the Zone of Influence (ZOI), in NUREG/CR-6850, "EPRI/NRC-RES Fire PRA Methodology for Nuclear Power Facilities: Detailed Methodology, Appendix M for Chapter 11, High Energy Arcing Faults" (NUREG/CR 6850) [2].

Electrical arc tests were generally conducted per IEEE C37.20.7 "IEEE Guide for Testing Metal-Enclosed Switchgear Rated Up to 38 kV for Internal Arcing Faults" that tests if SWGR cabinets remain intact and the HEAF cannot injure workers [3]. The key part of IEEE C37.20.7 for these tests is the initial arc was created by putting a wire between the bus bars to cause a direct short circuit at the desired position for the HEAF. Tests with electrical arcs were conducted at KEMA Laboratories Chalfont (KEMA), located in Chalfont, Pennsylvania between January 2013 and March 2015, using specialized large capacity electrical systems to create the arc and provide the high energy for the HEAF (usually 10-75 MJ over 2 or 3 seconds). The KEMA facilities are qualified to meet IEEE C37.30.7 requirements.

Tests with Rocket Fuel Arc Simulators (RFAS) to simulate the arc heat were conducted at Southwest Research Institute (SwRI) using aluminum-based solid rocket fuel. The RFAS were used to investigate thermal effects and ensuing fires using a large, industrial calorimeter at SwRI.

The 480 V tests on DP and MCC were the first tests performed to develop the test methods before the more important SWGR tests to simulate the Onagawa HEAF were performed. The test methods improved over the course of the tests with a key change to increase the number of arcs from one (1) to two (2) in the SWGR tests to be similar to the arcs at Onagawa. This confirmed that pre-heating of cable internal to the cabinet is important for rapid cable ignition in a second arc. The final SWGR and DP tests were completed in March 2015.

DP tests 1 through 3 were completed in January 2013 and DP tests 4 through 6 were completed in March 2015 using General Electric (GE) APN-B cabinets. The DPs were tested at nominal 480 V except Test 6 was conducted at nominal 400 V. The tests had target an arc duration of 2

seconds and a target current of 53 kA. The results were arc durations varying between 0.8 to 2 seconds, currents of 38 to 52 kA, and arc electrical energies ranging from 8.3 to 37.1 MJ. Cabinet pressures were 2.0 to 4.8 psi (13.8 to 33.1 kPa) and the maximum external measured flux¹ recorded was 158 kW/m², during the arc for a short duration (less than 1 second). There were ensuing internal cable fires in two tests.

The key observations for the DP tests were:

- It was difficult to repeat arc duration because the arcs could not be sustained.
- The energy threshold for an ensuing internal cable fire was about 28 MJ.
- The pressure was higher for the DP cabinet than the SWGR cabinet because there are fewer vents. The cabinet walls and roof had bending and deformation of several centimeters.

Four MCC tests were completed in May 2013 using GE Series 7700 MCCs. The MCCs were tested at nominal 480 V with a target arc duration of 2 seconds and a target current of 63 kA. The resulting arc durations varied from 0.15 to 0.95 seconds, currents varied between 21 and 46 kA and arc electrical energies ranged from 1.7 to 17.6 MJ. Cabinet pressures were 4.4 to 9.2 psi (30.3 to 63.4 kPa) and the maximum external flux recorded was 102 kW/m² during the arc for a short duration (less than 1 second). There were no ensuing fires.

The key observations for the MCC tests were:

- Test 2 demonstrates the important observation that hot gases and plasma can travel from the initial arc point to other locations in the cabinet and cause a second and in this case higher energy arc.
- Cabinets with few vents that are “tight” and have low ventilation like the MCC have higher pressures, as would be expected. The MCC tests had the maximum pressures of all tests including SWGR and DP. SWGR had the lowest pressures (most ventilated), DP had moderate pressure (less open than SWGR), and MCC had the highest (tight cabinets).
- As shown with the DP tests, it is difficult to maintain a steady arc with 480 V. The bus bars were not very substantial in the MCC, which bent during testing and caused large arc gaps and the voltage could not sustain the arc.

Three SWGR tests with single arcs were completed in June 2013 with a 5-cabinet lineup of GE Magneblast breakers modified to have geometry similar to the SWGR at Onagawa including aluminum bus bars. The SWGRs were tested at nominal 6.9 KV with a target arc duration of 2 seconds and a target current of 23 kA. The results were arc durations of 2 to 3 seconds, currents between 30 and 31 kA and arc electrical energies ranging from 42.6 to 64.2 MJ. Cabinet pressures were 0.7 to 2.4 psi (4.8 to 16.5 kPa) and the maximum external flux recorded was 107 kW/m² during the arc for a short duration (less than 1 second). There were ensuing internal cable fires in two tests.

Test 2 had a fully developed ensuing fire that completely burned the cables in Cabinets 7 and 8 over approximately 20 minutes. Cables in Cabinets 6, 9, and 10 were only partially burned.

¹ The reported flux is the average over the arc duration based on the temperature change of slug calorimeters where the slug temperature is caused by an unknown combination of radiation and convection heat transfer but the flux analysis assumes that the flux is predominately radiation during the arc. See Appendix A for more detail.

Test 3 showed similar results and an ensuing fire but the ensuing fire was extinguished after 4 minutes for safety reasons at the laboratory.

The key results from the SWGR 1-arc tests were:

- The electrical arcing tests at KEMA did not duplicate the Onagawa damage conditions because the damage was not as severe.
- An electrical energy of about 60 MJ was needed for the ensuing fire in the KEMA SWGR tests. One observation on all the tests is that the ensuing fire usually required an energy of around 25 MJ or greater. The higher 60 MJ in this case is probably due to the heat lost through the vents. Cabinets with vents and the vent location may be an important consideration in determining the heat damage effects from HEAF.

The 1-arc SWGR Tests 1 through 3 did not duplicate the assumed 2011 Onagawa HEAF event that may have had two large arcs in two different cabinets several minutes apart. So, the SWGR test items were re-designed to include a working circuit breaker to provide two arcs. SWGR Tests 4 and 5 with two initiated arcs each were completed in March 2014 with 5-cabinet lineups of GE Magneblast breakers identical to SWGR Test 1 through 3. An additional Test 6 was completed in March 2015 with a 3-cabinet lineup. The SWGR were tested at nominal 6.9 KV with Arc 1 target arc durations of 1.0 to 2.5 seconds and a target current of 23 kA. The Arc 1 results were durations between 1.1 and 2.4 seconds, currents of 24 to 25 kA and arc electrical energies ranging from 26.5 to 64.6 MJ. The Arc 2 target arc durations were 2 to 3 seconds and a target current of 35 kA. The Arc 2 results were durations of 0.6 (there was a failure that shortened the duration) to 2.1 seconds, current of 33 – 34 kA and arc electrical energies ranging from 21.1 to 78.4 MJ.

Cabinet pressures were 1.3 to 3.4 psi (19.0 to 23.4 kPa) and the maximum external flux was 220 kW/m² for a short duration (less than 1 second) during Test 4, Arc 2. This test also resulted in very large amount of aluminum oxidation from bus bar contact and shorting. There were ensuing internal cable fires in two tests.

The key results from the SWGR 2-arc tests at KEMA were:

- Test 4, Arc 2 had horizontal bus bar arcing that simulated the assumed second arc in the 2011 Onagawa HEAF event scenario with severe bus bar arcing. The energy and fire were very large and the damage on the front of Cabinet 7 was similar to Onagawa but not as severe. This test confirms that the aluminum bus bar oxidation likely contributed to the large ensuing fire at Onagawa.
- In Test 5 and Test 6 Arc 2, there were strong arcs in the secondary (rear) of Cabinet 8, as planned. However, the damage to the circuit breaker was not as severe as at Onagawa because the arc did not travel down into to the breaker to cause the severe damage observed at Onagawa. In Test 5, Arc 2 the hot gas and plasma went up through the top of the cabinet and out the vent rather than down toward the breaker. In Test 6, Arc 2 the hot gas and plasma remained in the rear of the cabinet but the damage to the breaker was still minimal.
- The energies for the arcs were greater than 60 MJ in SWGR Tests 4 and 5, and resulted in ensuing fires. This is similar to the results in SWGR Tests 1 through 3. The energies in Test 6 were not adequate for an ensuing fire because a shorter Arc 1 was planned (1

second versus 2 seconds) and the second arc was extinguished by a hot short that opened the Cabinet 8 breaker carrying the arc current from the KEMA source.

- Tests 4, 5 and 6 had higher total energies than Tests 2 and 3 because there were two electrical arcs and much more aluminum oxidation, especially in the case of Test 4, Arc 2. The fire in Test 4 quickly spread to the other cabinets. The cables were pre-heated by Arc 1 so the cable burning was very rapid after Test 4, Arc 2.
- Test 4, Arc 2 showed the highest external flux for any test in this report. None of the cables in the test cable trays 45.7 cm (18 in) above the top of the SWGR caught fire but there was some fire damage, such as charring and local burns where the cables were in contact with the tray rungs.
- Test 6, Arc 2 demonstrated the important behavior that arcs can move from the initial ignition point because the arc ignited at the insulator but moved to the end of the bus bars along the path of the current. This also demonstrates that arc behavior is difficult to predict because in an identical test configuration in SWGR Test 5, Arc 2 stayed at the initial ignition point.

Two RFAS tests in 5-cabinet lineups of GE Magneblast cabinets identical to SWGR Tests 1 through 3 were tested in July 2013. RFAS energies of 140 MJ single RFAS burst (Test 1) to 245 MJ in two bursts (like the two arcs assumed at Onagawa) were tested.

RFAS Test 2 was one of the most interesting tests because there was a full ensuing fire that was allowed to burn to extinguishment 90 minutes after ignition. In Test 1 both RFAS charges ignited at the start of the test and there was no major ensuing fire even though the energy was more than 2 times the energy of KEMA SWGR Test 2 that had a major fire. The cables in Test 1 reached a high temperature during the RFAS ignition but quickly cooled and there was no ensuing cable fire.

The key results from the RFAS SWGR tests at SwRI were:

- The RFAS is a good method to simulate the high energy of a HEAF and get more data about the ensuing fires. However, the energy required to get an ensuing fire is at least 2 to 4 times higher for an RFAS than for an electrical arc. This suggests that the rapid aluminum oxidation (combustion) energy in addition to the electrical energy was needed to cause the ensuing fires in electrical SWGR HEAF tests.
- The low pressure and rapid recovery of oxygen after the RFAS ignition show that the SWGR are well ventilated cabinets and much of the heat energy from a HEAF is lost. The KEMA tests suggest the energy is much higher to start an ensuing fire in a SWGR than for less-ventilated cabinets like the DP.
- Pre-heating from the first RFAS burst decreased the time needed to develop the ensuing fire and subsequently increased the growth of the ensuing fire to the peak temperature. However, cabinets without much pre-heat still can have an ensuing fire, but it took a longer time to ignite when the ramp up was slower.
- Even at the very high energies (245 MJ) in RFAS Test 2, the damage was not as severe as occurred at Onagawa NPP in 2011. The exterior of the cabinet was not as charred

and there was no major damage in the secondary (rear) of the SWGR cabinet. This suggests a large thermal energy release from the bus bar oxidation at Onagawa.

CITATIONS

This report was prepared by the following:

Division of Research for Reactor System Safety
Regulatory Standard and Research Department
Secretariat of Nuclear Regulation Authority
(S/NRA/R)
1-9-9 Roppongi, Mianto-ku, Tokyo, Japan 106-8450

S. Tsuchino, Senior Expert
H. Kabashima, Chief Researcher

Leidos, Inc.
301 Laboratory Road
Oak Ridge, TN 37830
S. Turner

Division of Risk Analysis
Office of Nuclear Regulatory Research
U.S. Nuclear Regulatory Commission
Washington, DC 20555-0001

S. Mehta
D. Stroup
N. Melly
G. Taylor
F. Gonzalez

Prepared as part of:
The Agreement on Research Participation and Technical Exchange under the Fire-Related
Research Program

ACKNOWLEDGMENTS

The authors acknowledge the dedicated team of individuals and international companies that contributed to the success of the HEAF tests.

Dr. Fumio Kasahara of NRA provided senior management oversight and technical advice.

Takeshi Saito and Masahiro Nagaki of Japan NUS Co, LTD (JANUS), Tokyo provided technical support and translation.

The NRC team observing and supporting the tests was led by Mark Henry Salley with support from Nicholas Melly, Gabriel Taylor, David Stroup, and Felix Gonzalez. Shivani Mehta was responsible for the final NUREG/IA preparation.

NRC was also supported by the National Institute of Standards and Technology (NIST) team that provided measurement support under the leadership of Anthony Putorti with test engineering support by Scott Bareham, Michael Selepak, Joseph Praydis Jr, and additional technical staff for test operations at NIST and KEMA.

NRC was also supported by Carlos Lopez and other staff at Sandia National Laboratories (SNL) that tested some measurement methods.

The tests were managed by Leidos, Inc. of Oak Ridge, Tennessee under the leadership of Stephen Turner and supported by various subcontractors. Jennie Henry was the Leidos Subcontract administrator. Karen Carpenter of Southwest Research Institute provided test management support and thermal imaging at KEMA and managed the tests at SwRI with support from the SwRI technical staff and oversight from Marc Janssens and Matt Blais. Matthew Muthard, Kresimir Starcevic, Victor Savulak, Richard McLaughlin, Dennis Samuel, and George Khoury coordinated and managed the tests at KEMA Laboratories Chalfont. Robert Taylor of Brendan Stanton Incorporated (BSI) managed the assembly and installation of the test items with engineering support from Benny Lee and fabrication and technician support by other technical staff. David Muir of Advanced Motor Controls in cooperation with Paul Grein and Kyle Fincher at Circuit Breaker Sales provided the test items. James Phillips of Brainfiller, Incorporated provided Subject Matter Expert advice on arc flash hazards.

ACRONYMS AND ABBREVIATIONS

AC	Alternating Current
AL	Aluminum
A	Ampere
ASTM	ASTM International
Bot	Bottom
Cab	Cabinet
cal	calorie
CRIEPI	Central Research Institute of the Electric Power Industry
CT	Cable Tray
CV	A type of cable
DFT	Directional Flame Thermometers
DP	Distribution Panel
F	Front
FS	Front Side
FLIR	Forward Looking Infrared, also a camera manufacturer
g	gram
GE	General Electric
HD	High Definition
HEAF	High Energy Arcing Fault
HRR	Heat Release Rate
HS	High Speed
HV	High Voltage
IEEE	Institute of Electrical and Electronics Engineers
in	Inch
ISO	International Organization for Standardization
JNES	Japan Nuclear Energy Safety Organization (now NRA)
k	1,000
kA	Kiloampere
KEMA	KEMA Power Test, LLC
kg	Kilogram
kJ	Kilojoule
KMS	Knowledge Management System
kPa	Kilopascal
KPT	KEMA Power Test (same as KEMA)
kV	Kilovolt
kVA	Kilovolt Ampere
kW	Kilowatt
LLC	Limited Liability Corporation
LV	Low Voltage
m	meter
MBB	MagneBlast Breaker
MC	Mitsubishi Corporation

MCC	Motor Control Center
MCCB	Molded Case Circuit Breaker
min	minutes
MJ	Megajoule
mol	moles
MV	Medium Voltage
MVA	Megavolt Ampere
N/A	Not Applicable
NIST	National Institute of Standards and Technology
NPP	Nuclear Power Plant
NRA	Nuclear Regulation Authority (Japan, also see S/NRA/R)
NRC	Nuclear Regulatory Commission (United State of America)
OECD	Organization for Economic Cooperation and Development
Pa	Pascal
PRA	Probabilistic Risk Assessment
psi	Pounds per Square Inch
psig	Pounds per Square Inch Gauge
PT	Plate Thermometer
PRT	Pressure Transducer
PVC	Polyvinyl Chloride
R	Rear
RS	Right Side
RFAS	Rocket Fuel Arc Simulators
s	Second
S	Slug calorimeter
S/NRA/R	Regulatory Standard and Research Department, Secretariat of the Nuclear Regulation Authority (S/NRA/R) (Japan)
SAIC	Science Applications International Corporation (now Leidos)
SB	Schmidt-Boelter (heat gauge)
SNL	Sandia National Laboratories
SPR	Smoke Production Rate
SS	Stainless Steel
SWGR	Switchgear
SwRI	Southwest Research Institute
T	Top
TC	Thermocouples
THR	Total Heat Released
US	United States (of America)
V	Volt
VAC	Volts Alternating Current
XLPE	Cross-Linked Polyethylene
ZOI	Zone of Influence

1 INTRODUCTION

1.1 Background

The High Energy Arcing Fault (HEAF) tests in this report were conducted to support research on a HEAF event that occurred during the 2011 Great East Earthquake at the Onagawa NPP that damaged a row of Switchgear (SWGR) panels [1].

HEAFs are a fast energy release that occurs in the form of heat, light, molten metal, and pressure rise from electrical shorts inside of electrical equipment cabinets. HEAFs are a hazard that can cause ensuing (or secondary) fires that destroy targets such as the power and control cables inside and outside the cabinet. Understanding HEAFs and their consequences is important, as demonstrated by a large HEAF in a high-voltage (HV)² 6.9 kV switchgear (SWGR) and ensuing fire that occurred at the Onagawa NPP during the March 11, 2011 Great East Japan Earthquake.

In general, the electrical power industry refers to HEAF as an “arc-blast” or “arc-flash” and the basic behavior is documented in IEEE 1584 [4], which has a case history of arc-flash events. Industry has mainly been concerned about the effects of arc flash on workers and the protective equipment that is needed for workers to safely operate, maintain, and install electrical systems. The nuclear industry has focused more on evaluating the impact of ensuing fires as part of Fire Hazards Analysis (FHA). NRC Probabilistic Risk Assessment (PRA) guidance in NUREG/CR 6850 [2] specifically addresses analysis of HEAFs. The Organization for Economic Cooperation and Development (OECD), Nuclear Energy Agency (NEA) began an international activity to investigate HEAFs in 2009 and compiled information on 48 HEAF events [5].

The guidance in NUREG/CR 6850, Appendix M prescribes that the ensuing fire(s) typically includes ignition of combustible material within the HEAF Zone of Influence (ZOI). The resulting fire may be due to the ejection of hot particles or piloted ignition of combustibles. HEAF events are of concern due to their potential to impact adjacent items important to safety and current limitations in characterizing the ZOI. The ZOI was determined based on a review and characterization of the damage and detection/suppression behavior for the energetic phase of high-energy-arcing faults of 11 incidents that occurred in U.S. nuclear power industry between 1979 and 2001. Specifically, the ZOI boundaries are at 1.5 m (5 ft) above the cabinet and 0.91 m (3 ft) from the sides of the cabinet, in all directions.

The NRA test series focuses on HEAFs in a 6.9 kV SWGR with a similar configuration to the Onagawa event, and includes tests for 480 V Motor Control Centers (MCC) and Distribution Panel (DP) cabinets. The test objective included determining if ensuing fires occur and confirm the events in the Onagawa HEAF event. The tests performed are to better understand the HEAF phenomena and the ZOI for damage from the ensuing fires, as described in NUREG/CR 6850, Appendix M.

1.2 Onagawa HEAF Event

The damaged Onagawa switchgear panels 7 through 10 are shown in Figure 1.2-1. The Onagawa arcing event is shown in Figure 1.2-2, in which the first arc occurred from a normal operating condition with “Common Use Power” in the Cabinet 7 SWGR from shaking during the

² Japan considers 6.9 kV as “High Voltage”, most other countries, including the US, consider 6.9 kV as “Medium Voltage”.

initial earthquake at 14:46, local time [1]. It appears that a second arc may have occurred from an abnormal operating condition, in which start up power was available at the Cabinet 8 SWGR through an unusual configuration of the startup power circuits. In both arcs, the heavy breakers hanging in the SWGR cabinets swung wildly, causing arcs where the SWGR bushings are mated with the insulation bushings.

The circuit for Cabinet 7 had a reported impedance of 9.5% at 6.9 kV at the time of the Arc 1. The circuit for Cabinet 8 had an unknown impedance at the time of Arc 2 because the circuit was irregular and not covered in the design.

The main goal of the SWGR tests in this report was to simulate these arcs. The initial SWGR Tests 1 through 3 attempted to simulate the Cabinet 7 arc only. However, based on the initial test results, the SWGR tests were redesigned to provide two arcs in Tests 4 through 6 to better simulate the Onagawa event.



Figure 1.2-1. Damage in Onagawa HEAF Event

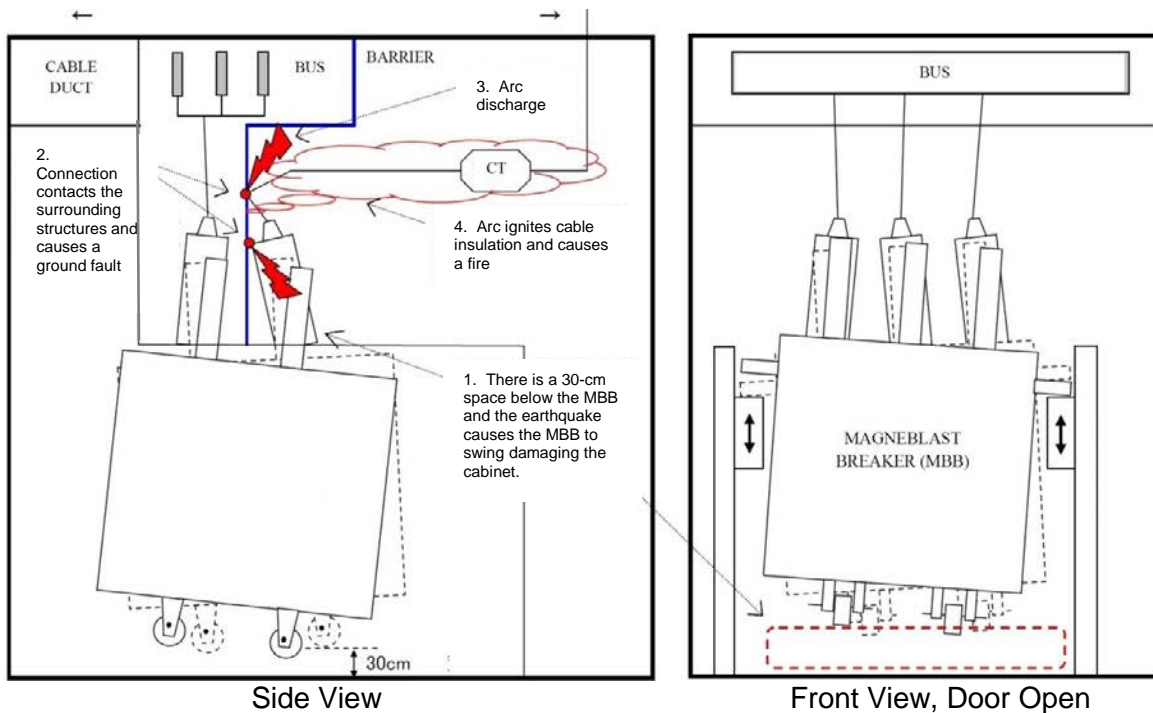


Figure 1.2-2. Onagawa Arching Scenario

1.3 Test Approach and Electrical Test Conditions

Tests were generally conducted per IEEE C37.20.7 [3] that evaluates SWGR to determine if it meets the “arc proof” requirements in IEEE 1584 [4]. “Arc proof” testing ensures that SWGR cabinets remain intact and the HEAF cannot injure workers. The key part of IEEE C37.20.7 used in these tests is the creation of the initial arc by putting a wire between the bus bars to cause a short at the desired position for the HEAF. The tests are intentionally creating an arc path at a specific location which will mimic event scenarios within cabinets. The cabinets are not connected to full electrical systems of breakers - this allows the arc to persist without safety mitigation strategies such as breaker trips.

Tests with electrical arcs were performed at the KEMA Laboratories Chalfont (KEMA) using specialized large capacity electrical systems to create the arc and provide the high energy for the HEAF (usually 10-75 MJ over 2 or 3 seconds). Details of the KEMA facilities are discussed in Appendix B. HEAFs have the ability to cause severe, short duration, thermal insults that were characterized by heat flux measurements using slug calorimeters at KEMA. HEAF heat release rate (HRR) is another important parameter to assess thermal properties but HRR cannot be measured at KEMA. To measure and understand the HRR, tests with Rocket Fuel Arc Simulators (RFAS) were conducted at Southwest Research Institute (SwRI) with their large-scale industrial calorimeter. The RFAS simulates the arc heat expected in a HEAF.

Table 1-1 summarizes the tests. The test conditions listed in the table are the target test conditions (not the voltage and current achieved) but the arc duration and energy from the tests are reported.

The arc current and arc duration for the tests were much higher than properly designed circuits allow. Circuits are designed to limit the arc energy and duration during a fault so HEAFs do not occur.

1.3.1 Arc Current

The bolted fault current that is the maximum feasible fault current for an electric circuit was used in the tests. KEMA used the bolted fault current as a target specified by NRA as a peak current target in no-load calibration runs with shorted busses before the current is applied to the test item. The actual symmetrical current in the tests is be slightly lower because of the impedance of the arc (it acts similar to a load). The peak current will be slightly higher than the symmetrical current but it only lasts for a few electrical cycles at the start of the arc. The calculations for the target test currents are provided in Appendix D.

1.3.2 Arc Duration

The planned target arc durations were nominally 2 seconds for most tests but were increased to 3 seconds in some cases to increase the energy in attempts to ignite ensuing fires. The 2 seconds was based on an assumption that older systems in Japan require long times for clearing a fault. This was a conservative duration to create very high energy. There are cases of reported HEAF events as long as 5 to 10 seconds [5].

Table 1-1. Summary of NRA HEAF Tests.

Date/Location	Test	Tests/ Type of Test	Test Conditions (1)	Results	Report Chapter
January 2013 SwRI	1-cabinet SWGR	3 RFAS tests to understand ensuing fires	Simulate 1 70 MJ arc 2 RFAS slabs (35 MJ each), 2 second burst time	No major ensuing fires HRR very low RFAS works	6
July 2013 SwRI	5-cabinet SWGR	2 RFAS tests	Test 1: Simulate 1 140 MJ arc, 2 seconds Test 2: Simulate 2 bursts, 70 MJ + 175 MJ, 2 seconds	Test 1: No ensuing fire Test 2: Ensuing 90-minute fire with good HRR measurements	6
June 2013 KEMA	5-cabinet SWGR	3 electrical arc tests, 1 arc	Test 1-3: 6.91 KV, 23 kA, 2 - 3 sec duration Arc energy of 43 to 64 MJ	Test 1: No ensuing fire with 43 MJ Test 2 and 3: Ensuing fires in cases with nominal 60 MJ energy, fire damage not as severe as Onagawa	4
March 2014 KEMA	5-cabinet SWGR	2 electrical arc tests, 2 arcs	6.9 KV, 23 kA, 2 - 3 sec duration Test 4: Arc 1: 67 MJ (Cab 7); Arc 2: 78 MJ (Cab 7, bus bars) Test 5: Arc 1: 57 MJ (Cab 7) Arc 2: 62 MJ (Cab 8, rear)	Test 4: Large ensuing fire and bus bar arcing like at Onagawa, highest energy fluxes and damage of all NRA tests Test 5: Ensuing fire and Arc 2 on secondary side like Onagawa but damage not as severe as Onagawa.	5

Date/Location	Test	Tests/ Type of Test	Test Conditions (1)	Results	Report Chapter
March 2015 KEMA	5-cabinet SWGR	1 electrical arc test, 2 arcs	Test 6: 6.9 KV, 23 kA Arc 1: 27 MJ (Cab 7), 1.1 sec Arc 2: 21 MJ (Cab 8), 0.6 sec	Test 6: No ensuing fire (low energy), minor bus bar oxidation, breaker failure caused a short Arc 2 duration, Arc 2 moved from the secondary insulator to the end of the secondary bus bars.	5
January 2013 KEMA	DP	3 electrical arc tests	Tests 1 – 3: 1 arc 480 V, 53 kA, 1.5- 2 seconds Energy 30 – 37 MJ	Difficult for arc to sustain, Ensuing fires in 2 tests.	2
March 2015 KEMA	DP	3 electrical arc tests	Test 4 and 5: 480 V, 53 kA, 0.7 – 1.7 seconds Energy 8 – 14 MJ Test 6: 400 V, 53 kA, 0.8 seconds Energy 8.2 MJ	Difficult for arc to sustain, no ensuing fires. All arcs short of the 2-second target.	2
May 2013 KEMA	MCC	4 electrical arc tests	Tests 1-4: 1 arc 480 V, 63 kA, 0.15 to 0.95 seconds, (2 second target) Energy 1.7 to 17.6 MJ	Difficult for arc to sustain – short arc times Proved that arcs could move inside the cabinet No ensuing fires. Arc penetrated the cabinet in 2 tests.	3

(1) The energy is the electrical energy input only; no energy from bus bar oxidation is included

1.4 Measurements and Instrumentation

The measurement items for the tests are shown in Table 1-2. The table includes the instruments used at SwRI and KEMA and additional instruments provided by Sandia National Laboratories (SNL) and the National Institute of Standards and Technology (NIST). SNL tested several instruments to potentially enhance the instruments available at KEMA. However the KEMA instruments were deemed adequate for the NRA testing [6]. NIST provided a portable oxygen-calorimetry hood and Plate Thermometers (PT) (described in Reference [7, 11]) for tests in March 2015. For this report, the results for plate thermocouples mounted on a cable tray above the cabinet are presented for DP Tests 4 through 6 and SWGR Test 6. Hood calorimetry results are not reported because, as noted in Reference [7, 11], the method was not effective during the arc but is useful for ensuing fires after the arc. However, none of the tests where the hood was used had ensuing fires.

Table 1-2. Measurements and Instrumentation.

Measurement Item	Measurement Method
1. Current waveform measuring device	Voltage dividers, coaxial shunts, and other coils provided current and voltage waveforms to calculate energy.
2. Pressure a. Internal b. External	a. Internal: Strain-gauge type pneumatic transducers were used by KEMA, SNL, and SwRI. b. External: Pencil-type gauges were used at the January 2013 tests at KEMA by SNL and at SwRI. The measurements were not useful in the swirling air around the HEAF and fire.
3. Temperatures	Thermocouples (TC), passive temperature indicator labels and plate thermometers (PT). The TCs could not be placed directly on the cabinets in the electrical tests for safety. They indicate local air temperatures 15.2 cm (6 in) from the cabinet. Results are reported but were not very useful. Not used in 2015 tests.
4. Heat Flux	Slug calorimeters built to ASTM F1959 [8] were used at the ZOI positions in tests at KEMA (see Appendix A). SwRI used dual plate thermometers, Schmidt-Boelter (SB) gauges, Gardon Gauges and ASTM F1959 calorimeters for comparison and analysis. Other methods used by SNL were not effective, see Reference [6].
5. Oxygen calorimeter	Industrial scale calorimeter used for ensuing fire HRR at SwRI. The NIST calorimetry hood was used in the March 2015 tests but was not useful during the arcs [7, 11].
6. Infrared and visible light high-speed photography	FLIR T300 Thermal Imaging camera to see the HEAF ensuing fire effects and general thermal conditions, High speed camera at 500 – 1000 frames per second to study ignition and cabinet deformation. Various High Definition videos from many positions were used to see the HEAF effects and timing of key events like ensuing fire ignition.
7. IEEE C37.20.7 indicators	Used to study debris that escapes the cabinet at KEMA. The DP and MCC cabinets are not arc proof so debris escaped. The SWGR cabinets showed little debris.

Measurement Item	Measurement Method
8. Oxygen monitor	Used at SwRI to measure oxygen depletion in Cabinet 8 caused by RFAS ignition in the SWGR tests. All oxygen calorimeter results include oxygen measurement.
9. Cable Samples	Short pieces of cable (less than 8 cm (3.15 in)) were placed at several internal and external positions and externally at the ZOI in DP Tests 1 through 3. Cable trays were placed above the DP and SWGR cabinets in the March 2015 tests.

2 Distribution Panel HEAF TEST – KEMA (January 2014 and March 2015)

2.1 DP Test Overview (2014 and 2015)

The purpose of these tests was to obtain the basic HEAF data such as arc duration, energy, flux, temperature, pressure, and ensuing fire effects for six (6) Distribution Panels (DP). All tests were conducted at KEMA; Tests 1 through 3 were conducted on January 29-31, 2014 and Tests 4 through 6 were conducted on March 18-19, 2015.

2.2 DP Tests Summary of Results

Each test consisted of one 480 V General Electric (GE) APN-B DP that contained three (3) Molded Case Circuit Breakers (MCCBs). The DP is nominally 1.11 m wide by 2.29 m high and 0.89 m deep (44 in by 90 in by 35 in). Japanese CV-2 cable that is typical of power cable was added as the combustible load. The key test parameters and results are in the Table 2-1. The target test voltage was nominally 480 V and the target test current was 53 kA bolted fault current. The final symmetrical current provided by the KEMA facility was nominally 38 to 43 kA during the arc.

The key results of the DP tests are:

- Arc durations were difficult to repeat; the resultant arcs demonstrated random behavior after initiation and often could not be sustained, especially in Tests 4 through 6.
- The energy threshold for the ensuing fire in these tests was about 28 MJ.
- The cabinet walls and roof exhibited bending and deformation of several centimeters, potentially due to the use of thin materials for the walls and doors.

Table 2-1. DP Test Summary of Results.

Test	Volt (V) (1) Current (kA) (2)	Test Peak Current (kA) (3)	Arc Duration (sec) (4)	Arc Energy (MJ)	Internal Max Press (kPa/psi) (5)	Ext Max Flux (6) (kW/m ²)	Ensuing fire? Key Observations
1	484 / 404 43.3 / 30	71.2	2.0 1.574	29.6	14.5 ± 2.8 2.1 ± 0.4	54 (7)	Yes. After 7 minutes.
2	484/ 394 38.4 / 31.6	66.9	2.0 1.446	26.2	18.6 ± 2.1 2.7 ± 0.3	63 (7)	No. Arc energy too low.
3	484/ 416 41.4 / 32.0	63.0	2.0 2.011	37.1	13.8 ± 6.9 2.0 ± 0.3	27 (8)	Yes. After 50 seconds.
4	484 / 403 50.3 / 19.3	95.0	2.0 0.698	8.3	33.1 ± 1.4 4.8 ± 0.2	91 (9)	No. Arc energy too low.
5	484 / 363 44.7 / 37.9	105	2.0 1.659 (10)	14.3 (10)	22.1 ± 2.1 3.2 ± 0.3	158 (9)	No. Arc energy too low.
6	400 / 305 51.8 / 30.3	106	2.0 0.781 (11)	8.2 (11)	16.5 ± 1.4 2.4 ± 0.2	73 (9)	No. Arc energy too low.

Notes:

- (1) The voltage is shown as the target voltage / arc Line-to- Line (L-L) voltage.
- (2) The symmetric arc current slowly drops during the test as the arc impedance increases. This shows the *test start current/ test end current*. These are average currents of all 3 phases.
- (3) This is the peak current for any phase or time, usually the asymmetric current at the start.
- (4) The duration is shown as the target duration and the actual test duration is below it.
- (5) The uncertainty is described in Appendix A.
- (6) The flux is reported for the outer boundary of the NUREG/CR 6850 ZOI at 0.91 m (3 ft) for the sides or 1.5 m (5 ft) at the top.
- (7) The maximum flux was seen at 0.91 m (3 ft) at the rear of the cabinet at the height of the arc, 78.7 cm (31 in) from the floor (S8).
- (8) The maximum flux was seen at the top, 0.91 m (3 ft) to the left side of the cabinet (S5). A higher flux of 187 kW/m² was seen at 30.48 cm (1 ft) from the cabinet (S8), not at the 0.91 m (3 ft), as in other tests.
- (9) The highest flux during the arc was measured at the top left side of the cabinet (S8).
- (10) This includes the initial arc for 1.001 seconds and a re-strike.
- (11) This includes the initial arc for 0.550 seconds and several re-strikes.

2.3 DP Test Configuration

The GE APN-B DP has horizontal and vertical bus bars, as shown in Figure 2.3-1. The horizontal buses are extended outside the cabinet for KEMA to connect (gray). A wire to start the arc is connected to the buses inside (red lines). The breakers and components in the DP are the combustible load. An arc at the bottom below the combustibles should cause the largest fire in the cabinet. DP Tests 1 through 3 used an arc at the bottom of the cabinet. DP Tests 4 through 6 used an arc at the top of the cabinet.

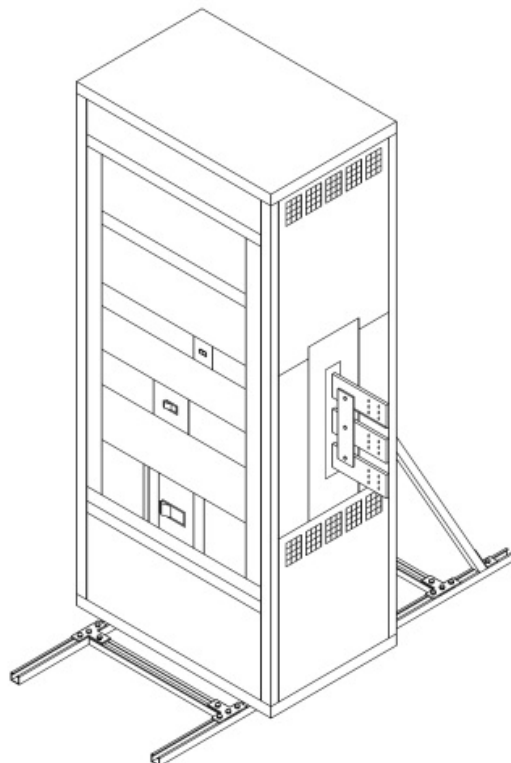
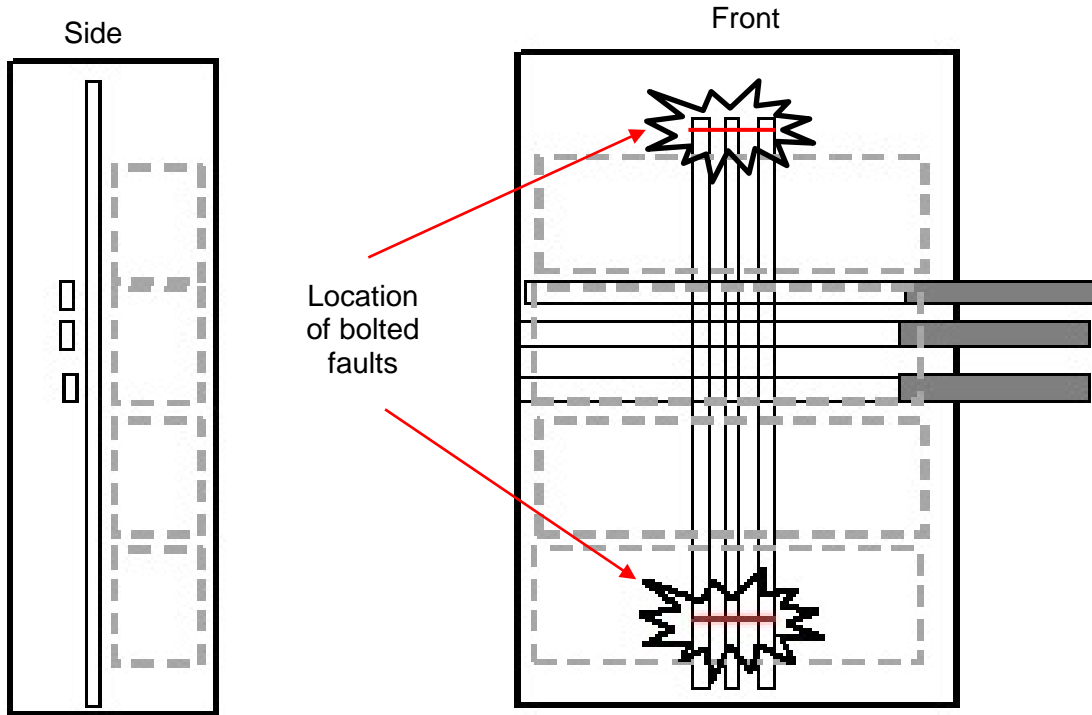


Figure 2.3-1. DP Test Configuration

2.4 DP Test Configuration

This DP test item is a GE Spectra Series APN-B, shown in Figure 2.4-1. Small, medium, and large Molded Case Circuit Breakers (MCCB) were used in the cabinet. The MCCBs were evenly spaced to encourage an ensuing fire. The horizontal bus is rated for 3 kA and the busses are connected from the right side of the cabinet.

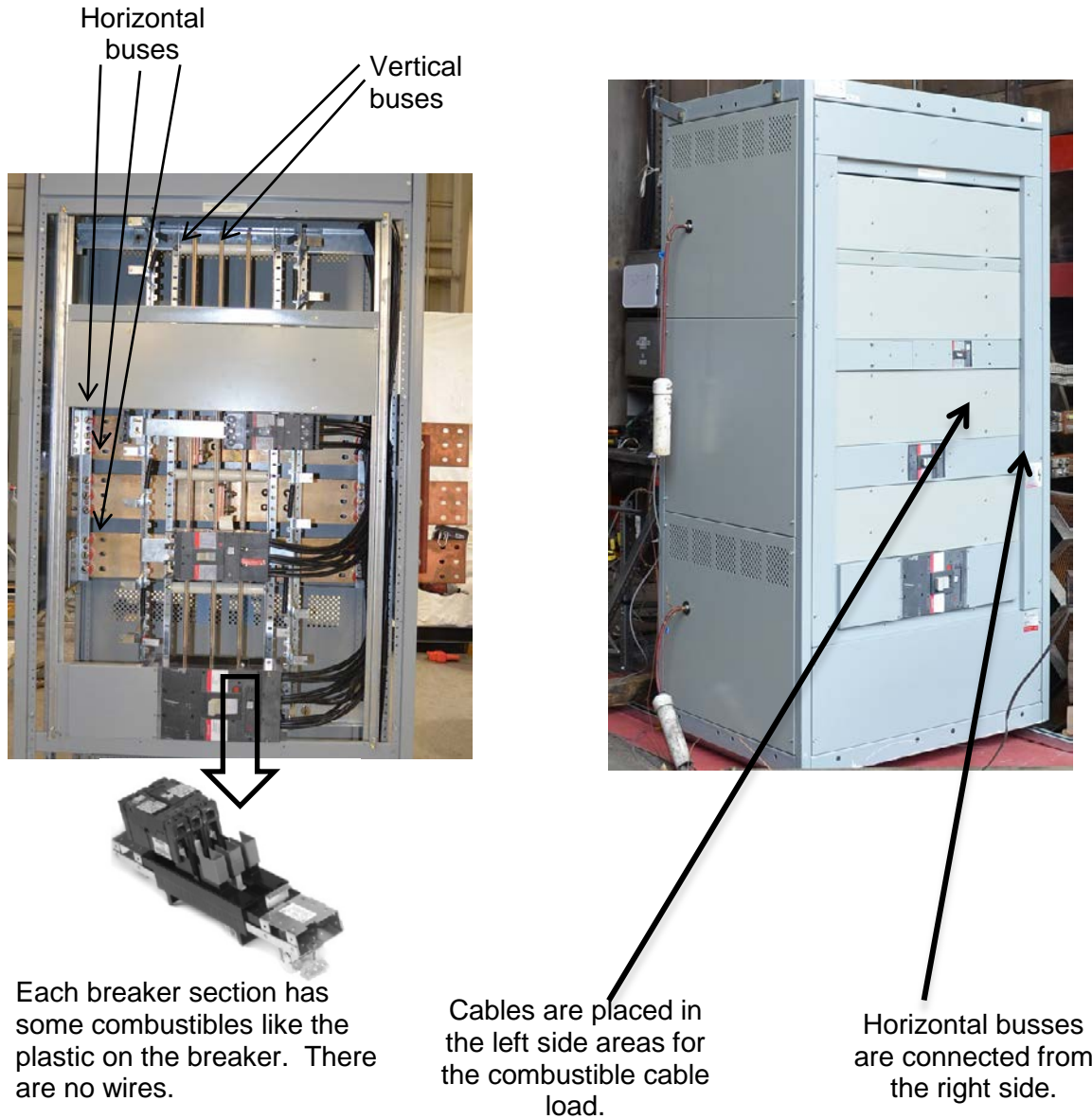


Figure 2.4-1. DP Used in Tests

2.5 DP Test Cable Combustible Loading

2.5.1 Internal Combustible Loading

Japanese Type CV control cables with heat resistant PVC (Polyvinyl Chloride) sheath and XLPE (Cross-Linked Polyethylene) insulation were used for the combustible cable load in each test (see Appendix C for the properties). In actual use, power cables are used from the MCCB controllers to motors, and from the DP breakers to the loads. In these cases, typical large 4-conductor cables are used (3 phases plus ground) but none were available for testing. Multiple 2-conductor (CV-2) and 4-conductor (CV-4) cables were used to realistically model large power cables.

The number of CV cables was changed for each breaker to represent larger power conductors for larger breakers. The cables loop over the top internal support bar and then to the floor as in a realistic cabinet where they exit the bottom of the cabinet, as seen in Figure 2.5-1. A total of 78 m (255 ft, about 9.4 kg of combustible load) of CV cable was included for Tests 1 through 6, with the following grouping:

- Two (2) CV cables (like small power cables) 1.5 m (5 ft) long installed per phase to the small breaker (9.1 m (30 ft) total).
- Three (3) CV cables (like medium power cables) 2.1 m (7 ft) long installed per phase to medium breaker (19.2 m (63 ft) total).
- Six (6) CV cables (like large power cables) 2.7 m (9 ft) long installed per phase to large breaker (49.4 m (162 ft) total).

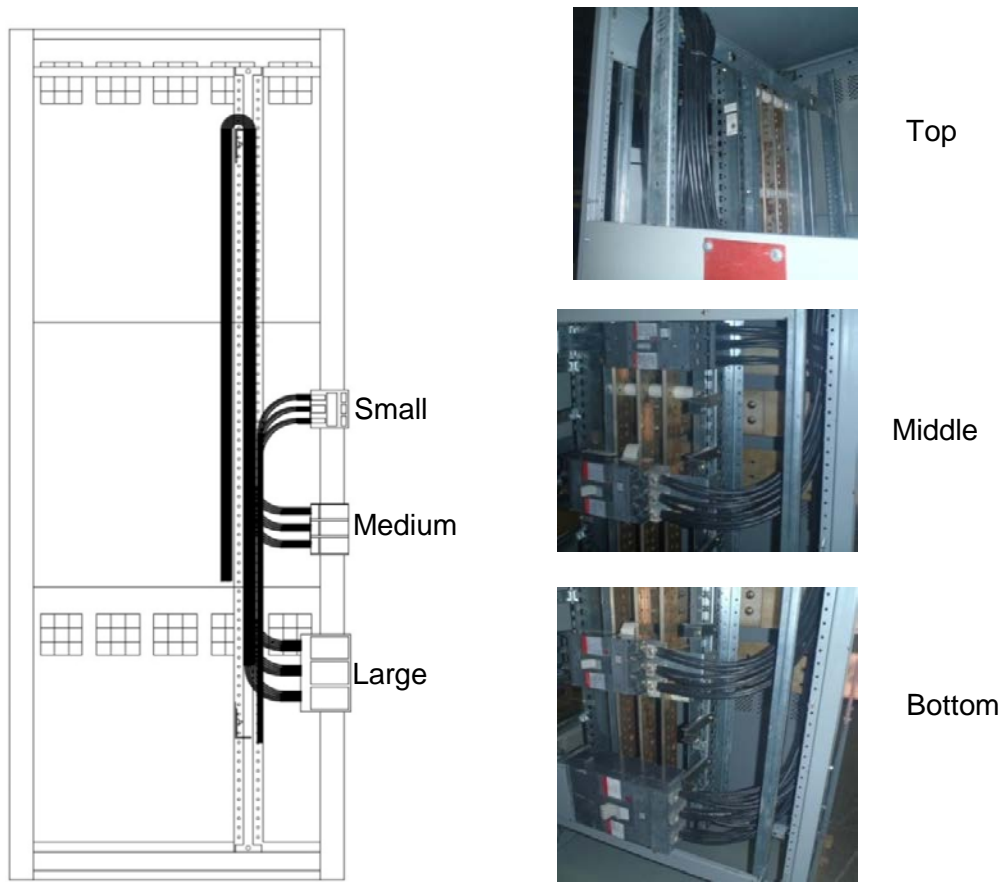


Figure 2.5-1. DP Test Cable Combustible Load

2.6 DP Test Temperature and Heat Flux Instrumentation

Slug calorimeter (slug, S) and thermocouple (TC) locations are in Figure 2.6-1 and Figure 2.6-2 for DP Tests 1 through 3 and Figure 2.6-3 for DP Tests 4 through 6. The TC and slug positions and names are in Table 2-2 and Table 2-3.

For DP Tests 1 through 3 slugs are nominally 0.91 m (3 ft) from the cabinet sides (labeled as S5, S6, S7, S8, S10) and 1.5 m (5 ft) from the cabinet top (S9), as shown in the figures. These are located at the boundary of the postulated NUREG/CR 6850 ZOI distances. For DP Tests 1 through 3, external TCs, TC2, TC3, TC11, TC12, and TC13, are approximately 15.2 cm (6 in) from the cabinet in open air and not in contact with the cabinet. The air temperatures are likely much lower than the actual metal temperature. Therefore, the temperatures are only a qualitative measure of thermal behavior. See Appendix A for more information on the slug calorimeters and calculations.

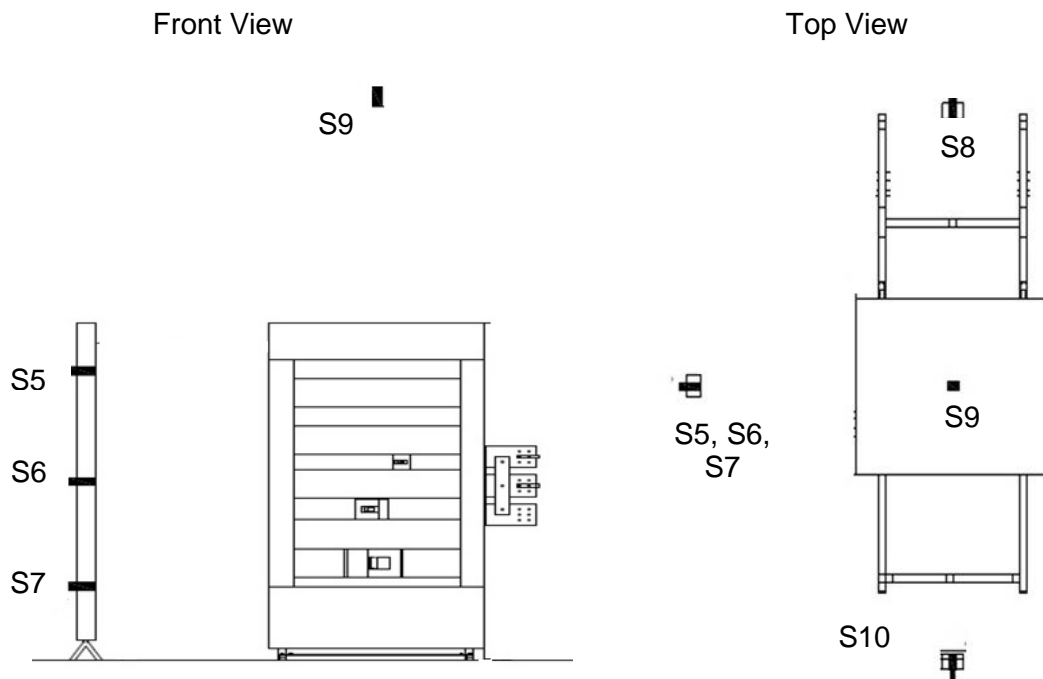


Figure 2.6-1. DP Tests 1 through 3 Calorimeter Locations

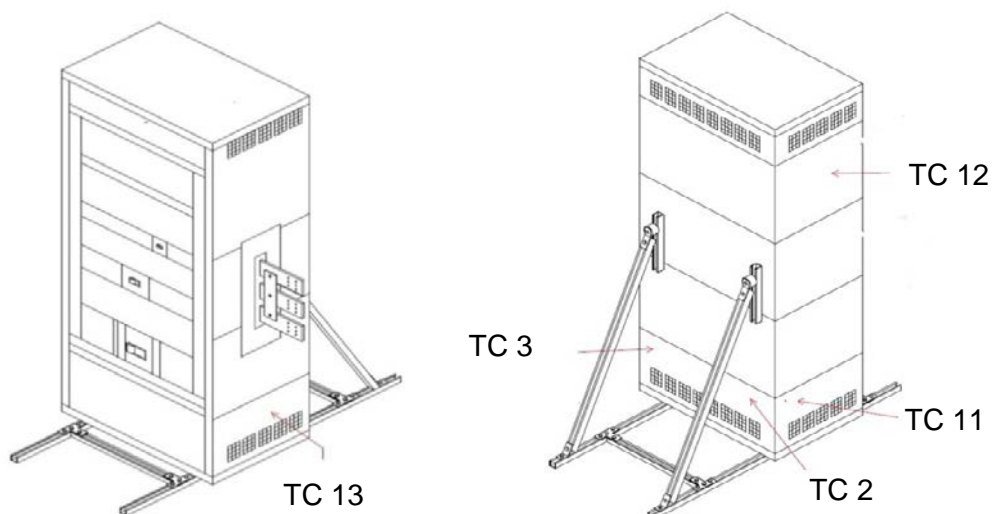


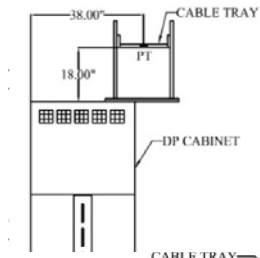
Figure 2.6-2. DP Tests 1 through 3 TC Locations

Table 2-2. DP Tests 1 through 3 Calorimeter and TC Locations.

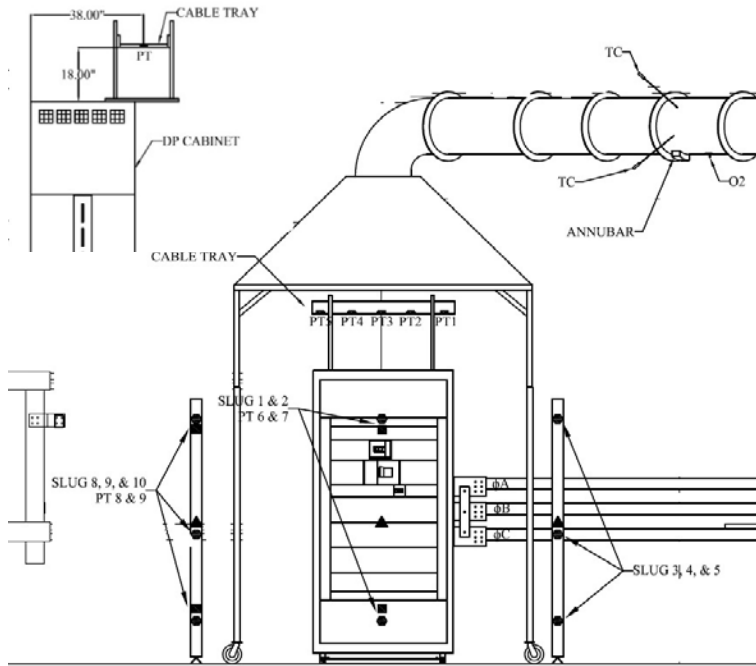
Slug or TC	From Floor cm (in)	Position	Slug or TC Name
TC2	61 (24)	Rear (R) Bottom	TC2-R-24-LS
TC3	61 (24)	Rear Bottom	TC3-R-24-RS
S5	198 (78)	Left Side (LS) Top	S5-LS-78-CL
S6	119 (47)	Left side Middle	S6-LS-47-CL
S7	89 (35)	Left side Bottom	S7-LS-35-CL
S8	78 (31)	Rear Bottom	S8-R-31-CL
S9	381 (150)	Top (T)	S9-T-150-CL
S10	78 (31)	Front (F) Bottom	S10-F-31-CL
TC11	61 (24)	Left Side Bottom	TC11-LS-24-R
TC12	196 (77)	Left Side top	TC12-LS-77-CL
TC13	61 (24)	Right Side (RS) Bottom	TC13-RS-24-CL

For DP Tests 4 through 6, slug calorimeters were located at 0.91 m (3 ft) and at the centerline (CL) of the cabinet except Slugs 3 through 5 on the right side, which were closer to the front (F) of the cabinet. The open air TCs were not used since useful data was not obtained in the previous tests. The tests also included a portable oxygen calorimeter and plate thermometers (PT) provided by NIST [7]. A cable tray with PTs was added as an ignition test target on the top of the DP as described in Section 2.5.2. These tests were conducted in KEMA Test Cell 7 rather than Test Cell 1 as in the previous DP tests to accommodate the hood. There was no slug calorimeter above the cabinet because of the hood. See Figure 2.6-3 for additional detail.

Cable Tray Detail



Front View



Top View

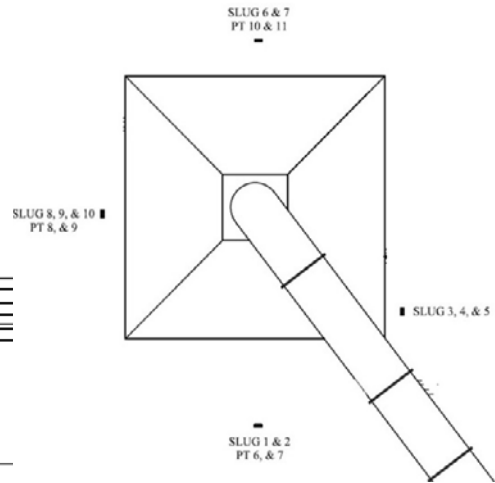


Figure 2.6-3. DP Tests 4 through 6 Calorimeter Hood and PT Locations

Table 2-3. DP Tests 4 through 6 Calorimeter Locations.

Slug	From Floor cm (in)	Position	Slug Name
S1	193 (76)	Front (F) Top	S1-F-76-CL
S2	41 (16)	Front Bottom	S2-F-16-CL
S3	193 (76)	Right Side (RS) Top	S3-RS-76-F
S4	122 (48)	Right Side Middle	S4-RS-48-F
S5	41 (16)	Right Side Bottom	S5-RS-16-F
S6	193 (76)	Rear (R) Top	S6-R-76-CL
S7	41 (16)	Rear Bottom	S7-R-16-CL
S8	193 (76)	Left Side (LS) Top	S8-LS-76-CL
S9	122 (48)	Left Side Middle	S9-LS-48-CL
S10	41 (16)	Left Side Bottom	S10-LS-16-CL

2.6.1 Cable Tray Combustible Loading

In DP Tests 4 through 6, a cable tray, loaded with cable was installed 46 cm (18 in) above the cabinet. In each test, the tray was loaded with 30 CV-2 cables, each 1.05 m (41.3 in) long and 16 CV-4 cables, each 1.14 m (44.9 in) long.

2.7 DP Test Pressure Instrumentation

Two Dynisco Pressure Transducer PT150-50 strain gauge type pressure transducers (PRT) strain-gauge were used on the right side of the DP, at the top and bottom, as shown below in Figure 2.7-1. The gauges are in PVC pipe to protect them from fire. The measurement analysis method is discussed in Appendix A.

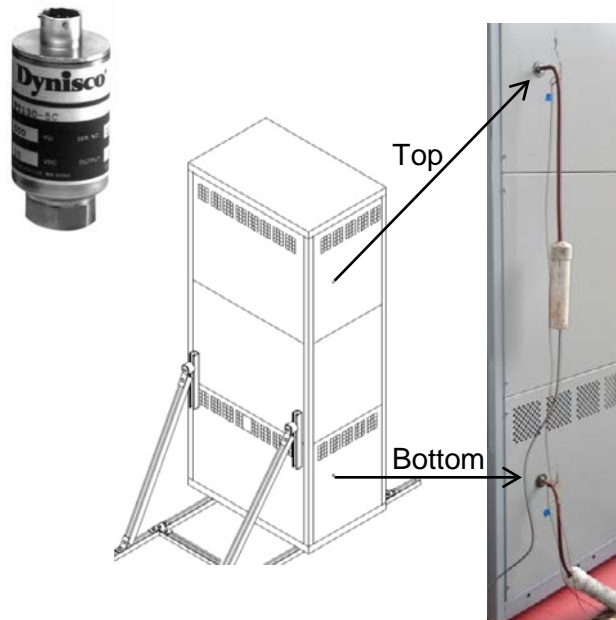


Figure 2.7-1. DP Tests 1 through 6 Pressure Transducer and Locations (Rear View)

2.8 DP Test 1 Key Observations (January 2013)

This cabinet test was initiated at 484 V and 43.3 kA, with a target duration of 2 seconds but the arc quenched at 1.6 seconds. It is theorized that the arc length from the bus bar to the cabinet increased as the arc connection points melted and vaporized and the voltage could not sustain the arc. The total energy was 29.6 MJ. Figure 2.8-1 shows the explosion after the arc at 0.012 seconds, 0.052 seconds, 1 second, and 2 seconds after the arc was initiated. Note the white-hot lower panel at 2 seconds in Figure 2.8-1(d). A cable fire flame was visible out of the top vents about 7 minutes after the arc with a maximum flame about 5 minutes after that (12 minutes from start of test) as seen in Figure 2.8-2 then the fire was visible for approximately another 12 minutes, for a total of 24 minutes. Post-test inspection showed the cable bundle was completely burned, demonstrating that the arc energy was enough to cause an ensuing cable fire. The fire self-extinguished.

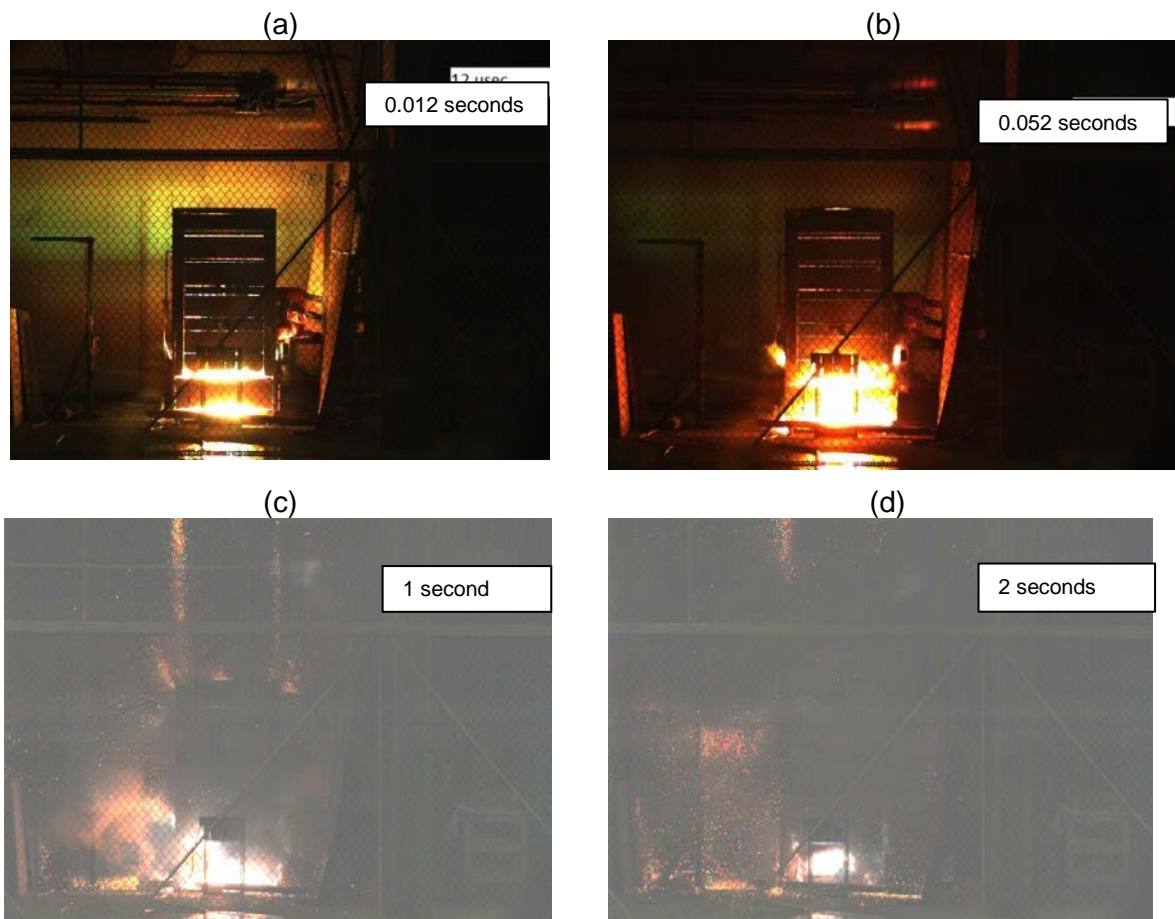


Figure 2.8-1. DP Test 1 Arc

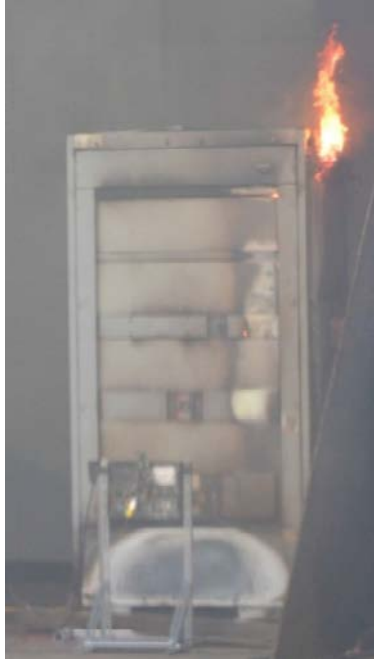


Figure 2.8-2. DP Test 1 Ensuing Fire, 12 Minutes After Arc

The front was heavily damaged by the arc and ensuing fire. The top, sides and rear was also damaged, as seen in Figure 2.8-3. The top bulged out several centimeters.

(a)



Figure 2.8-3. DP Test 1 Exterior Damage

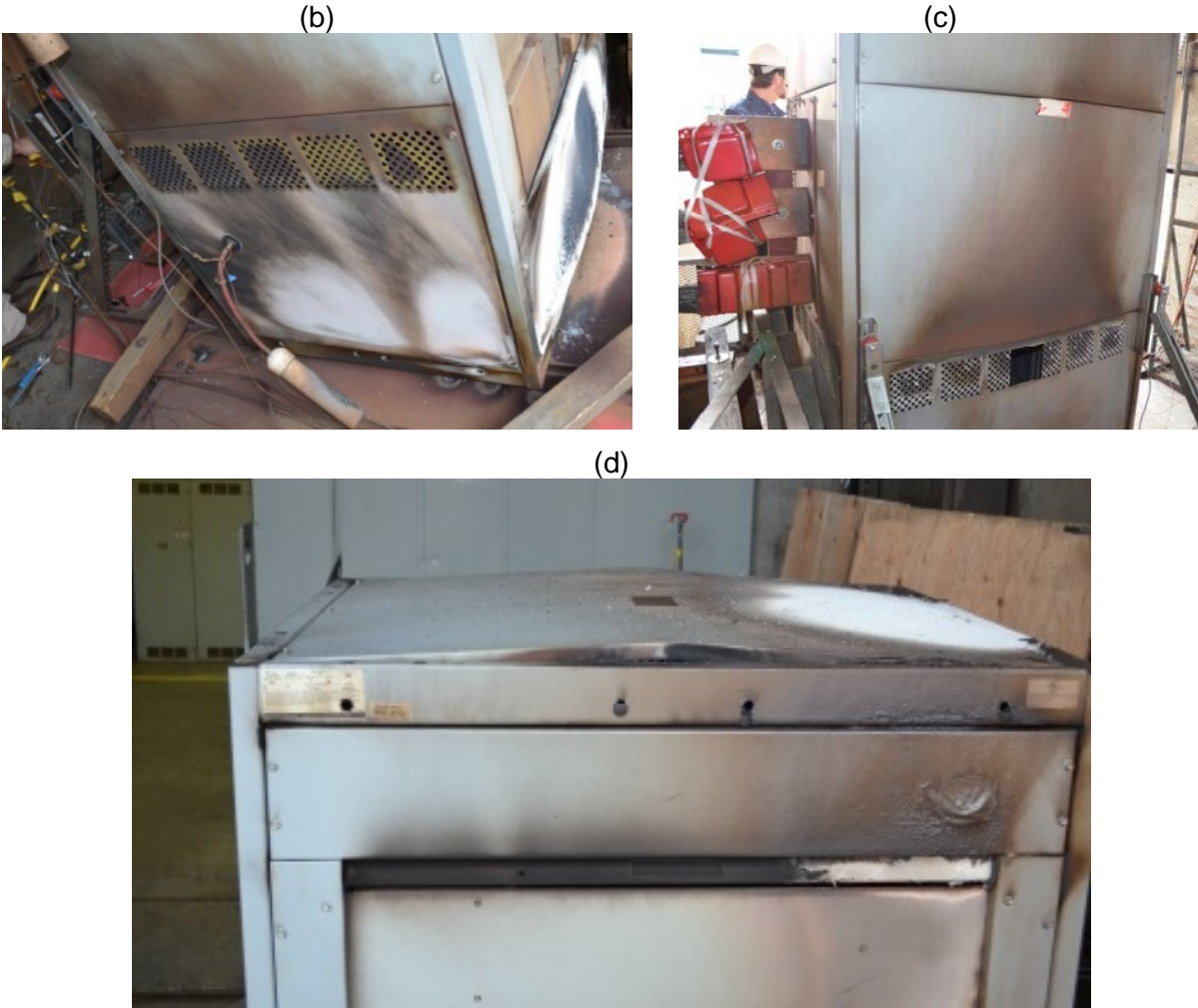


Figure 2.8-3. DP Test 1, Exterior Damage, Continued

The internal damage is shown in Figure 2.8-4. The arc moved downward to the bottom end of the vertical bus bars, melting several centimeters of the bus bars and burning through the horizontal support nearby. The cables were burned completely; the CV-2 cables burned like a typical thermoset (TS) with charring, flaking and no drips. Notice the burned insulation in the bottom of the cabinet, also indicating burning like a TS material.

(a)



(b)



(c)

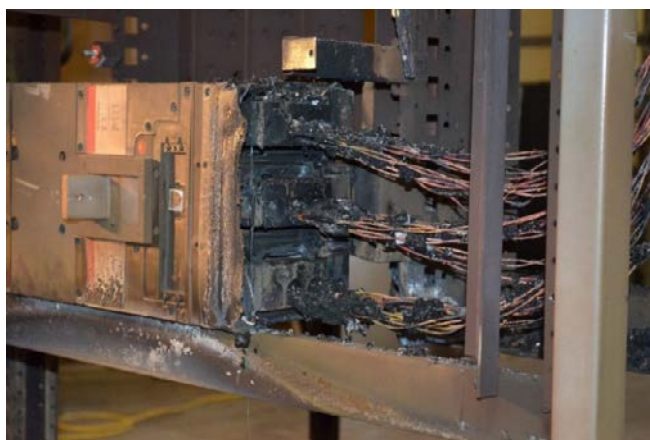


Figure 2.8-4. DP Test 1 HEAF and Fire Interior Damage

2.8.1 DP Test 1 Calorimetry Data

Temperatures measured at the slug locations are shown in Figure 2.8-5. Data collection stopped at 4 minutes so some of the data for the ensuing fire was not recorded. Slug 10 is directly in front of the white-hot bottom panel at the bottom of the DP and shows the highest response to the ensuing fire at 7 minutes. The internal cabinet fire had been burning since the arc occurred, based on the Slug 10 response. Slug 8 located at the rear had the strongest response to the initial arc. Slug 8 also showed some heating from heat escaping from the cabinet after the arc, probably from the ensuing fire. Slug 9 above the cabinet shows a small increase from the ensuing fire. The spikes during the arc indicate large variations in the slug temperature from noise and because the energy produced during the arc is not uniformly distributed external to the cabinet and varies during the arc. Venting conditions and cabinet integrity such as DP panel deformation and the associated plasma and flame leakage also affect the slug responses seen during the test series.

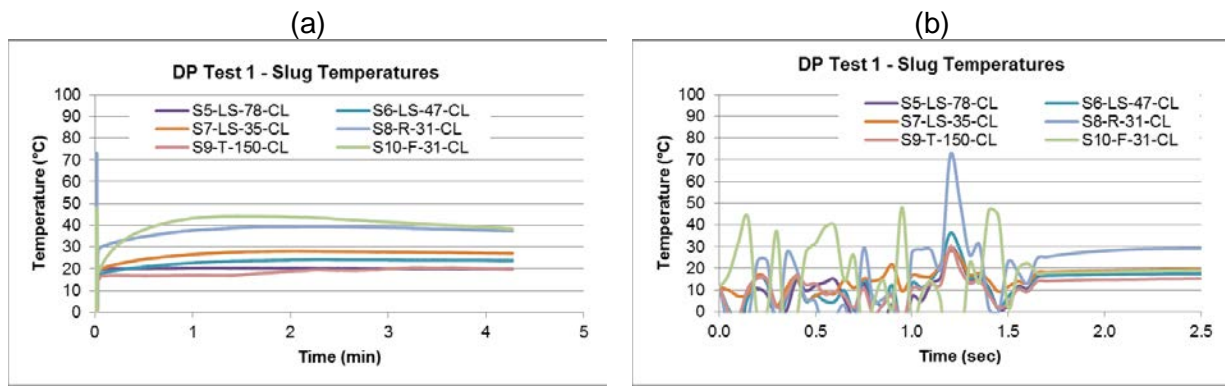


Figure 2.8-5. DP Test 1 Slug Calorimeter Data: Temperature

Table 2-4 shows the flux results based on the ASTM F1959 method in Appendix A using the change in temperature (ΔT) between the start and end of the arc. A maximum flux of 54 kW/m² is reported in the results 0.91 m (3 ft) from the rear, bottom of the cabinet (S8). As discussed in Section A.1, the maximum slug temperatures are also shown to indicate the maximum temperature a metal object could reach.

Table 2-4. DP Test 1 Flux Results.

Slug	ΔT (°C)	Flux (kW/m ²)	Max T (°C)
S5-LS-78-CL	4.5	17	29
S6-LS-47-CL	5.7	21	36
S7-LS-35-CL	6.7	25	28
S8-R-31-CL	14.5	54	72
S9-T-150-CL	2.8	10	30
S10-F-31-CL	6.2	23	48

2.8.2 DP Test 1 Temperature Data

The temperatures measured by the TCs are seen in Figure 2.8-6 below. The strongest response was at the bottom rear panel (TC2, TC3) because this panel directly views the arc through the vent openings. Table 2-5 shows the maximum temperature results. The thermocouple maximum temperature is a general indication of the air temperature 15.2 cm (6 in) from the cabinet and as expected TC2 and TC3 at the rear, lower panel near the arc had the highest temperatures. The thermocouples cannot be practically used to estimate flux.

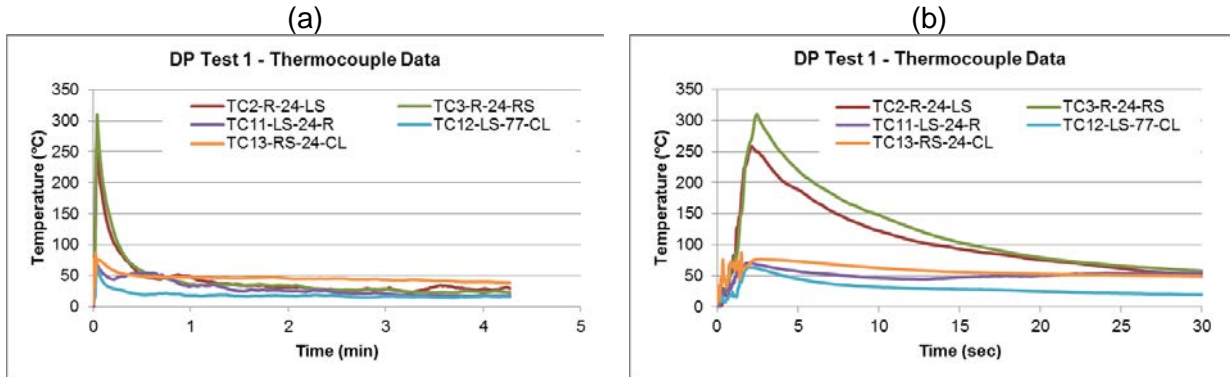


Figure 2.8-6. DP Test 1 Thermocouple Data

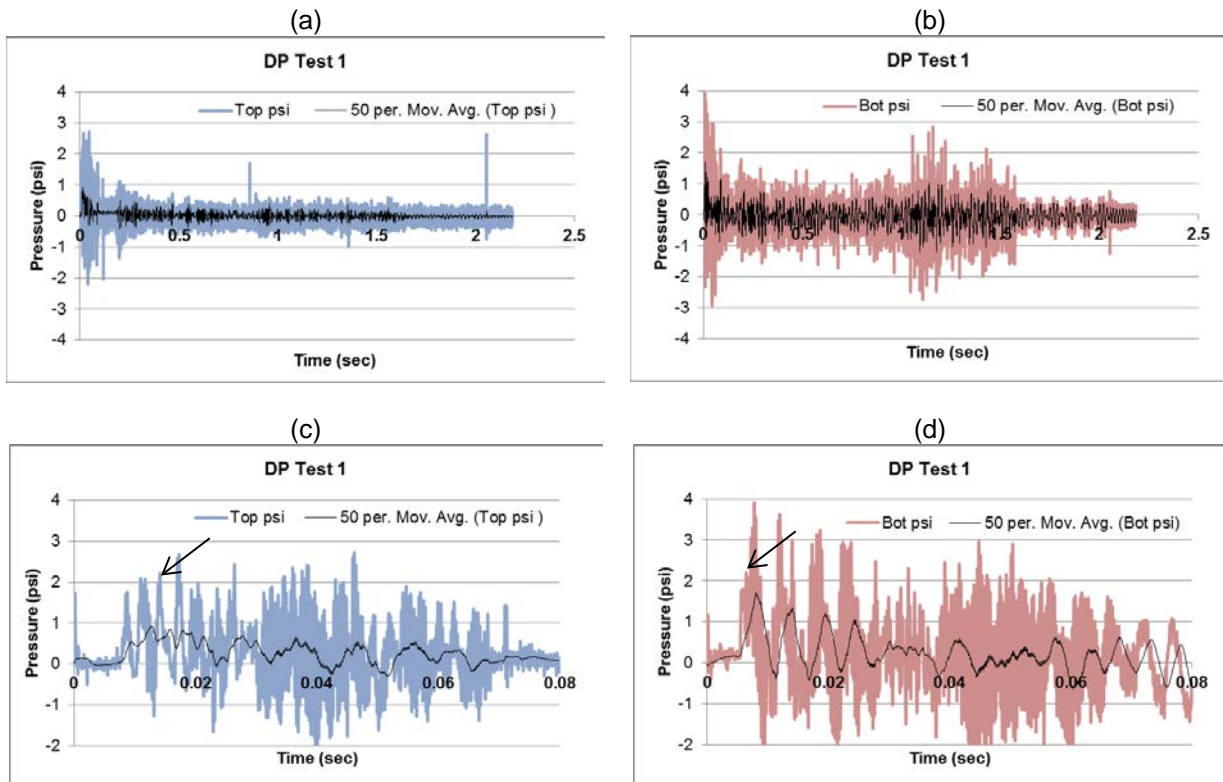
Table 2-5. DP Test 1 TC Results.

TC	Max T (°C)
TC2-R-24-LS	258
TC3-R-24-RS	310
TC11-LS-24-R	71
TC12-LS-77-CL	64
TC13-RS-24-CL	88

2.8.3 DP Test 1 Pressure Data

The pressures during the arc are depicted in Figure 2.8-7. Notice the higher level of noise in the measurements at the bottom location pressure near the arc. There are spikes near 2 seconds on the top pressure and at 2.1 seconds for the bottom pressure, both appear to be noise. The bottom pressure closer to the arc occurred earlier than the top pressure that was further from the arc. The maximum pressures are indicated by the arrows in Figure 2.8-7(c) and (d). The distinct sinusoidal responses on the bottom pressure transducer had a frequency of about 195 Hz and could have been resonant pressure waves in the cabinet, as seen in other DP tests.

The pressure analysis methods are in Appendix A and involved picking the maximum near the start of the arc then including a nominal uncertainty for the noise in the signal just before the arc.



Test 1 Pressure Transducer 1 Top
 14.5 ± 2.1 kPa (2.1 ± 0.3 psi)
 @ 0.0171 s

Test 1 Pressure Transducer 2 Bottom
 14.5 ± 2.8 kPa (2.1 ± 0.4 psi)
 @ 0.0079 s

Figure 2.8-7. DP Test 1 Pressure

2.8.4 DP Test 1 Arc Energy

The total energy was 28.6 MJ, seen in Figure 2.8-8. The energy analysis methods are in Appendix A. The “Energy” is calculated as volts multiplied current multiplied by the time step and each time step is shown. “Energy Total” is the cumulative sum of the energy in each time step. The smooth increase of the cumulative energy, labeled as Energy Total shows a steady increase, indicating a stable arc (a smooth increase) in total energy during the arc.

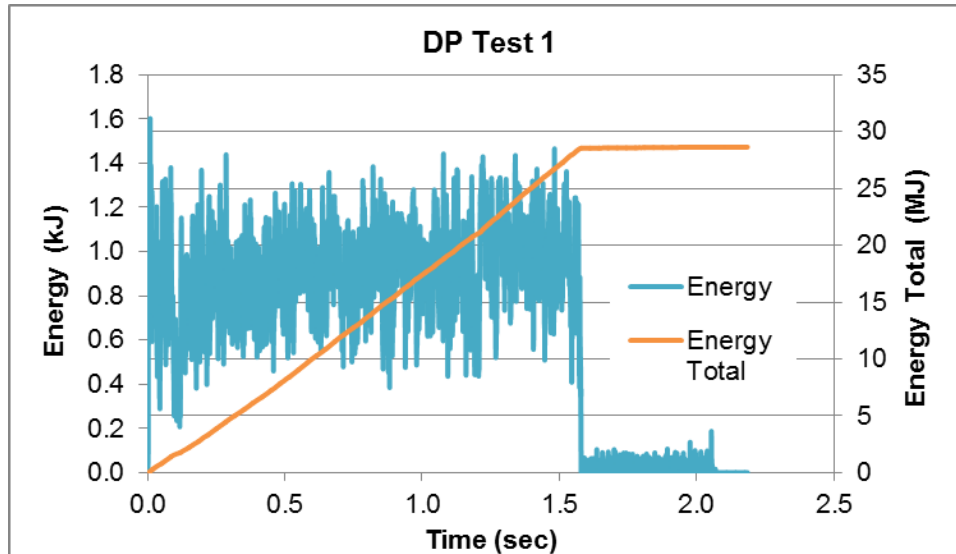


Figure 2.8-8. DP Test 1 Arc Energy

DP Test 1 resulted in an ensuing fire, which lasted about 24 minutes after the initial arc. The arc energy was sufficient to ignite the cables within the cabinet.

2.9 DP Test 2 Key Observations (January 2013)

This cabinet test was initiated at 484 V and 38.4 kA, with a target duration of 2 seconds but the arc quenched at 1.4 seconds probably because the arc length increased and the voltage could not sustain the arc. The total energy was 26.2 MJ. Figure 2.9-1 shows the explosion after the arc at 0.012 seconds, 0.052 seconds, 1 second, and 2 seconds after the arc. There was no ensuing cable fire but the cable damage showed this energy was almost enough to cause an ensuing fire.

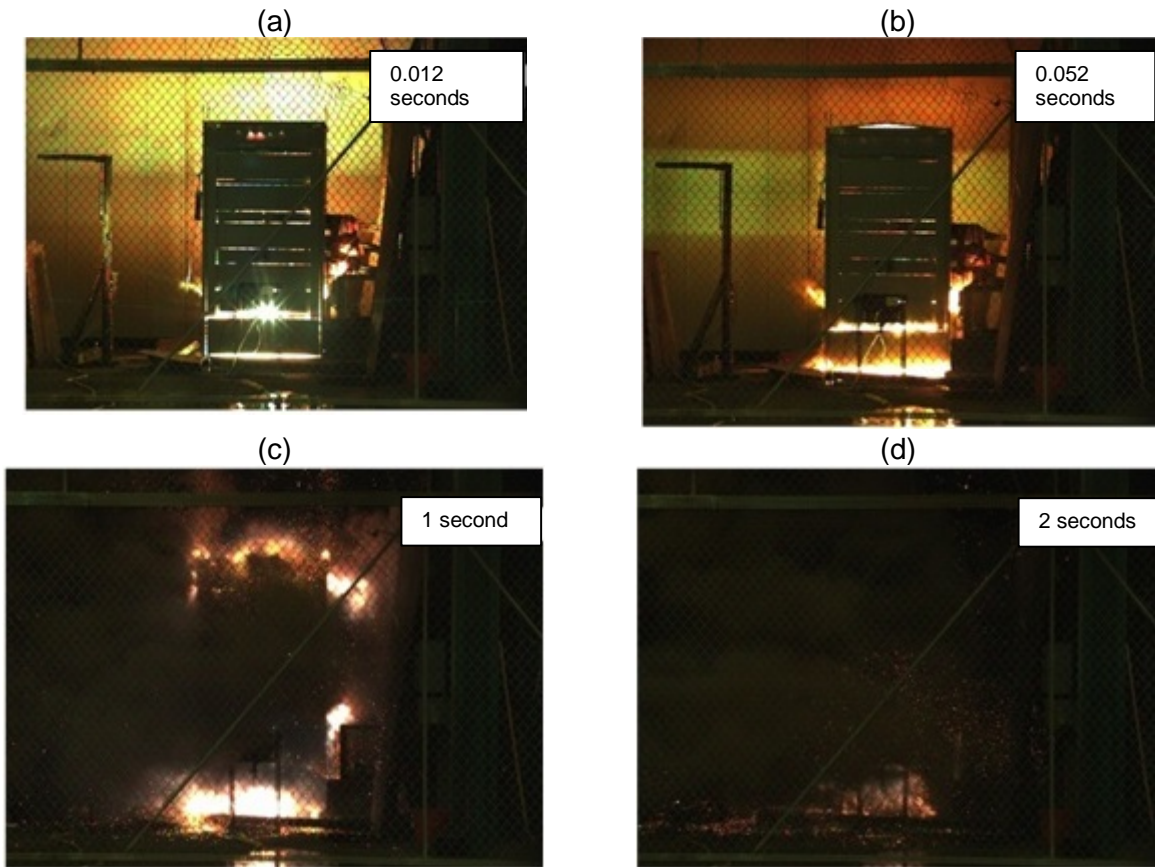


Figure 2.9-1. DP Test 2 Arc

The cabinet front was heavily damaged by the arc. The sides and rear were damaged, as seen in Figure 2.9-2. The cabinet top had a deformation that occurred at about 0.022 seconds after the arc based on high speed images as shown in Figure 2.9-3.

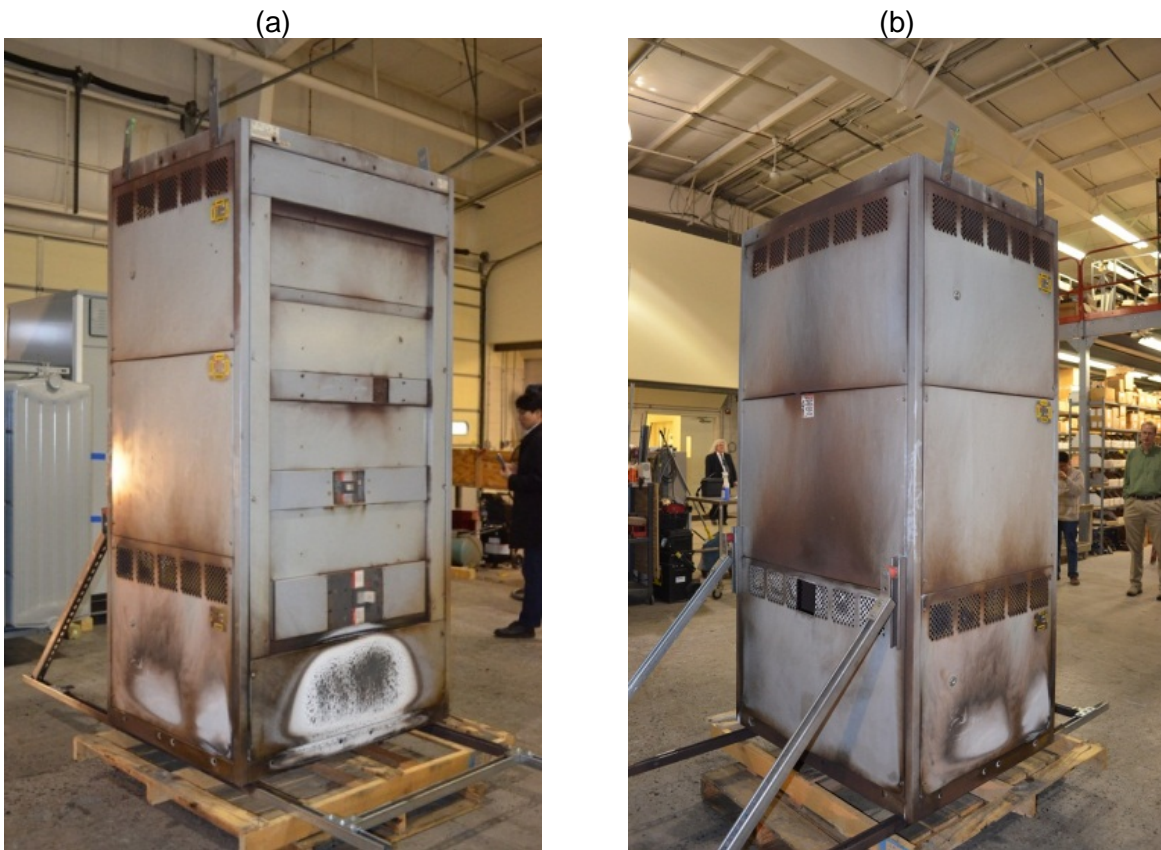


Figure 2.9-2. DP Test 2 HEAF Exterior Damage



Figure 2.9-3. DP Test 2 Cabinet Top Deformation

The interior damage seen in Figure 2.9-4 shows that the arc moved downward to the bottom end of the vertical bus bars, where several centimeters of bus bar were melted. The cables did not ignite but showed damage indicating that they were pyrolyzing. Notice the inside of the cabinet is coated with copper from the damaged bus bars.

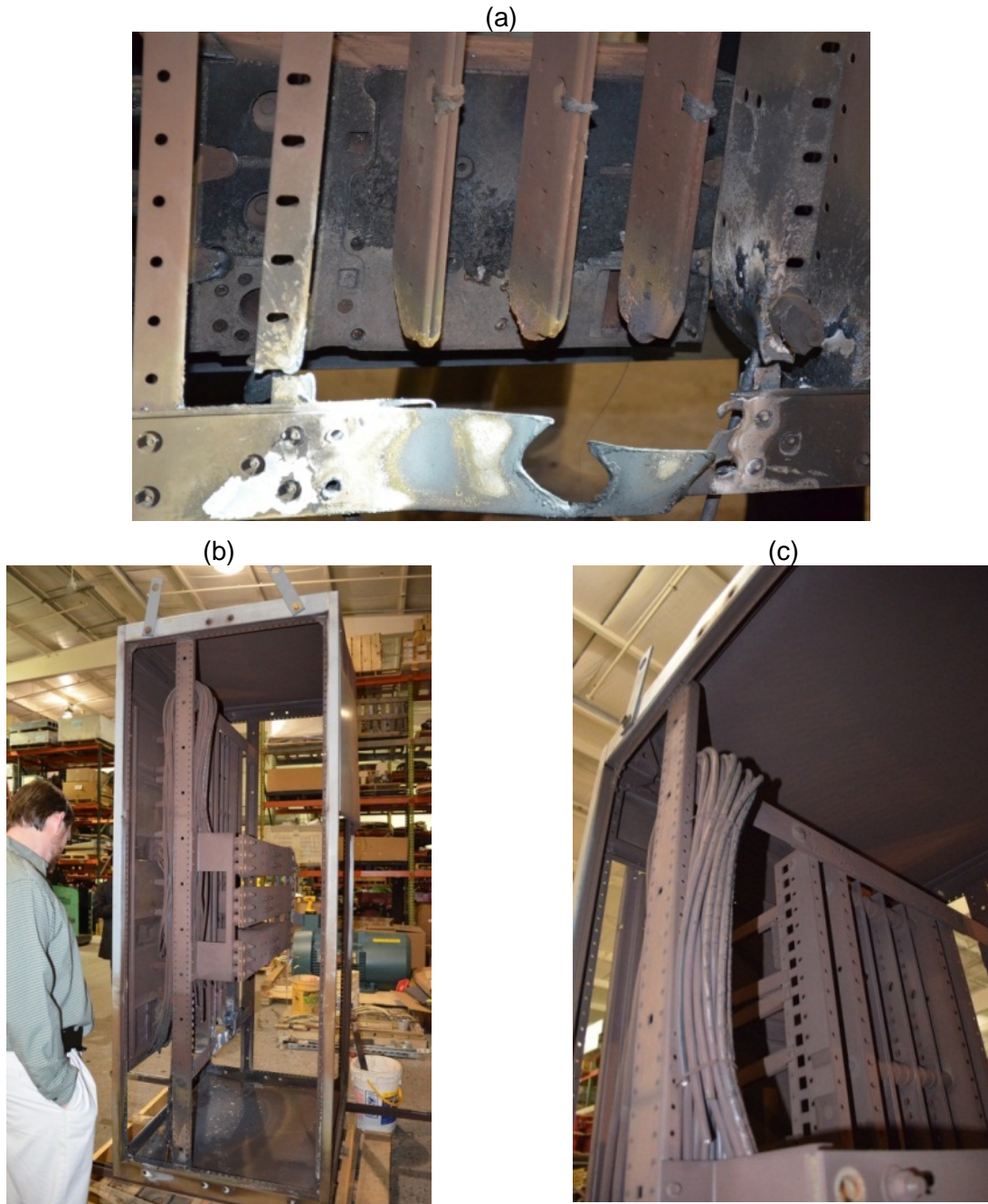


Figure 2.9-4. DP Test 2 Interior Cabinet Damage

2.9.1 DP Test 2 Calorimetry Data

Temperatures measured at the slug locations are shown Figure 2.9-5. Temperatures at the rear (S8) were higher than in the front (S10), indicating more heat escaped out the rear of the cabinet in this test. As expected, there are no heat increases in the later part of the test because there was no ensuing fire. The heating in the first few minutes after the arc was from heat escaping from the cabinet.

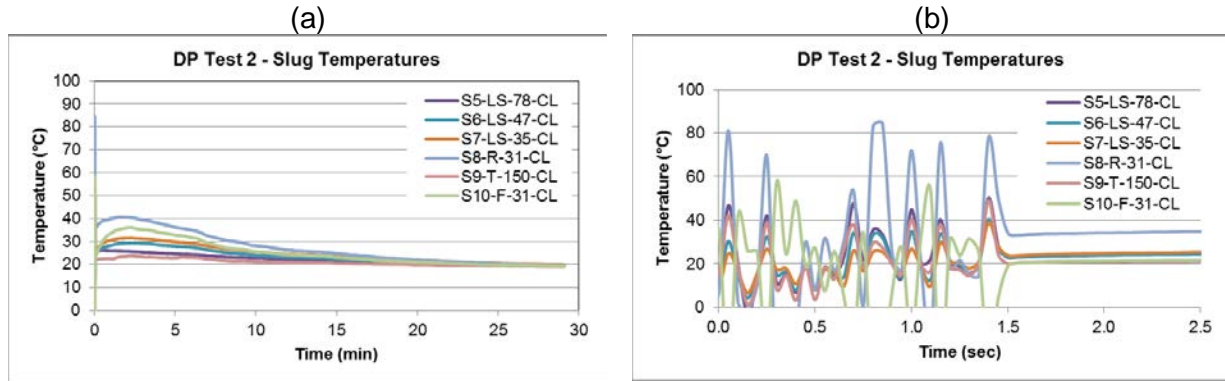


Figure 2.9-5. DP Test 2 Calorimetry Temperature Data: Temperature

Table 2-6 shows the flux results based on the ASTM F1959 method in Appendix A using the change in temperature (ΔT) between the start and end of the arc. The maximum flux of 63 kW/m² is reported at the rear of the cabinet (S8). The maximum slug temperatures are also shown to indicate the maximum temperature a metal object could reach.

Table 2-6. DP Test 2 Flux Results.

Slug	ΔT (°C)	Flux (kW/m ²)	Max T (°C)
S5-LS-78-CL	5.9	23	50
S6-LS-47-CL	5.8	22	40
S7-LS-35-CL	6.3	24	39
S8-R-31-CL	16.5	63	84
S9-T-150-CL	3.1	12	49
S10-F-31-CL	3.4	13	57

2.9.2 DP Test 2 Temperature Data

The temperatures measured by the TCs are in the Figure 2.9-6. The highest response was at the rear bottom TCs (TC2, TC3), similar to all DP tests. Table 2-7 shows the maximum temperature results. The thermocouple maximum temperature is a general indication of the air temperature 15.24 cm (6 in) from the cabinet, and as expected TC2 and TC3 at the rear, lower panel near the arc had the highest temperatures. The thermocouples cannot be practically used to estimate flux.

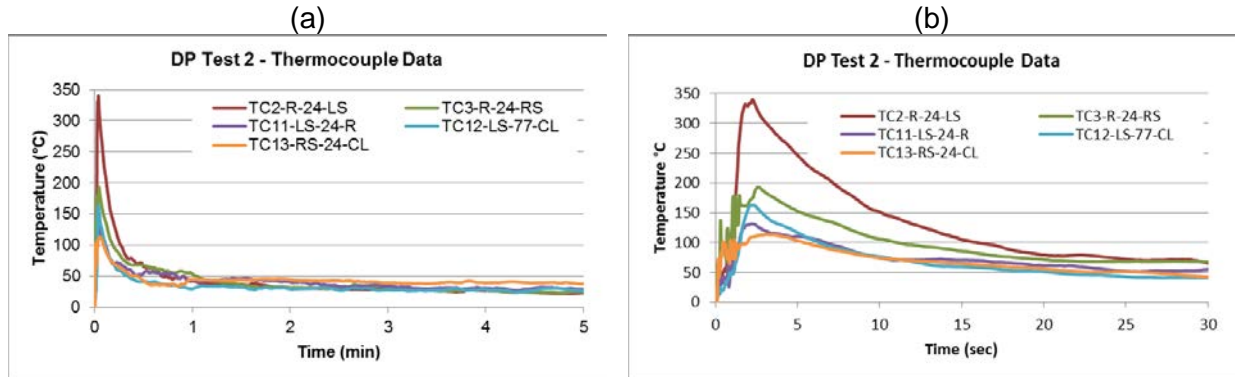


Figure 2.9-6. DP Test 2 Thermocouple Data

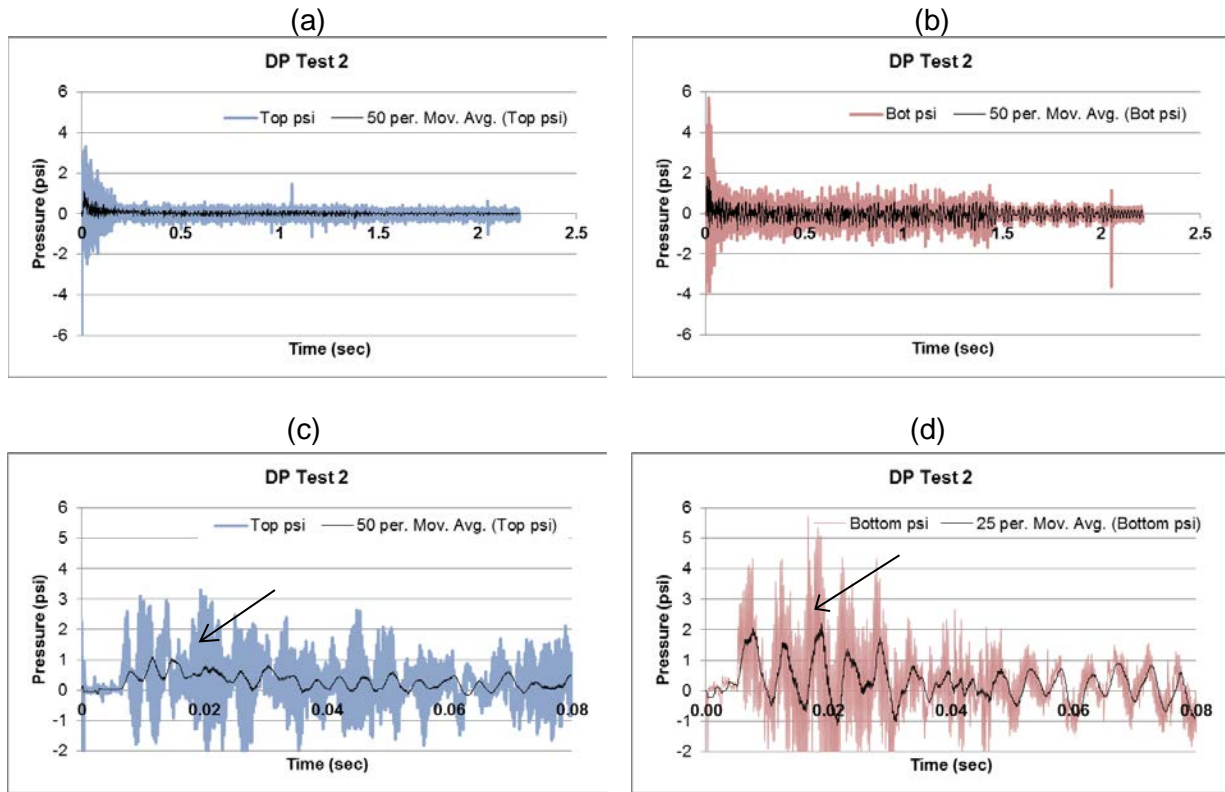
Table 2-7. DP Test 2 TC Results.

TC	Max T (°C)
TC2-R-24-LS	340
TC3-R-24-RS	193
TC11-LS-24-R	132
TC12-LS-77-CL	163
TC13-RS-24-CL	114

2.9.3 DP Test 2 Pressure Data

The pressures during the arc are seen in Figure 2.9-7. Notice the result for the bottom pressure, near the arc has much more noise. There is a spike near 1.2 seconds on the top pressure and at 2.1 seconds for the bottom pressure, which both appear to be noise. The bottom pressure closer to the arc had a higher maximum and occurred earlier than the top pressure that was further from the arc. The maximum pressures are indicated by the arrows in Figure 2.9-7 (c) and (d). The distinct sinusoidal responses on both pressure transducers had a frequency of about 195 Hz and could have been resonant pressure waves in the cabinet.

The pressure analysis methods are in Appendix A and involved picking the maximum near the start of the arc (using the middle charts below) then including a nominal uncertainty for the noise in the signal just before the arc.



Test 2 Pressure Transducer 1 Top
 11.7 ± 2.1 kPa (1.7 ± 0.3 psi)
 @ 0.0194 s

Test 2 Pressure Transducer 2 Bottom
 18.6 ± 2.1 kPa (2.7 ± 0.3 psi)
 @ 0.0183 s

Figure 2.9-7. DP Test 2 Pressure

2.9.4 DP Test 2 Arc Energy

The total energy was 26.2 MJ, seen in Figure 2.9-8. The energy analysis methods are in Appendix A. The “Energy” is calculated as volts multiplied current multiplied by the time step and each time step is shown. “Energy Total” is the cumulative sum of the energy in each time step. The result shows a smooth increase in the total energy, indicated by the total energy showing that the energy provided by the KEMA power system was steady.

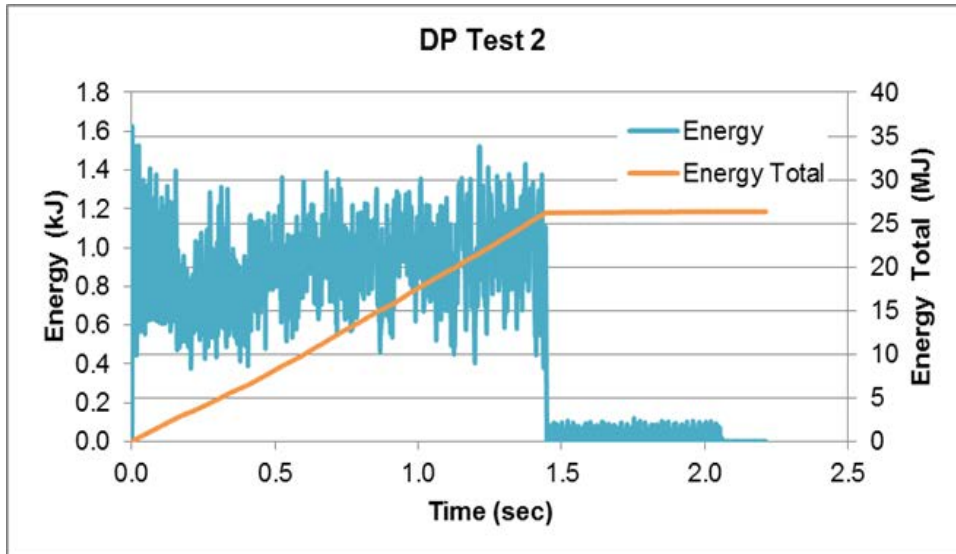


Figure 2.9-8. DP Test 2 Arc Energy

2.10 DP Test 3 Key Observations (January 2013)

This cabinet test was initiated at 484 V and 41.4 kA, with a target duration of 2 seconds that was achieved with a total energy of 37.1 MJ. Figure 2.10-1 shows the explosion after the arc initiated at 0.012 seconds, 0.052 seconds, 1 second, and 2 seconds. One panel popped open based on the high speed images. A small fire was visible immediately after the arc but it self-extinguished in a few seconds (Figure 2.10-21(d)). An ensuing cable fire 50 seconds after the arc was visible at the bottom of the cabinet and half-way up the cabinets as shown in Figure 2.10-1(a). The fire reached the top of the cabinet in about 4 minutes (Figure 2.10-2(b)) then the fire self-extinguished after 14 minutes. The energy from the 2 second arc was enough energy to start a fire.

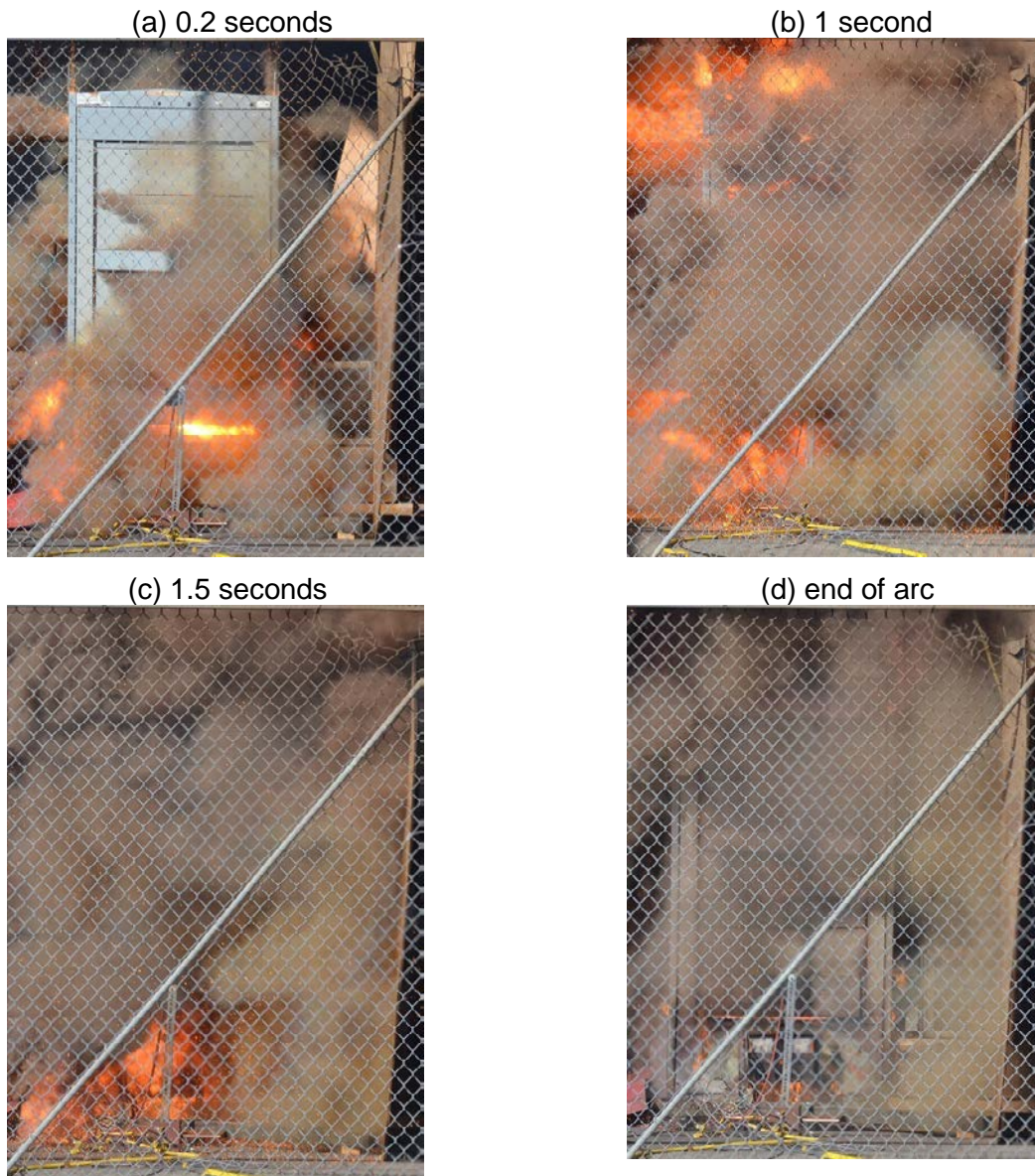


Figure 2.10-1. DP Test 3 Arc

(a) 50 seconds after arc



(b) 4 minutes after arc



Figure 2.10-2. DP Test 3 Ensuing Fire

The front was heavily damaged by the arc and ensuing fire, as seen in Figure 2.10-3 through Figure 2.10-5. The sides and rear was also damaged. One panel opened from the high pressure at 0.024 seconds and roof deformation occurred at the same time, as seen in Figure 2.10-3(c). The roof deformation was smaller than Tests 1 and 2, probably because the pressure was relieved by the panel coming off during the test. The pressures seen in Test 3 were between those in Tests 1 and 2.



Figure 2.10-3. DP Test 3 Exterior Cabinet Damage

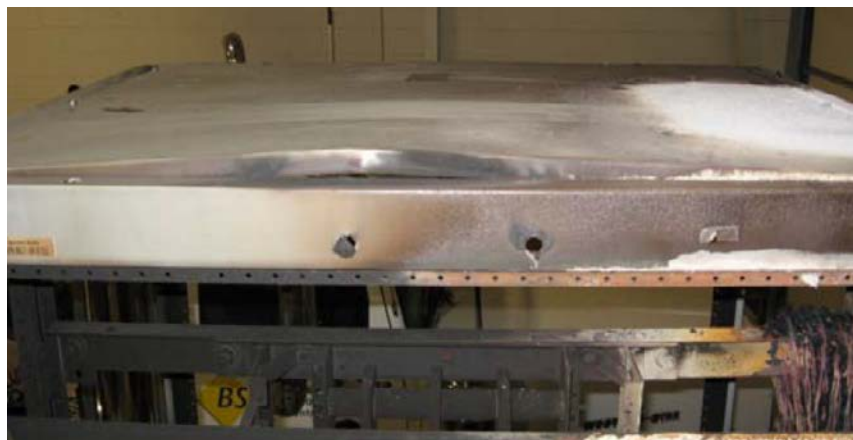


Figure 2.10-4. DP Test 3 Cabinet Top Deformation

The arc moved downward to the bottom end of the vertical bus bars and where several centimeters of bus bar were melted, similar to Tests 1 and 2. More of the bus bars burned in Test 3 because of the higher energy and longer arc duration. The cables were burned completely, as in Test 1, and can be seen on the right side of the cabinet.

(a)



(b)



Figure 2.10-5. DP Test 3 Interior Damage

2.10.1 DP Test 3 Calorimetry Data

Temperatures measured at the slug locations are shown in Figure 2.10-6. Slug 8 showed the highest reading of all DP tests. Slug 8 responded strongly to the initial arc and the fire afterwards, and Slug 10 also had high response. There is an increase in temperatures due to the ensuing fire (between 2 and 8 minutes), and S10, located near the bottom of the cabinet, responded before S9, located near the top of the cabinet as expected since the cable fire started near the arc at the bottom.

NOTE: In this test, S8 was 0.31 m (1 ft) from the cabinet and S10 was 0.16 m (0.5 ft) from the cabinet, whereas in other tests, they were 0.91 m (3 ft) from the cabinet. This is indicated by the “*” in the series titles on the charts in Figure 2.10-6. The positions were changed to test the calorimeter sensitivity. The close distance for S8 contributed to its very high response.

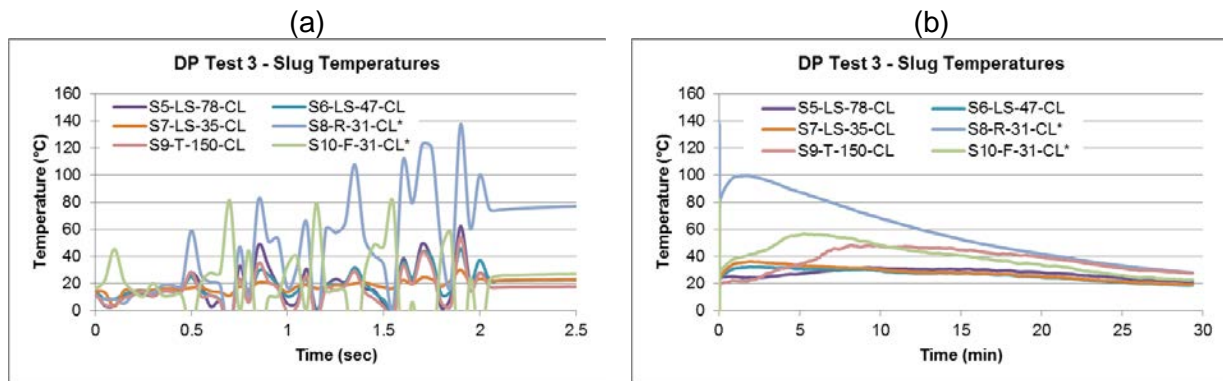


Figure 2.10-6. DP Test 3 Calorimetry Data: Temperature

Table 2-8 shows the flux results based on the ASTM F1959 method in Appendix A using the change in temperature (ΔT) between the start and end of the arc. The maximum flux of 187 kW/m² was at the rear (S8) and the maximum at a 0.91m (3 ft) on the left side (S5) was 27 kW/m². The maximum slug temperatures are also shown to indicate the maximum temperature a metal object could reach during or after the arc.

Table 2-8. DP Test 3 Flux Results.

Slug	ΔT (°C)	Flux (kW/m ²)	Max T (°C)
S5-LS-78-CL	9.2	27	62
S6-LS-47-CL	8.1	24	46
S7-LS-35-CL	7.6	22	36
S8-R-31-CL*	63.6	187*	137
S9-T-150-CL	4.5	13	54
S10-F-31-CL*	9.8	29	81

* S8 is 0.32 m (1 ft) from cabinet and S10 is 0.16 m (0.5 ft) from the cabinet.

2.10.2 DP Test 3 Temperature Data

The temperatures measured by the TCs are seen in the Figure 2.10-7. As seen in previous tests, the highest temperatures were at the rear (TC2, TC3). However, it is not clear why TC2 and TC3 are 100 to 140°C lower than in previous tests. At about 1.7 minutes, it appears that TC12 at the top of the cabinet is detecting the ensuing fire. All TCs show an unsteady response, indicating the turbulent nature of the ensuing fire. The thermocouples cannot practically be used to estimate flux.

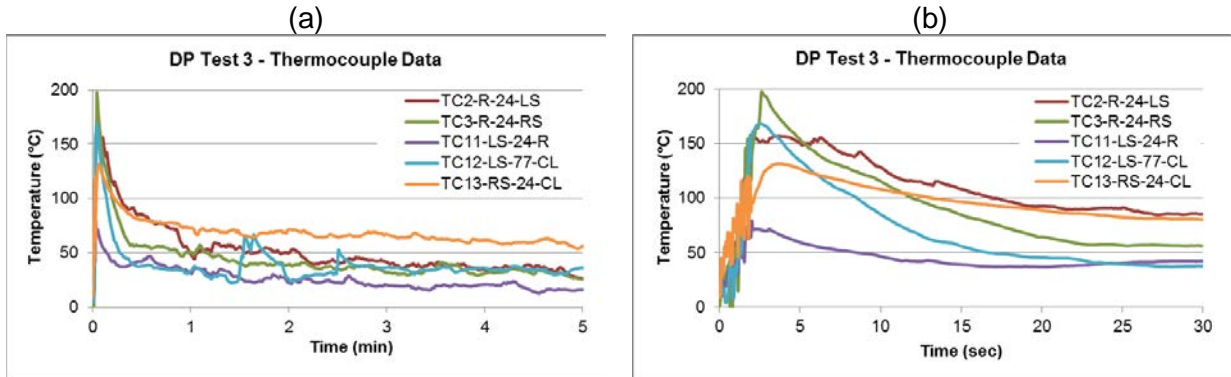


Figure 2.10-7. DP Test 3 Thermocouple Data

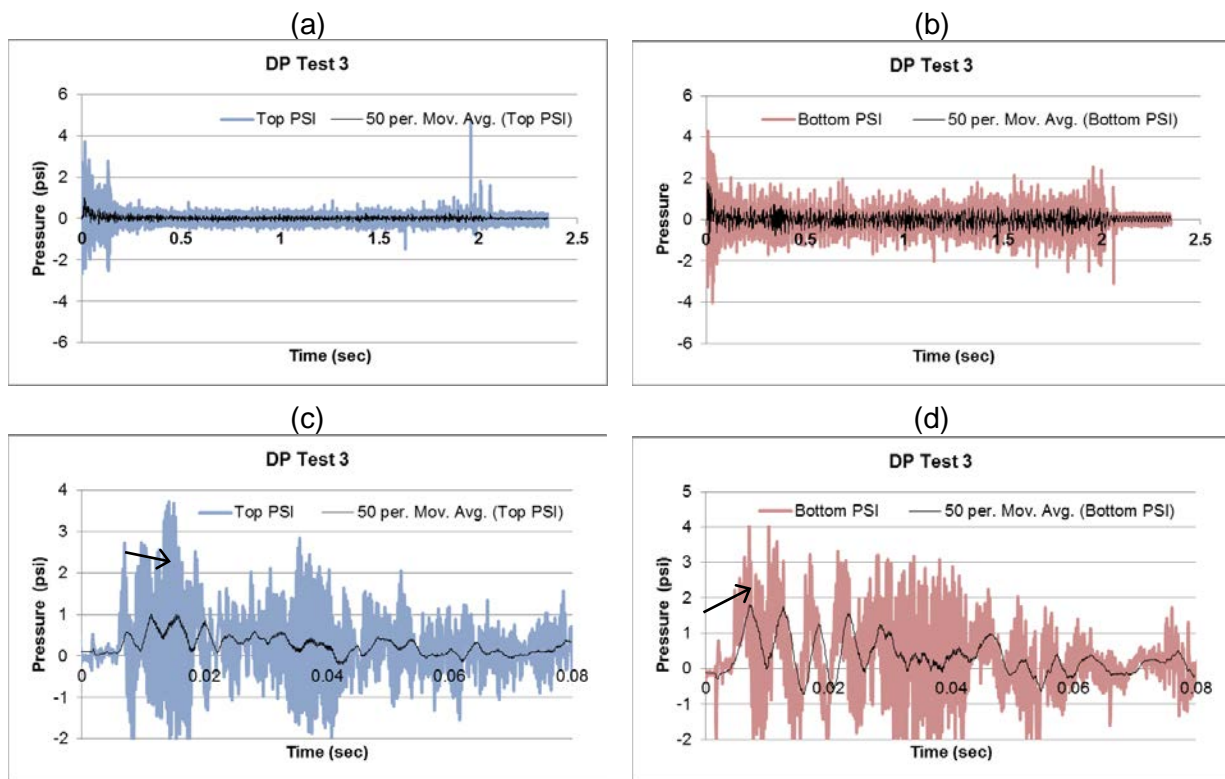
Table 2-9. DP Test 3 TC Results.

TC	Max T (°C)
TC2-R-24-LS	158
TC3-R-24-RS	198
TC11-LS-24-R	79
TC12-LS-77-CL	169
TC13-RS-24-CL	132

2.10.3 DP Test 3 Pressure Data

Figure 2.10-7 depicts the pressure measurement during the arc. Notice the result for the bottom pressure, measured near the arc, has much more noise. There are spikes near 0.13 and 2.0 seconds at the top and several more around 2 seconds for the bottom pressure location. These appear to be noise. The bottom pressure closer to the arc had a slightly higher maximum and occurred earlier than the top that was further from the arc. The maximum pressures are indicated by the arrows in Figure 2.10-8(c) and (d). The distinct sinusoidal responses on the bottom at the arc initiation had a frequency of about 195 Hz, similar to Test 2, and was probably caused by resonant pressure waves in the cabinet.

The pressure analysis methods are in Appendix A and involved picking the maximum near the start of the arc then including a nominal uncertainty for the noise in the signal just before the arc.



Test 3 Pressure 1 Top
 13.8 ± 2.1 kPa (2.0 ± 0.3 psi)
 @ 0.0142 s

Test 3 Pressure 2 Bottom
 13.8 ± 2.1 kPa (2.0 ± 0.3 psi)
 @ 0.0072 s

Figure 2.10-8. DP Test 3 Pressure

2.10.4 DP Test 3 Arc Energy

The total energy was 37.1 MJ, as shown in Figure 2.10-9. The energy analysis methods are in Appendix A. The “Energy” is calculated as volts multiplied current multiplied by the time step and each time step is shown. “Energy Total” is the cumulative sum of the energy in each time step. The result shows a smooth increase in the total energy, indicating that the energy provided by the KEMA power system was steady.

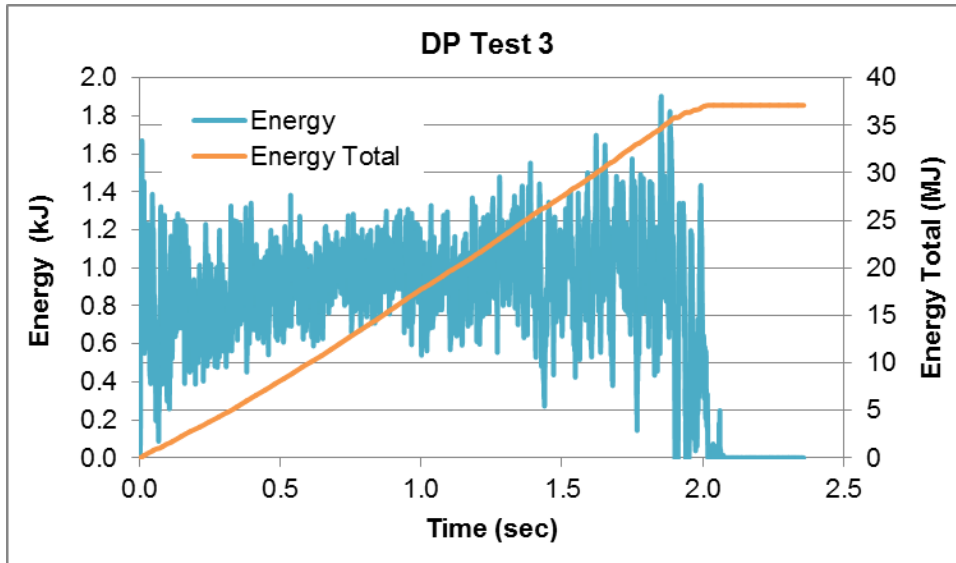


Figure 2.10-9. DP Test 3 Arc Energy

2.11 DP Test 4 Key Observations (March 2015)

This cabinet test was initiated at 484 V and 50.3 kA, with a target duration of 2 seconds. The arc quenched at 0.698 seconds due to a ground failure. The total energy was 8.3 MJ. Figures 2.11-1 through 2.11-3 show the arc with High Speed (HS) camera, and High Definition (HD) camera, and Forward Looking Infrared (FLIR) camera. Note the arc flames extend to the postulated ZOI of 0.91m (3 ft) at 0.350 sec. There was no ensuing fire.

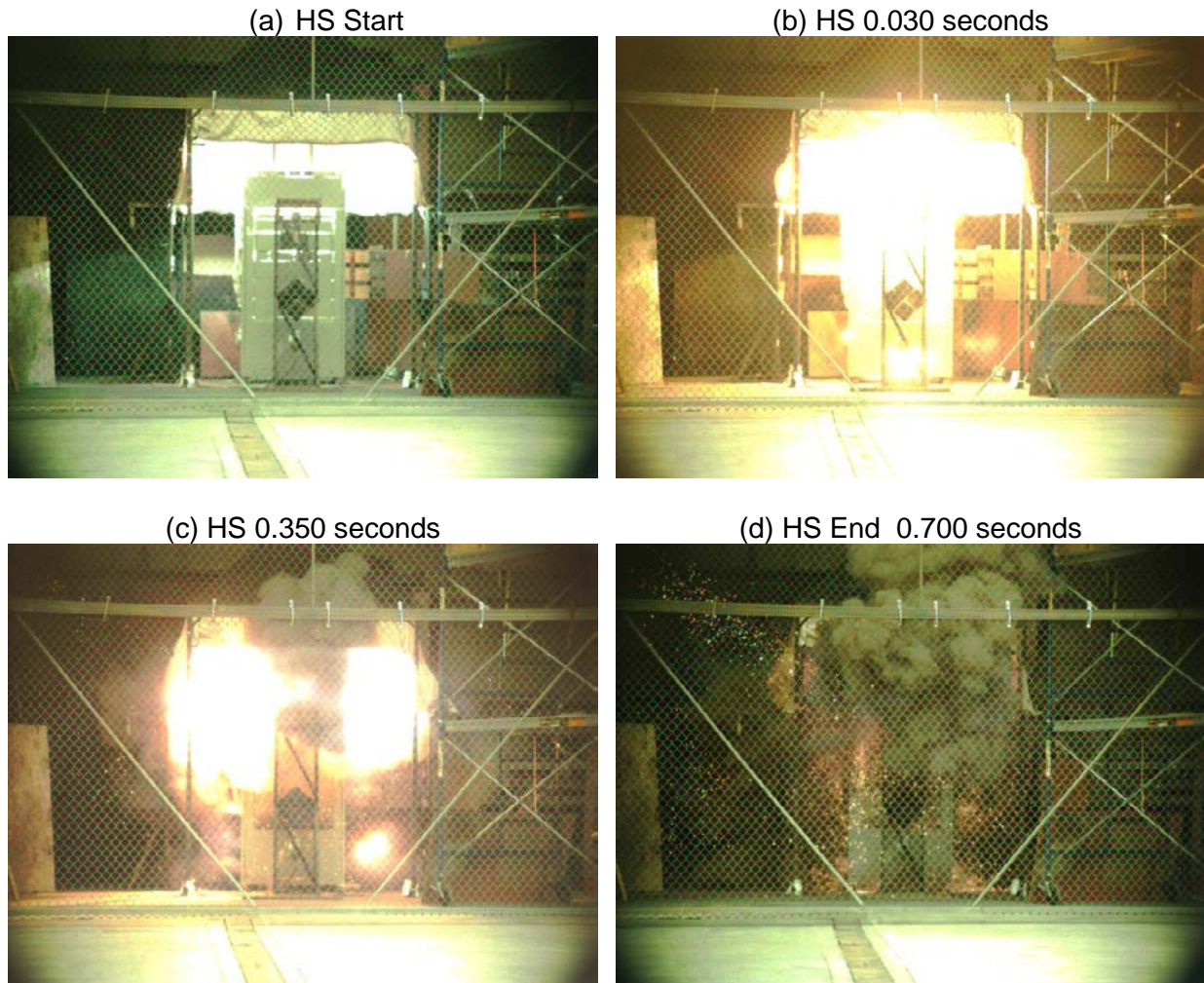


Figure 2.11-1. DP Test 4 Arc

Flames escaped the vents at the top and reached 0.91 m (3 ft), as shown in Figure 2.11-2.



Figure 2.11-2. DP Test 4 Arc Flames

The FLIR camera indicated a maximum temperature of 350 °C at the top front “hot spot” that cooled 100 °C in 2 minutes, see Figure 2.11-3. The flux from this hot spot was detected by the slug calorimeter at the top front of the cabinet as discussed later. This hot spot on the panel near the arc was similar to previous DP tests in 2013. There was no ensuing fire.

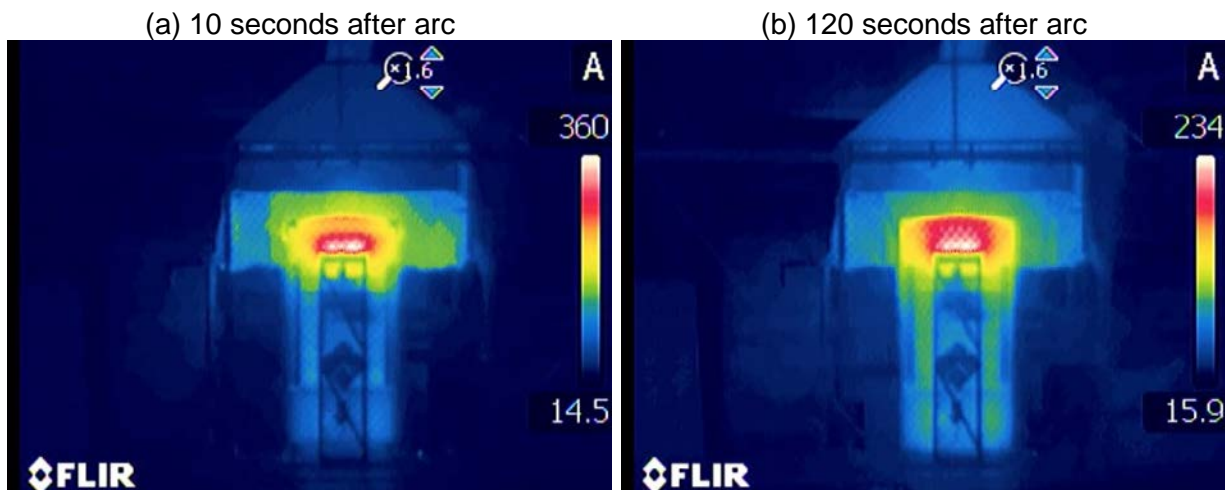


Figure 2.11-3. DP Test 4 Thermal Images

The damage is shown in Figure 2.11-4 through Figure 2.11-8. Figure 2.11-4 shows the exterior charring and discoloration on the top panel near the arc. There was minor deformation of the front and rear panels. The external cable tray showed no damage. The arc was shorter than planned because there was an external ground fault from a poor connection as shown in Figure 2.11-7. Figure 2.11-6 shows the interior damage with charring and copper plated on the surfaces but no major fire. Figure 2.11-8 shows the interior bus bar damage.



Figure 2.11-4. DP Test 4 Exterior Cabinet Damage



Figure 2.11-5. DP Test 4 External Cable Tray Damage



Figure 2.11-6. DP Test 4 Interior Cable Damage

(a) Before Failure



(b) At failure



Figure 2.11-7. DP Test 4 Ground Fault during the Arc

(a) From Front



(b) From Rear

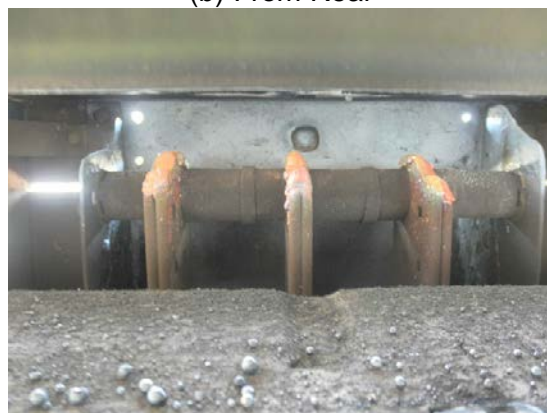


Figure 2.11-8. DP Test 4 Bus Bar Damage at Arc Location

2.11.1 DP Test 4 Calorimetry Data

Temperatures measured at the slug locations are shown in Figure 2.11-9. Slugs 3 to 5 had high noise during the arc probably due to electro-magnetic interference (EMI); the power supply was directly next to the slug calorimeters. The highest temperatures at the end of the arc were seen at the bottom of the cabinet (S7 and S8). These both showed cooling after the arc because there was no ensuing fire. After the arc the S1 calorimeter was the only calorimeter with increasing temperature caused by the hot spot on the front panel near the arc.

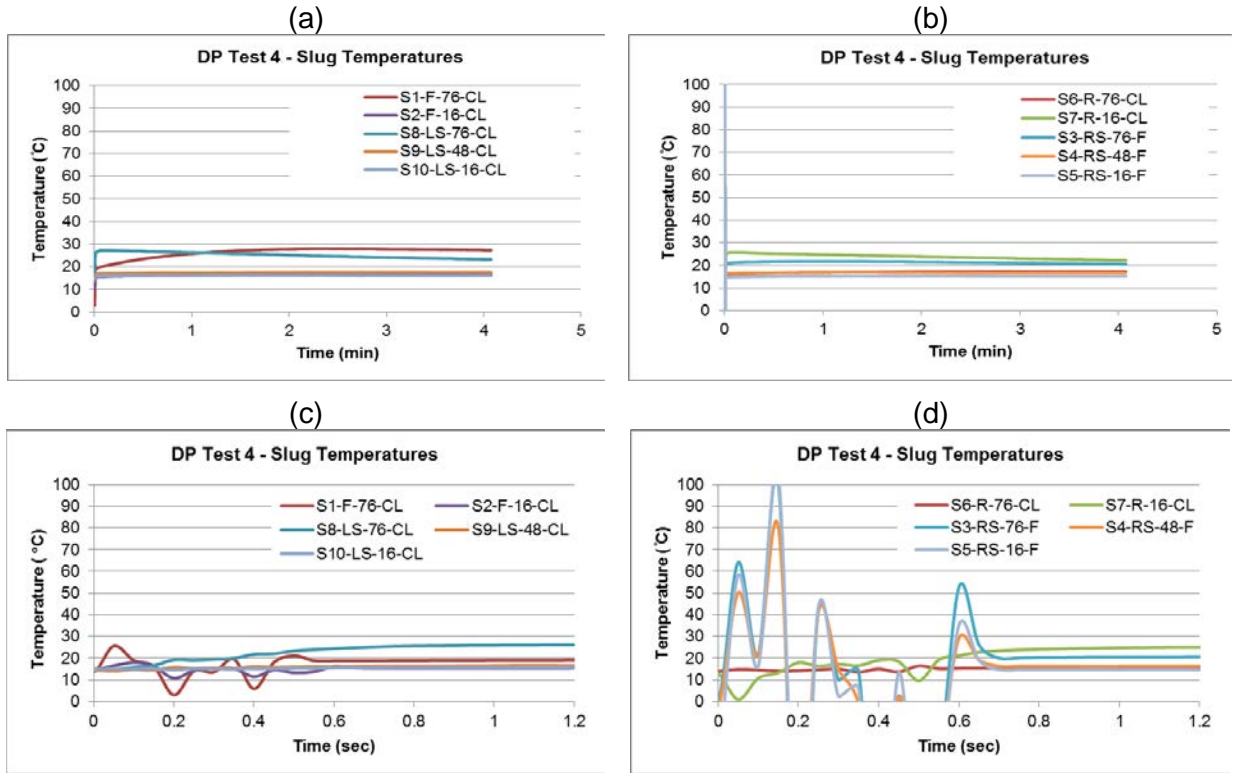


Figure 2.11-9. DP Test 4 Calorimetry Data: Temperature

Table 2-10 shows the flux results based on the ASTM F1959 method in Appendix A using the change in temperature (ΔT) between the start and end of the arc. The maximum flux of 91 kW/m² was at 0.91 m (3ft) at the top, left (S8). The maximum slug temperatures are also shown to indicate the maximum temperature a metal object would reach during the arc or after the arc.

Table 2-10. DP Test 4 Flux Results.

Slug	ΔT (°C)	Flux (kW/m²)	Max T (°C)
S1-F-76-CL	3.8	33	28
S2-F-16-CL	0.5	4	19
S3-RS-76-F	5.5	48	20*
S4-RS-48-F	1.7	15	16*
S5-RS-16-F	0.1	0.9	15*
S6-R-76-CL	1.5	13	17
S7-R-16-CL	9.4	82	26
S8-LS-76-CL	10.4	91	27
S9-LS-48-CL	1.8	16	18
S10-LS-16-CL	0.8	7	16

* Maximums at the noise spikes in Figure 2.10-7 are excluded.

2.11.2 DP Test 4 Temperature Data

PTs were used in this test to measure temperature; TCs were not used based on experience in previous DP tests. The temperatures measured by the PTs on the Cable Tray (CT) are seen in Figure 2.11-10. Table 2-11 shows the maximum PT temperature during the test. The PTs indicated the maximum temperature a metal object with gray surface emissivity of approximately 0.85, 46 cm (18 in) above the cabinet in the rear could reach during the arc.

As expected, the temperature in the center of the cable tray was the highest but all temperatures were low, indicating the heat released through the top rear vents below the cable tray were low. These low temperatures were consistent with no cable damage, as shown earlier. The maximum temperatures occurred at about 1.5 minutes after the arc, indicating that heat escaped from the cabinet after the arc heating the PT.

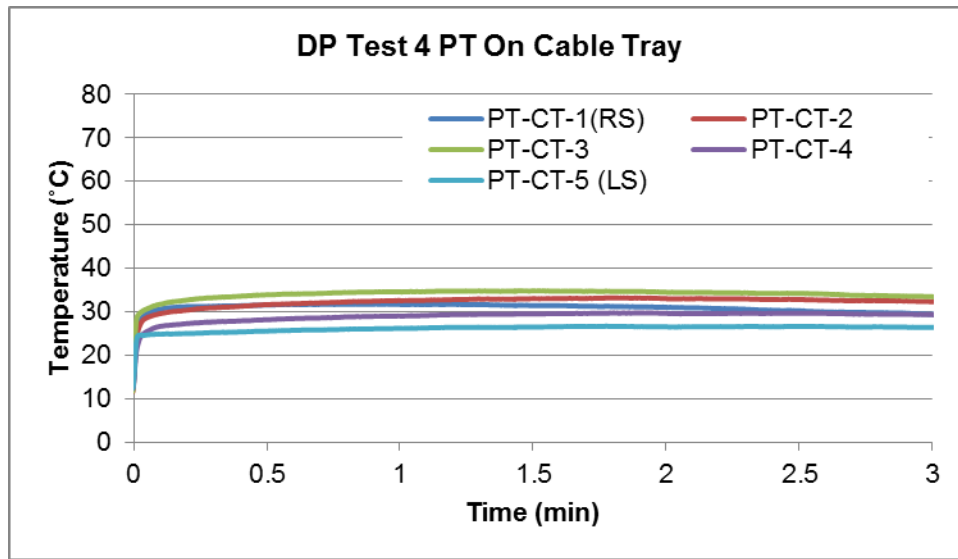


Figure 2.11-10. DP Test 4 Cable Tray Plate Thermometer Data

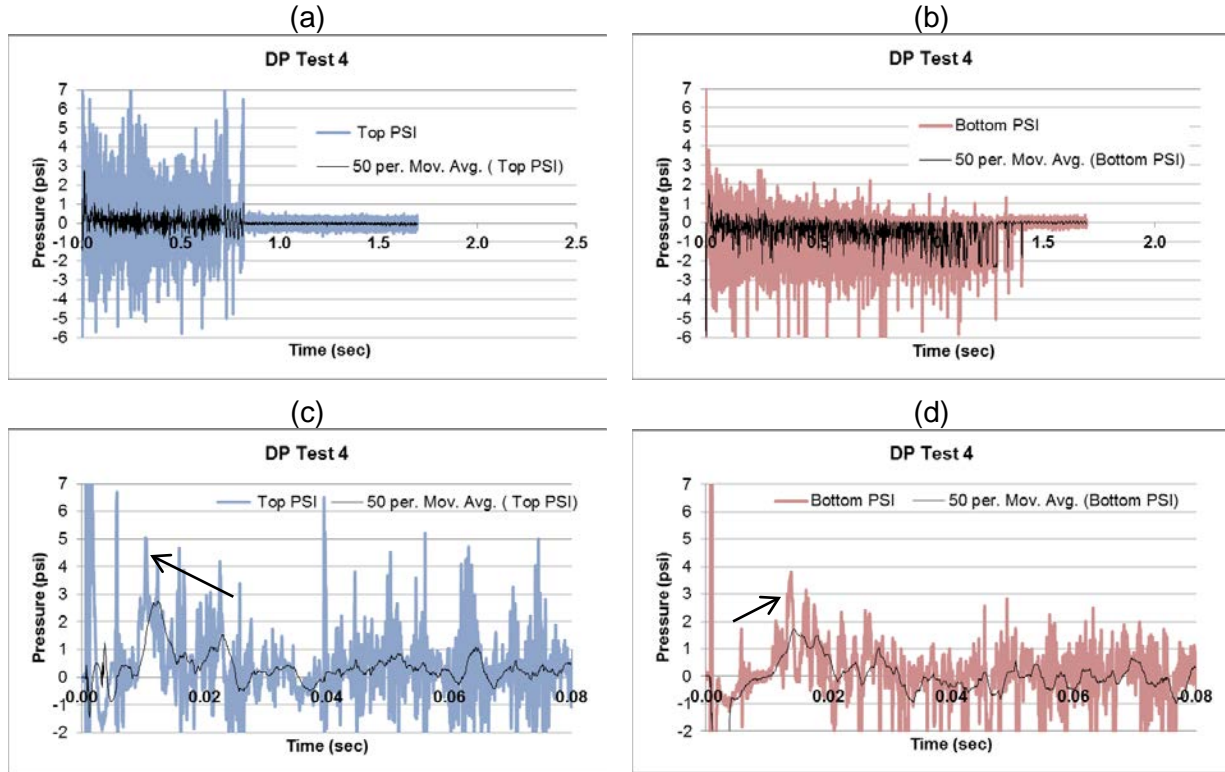
Table 2-11. DP Test 4 Plate Thermometer Results.

PT	Max T (°C)
PT-CT-1(RS)	32
PT-CT-2	33
PT-CT-3	35
PT-CT-4	30
PT-CT-5 (LS)	27

2.11.3 DP Test 4 Pressure Data

The pressures during the arc are seen in Figure 2.11-11. The top pressure, measured near the arc had a higher noise than at the bottom. The noise was significant towards the end of the arcing at the top; throughout the entire test, there was noise in the bottom measurement. A maximum pressure was indicated at the top of the cabinet, closer to the arc, before it was seen at the bottom of the cabinet. The maximum pressures are indicated by the arrows in Figure 2.11-11(c) and (d).

The pressure analysis methods are in Appendix A and involved picking the maximum near the start of the arc then including a nominal uncertainty for the noise in the signal just before the arc.



Test 4 Pressure 1 Top
 33.1 ± 1.4 kPa (4.8 ± 0.2 psi)
@ 0.0105 sec

Test 4 Pressure 2 Bottom
 23.4 ± 1.4 kPa (3.4 ± 0.2 psi)
@ 0.0139 sec

Figure 2.11-11. DP Test 4 Pressure

2.11.4 DP Test 4 Arc Energy

The total energy was 8.3 MJ, as shown in Figure 2.11-12. The energy analysis methods are in Appendix A. The “Energy” is calculated as volts multiplied current multiplied by the time step and each time step is shown. “Energy Total” is the cumulative sum of the energy in each time step. Note the arc quenched momentarily at about 0.3 seconds.

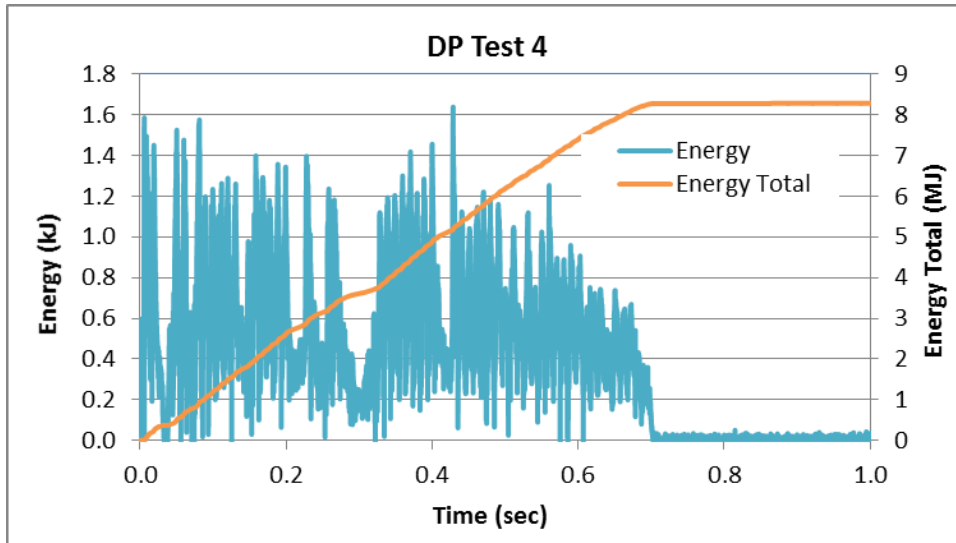


Figure 2.11-12. DP Test 4 Arc Energy

2.12 DP Test 5 Key Observations (March 2015)

This cabinet test was initiated at 484 V and 44.7 kA with a target duration of 2 seconds. The arc quenched at 1.001 seconds with an additional restrike arc, 0.150 seconds in duration, and 0.55 seconds after the main arc. The total energy with the restrike was 14.3 MJ. Figure 2.12-1 shows the arc with High Speed (HS) camera, Figure 2.12-2 shows the HD camera images and Figure 2.12-3 shows the FLIR camera images. Note the arc flames extend to the NUREG/CR 6850 specified ZOI of 0.9 m (3 ft) ZOI as in Figure 2.12-2.

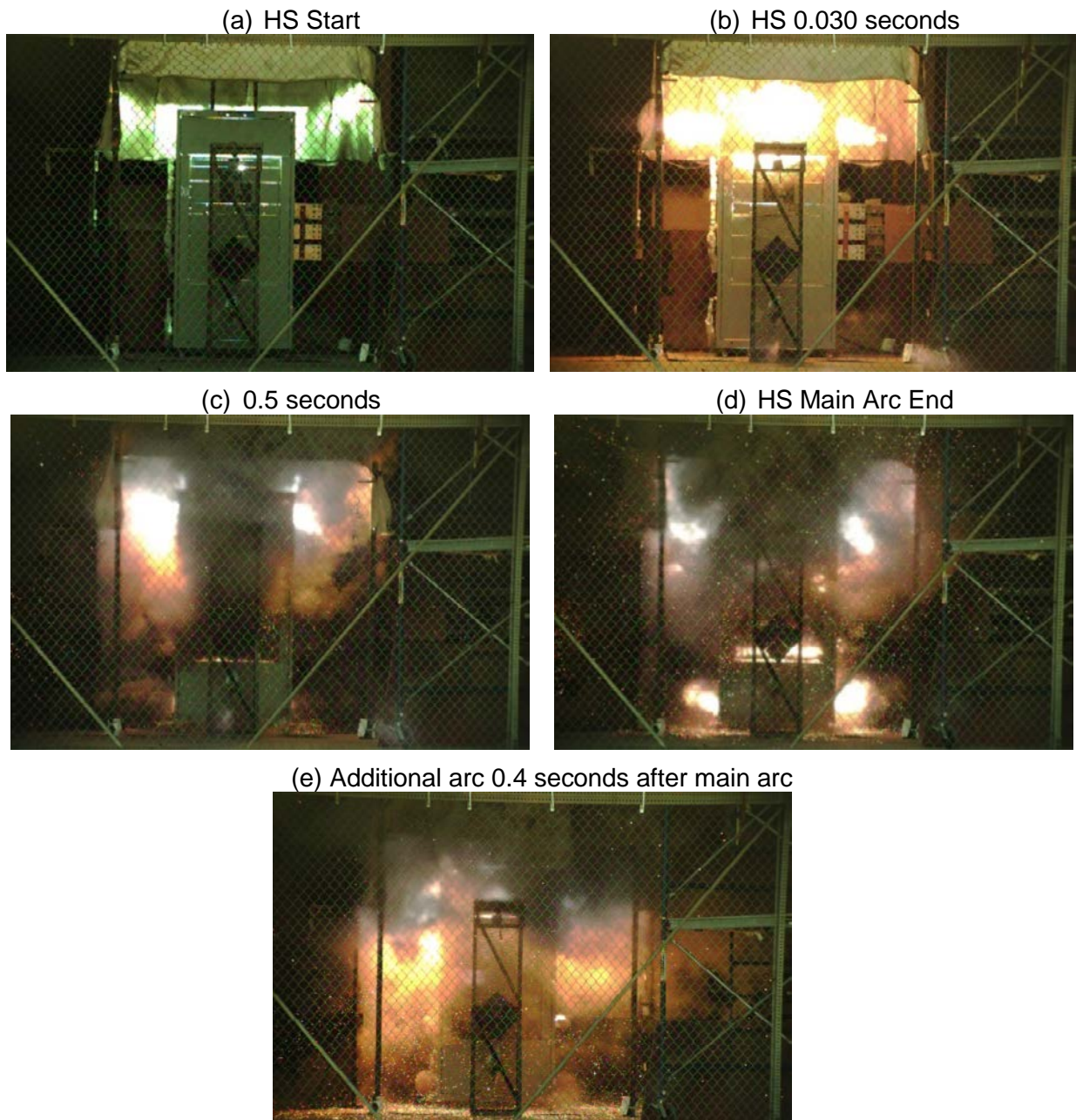


Figure 2.12-1. DP Test 5 Arc

Flames escaped the vents at the top and reached the 0.91 m (3 ft), as seen in Figure 2.12-2. Some flames were visible inside the top vent on the left side of the cabinet immediately after the arc but these extinguished quickly, as seen in Figure 2.12-2(d).

(a) Front start



(b) Rear start



(c) Flame contact with calorimeter
(rear and side)



(d) Flames in cabinet at end of arc



Figure 2.12-2. DP Test 5 Arc Flames

The FLIR camera was manually set at a fixed maximum of 150 °C. The flux from the hot spot is detected by the slug calorimeter at the top front of the cabinet. There was no ensuing fire.

(a) 10 seconds after arc



(b) 120 seconds after arc



Figure 2.12-3. DP Test 5 Thermal Images

The damage caused by the HEAF is shown in Figure 2.12-4 through Figure 2.12-6. Figure 2.12-4 shows the exterior damage as char and discoloration on the top panel near the arc. There was minor deformation of the front and rear panels. The top front plate was dislodged during fire suppression. The external cable tray showed no damage. Figure 2.12-5 shows the interior damage with charring and copper plated on the surfaces but no major fire and no cable damage. Figure 2.12-6 shows the interior bus bar damage and the insulators that were dislodged when the arc reached that point.

(a) Front in-situ



(b) Front



(c) Rear cable tray



(d) Rear



Figure 2.12-4. DP Test 5 Exterior Damage

(a) Plate on



(b) Plate off

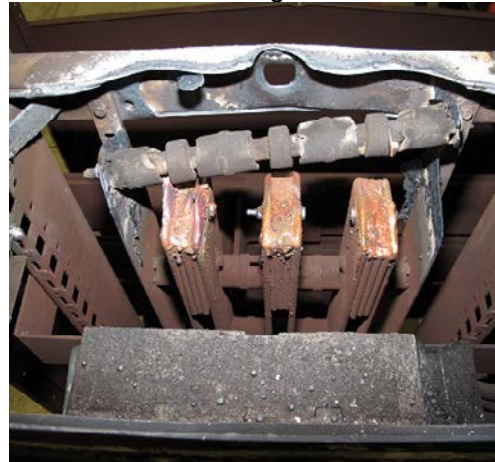


Figure 2.12-5. DP Test 5 Interior and Cable Damage

(a) With bus bar cover



(b) Without bus bar cover, insulator dislodged



(c) Top of bus bars with no cover



Figure 2.12-6. DP Test 5 Bus Bar Damage at Arc Location

2.12.1 DP Test 5 Calorimetry Data

Temperatures measured at the slug locations are shown Figure 2.12-7. The slug temperatures (in addition to the arc energy results shown in Section 2.12.4) show that the arc quenched at 1.001 seconds then re-struck on its own and quenched at 1.659 seconds. Slugs 3 to 5 had high noise during the arc probably due to EMI; the power supply was directly next to the slug calorimeters. Note there were additional noise spikes at the restrike. The noise was very high in some places causing the data to go off scale, see Figure 2.12-7. The highest temperatures at the end of the arc were measured near the top of the cabinet (S8 and S7). S7 and S8 cooled after the arc because there was no ensuing fire. After the arc, the temperature was seen to increase at a hot spot on the front panel near the arc (S1).

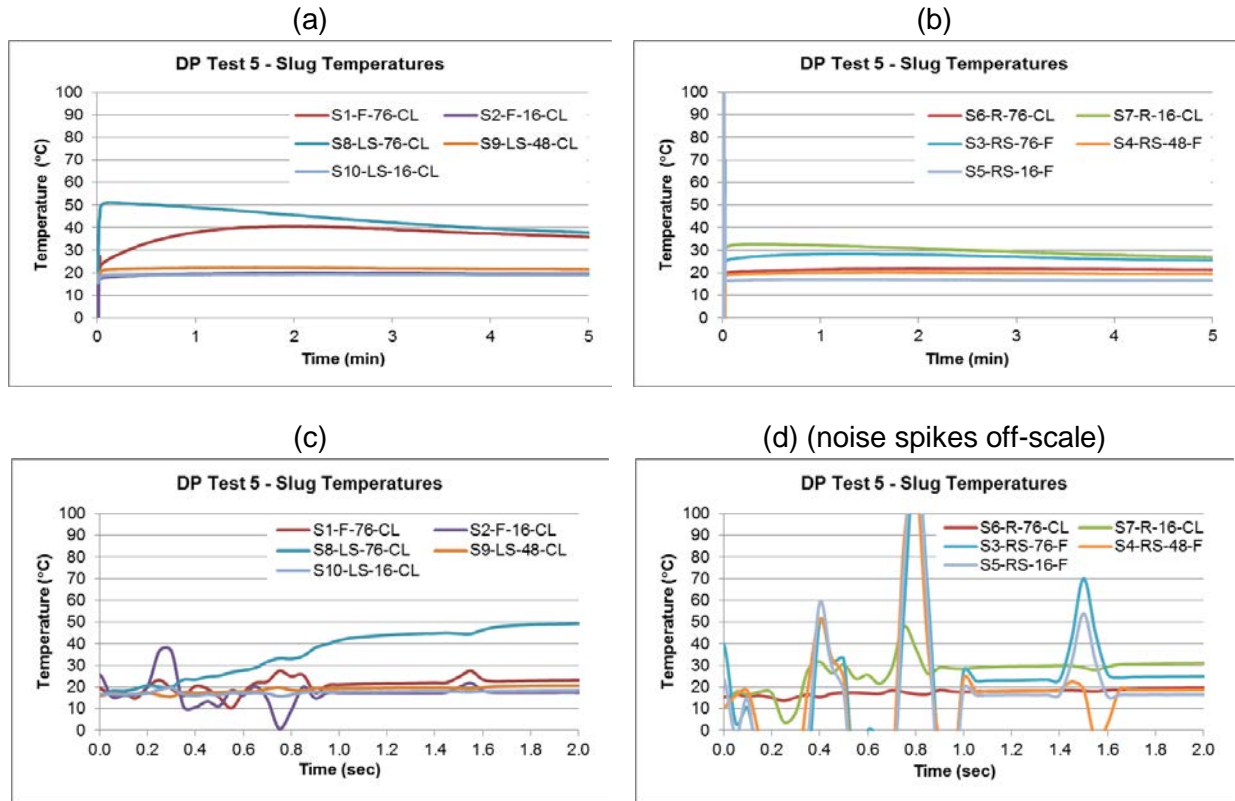


Figure 2.12-7. DP Test 5 Calorimetry Data: Temperature

Table 2-12 shows the flux results based on the ASTM F1959 method in Appendix A using the change in temperature (ΔT) between the start and the time the arc quenched. The maximum flux of 158 kW/m² was at the top left side of the cabinet (S8). The maximum slug temperatures are also shown to indicate the maximum temperature a metal object could reach during or after the arc.

Table 2-12. DP Test 5 Flux Results.

Slug	ΔT (°C)	Flux (kW/m ²)	Max T (°C)
S1-F-76-CL	4.4	27	41
S2-F-16-CL	0.9	6	17*
S3-RS-76-F	5.8	36	23*
S4-RS-48-F	1.6	10	18*
S5-RS-16-F	0.1	0.6	16*
S6-R-76-CL	1.9	12	22
S7-R-16-CL	12.3	75	48
S8-LS-76-CL	25.7	158	51
S9-LS-48-CL	2.8	17	22
S10-LS-16-CL	1.3	8	20

*Maximums at the noise spikes in Figure 2.12-7 are excluded.

2.12.2 DP Test 5 Temperature Data

PTs were used in this test to measure temperature; TCs were not used based on experience in previous DP tests. The temperatures measured by the PTs on the CT are seen in Figure 2.12-8. Table 2-13 shows the maximum PT temperature during the test. The PTs indicated the maximum temperature a metal object 46 cm (18 in) above the cabinet rear could reach during the arc.

As expected, the temperature in the center of the cable tray was the highest but all temperatures were low indicating the heat released through the top rear vents below the cable tray was low. These low temperatures were consistent with no cable damage, as shown earlier. The maximum PT temperatures were higher than DP Test 4 because the duration was longer and there was more energy in Test 5. The maximum temperatures were about 1.5 minutes after the arc indicating that heat escaped from the cabinet after the arc heating the PT.

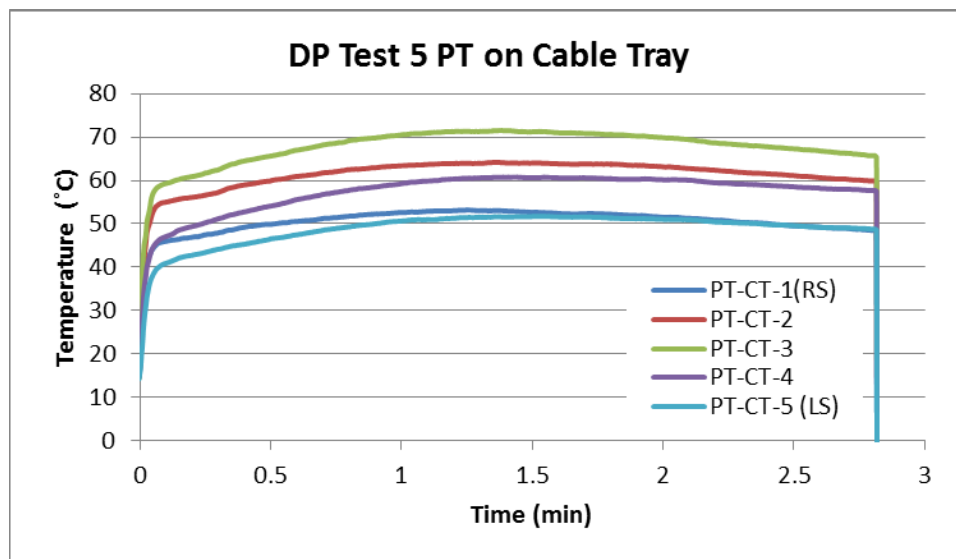


Figure 2.12-8. DP Test 5 Cable Tray Plate Thermometer Data

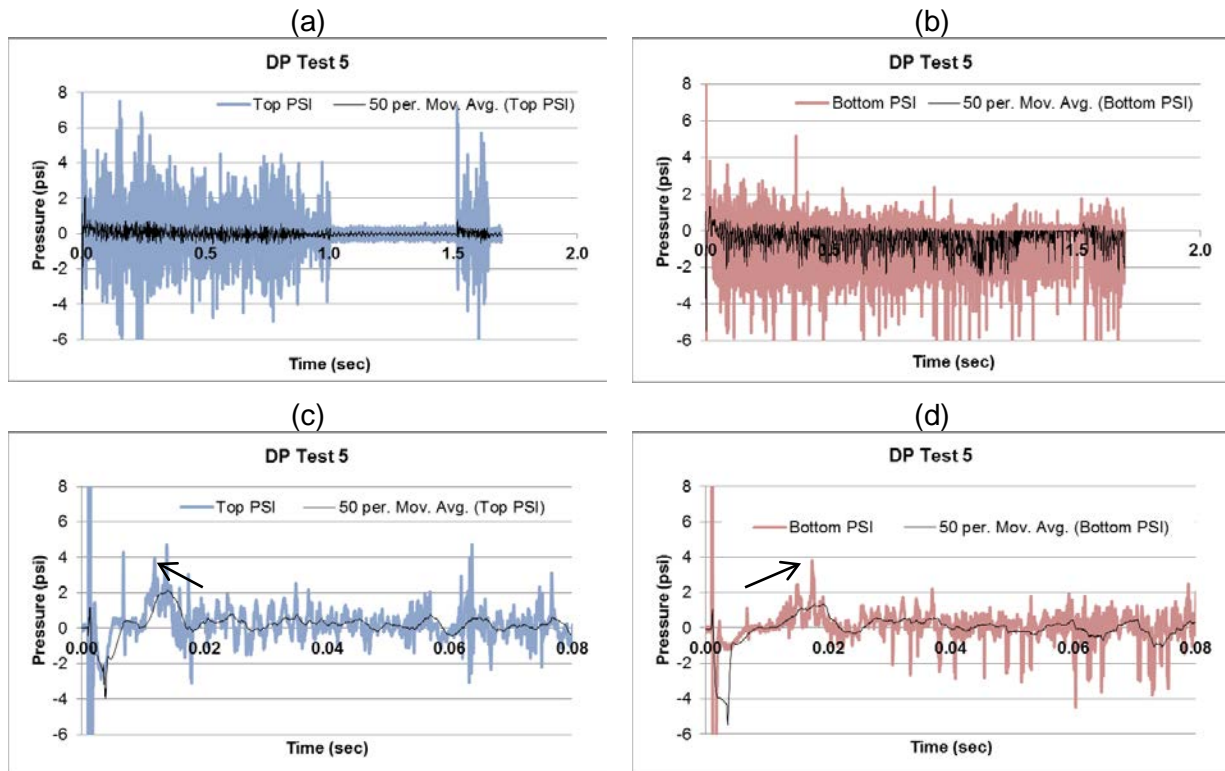
Table 2-13. DP Test 5 Plate Thermometer Results.

PT	Max T (°C)
PT-CT-1(RS)	53
PT-CT-2	64
PT-CT-3	72
PT-CT-4	61
PT-CT-5 (LS)	52

2.12.3 DP Test 5 Pressure Data

The pressures during the arc are seen in Figure 2.12-9. There were noise spikes at 0.16, 0.24 seconds on the top and 0.365 seconds on the bottom. The top pressure, measured closer to the arc had a higher maximum and occurred earlier than the bottom pressure, which was measured further from the arc. The maximum pressures are indicated by the arrows in Figure 2.12-9(c) and (d). There were additional pressure and noise spikes with the re-strike at 1.6 seconds.

The pressure analysis methods are in Appendix A and involved picking the maximum near the start of the arc then including a nominal uncertainty for the noise in the signal just before the arc.



Test 5 Pressure 1 Top
 22.1 ± 2.1 kPa (3.2 ± 0.3 psi)
 @ 0.0136 s

Test 5 Pressure 2 Bottom
 20.0 ± 1.4 kPa (2.9 ± 0.2 psi)
 @ 0.0174 s

Figure 2.12-9. DP Test 5 Pressure

2.12.4 DP Test 5 Arc Energy

The arc duration including the restrike was 1.659 seconds with total energy of 14.3 MJ, labeled as seen in Figure 2.12-10. The energy analysis methods are in Appendix A. The “Energy” is calculated as volts multiplied current multiplied by the time step and each time step is shown. “Energy Total” is the cumulative sum of the energy in each time step. There was a restrike of 0.150 seconds that was 0.508 seconds after the main arc.

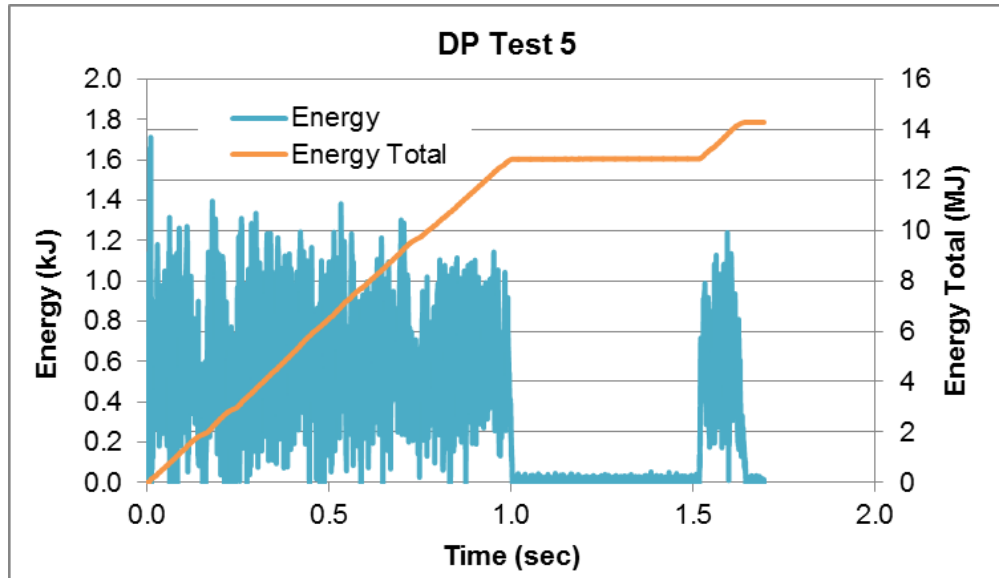


Figure 2.12-10. DP Test 5 Arc Energy

2.13 DP Test 6 Key Observations (March 2015)

This cabinet test was initiated at 400 V and 51.8 kA with a target duration of 2 seconds. The arc quenched at 0.550 seconds and there were additional short duration arc restrikes at 0.60, 0.71, and 0.78 seconds after the arc initiation. The total energy including the restrikes was 8.2 MJ. Figure 2.13-1 through Figure 2.13-3 show the arc with the HS camera, the HD camera, and the FLIR camera. Note the arc flames extend to the NUREG/CR 6850 ZOI. There was no ensuing fire because the energy was too low.

For this test, a top steel plate cover was placed above the ends of the bus bars to act as a ground surface for the arc to attach in order to achieve the full 2-second arc duration but this did not work.

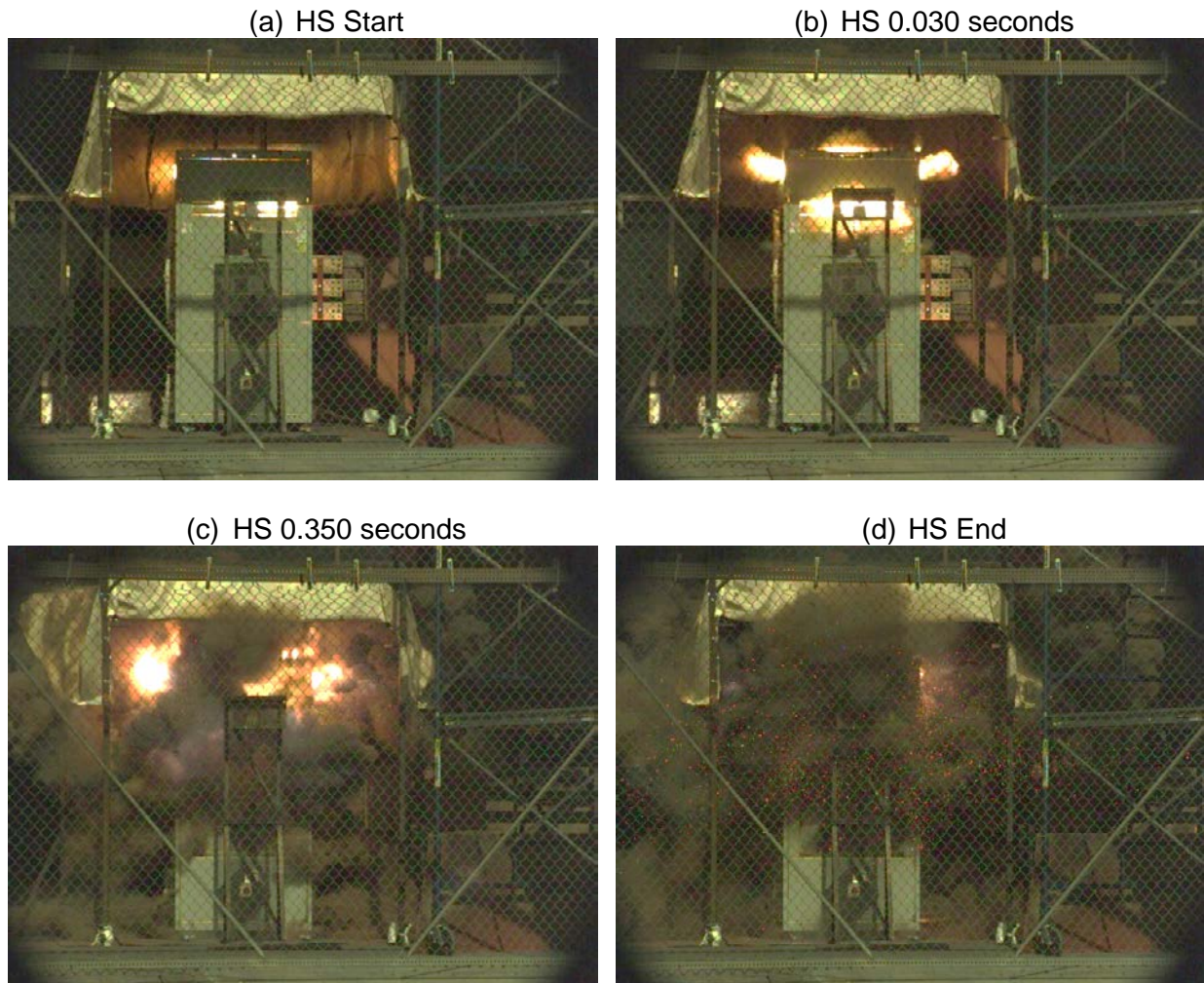


Figure 2.13-1. DP Test 6 Arc

Flames escaped the vents at the top and reached the 0.91 m (3 ft), as shown in Figure 2.13-2.

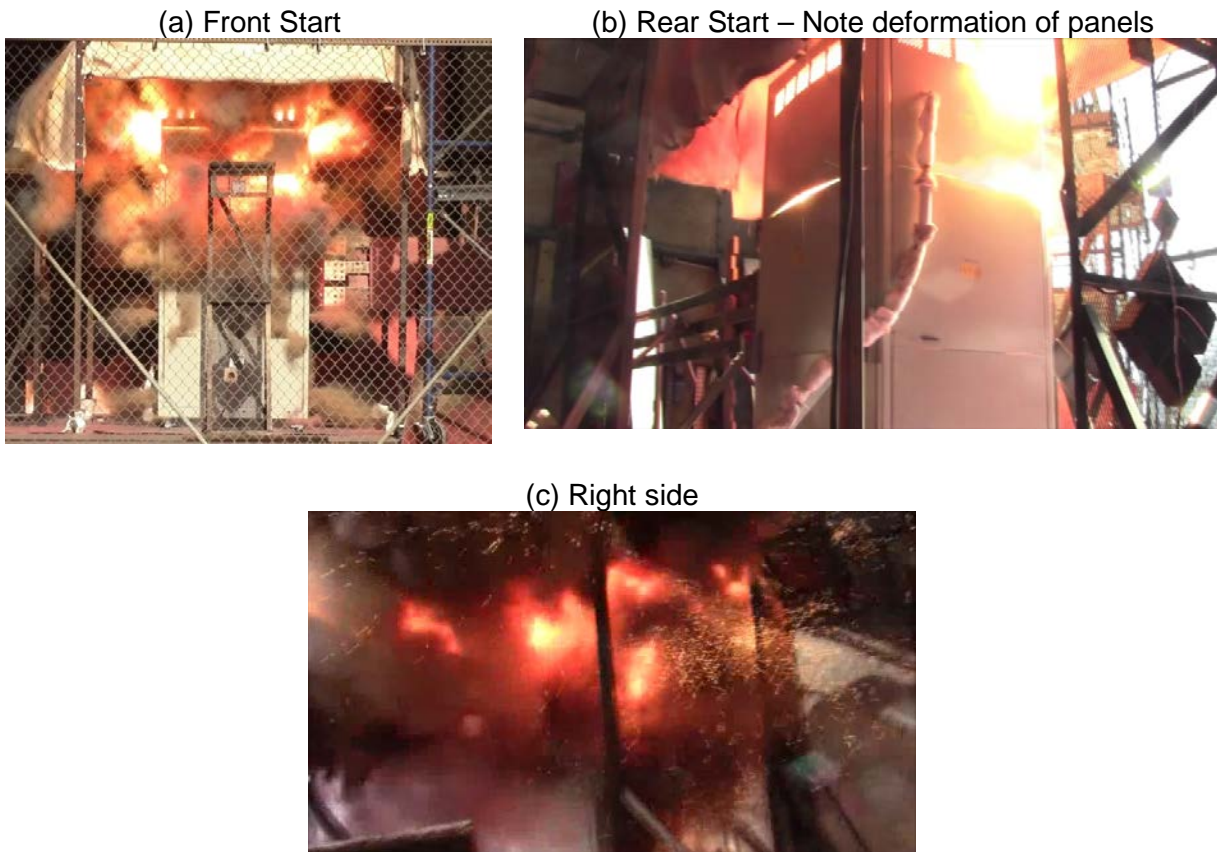


Figure 2.13-2. DP Test 6 Arc Flames

The FLIR camera indicated a maximum temperature of 360 °C at the top front “hot spot” that cooled by 140 °C in 2 minutes. The flux from this hot spot was detected by the slug calorimeter at the top front of the cabinet (see Figure 2.13-3). This hot spot was a little smaller than in Test 4, with a similar arc. There was no ensuing fire.

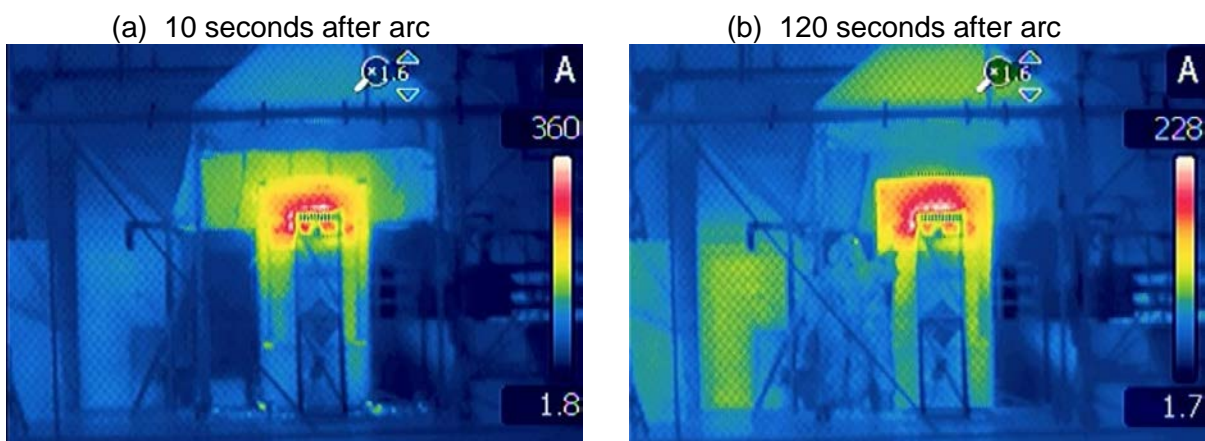


Figure 2.13-3. DP Test 6 Thermal Images

Figure 2.13-4 shows the exterior charring and discoloration on the top panel near the arc. There was minor deformation of the front and rear panels. The external cable tray showed no damage. Figure 2.13-5 shows the interior damage with minor charring of the cables and copper plated onto the surfaces but no major fire. Figure 2.13-6 shows the interior bus bar damage was only burning at the top of the bus bars.



Figure 2.13-4. DP Test 6 Exterior Damage

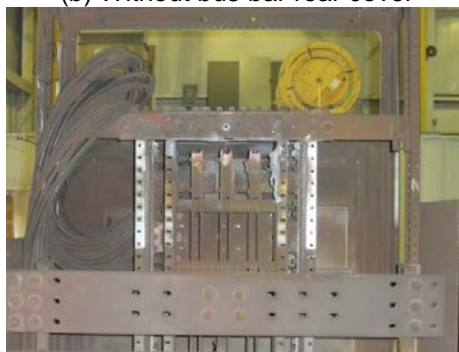


Figure 2.13-5. DP Test 6 Interior Cable Damage

(a) Bus Bar Rear Cover



(b) Without bus bar rear cover



(c) Top of bus bars with no cover plate

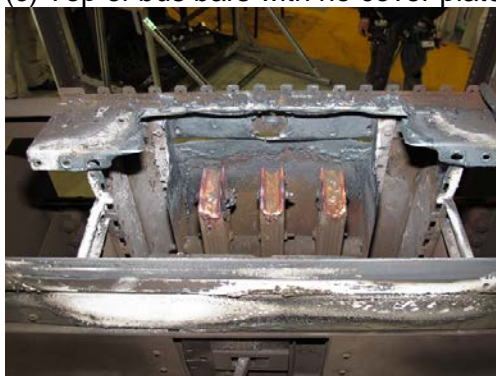


Figure 2.13-6. DP Test 6 Bus Bar Damage at Arc Location

2.13.1 DP Test 6 Calorimetry Data

Temperatures measured at the slug locations are shown in Figure 2.13-7. The slug temperatures (in addition to the arc energy results shown in Section 2.12.3) show that the arc quenched at 0.55 seconds then re-struck many times for short durations. Slugs 3 to 5 had high noise during the arc probably due to EMI; the power supply was located nearby. Note there were additional noise spikes at the restrike. The highest temperatures at the end of the arc were measured at the top of the cabinet (S1 and S8). Slug 8 cooled after the arc because there was no ensuing fire. After the arc, the temperature was seen to increase at a hot spot on the front panel near the arc (S1).

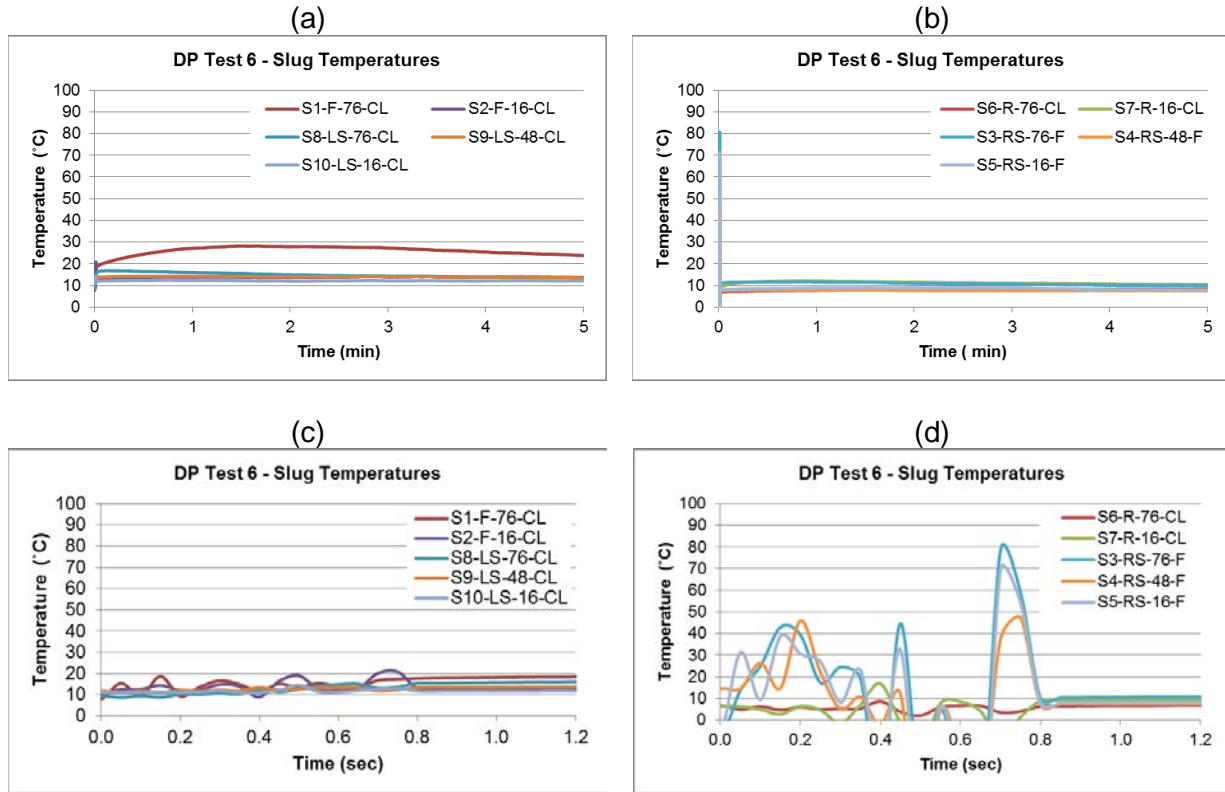


Figure 2.13-7. DP Test 6 Calorimetry Data: Temperature

Table 2-14 shows the flux results based on the ASTM F1959 method in Appendix A using the change in temperature (ΔT) between the start and the time the arc quenched. The results report a maximum flux of 73 kW/m² at the left top of the cabinet (S8). The maximum slug temperatures are also shown to indicate the maximum temperature a metal object would obtain during or after the arc.

Table 2-14. DP Test 6 Flux Results.

Slug	ΔT ($^{\circ}C$)	Flux (kW/m^2)	Max T ($^{\circ}C$)
S1-F-76-CL	6.0	67	28
S2-F-16-CL	0.7	8	13*
S3-RS-76-F	4.2	47	11*
S4-RS-48-F	1.8	20	8*
S5-RS-16-F	0	0	8*
S6-R-76-CL	0.8	9	9
S7-R-16-CL	3.2	35	17
S8-LS-76-CL	6.6	73	17
S9-LS-48-CL	1.9	21	14
S10-LS-16-CL	0.5	6	15

*Maximums at the noise spikes in Figure 2.13-7 are excluded.

2.13.2 DP Test 6 Temperature Data

PTs were used in this test to measure temperature; TCs were not used based on experience in previous DP tests. The temperatures measured by the PTs on the CT are seen in Figure 2.13-9. Table 2.13-2 shows the maximum PT temperature during the test. The PTs indicated the maximum temperature a black-body, metal object 46 cm (18 in) above the cabinet rear could reach during the arc.

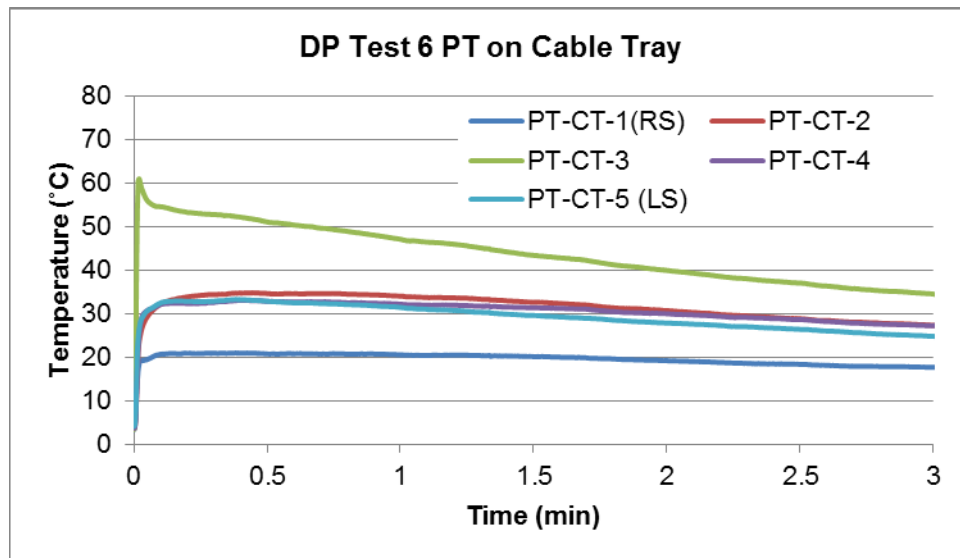


Figure 2.13-8. DP Test 6 Cable Tray Plate Thermometer Data

As expected, the temperature in the center of the cable tray was the highest but all temperatures were low, indicating the heat released through the top rear vents below the cable tray was low. These low temperatures were consistent with no cable damage, as shown earlier. The temperature response was different than Tests DP-4 and DP-5 with the maximum occurring soon after the arc or in the case of the center temperature PT-CT-3 at the end of the arc. PT-CT-3 also had a much higher temperature than test DP-4 even though the arc energies were nominally the same. It is theorized that flame/plasma escaped near the center rear of the cabinet in this test but this is not detectable on the videos and the discoloration and charring were similar in all tests.

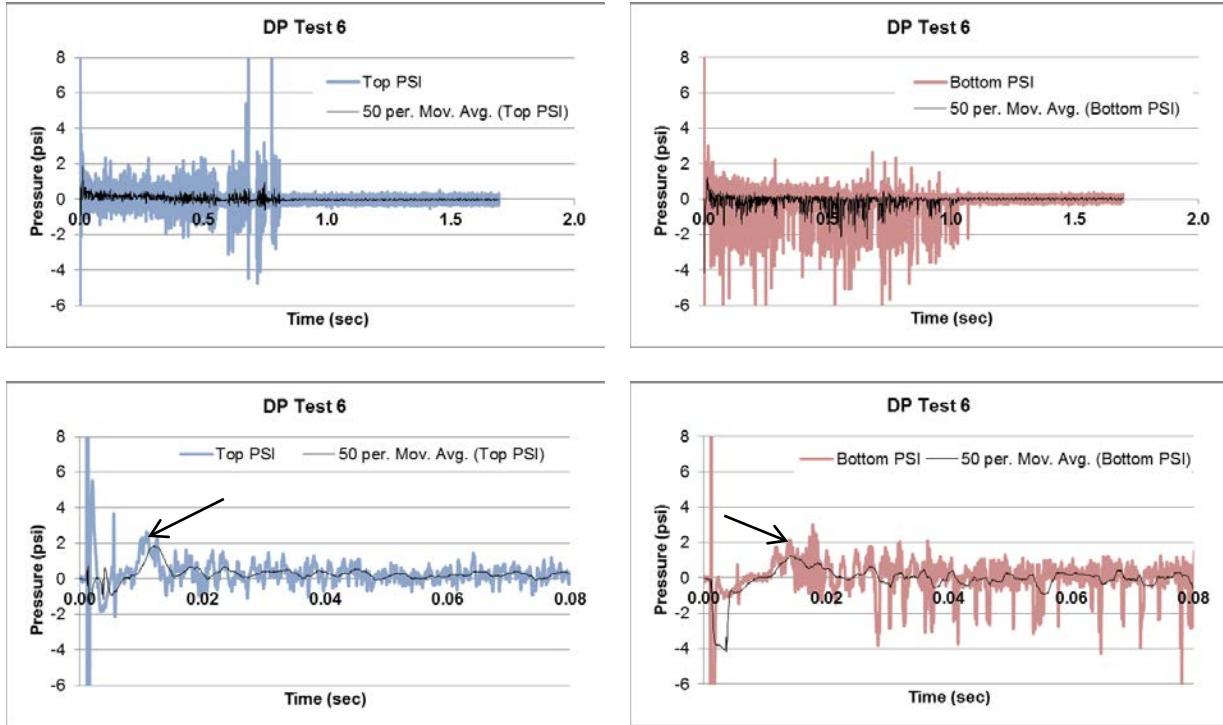
Table 2-15. DP Test 6 Plate Thermometer Results.

PT	Max T (°C)
PT-CT-1(RS)	21
PT-CT-2	35
PT-CT-3	61
PT-CT-4	33
PT-CT-5 (LS)	33

2.13.3 DP Test 6 Pressure Data

The pressures during the arc are shown in Figure 2.13-9. The top pressure, measured closer to the arc had a higher maximum and occurred earlier than the bottom pressure, which was measured further from the arc. At 0.67 and 0.77 seconds, there appears to be pressure spikes and noise related to the restrikes. The maximum pressures are indicated by the arrows in Figure 2.13-9 (c) and (d).

The pressure analysis methods are in Appendix A and involved picking the maximum near the start of the arc then including a nominal uncertainty for the noise in the signal just before the arc.



Test 6 Pressure 1 Top
 16.5 ± 1.4 kPa (2.4 ± 0.2 psi)
@ 0.0111 s

Test 6 Pressure 2 Bottom
 13.1 ± 1.4 kPa (1.9 ± 0.2 psi)
@ 0.0142 s

Figure 2.13-9. DP Test 6 Pressure

2.13.4 DP Test 6 Arc Energy

Figure 2.13-10 shows the initial arc was 0.55 seconds before the first extinction with a smooth and steady energy increase then there were several restrikes after the initial arc. The arc duration, including the restrikes was 0.781 seconds with total energy of 8.2 MJ. The energy analysis methods are in Appendix A. The “Energy” is calculated as volts multiplied current multiplied by the time step and each time step is shown. “Energy Total” is the cumulative sum of the energy in each time step.

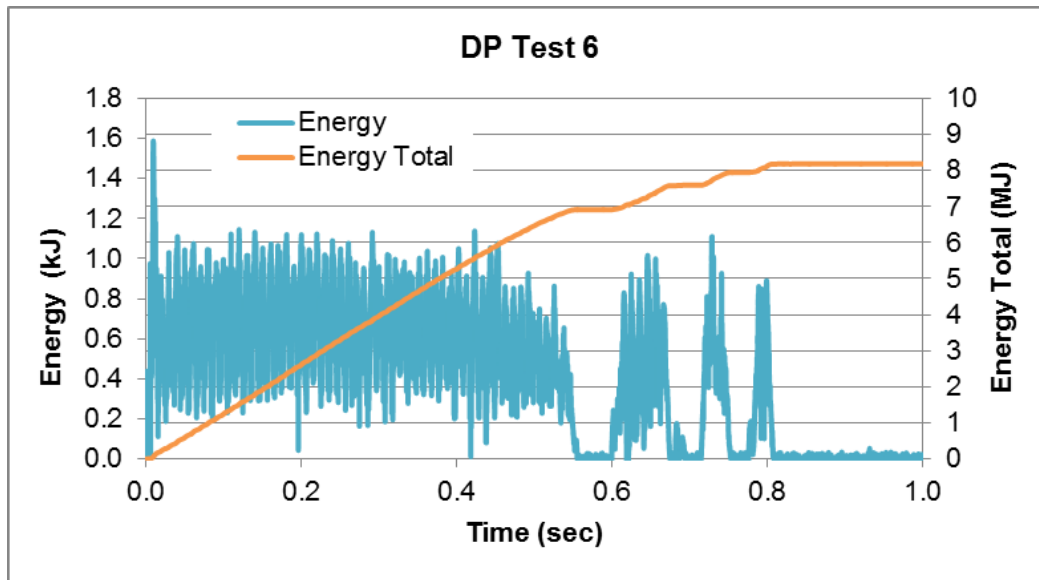


Figure 2.13-10. DP Test 6 Arc Energy

2.14 DP Tests 1 through 6: Summary of Electrical Conditions

The table shows the electrical conditions measured by KEMA. KEMA does not include any restrikes in their analysis so Tests 5 and 6 have shorter duration and lower energy than reported in the previous sections.

Table 2-16. DP Tests Electrical Results.

Test	Arc Location	OCV (V)	Phase	Sym (kA)	Peak (kA)	Sym @End (kA)	Curr. Dur. (sec) (1)	Arc Energy (MJ)	Freq @End (Hz)	Phase Arc Volts
1	Bottom of bus bars	484	A	42.7	63.5	32.2	1.574	11	47.7	A-N 248
			B	40.0	66.3	28.1		8		B-N 220
			C	47.2	71.2	29.7		9		C-N 231
			AVG	43.3	67	30.0		Σ 28		AVG L-L 404
2	Bottom of bus bars	484	A	40.7	60.8	33.6	1.446	10	47.7	A-N 246
			B	35.9	60.5	25.6		8		B-N 211
			C	38.6	66.9	35.5		9		C-N 225
			AVG	38.4	62.73	31.6		Σ 27		AVG L-L 394
3	Bottom of bus bars	484	A	41.9	60.7	33.6	2.011	14	46.6	A-N 257
			B	39.5	61.5	29.8		10		B-N 227
			C	42.9	63.0	32.5		12		C-N 237
			AVG	41.4	61.73	32.0		Σ 36		AVG L-L 416
4	Top of bus bars	484	A	55.0	95.0	19.4	0.698	4	49.3	A-N 238
			B	42.4	69.0	21.9		2		B-N 230
			C	53.5	87.1	16.7		3		C-N 230
			AVG	50.3	83.7	19.9		Σ9 (2)		AVG L-L 403
5	Top of bus bars	484	A	44.2	97.9	45.0	1.001	7	48.1	A-N 216
			B	45.2	84.4	34.9		2		B-N 212
			C	44.6	105.0	33.9		4		C-N 201
			AVG	44.7	95.8	37.9		Σ13(2)		AVG L-L 363
6	Top of bus bars	400	A	51.1	100.9	30.5	0.550	4	50.0	A-N 177
			B	52.9	93.7	32.7		1		B-N 176
			C	51.3	105.8	27.8		2		C-N 176
			AVG	51.8	100.1	30.3		Σ7(2)		AVG L-L 305

Notes:

- (1) Does not include restrikes.
- (2) As reported by KEMA instruments and results for the main arc. This does not include the restrike arcs after the main arc for Tests 5 (see section 2.12.4) and 6 (see section 2.13.4). Target energy was 35 MJ.
- (3) Target current duration was 2 seconds.

Table 2-17. Acronyms and Abbreviations for Electrical Test Results.

@End	At the end of the test
AVG	Average
Bot	Bottom
Curr	Current
Dur	Duration
Freq	Frequency
L-L	Line to Line
Max	Maximum
N	Neutral
OCV	Open Circuit Voltage
Press	Pressure
psi	pounds per square inch
Sym	Symmetrical

2.15 DP Tests 1 through 6 Qualitative Summary

Although the tests in this series were planned to be similar, there were some differences in the results. Some important or interesting items to note are discussed below.

1. **Ensuing Fire:** Only two of the tests (1, 3), with the arc at the bottom, resulted in ensuing fires in which all the internal combustibles were consumed. The damage to the internal combustibles in Test 2 suggests that an ensuing fire would be possible with a slightly more energetic arc; Test 2 was slightly less energetic than Test 1. The remaining three tests (4, 5, 6), with the arc at the top, showed little or no damage to the internal cables. Generally, the energy required for an ensuing fire was much less in the DP tests than what was required for the SWGR tests discussed later because the DP had less venting than the SWGR, so heat was better retained and lower electrical energy started the fire in the DP tests.
2. **Damage:** All of the tests resulted in bus bar damage, as would be expected from oxidation during the arc. In Tests 1 and 3 several centimeters of the bus bar was consumed during the arc. Test 2 had bus bar losses which were not as severe as Tests 1 or 3 because of the shorter arc duration. As expected Tests 4, 5 and 6 showed much less damage to the bus bars because of the very short arc durations.

Tests 1, 2 and 3 all showed heavy damage to the front of the cabinet, due to the high energy and ensuing fires. These tests also resulted in deformations of the panels. However, the deformation in Test 3 was smaller than Tests 1 and 2, probably because the pressure was relieved by the panel opening during the test.

Tests 4, 5, 6 all resulted in minor deformation of the front and rear panels. These tests also included an external cable tray, which showed no damage in all tests.

3. Calorimetry: The maximum measured flux varied between the tests. Tests 1, 2 and 3 showed the maximum heat flux in the same location: at the bottom rear of the cabinet where the cabinet panel was directly exposed to the arc. The slug calorimeter located at the top left in Tests 4, 5 and 6 showed the maximum flux. Tests 4, 5 and 6 also showed high heat flux at the rear bottom (Tests 4 and 5 were particularly high), which was unexpected because the arc was at the top, front of the cabinet. The flux at the top rear was low for Tests 4, 5 and 6 that was also unexpected for the top arc location.

In all the tests, there were spikes during the arc, which indicate large variations in the slug temperature from noise and because the energy produced during the arc is not uniformly distributed external to the cabinet and varies during the arc. Venting conditions and cabinet integrity such as DP panel deformation and the associated plasma and flame leakage also affect the slug responses seen during the test series

4. Temperature: Thermocouples to measure air temperature were only used in Tests 1, 2 and 3. Since the arcs were in the rear of the cabinets, the highest temperatures occurred in this area for all three tests. However, the temperatures for Test 2 were less than Tests 1 and 3 because the energy was lower.

Plate thermometers were used for Tests 4, 5 and 6 in the external cable trays to measure temperature above the cabinet. The highest temperatures were seen in the center of the cable trays as expected. Tests 5 and 6 had similar maximum temperatures whereas Test 4 showed a lower temperature, probably related to the random nature of flames and plasma exiting the rear of the cabinet at the top just below the cable tray.

5. Pressure Data: In Tests 1 through 5, the highest pressures were measured near the arc; Tests 1 through 3 at the bottom, and Tests 4 through 6 at the top of the cabinets, as expected. Tests 4 through 6 had considerably higher pressures than Tests 1 through 3, perhaps because the top location had a different flow path from the initial arc shock to the PRT.

The pressure was, on average, higher for the DP cabinets than in the SWGR cabinets (Chapters 4 and 5) because there was less vent area in the DP and the SWGR vent was directly above the arc. Additionally, the SWGR had interior walls between the arc and the pressure measurement points. The cabinet walls and roof exhibited bending and deformation of several centimeters. The DP also had thinner materials for the walls and doors than the SWGR.

6. Arc Energy: In all tests the total energy was proportional to the arc duration for the given electrical testing conditions, as expected. Tests 1 through 3 showed a smooth increase of the total energy during the arc indicating stable arc conditions for the bottom bus bar and cabinet arrangement. Tests 4 through 6 showed severe decreases in the energy and restrikes indicating less stable arc conditions at the top of the cabinet. Based on the occurrence of ensuing fires, the electrical energy threshold for an ensuing internal cable fire was about 28 MJ.

3 Motor Control Center HEAF TEST – KEMA (May 2013)

3.1 MCC Test Overview

The purpose of these tests was to obtain the basic HEAF data such as duration, energy, flux, temperatures, pressures, and ensuing fire effects for three (3) Motor Control Centers (MCC) at KEMA on May 22-23, 2013.

3.2 MCC Summary of Results

Each test consisted of one GE Series 7700 MCC with a horizontal bus rating of 2.8 kA. Japanese CV-2 cable that is typical of power cable was added as the combustible load.

The key test parameters and results are in Table 3-1. The target test values were nominally 480 V and 63 kA bolted fault current and the symmetric current achieved was nominally 21 to 46 kA. The target arc duration was 2 seconds.

There were no ensuing fires in any of the tests. The resulting arc energies for the tests were low, and the cabinets panels bent or came off, allowing the heat to escape out of the cabinets. The small bus bars bent away from each other in every test and increased the distance between the bus bars so the arcs quenched quickly (all tests resulted in less than 1 second arc duration).

The key results from the MCC tests at KEMA were:

- Hot gases and plasma can travel from the initial arc point to other locations in the cabinet and cause a second and in this case higher energy arc (Test 2).
- MCC cabinets have few vents and are “tight” and minimally ventilated, causing higher pressure increases, as to be expected.
- It is difficult to maintain a steady arc with 480 V, which was also the case in the DP tests. The bus bars bent away from each other due to the strong magnetic fields from large current imbalances in the three phases during the arc causing large arc gaps, and providing a condition under which the voltage could not sustain the arc.

Table 3-1. MCC Test Summary of Results.

Test	Volt (V) (1) Current (kA) (2)	Test Peak Current (kA) (3)	Arc duration (sec) (4)	Arc Energy (MJ)	Internal Max Press (kPa/psi)	External Max Flux (9) (kW/m ²)	Ensuing fire? Key Observations (10)
1	484 / 432 21.4 / 11.2	45.9	2.0 0.145	1.7	37.9 ± 1.4 5.5 ± 0.2	38 (6)	No. Low duration and low energy. Bottom arc.
2	492 / 384 34.1 / 25.2	80.3	2.0 0.952 (5)	17.4	30.3 ± 1.4 4.4 ± 0.2	46 (7) (11)	No. Two Arcs-arc moved from bottom to top of MCC
3	492 / 384 40.4 / 26.8	67.7	2.0 0.256	4.2	31.0 ± 1.4 4.5 ± 0.2	102 (8)	No. Bottom arc.
4	492 / 374 46.4 / 37.0	91.0	2.0 0.922	17.6	63.4 ± 1.4 9.2 ± 0.2	65 (9)	No. Top arc was planned and occurred.

Notes:

- (1) The voltage is shown as the target voltage / arc Line-to- Line (L-L) voltage.
- (2) The symmetric arc current slowly drops during the test as the arc impedance increases. This shows the *test start current/ test end current*. These are average currents of all 3 phases.
- (3) This is the peak current for any phase or time, usually the asymmetric current at the start.
- (4) The duration is shown as the target duration and the actual test duration is below it.
- (5) This is for the total duration of the 2 arcs: one at the bottom then one at the top.
- (6) The maximum flux was seen on the side at 0.91 m (3 ft), and 0.9 m (35.5 in) from the floor (S1).
- (7) The maximum flux was seen on the rear at 1.5 m (5 ft), behind the cabinet, 79 cm (31 in) from the floor (S6). Flames reached and contacted the slug calorimeters on the left side of the cabinet (S1, S2, and S3).
- (8) The maximum flux was seen at the bottom, left side at 0.91 m (3 ft) (S1), which viewed the opening in the bottom left of the cabinet. The left side slug at 0.91 m (3ft) saw flames directly but was not contacted by the flame (S1).
- (9) The maximum valid flux was seen at the top, 1.5 m (5 ft) above the cabinet that could directly view the flames at the top of the cabinet (S4). The flux at the rear (S6) was greater but the slug calorimeter was closer than 0.91 meters to the cabinet. Three other slugs on the left side also had higher fluxes but flames made contact with these slugs and the flux measurements were not valid.
- (10) No ensuing fires so the maximum flux was during the arc or within 1 second after. Low flux in general. The arc caused large releases of hot gases and fire from the cabinet to the left toward the slug calorimeters. These gases and fire contacted the calorimeters increasing their temperature so they cannot measure the flux. As discussed in Appendix A, results from slugs contacted by flames are not reported.

3.3 MCC Test Configuration

GE Series 7700 equipment was used in the test because it is most similar to Japanese equipment. The MCC is nominally 0.51 m wide by 2.32 m high by 0.51 m deep (20 in wide by 91.5 in high and 20 in deep). The test configuration is shown in Figure 3.3-1 and Figure 3.3-2. The latter figure shows the three cabinets together in a line-up and each cabinet was tested individually. The combustible load consisted of plastics and wire in three motor starter sections, the two switch sections at the bottom and CV-2 cables.

There were horizontal and vertical buses in each cabinet. The horizontal buses were extended outside the cabinet to the connection for the incoming KEMA power supply. Wire per IEEE C37.20.7 for low voltage tests was connected to the three phase of the buses to make the arc at the bottom of the MCC. This location was selected conservatively below the combustibles to provide the highest likelihood of causing a fire in the cabinet. The motor starter sections were not connected to the bus because the component could have arced at the connection rather than at the arc wire. The bottom 15.24 cm (6 in) of the bus covers (white) called "arc chutes" were removed to place the wire then the covers were put back in place in Test 1. In Tests 2 and 3, the lower 61 cm (24 in) of the arc chute were removed to ensure the arc chutes did not extinguish the arc prematurely. Test 4 was at the top bus bars and the arc chutes were not involved.

In Tests 2 through 4, the cabinets were wrapped with six (6) steel bands around the MCC, two vertically and three horizontally. This was done to prevent the panels from blowing off the MCC, as was seen in MCC Test 1.

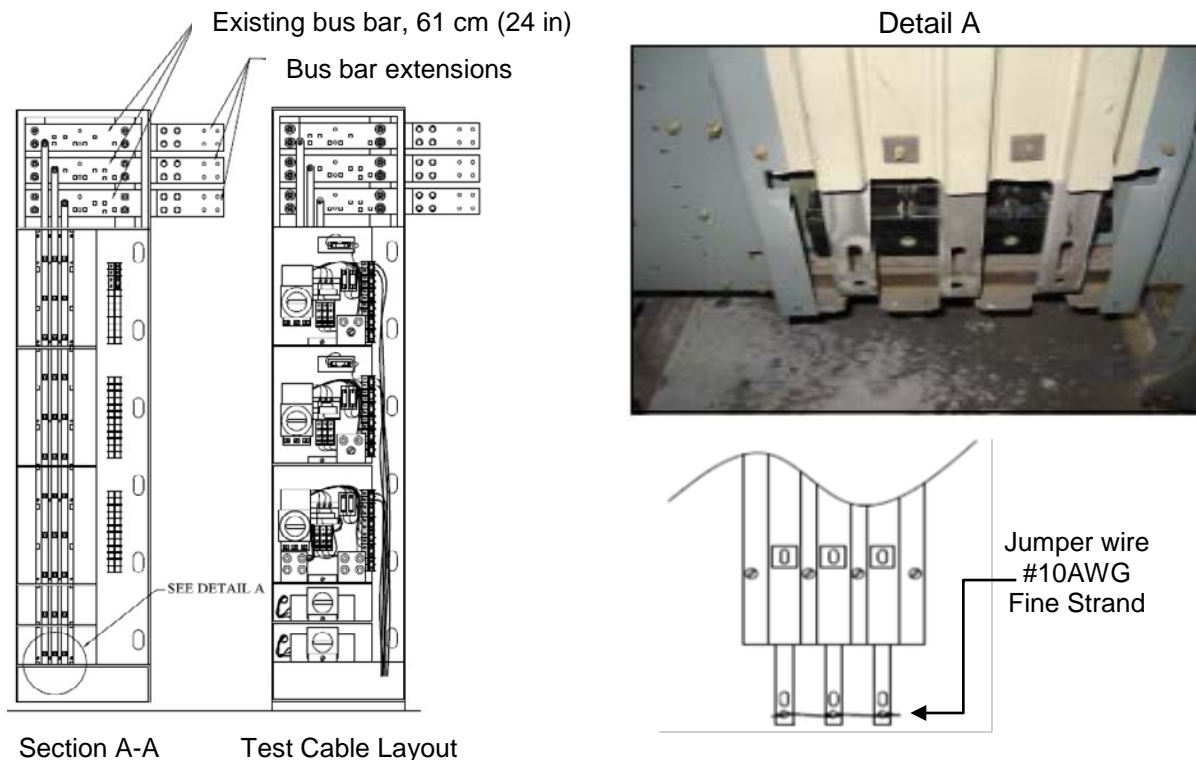
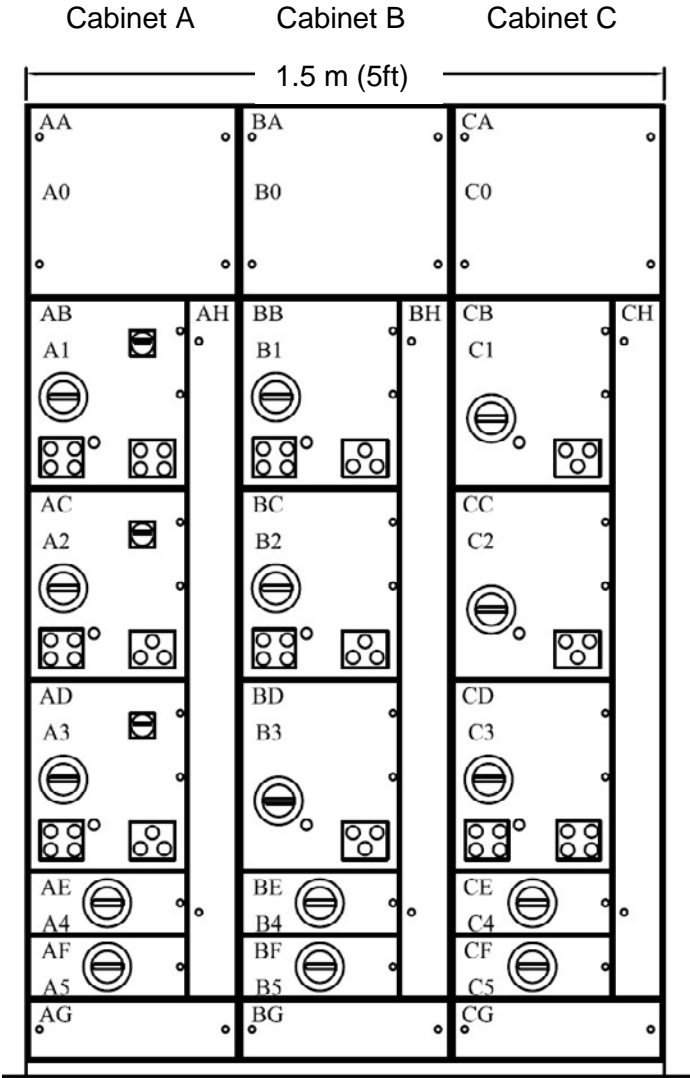


Figure 3.3-1. MCC Test Configuration



Each MCC section has some combustibles like the plastic on the breaker, the starter and some wires.



Figure 3.3-2. MCC for Test

3.4 MCC Cable Combustible Loading

Japanese CV-2 cable with heat resistant PVC sheath and XLPE insulation was used for the combustible cable load to simulate the power cables that are typically used from the MCC controllers to motors. The number of CV-2 cables was realistic for motor and control connections for a typical section/bucket. There were five (5) CV-2 cables in each of the top three (3) sections that dropped from each section to the bottom of the cabinet. Three (3) CV-2 cables represented the power cable and two (2) CV-2 cables represented the control cables. For the bottom two sections, only power cable was needed and three (3) CV-2 cables were used. The total cable combustible load was 18.29 m (60 ft) of CV-2 or 5 kg. Cable properties are in Appendix C.

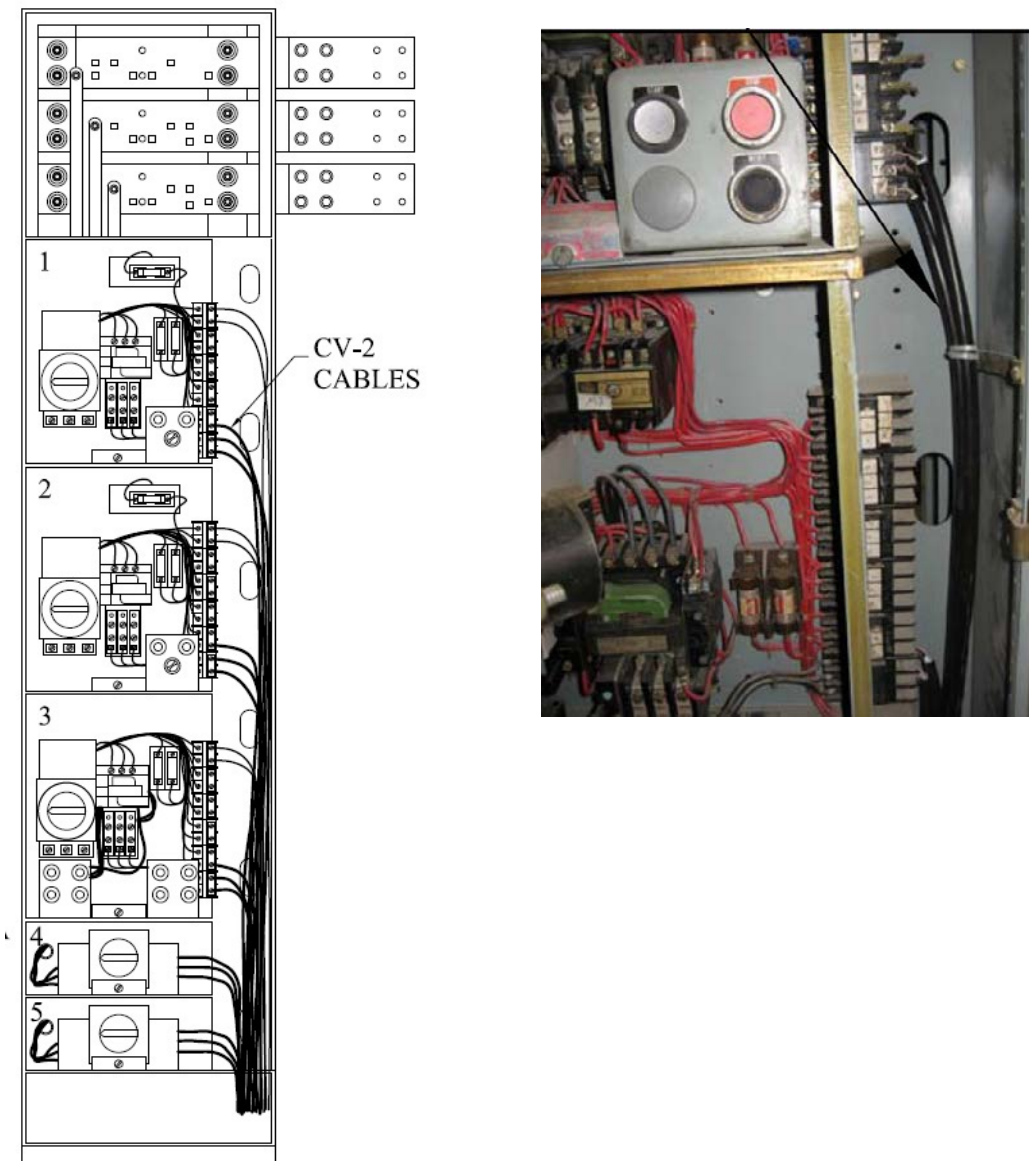


Figure 3.4-1. MCC Cable Combustible Load

3.5 MCC Temperature and Heat Flux Instrumentation

Slug calorimeters (slug, S) and thermocouples (TC) locations for these tests are shown in Figure 3.5-1. Slugs were nominally 0.91 m (3 ft) from the cabinet sides (S1, S2, S3, S5, S6) and 1.5 m (5 ft) from the cabinet top (S4). TCs were 15.2 cm (6 in) from the cabinet in open air and not in contact with the cabinet. The air temperatures are likely much lower than the actual metal temperature. Therefore, the temperatures are only a qualitative measure of thermal behavior. Table 3.5-1 shows the slug calorimeter and MCC locations.

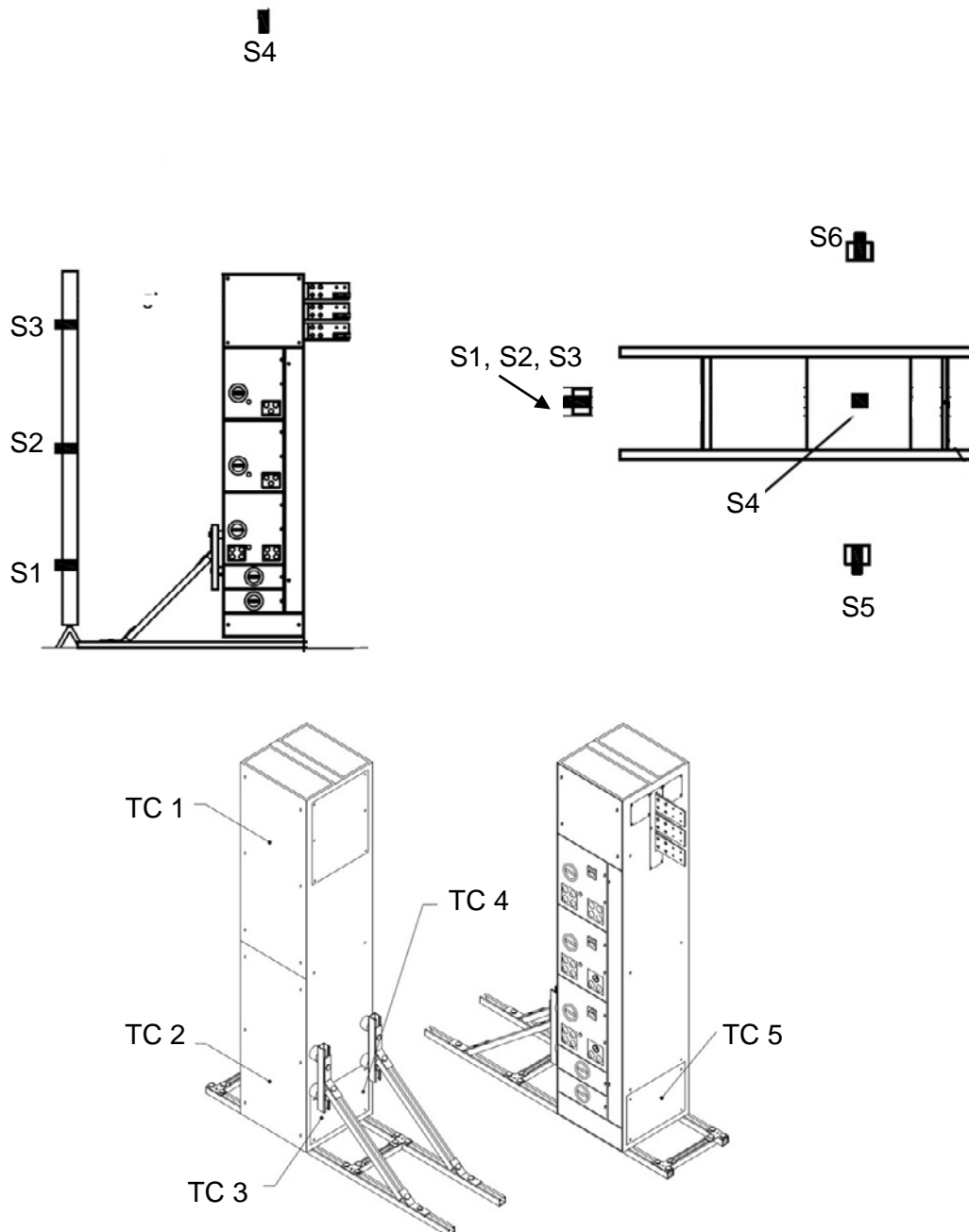


Figure 3.5-1. MCC Calorimeter and TC Location

Table 3-2. MCC Calorimeter and TC Locations.

Slug or TC	From Floor cm (in)	Position	Slug or TC Name
S1	90 (35.5)	Left side (LS)	S1-LS-36-LS
S2	119 (47)	Left side	S2-LS-47-CL
S3	198 (78)	Left side	S3-LS-78-CL
S4	381 (150)	Top (T)	S4-T-150-CL
S5	79 (31)	Front (F)	S5-F-31-CL
S6	79 (31)	Rear (R)	S6-R-31-CL
TC1	198 (78)	Rear	TC1-R-78-CL
TC2	61 (24)	Rear	TC2-R-24-CL
TC3	61 (24)	Left Side	TC3-LS-24-R
TC4	61 (24)	Left Side	TC4-LS-24-F
TC5	61 (24)	Right Side (RS)	TC5-RS-24-CL

*TC3, TC4, TC5 data was corrupted for all tests and no results are provided.

3.6 MCC Test Pressure Instrumentation

Two Dynisco PT150-50 strain-gauge type pressure transducers were used. The pressure transducer was isolated from the cabinet with a fiber-reinforced rubber tube. The sensors are on the left side of the cabinet. The gauges were in PVC pipe to protect them from fire.

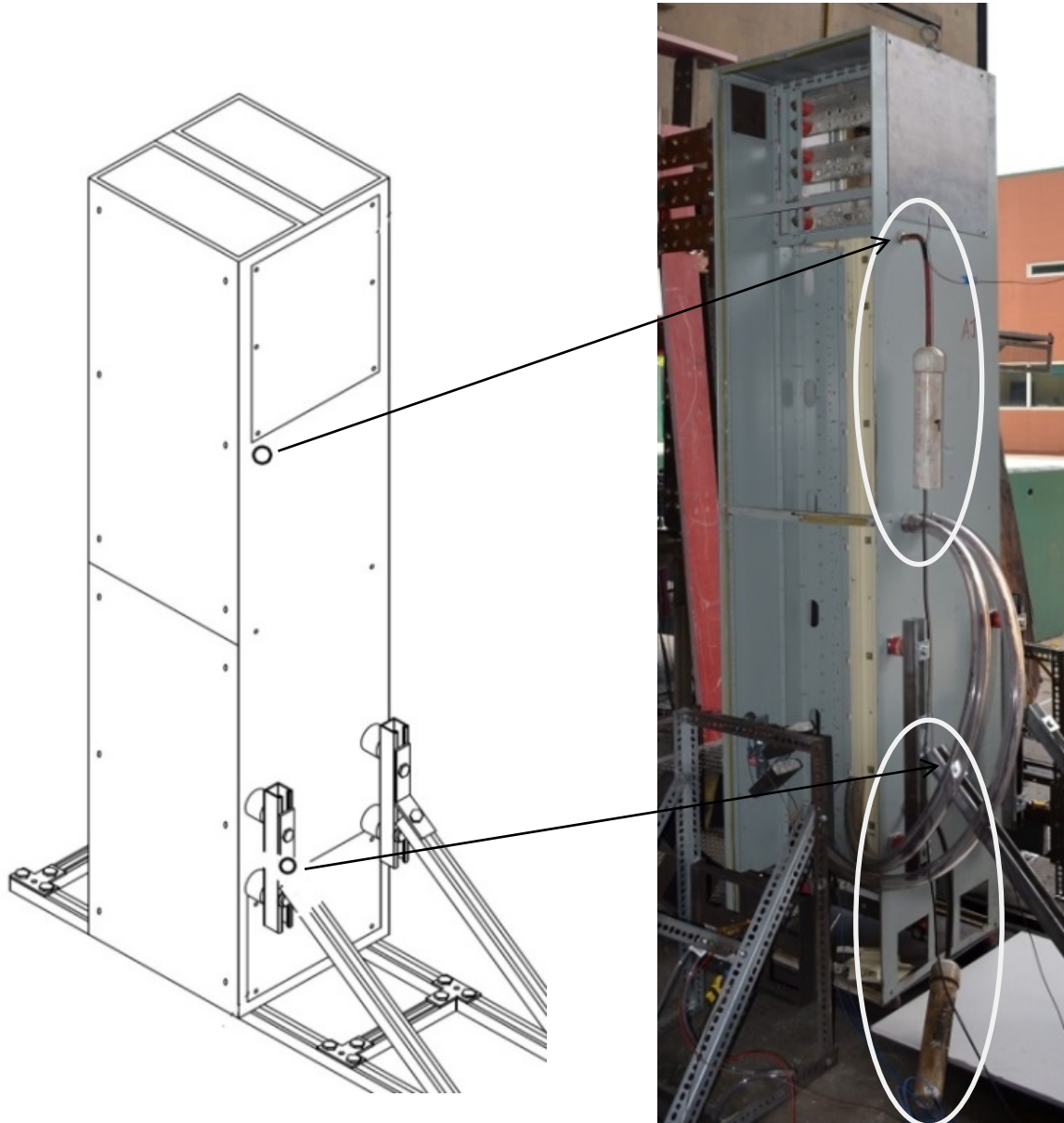


Figure 3.6-1. MCC Pressure Measurement Locations

3.7 MCC Test 1 Key Observations

This cabinet test was initiated at 484 V and 21.4 kA with a target duration of 2 seconds. The arc quenched at 0.145 seconds with a total energy of 1.7 MJ. Figure 3.7-1 shows the explosion after the arc at about 0.050 seconds.

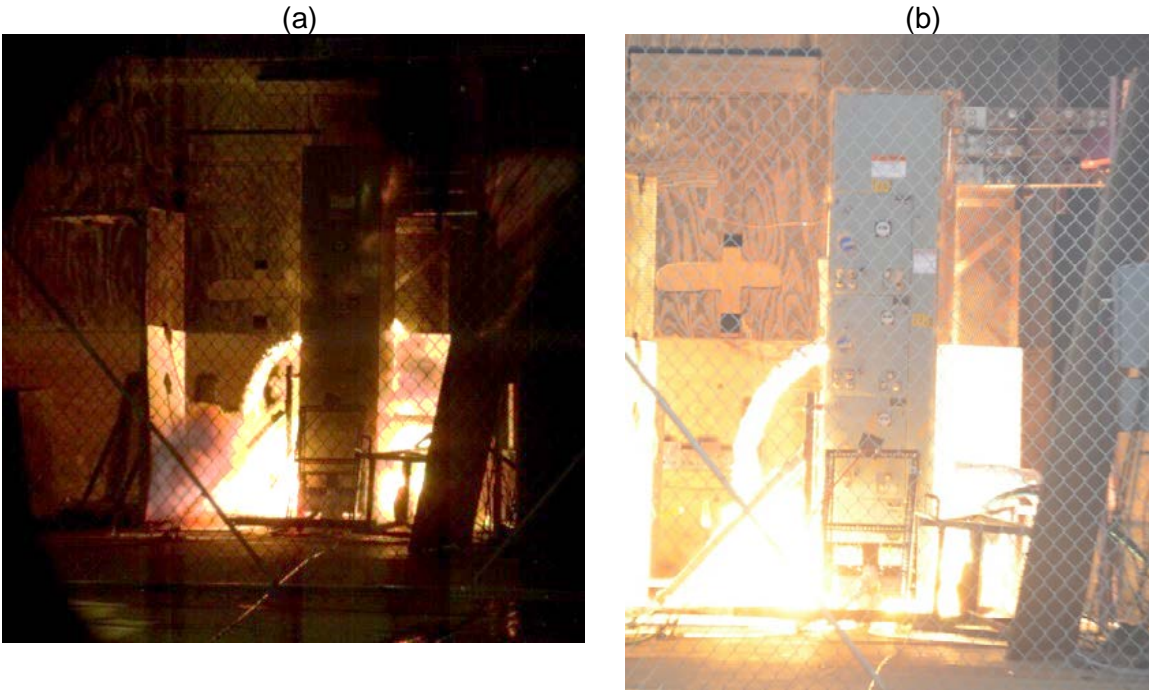


Figure 3.7-1. MCC Test 1 Arc

There was no ensuing fire and the thermal image in Figure 3.7-2 shows only a brief burst of heat from hot gas escaping at the bottom at the time of the arc. The FLIR camera was set at the maximum 750 °C and no residual heat was detected. The only visible response by the FLIR was during the arc.

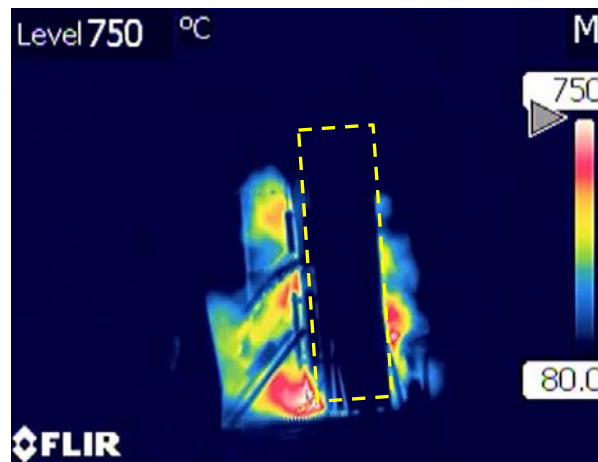


Figure 3.7-2. MCC Test 1 Thermal Image
(the yellow box represents the cabinet perimeter)

Damage was minor with only light charring and soot at the bottom of the cabinet and on a white external poster-board target, as seen in Figure 3.7-3(a). As shown in Figure 3.7-3(b) the top rear panel blew off during the arc; to avoid this in the future tests, steel bands were used to hold the cabinet panels in place.

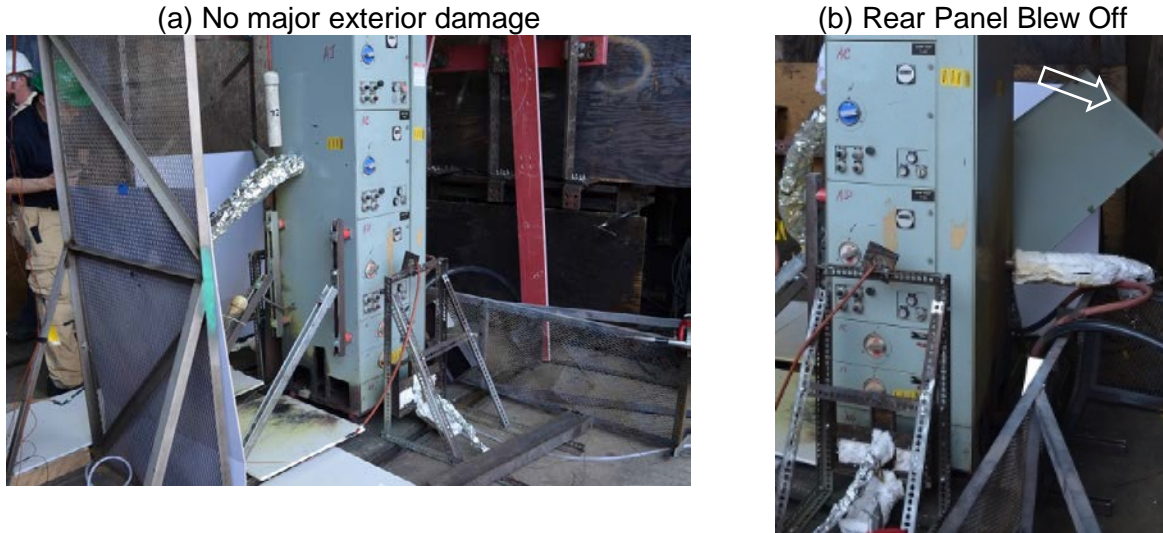
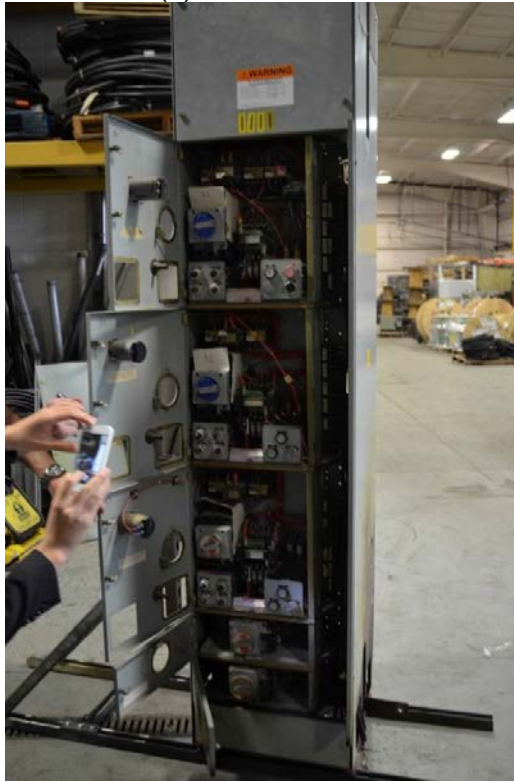


Figure 3.7-3. MCC Test 1 Exterior Damage

Figure 3.7-4(a) shows only minor soot deposits on the interior, and no evidence of an ensuing cable fire (cables are on the right in the picture). Figure 3.7-4(b) shows no damage to the white plastic composite arc chutes covering the bus bars and only minor melting of the strut near the ends of the bus bars where the arc briefly attached. The bus bars burned upward and cannot be seen in the photo under the arc chutes. The bottom 15.24 cm (6 in) of bus duct had been removed before the test to expose the bus bars. Based on this result, it appeared that the arc chutes were obstructing the arc path, causing the arc to extinguish. In order to allow the arc to fully occur, the arc chutes were cut further from the end of the bus bars in Tests 2 and 3.

(a) No cable fire



(b) No major damage to arc chutes



(c) lower bus bar damage



Figure 3.7-4. Test 1 Exterior and Interior Damage

3.7.1 MCC Test 1 Calorimetry Data

Temperatures measured at the slug locations are shown in Figure 3.7-5. The arc quenched at 0.145 seconds. Slugs S5 and S6 recorded high noise during the arc, probably due to EMI; the power supply was directly next to the slug calorimeters. The highest temperature at the end of the arc was measured on the left side, 90 cm (35.5 in) from the floor (S1). After the arc these temperatures stopped increasing and there was no flux after that since there was no ensuing fire. Other slugs had a similar steady temperature response after the arc.

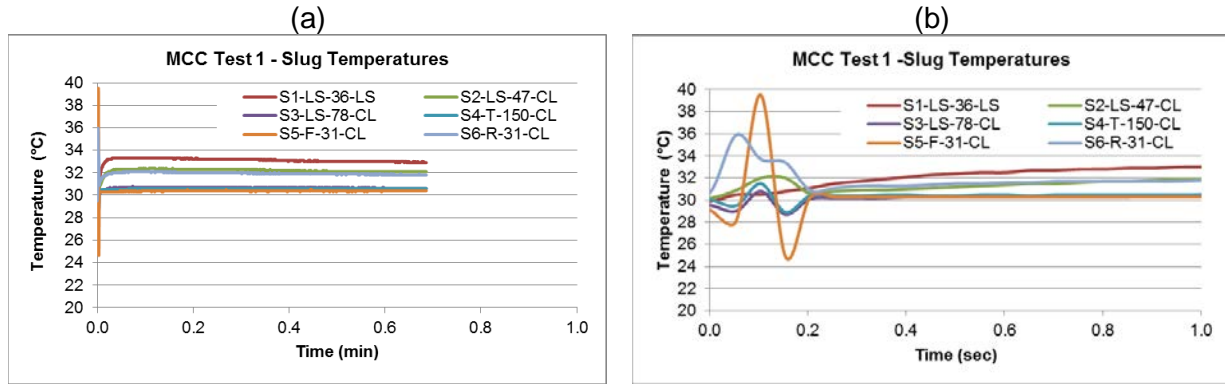


Figure 3.7-5. MCC Test 1 Calorimetry Temperature Data

Table 3-3 shows the flux results based on the ASTM F1959 method in Appendix A using the change in temperature (ΔT) between the start and end of the arc. The maximum flux of 38 kW/m² is reported at the bottom, left side (S1). The maximum slug temperatures are also shown to indicate the maximum temperature a metal object could reach during the arc.

Table 3-3. MCC Test 1 Flux Results.

Slug	ΔT (°C)	Flux (kW/m ²)	Max T °(C)
S1-LS-36-LS	1.9	38	33
S2-LS-47-CL	0.8	16	32
S3-LS-78-CL	0.4	8	31
S4-T-150-CL	0.1	2	32
S5-F-31-CL	0.1	2	40
S6-R-35-CL	1.8	36	36

3.7.2 MCC Test 1 Temperature Data

The temperatures measured by the TCs are shown in the Figure 3.7-6. Table 3-4 shows the maximum temperature results. The thermocouple maximum temperature is a general indication of the air temperature 15.2 cm (6 in) from the cabinet. The highest recorded temperature was seen at TC1, located at the rear top where the panel blew off. The TCs cannot be used to estimate flux.

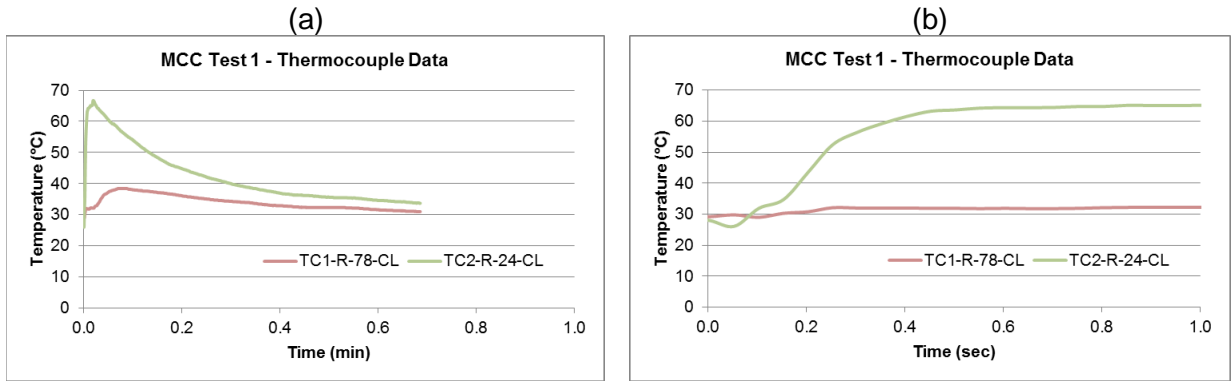


Figure 3.7-6. MCC Test 1 Thermocouple Data

Table 3-4. MCC Test 1 TC Results.

TC	Max T (°C)
TC1-R-78-CL	38
TC2-R-24-CL	67
TC3-LS-24-R	*
TC4-LS-24-F	*

*Data was corrupt

3.7.3 MCC Test 1 Pressure Data

The pressures during the arc are seen in Figure 3.7-7. The two pressure probes, top and bottom, exhibited similar noise. The maximum pressure at the bottom, measured closer to the arc was higher and occurred earlier than the pressure measurement at the top. The top pressure measurement probe was further from the arc location. The maximum pressures are indicated by the arrows in Figure 3.7-7(c) and (d). The pressure dropped quickly and the pressure after the peak was low when the back panel blew off.

The pressure analysis methods are in Appendix A and involved picking the maximum near the start of the arc then including a nominal uncertainty for the noise in the signal just before the arc.

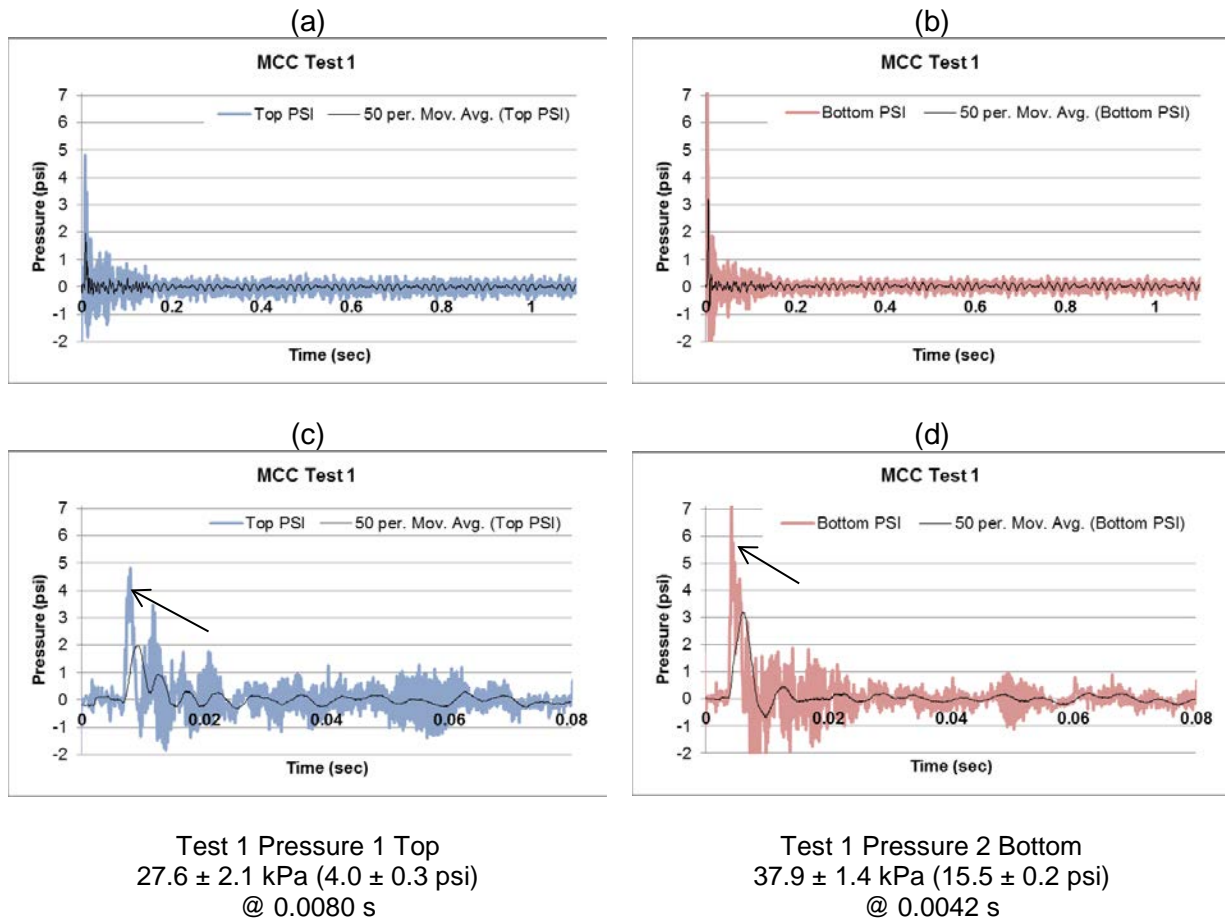


Figure 3.7-7. MCC Test 1 Pressure Data

3.7.4 MCC Test 1 Arc Energy

The arc duration was 0.145 seconds with total energy of 1.7 MJ, seen in Figure 3.7-8. The energy analysis methods are in Appendix A. The “Energy” is calculated as volts multiplied current multiplied by the time step and each time step is shown. “Energy Total” is the cumulative sum of the energy in each time step.

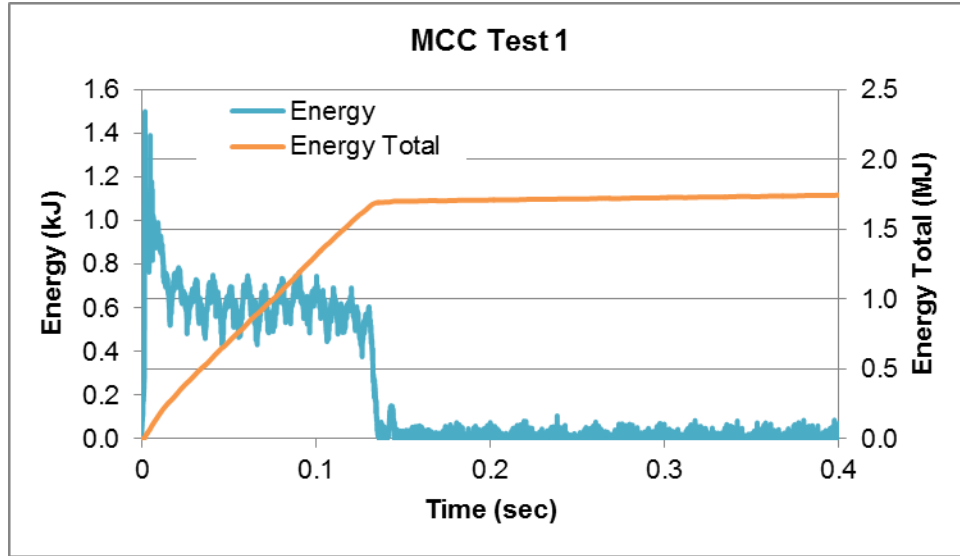


Figure 3.7-8. MCC Test 1 Arc Energy

3.8 MCC Test 2 Key Observations

This cabinet test was initiated at 492 V and 34.1 kA with a target duration of 2 seconds. The arc quenched at 0.952 seconds with a total energy of 17.4 MJ. There was no ensuing internal cable fire, and only soot deposits on the cables.

The Test 2 arc started at the bottom of the cabinet, as planned, but quenched at about 0.1 seconds then the hot gases from the initial arc moved to the top of the cabinet and caused the horizontal bus bars at the top of the cabinet to arc to the left side of the cabinet at 0.141 seconds as shown in Figure 3.8-1. This additional arc lasted until 0.952 seconds after arc initiation and caused significant damage to the cabinet.

As discussed earlier, six steel bands were wrapped around the MCC to hold the cabinet panels in place. In addition, to prevent the arc chutes from interfering with the arc, the bottom 61 cm (24 in) of the arc chutes were cut and removed.

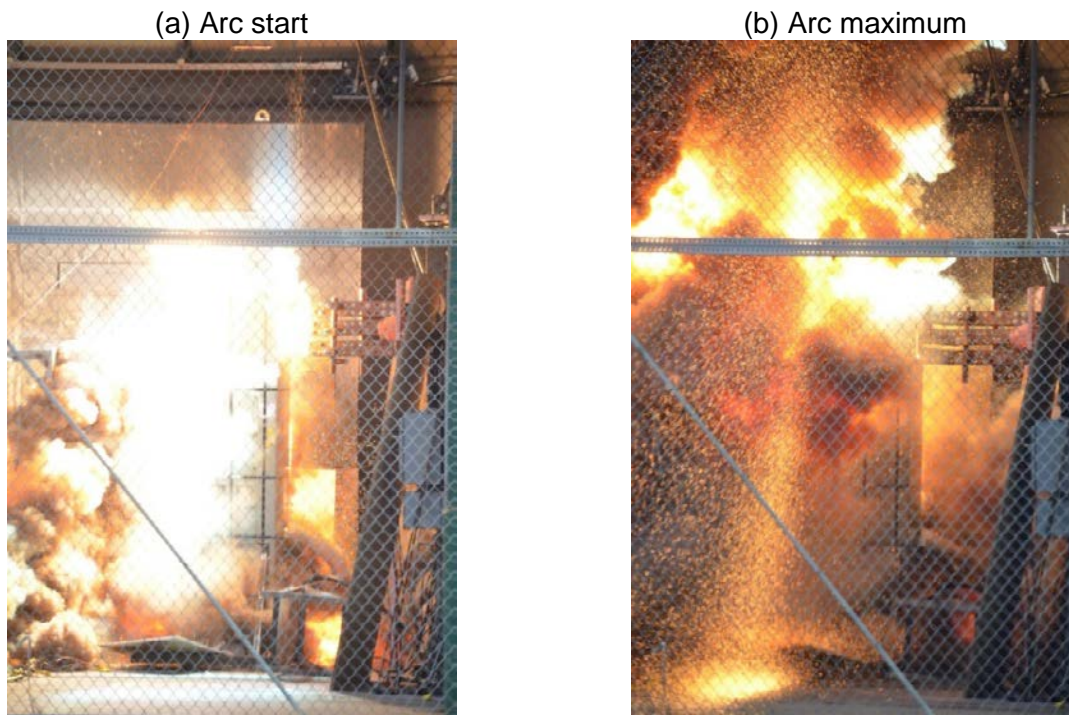


Figure 3.8-1. MCC Test 2 Arcs at Bottom and Top

The arc sequence is shown in Figure 3.8-2: (a) the initial arc at 0.018 seconds, (b) the initial arc almost quenches and is not visible, (c) the hot gases traveled up the right side of the cabinet and some escaped out of the panels (at this point the gases are about half way up the cabinet), and (d) the hot gases caused the arc at the top horizontal bus bars. This is the only test where the arc quenched at the ignition point at the arc wire followed by the hot gases causing a second arc in a separate location.

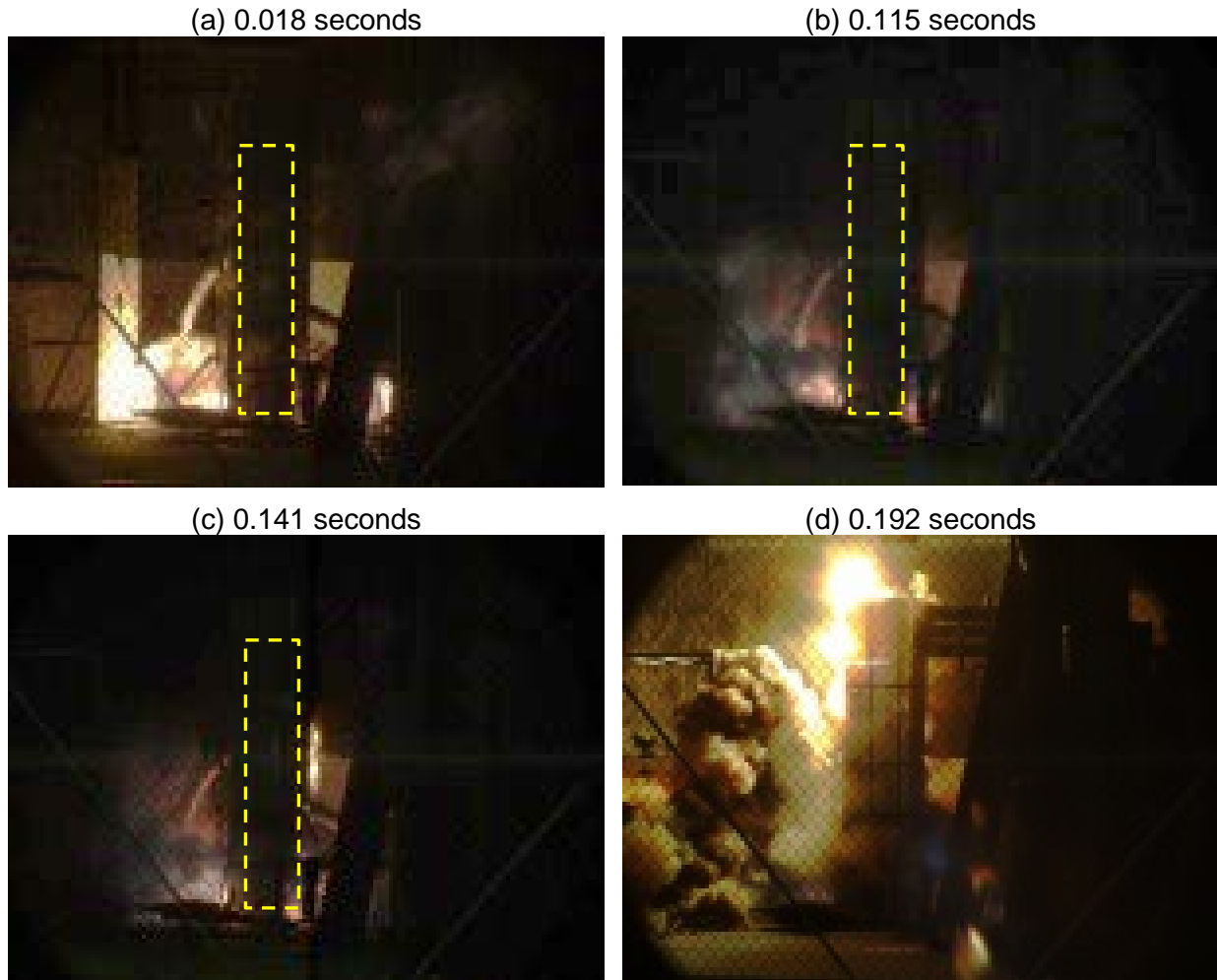


Figure 3.8-2. MCC Test 2 Sequence for 2 Arcs
(the cabinet is outlined in yellow)

Figure 3.8-3 shows thermal images during the arc. Based on the poor sensitivity in the MCC Test 1 FLIR images, the FLIR was set to a fixed 350 °C (662 °F) maximum temperature. Figure 3.8-3(a) shows a plume of plasma and hot gas coming out of the rectangular openings at the left bottom of the cabinet and gases escaping from the openings to the left. The heat was initially at the arc at the bottom then the heat progressed up the right side of the cabinet, as shown in Figure 3.8-3(b) and the second arc the top left occurred. Figure 3.8-3(c) shows there were large balls of hot gas and plasma on the left side of the cabinet, extending out 1 to 2 meters. However, 30 seconds after the arc shows there were no internal fires on the left rear even where the hot gas contacted the target cardboard poster boards (see Figure 3.8-3(d)). Some poster boards that were placed as targets near the front left out of view of the FLIR did ignite. After the arc extinguished, cooling was seen in the area at the top where the panels had burned through, as shown in Figure 3.8-3(e), indicating no sustained internal fire. The cabinet exterior showed no other hotspots that would indicate an internal fire as the top panels cooled.

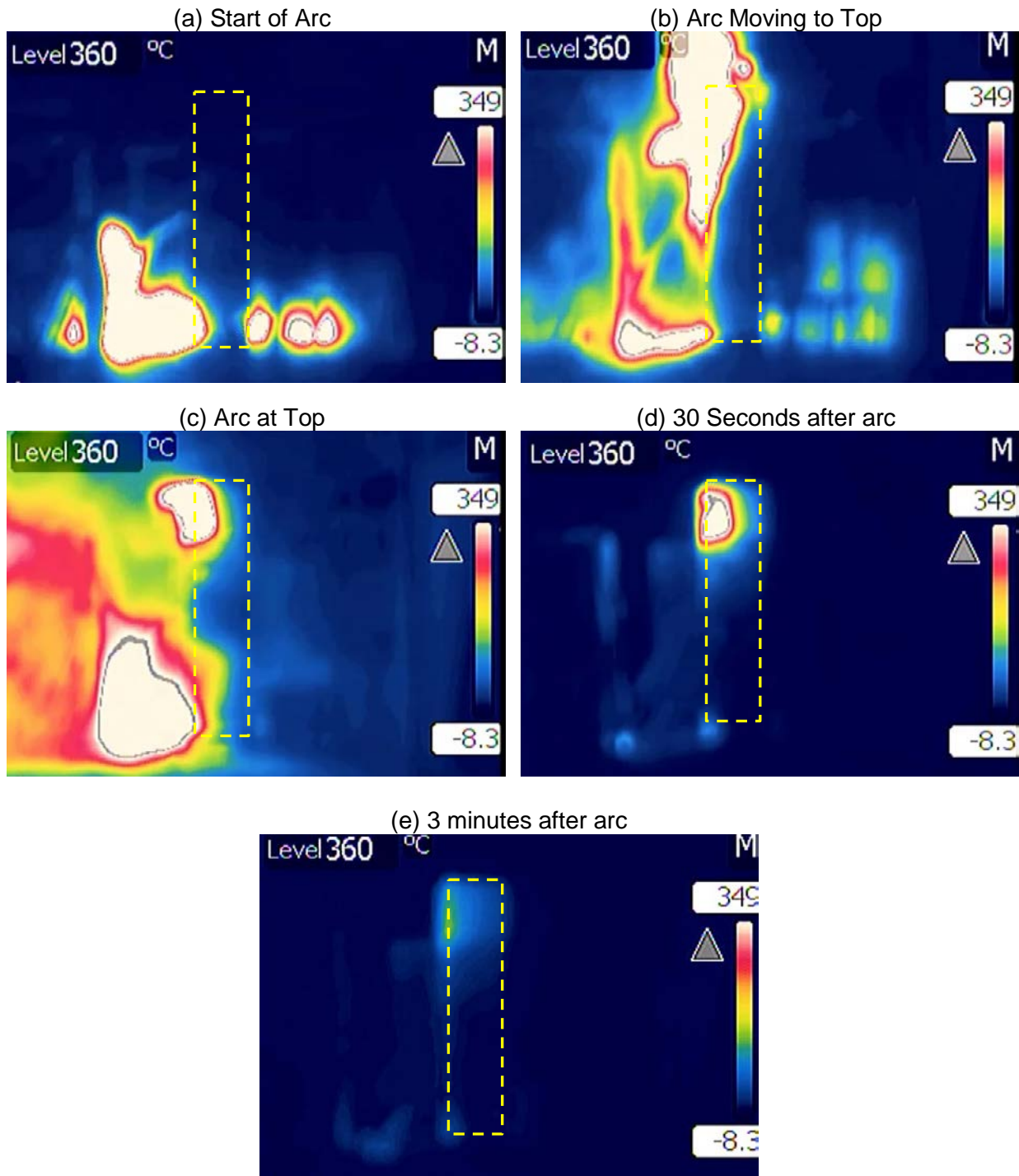


Figure 3.8-3. MCC Test 2 Thermal Images

Figure 3.8-4(a) shows there was heavy soot damage and copper coating on the exterior of the cabinets with heavy damage at the top. No panels were blown off but the front top panel opened about 5 cm (2 in). Figure 3.8-4(b) shows that the exterior top left panel was burned through by the strong arc at the top bus bars. About 5 cm (2 in) of the bus bars burned until the arc reached the vertical strut supporting the bus bars and the arc extinguished, as shown in Figure 3.8-4(c).

(a) Exterior damage



(b) Top Arc Burn Through



(c) Top Bus Bar Damage



Figure 3.8-4. MCC Test 2 Exterior Damage

Figure 3.8-5(a) shows that the thin bus bars at the bottom bent outward where the bottom arc quickly quenched. The arc appears to have attached to the bottom horizontal strut and when the bus bars bent they were too far from the bar to maintain the arc. Figure 3.8-5(b) shows interior soot deposits along the cables but the internal cables on the right did not ignite.

(a) Bottom Arc Damage



(b) No cable fire



Figure 3.8-5. MCC Test 2 Interior Damage

3.8.1 MCC Test 2 Calorimetry Data

Temperatures measured at the slug locations are shown in Figure 3.8-6. The arc quenched at 0.952 seconds. Several slugs had high noise during the arc, probably due to EMI; the power supply was directly next to the slug calorimeters. The highest temperature at the end of the arc was at top left side (S3), which was struck by flames. The highest slug response that was not struck by flames was at the rear of the cabinet (S6).

All slugs except S2 showed cooling temperatures after the arc because there was no ensuing fire. The temperature is increasing after 0.2 minutes at the left side (S2) because the poster board used to detect debris ignited and the slug was in the flames. Although Slug 5 was only 12.7 cm (5 in) from the panel (rather than the usual 0.91 m (3 ft)), it had low response.

The left side slugs (S1 through S3) had very high response from the arc breaking through the top left panel and the hot gases and plasma exiting directly to the slugs.

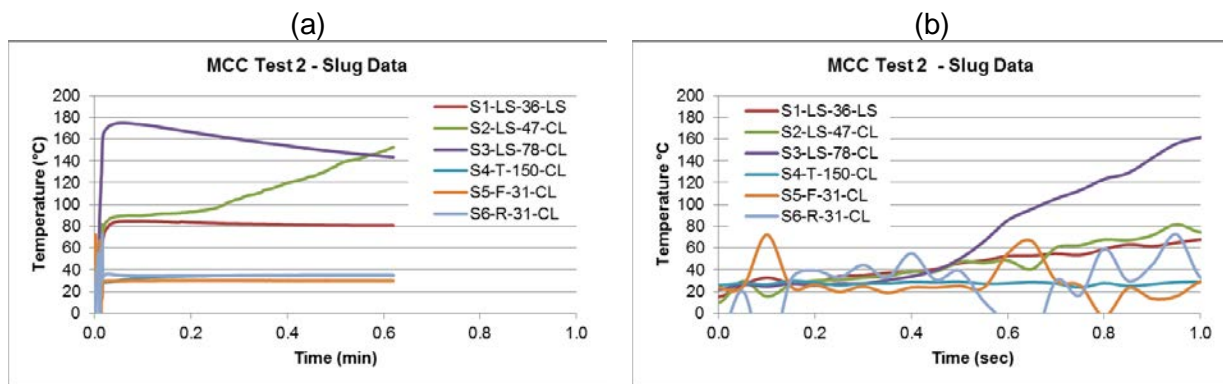


Figure 3.8-6. MCC Test 2 Calorimetry Temperature Data

Table 3-5 shows the flux results based on the ASTM F1959 method in Appendix A using the change in temperature (ΔT) between the start and end of the arc. The maximum valid flux of 46 kW/m², measured at the rear (S6) is reported. The maximum slug temperatures are also shown to indicate the maximum temperature a metal object would reach during the arc and after the arc. Except for at the left side, center (S2), all of these maximums were shortly after the arc extinguished. At this location (S2), the maximum was during the external ensuing fire (the poster boards in front of the cabinet).

Table 3-5. MCC Test 2 Flux Results.

Slug	ΔT ($^{\circ}C$)	Flux (kW/m^2)	Max T ($^{\circ}C$)
S1-LS-36-LS	47.7	246	85
S2-LS-47-CL	54.6	282*	153
S3-LS-78-CL	140.6	736*	175
S4-T-150-CL	2.4	12	35
S5-F-31-CL	3.4	17	30
S6-R-35-CL	9.0	46	73

* Slugs in contact with flames, therefore calculated flux is not valid, see Appendix A, Section A.1

3.8.2 MCC Test 2 Temperature Data

The temperatures measured by the TCs are shown in Figure 3.8-7 and Table 3-6 shows the maximum temperature results. The thermocouple maximum temperature is a general indication of the air temperature 15.2 cm (6 in) from the cabinet and as expected TC1 at the rear top where near the final arc location had the highest temperature. TC1 was also near the point where the hot gases and plasma were released as shown in Figure 3.8-3(b). The TCs cannot be used to practically estimate flux.

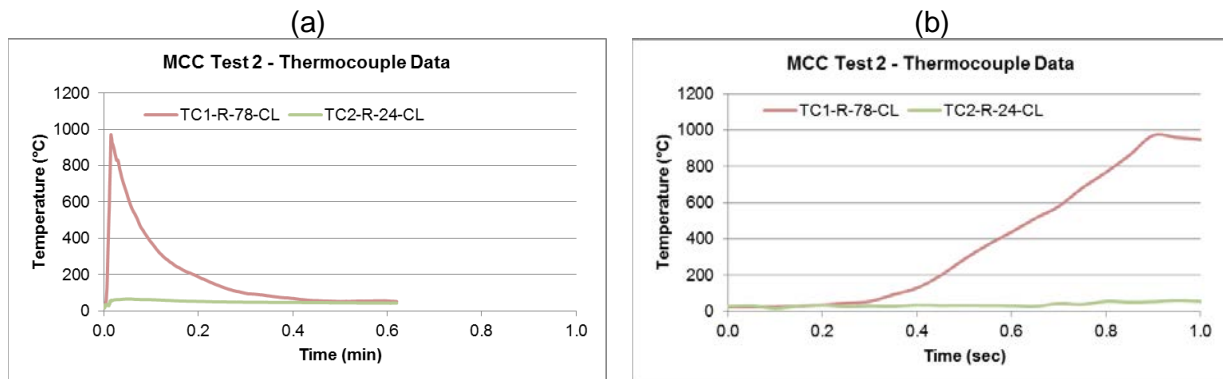


Figure 3.8-7. MCC Test 2 Thermocouple Data

Table 3-6. MCC Test 2 TC Results.

TC	Max T ($^{\circ}C$)
TC1-R-78-CL	970
TC2-R-24-CL	65
TC3-LS-24-R	*
TC4-LS-24-F	*
TC5-RS-24-CL	*

*Data was corrupt

3.8.3 MCC Test 2 Pressure Data

The pressures during the arc are seen in Figure 3.8-8. The two pressure probes, top and bottom, exhibited similar noise. There were noise spikes at 0.87 seconds on the top and 0.64 seconds on the bottom. The bottom pressure, measured closer to the arc, had a higher maximum and occurred earlier than the top pressure, which was measured further from the arc. The maximum pressures are indicated by the arrows in Figure 3.8-8(c) and (d).

The pressure analysis methods are in Appendix A and involved picking the maximum near the start of the arc then including a nominal uncertainty for the noise in the signal just before the arc.

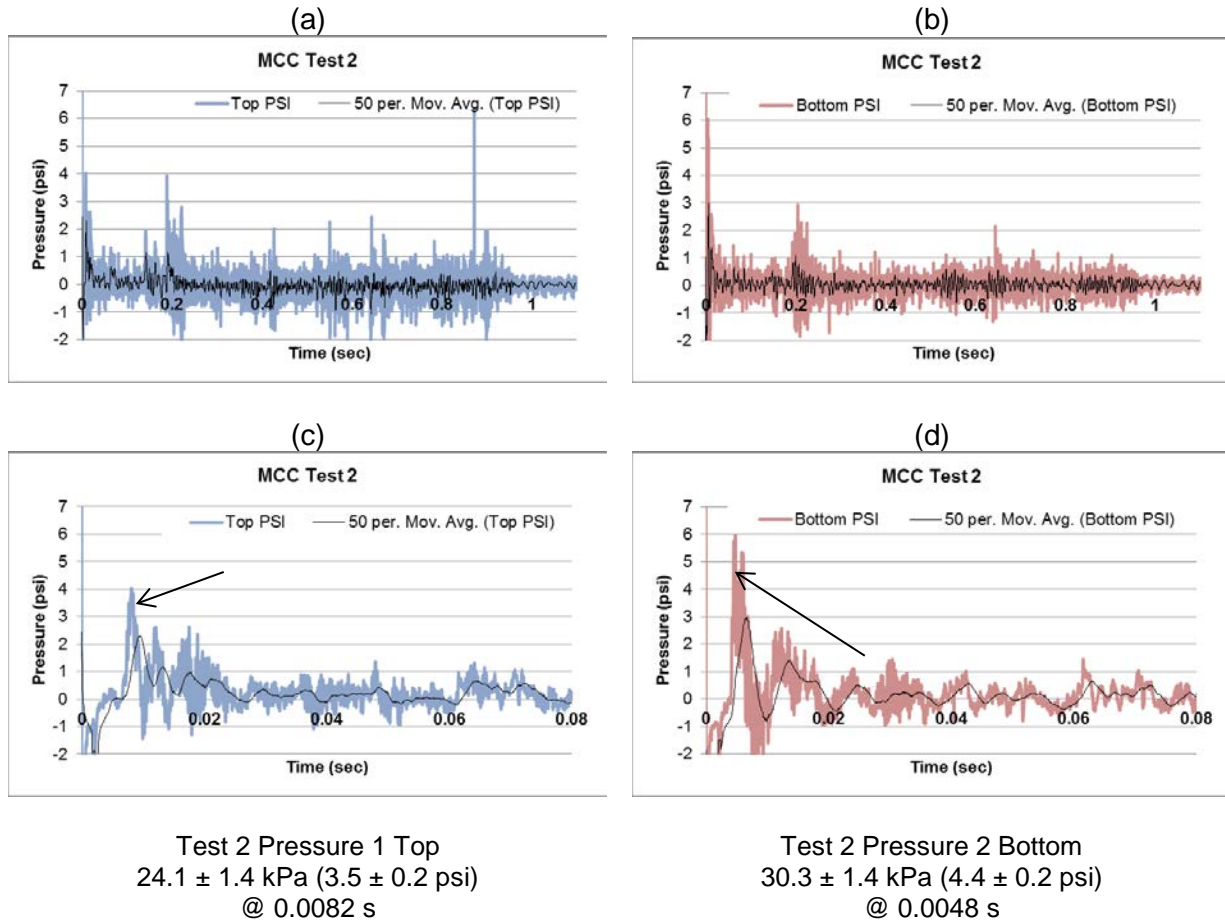


Figure 3.8-8. MCC Test 2 Pressure Data

3.8.4 MCC Test 2 Arc Energy

The arc duration including at the bottom and top positions was 0.952 seconds with total energy of 17.4 MJ, as shown in Figure 3.8-9. The energy analysis methods are in Appendix A. The “Energy” is calculated as volts multiplied current multiplied by the time step and each time step is shown. “Energy total” is the cumulative sum of the energy in each time step. The initial arc at the bottom almost quenched about 0.154 seconds then the arc re-struck in the top position 0.19 seconds.

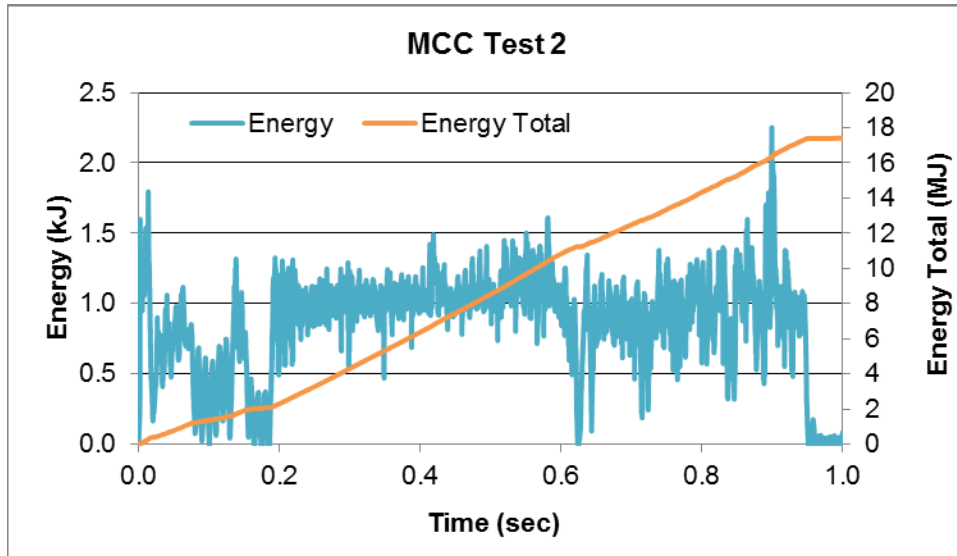


Figure 3.8-9. MCC Test 2 Arc Energy

3.9 MCC Test 3 Key Observations

This cabinet test was initiated at 484 V and 40.4 kA with a target duration of 2 seconds. The arc quenched at 0.256 seconds with a total energy of 4.2 MJ. For Test 3, the arc chutes were removed as in Test 2. Red board bands were placed across the bus bars at the bottom in an attempt to prevent the bus bar from bending, as observed in MCC Test 2. The arc broke the bands and the arc quenched. Figure 3.9-1 shows the arc at about 0.050 seconds. The arc was very short and the damage was minor. There was no ensuing cable fire.

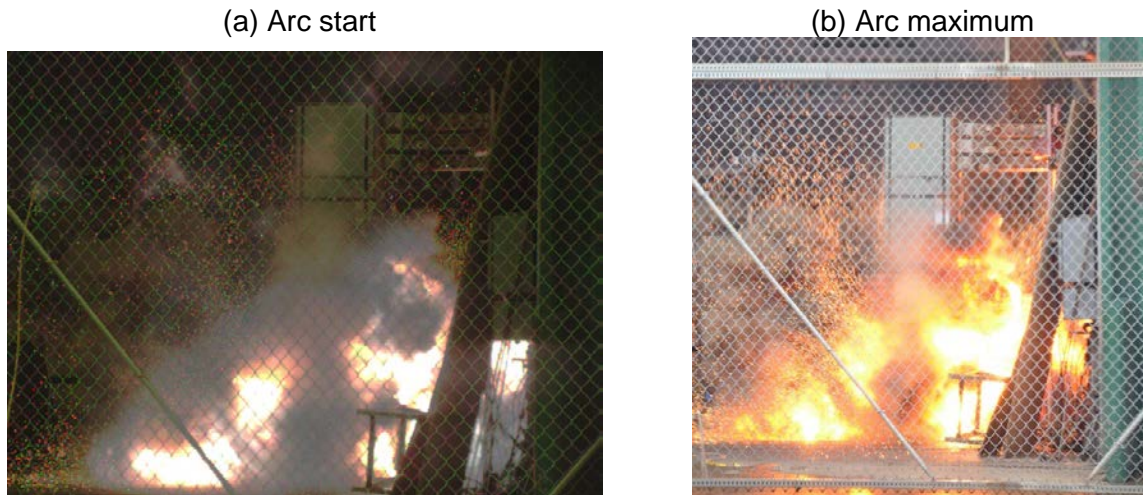


Figure 3.9-1. MCC Test 3 Arc

Figure 3.9-2 shows FLIR images from the rear, left corner of the tests cell (other videos are from the front) to get a close view if the arc moved to the top of the MCC. In these views the right side of the cabinet is on the left side and the camera was turned upward to view more of the MCC. The FLIR was set at a constant 355 °C (671 °F) maximum. Arc plasma and hot gases escaped the lower part of the cabinet during the arc. After the arc, there was no detectable indication of high temperatures on the exterior of the cabinet or of internal fires.

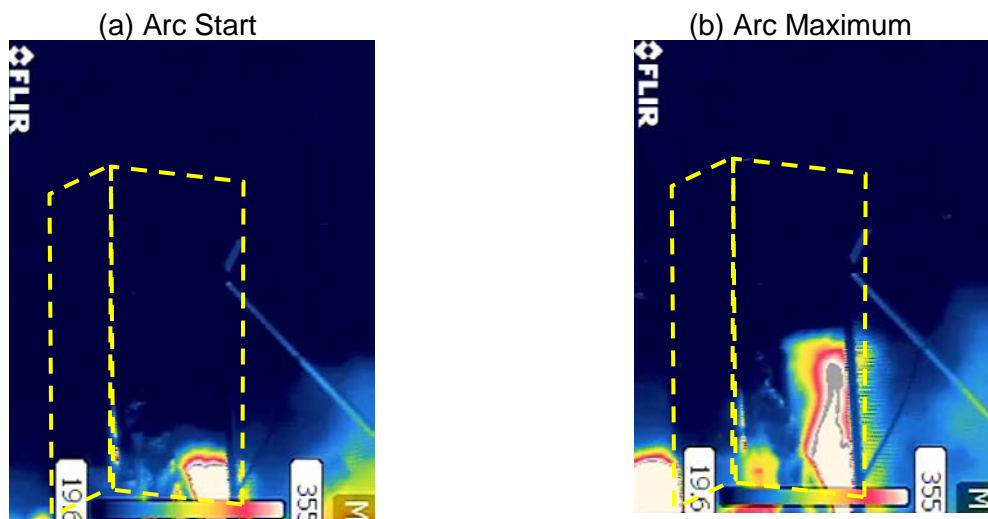


Figure 3.9-2. MCC Test 3 Thermal Images (Rear View)

Figure 3.9-3 shows the only major exterior damage; the rear top panel opened about a 1 centimeter (0.5 in) but was held in place by steel bands and did not blow off.



Figure 3.9-3. MCC Test 3 Exterior Damage.

Figure 3.9-4 shows the lower bus bar damage for the arc position in Test 3. Figure 3.9-4(a) shows the bus bar configuration before the test. The thin, copper bus bars were held in place by three red boards (fiber-reinforced composite) at approximately 20.3 cm (8 in), 35.6 cm (14 in), and 50.8 cm (20 in) from the bottom as shown in Figure 3.9-4(a). Figure 3.9-4(b) and (c) shows that the bus bars bent despite the bands and caused the arc to quench.

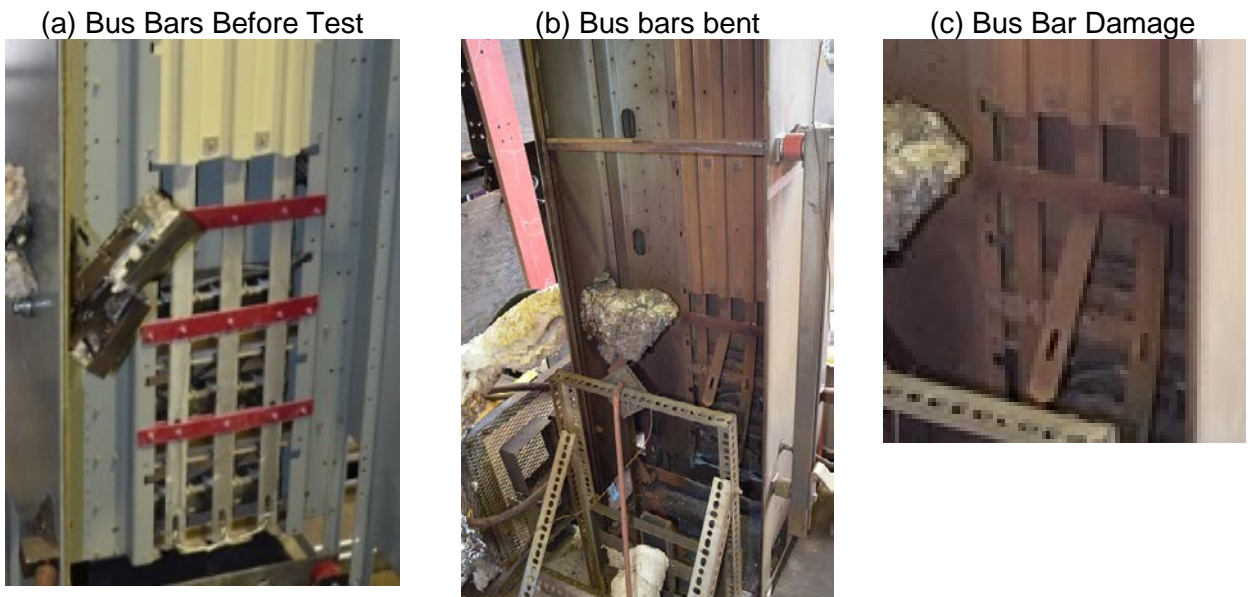


Figure 3.9-4. MCC Test 3 Interior Damage

3.9.1 MCC Test 3 Calorimetry Data

Temperatures measured at the slug locations are shown in Figure 3.9-5. The arc quenched at 0.256 seconds. All slugs had high noise during the test, probably due to EMI; the power supply was directly next to the slug calorimeters. The highest temperature at the end of the arc was measured at the bottom left side (S1) but this slug was contacted by flames when the arc initiated. S2 and S3 were also contacted by flames. All slugs had steady temperatures after the arc because there was no ensuing fire.

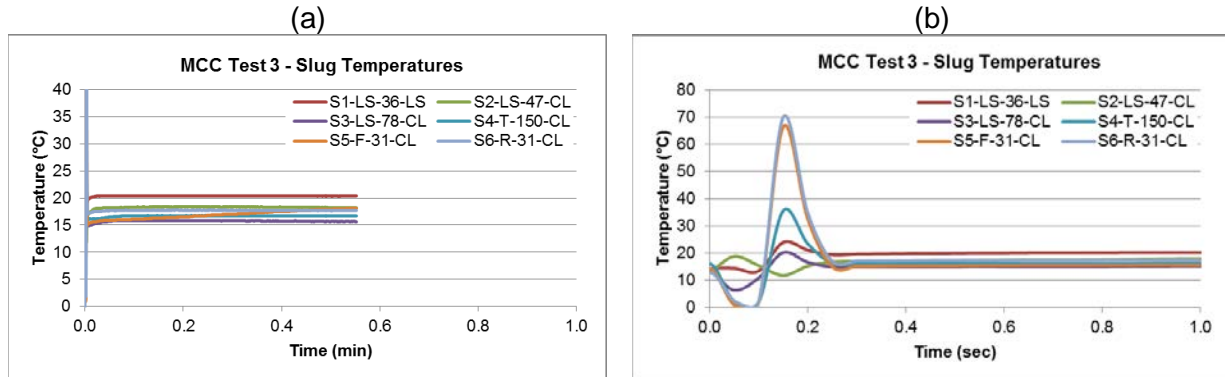


Figure 3.9-5. MCC Test 3 Calorimetry Data

Table 3-7 shows the flux results based on the ASTM F1959 method in Appendix A using the change in temperature (ΔT) between the start and end of the arc. The maximum flux of 102 kW/m² was seen at the left side (S1). The maximum slug temperatures are also shown to indicate the maximum temperature a metal object could reach.

Table 3-7. MCC Test 3 Flux Results.

Slug	ΔT (°C)	Flux (kW/m ²)	Max T (°C)
S1-LS-36-LS	5.0	102	20
S2-LS-47-CL	2.1	43	18
S3-LS-78-CL	0.3	6	16
S4-T-150-CL	0.2	4	17
S5-F-31-CL	1.2	24	18
S6-R-35-CL	2.2	45	18

3.9.2 MCC Test 3 Temperature Data

The temperatures measured by the TCs are shown in the Figure 3.9-6. Table 3-8 shows the maximum temperature results. The thermocouple maximum temperature is a general indication of the air temperature 15.2 cm (6 in) from the cabinet and as expected TC2 at the rear bottom near the arc had the highest temperature. The TC2 temperatures were lower than expected because hot gas should have escaped from the panel opening shown in Figure 3.9-3. The TCs cannot be used to estimate flux.

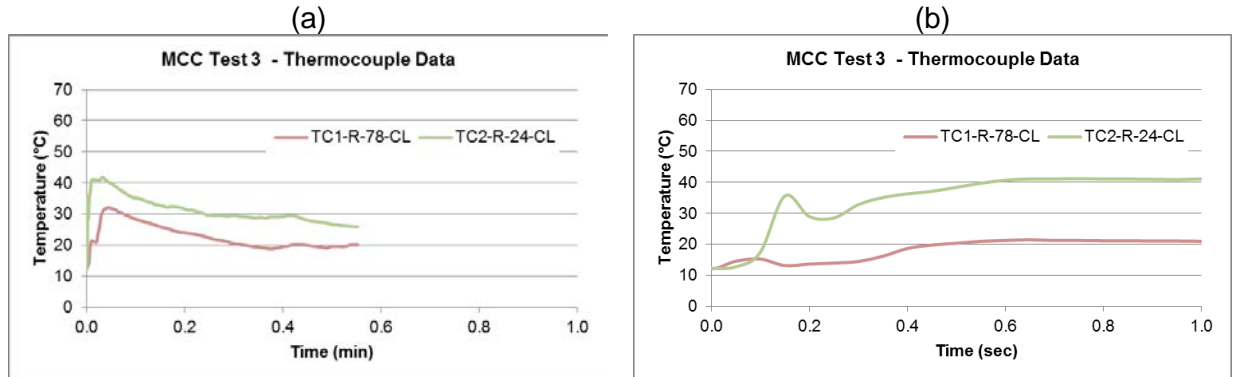


Figure 3.9-6. MCC Test 3 Thermocouple Data

Table 3-8. MCC Test 3 TC Results.

TC	Max T (°C)
TC1-R-78-CL	32
TC2-R-24-CL	42
TC3-LS-24-R	*
TC4-LS-24-F	*
TC5-RS-24-CL	*

*Data was corrupt

3.9.3 MCC Test 3 Pressure Data

The pressures during the arc are seen in Figure 3.9-7. The two pressure probes, top and bottom, exhibited similar noise. There was a significant spike in noise at 0.24 seconds at the bottom pressure. The bottom pressure, measured closer to the arc, had a higher maximum and occurred earlier than the top pressure, which was measured further from the arc.

The pressure analysis methods are in Appendix A and involved picking the maximum near the start of the arc then including a nominal uncertainty for the noise in the signal just before the arc.

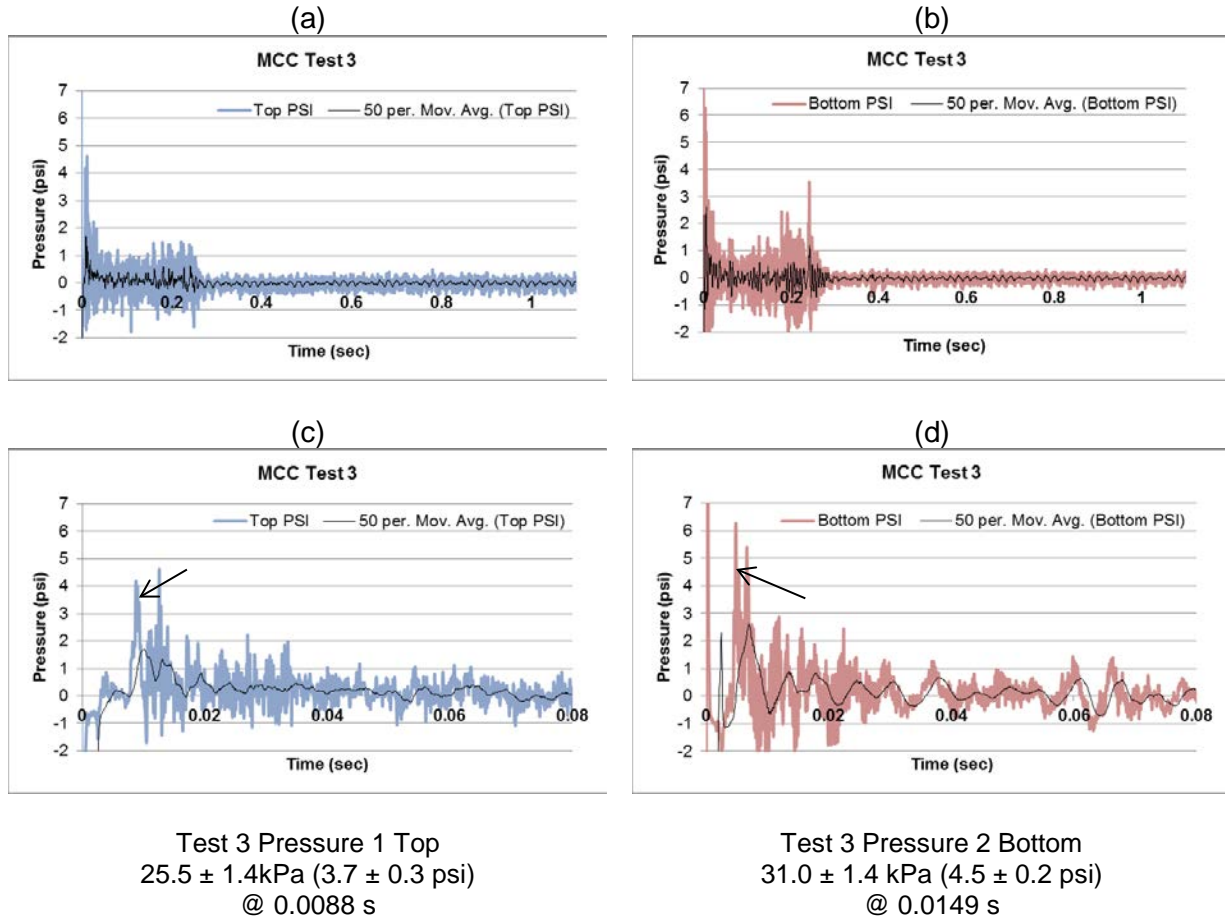


Figure 3.9-7. MCC Test 3 Pressure Data

3.9.4 MCC Test 3 Arc Energy

The arc duration was 0.256 seconds with total energy of 4.2 MJ, as seen in Figure 3.9-8. The energy analysis methods are in Appendix A. The “Energy” is calculated as volts multiplied current multiplied by the time step and each time step is shown. “Energy total” is the cumulative sum of the energy in each time step.

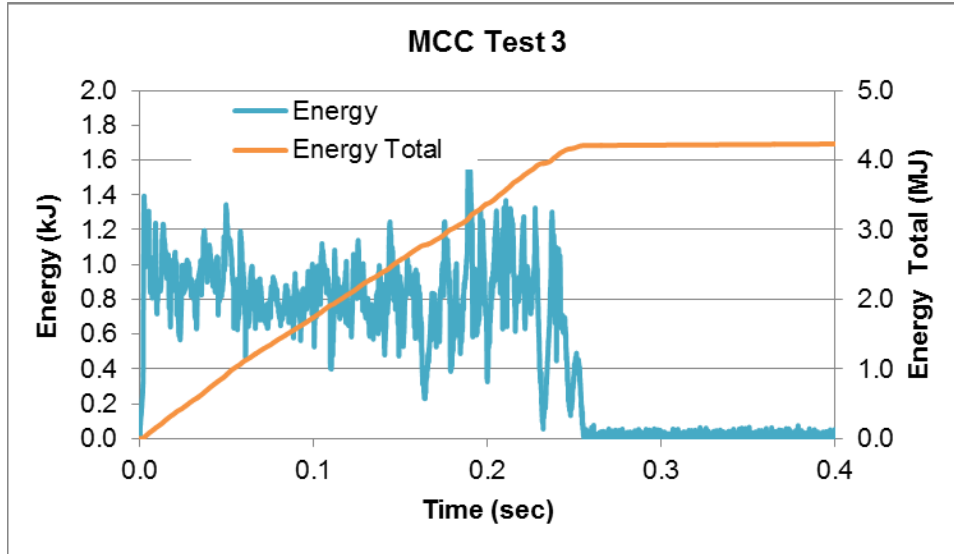


Figure 3.9-8. MCC Test 3 Arc Energy

3.10 MCC Test 4 Key Observations

The cabinet from Test 3 was left in place and reused for Test 4 with the arc wire at the top bus bars to repeat the second arc that was observed in Test 2. This cabinet test was initiated at 492 V and 46.4 kA and a target duration of 2 seconds. The arc quenched at 0.922 seconds with a total energy of 17.6 MJ. Figure 3.10-1 shows the explosion at 0.1 sec and 0.8 sec after the arc. There was a small metal fire at the top bus bars for a few minutes but there was no major ensuing cable fire. The plasma escaped through the small cracks between the panels and burned through the steel bands. The top front panel was blown off and traveled about 3.66 m (12 ft) as shown in Figure 3.10-1(a).

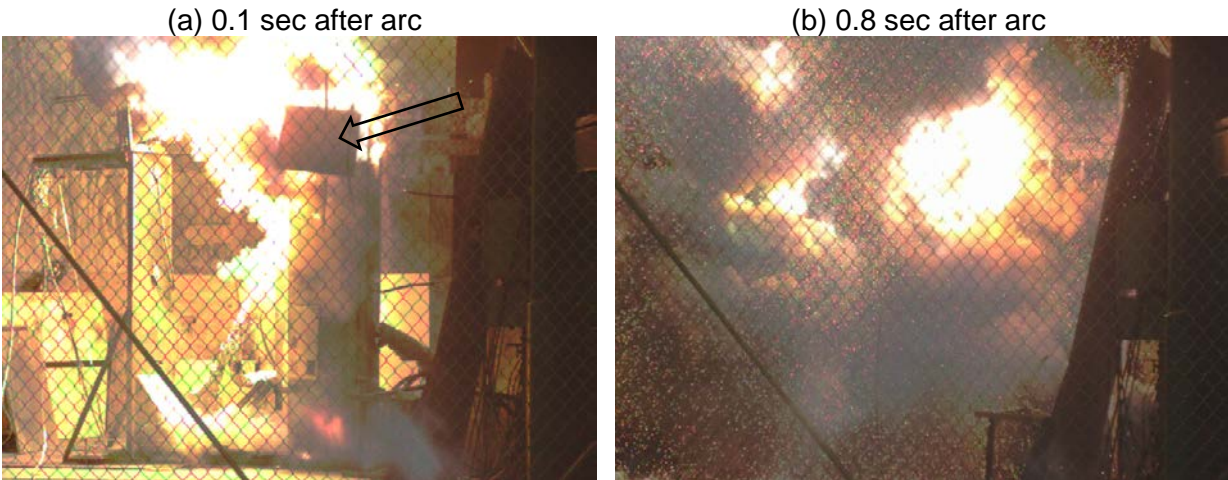


Figure 3.10-1. MCC Test 4 Arc

Figure 3.10-2 shows FLIR images (set at a constant 355 °C (671 °F) maximum) from the rear, left corner of the test cell. In these views the right side of the cabinet is on the left side of the view. Arc plasma and hot gases escaped the top part of the cabinet during the arc when the top and rear front panels blew off, and the top, left panel opened. After the arc, there was no detectable indication of high temperatures on the exterior of the cabinet or of internal fires.

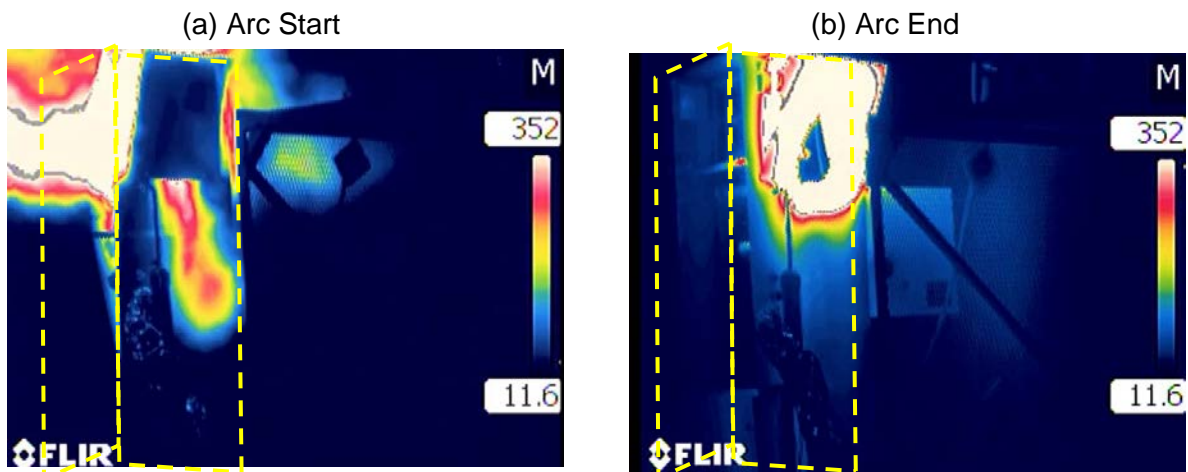


Figure 3.10-2. MCC Test 4 Thermal Images (Rear View)

Figure 3.10-3(a) shows the damage caused by the arc was extensive at the top of the cabinet. The top rear panel blew off, as indicated by the white arrow, when the steel bands were burned through by plasma escaping the cabinet. Figure 3.10-3(b) shows that the arc burned through the top right panel, similar to MCC Test 2 and it almost detached from the cabinet. The exterior had charring, soot damage, and copper disposition and the MCCB panel on the front top also opened. The top front cover was blown off during the arc. The heat caused the metal in the area of the left top to glow for several minutes after the arc as seen from the front view in Figure 3.10-3(c).

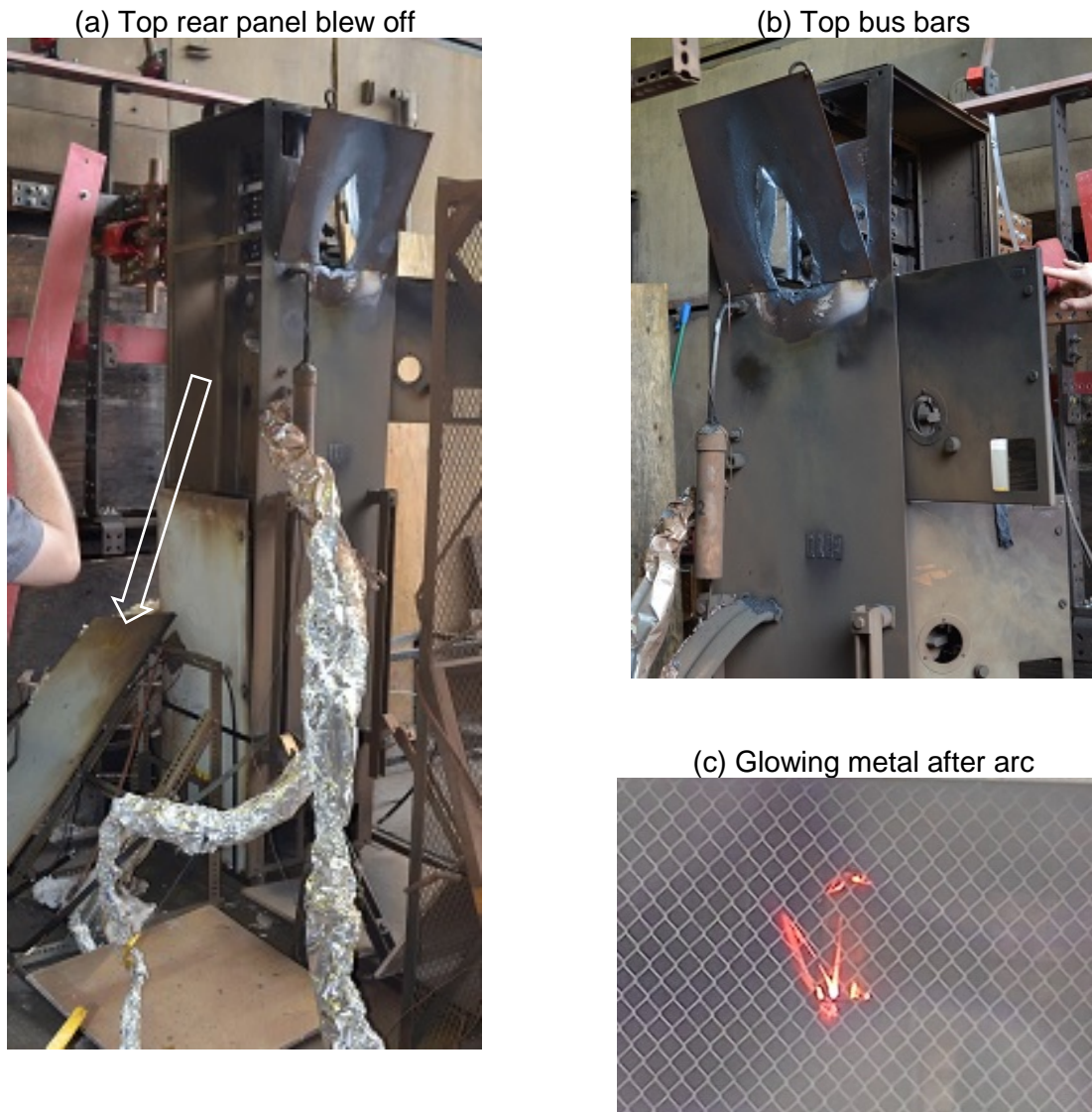


Figure 3.10-3. MCC Test 4 Exterior Damage

Figure 3.10-4(a) shows that about 5 cm (2 in) of the copper bus bars burned during the arc before the arc progression ended at the vertical bus support; the yellow dashed lines show the initial length of the bus bars before oxidation. There was similar bus bar loss in MCC Test 2. Figure 3.10-4(b) shows that there was soot inside the cabinet but there were only small amounts inside the switch and motor starter sections that were protected by the doors on the bucket (the door is open in the photo). The cables were not charred, just coated with soot and

there was no ensuing cable fire. Most of the energy escaped through the open panels and did not build up inside the cabinet.

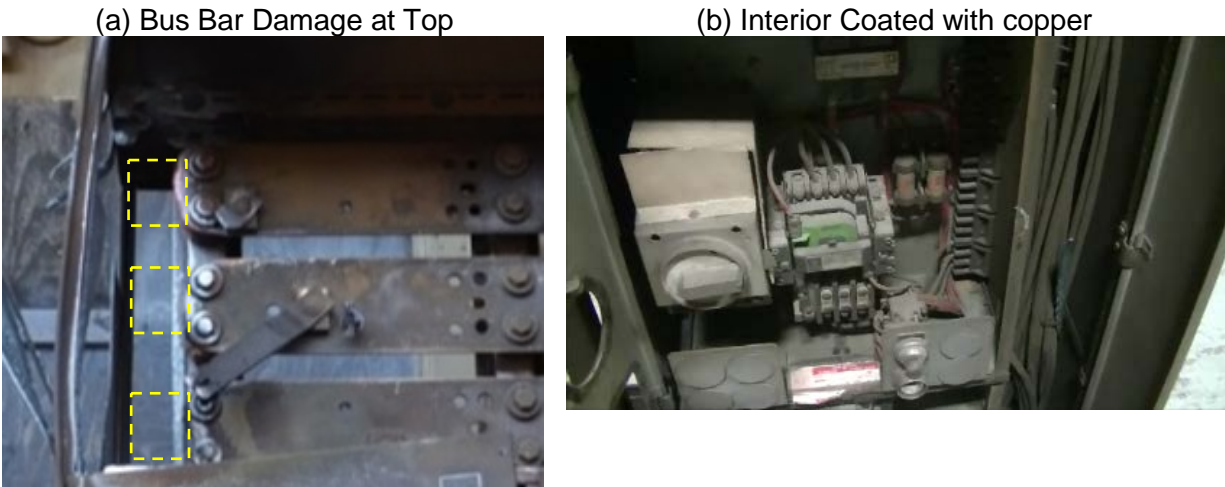


Figure 3.10-4. MCC Test 4 Interior Damage

3.10.1 MCC Test 4 Calorimetry Data

Temperatures measured at the slug locations are shown in Figure 3.10-5. The arc quenched at 0.922 seconds. Several slugs had high noise during the arc probably due to EMI; the power supply was directly next to the slug calorimeters. Similar to Test MCC 2, the highest temperature at the end of the arc was at the top left side (S3) where flames had contacted the slug; the highest response that was not contacted by flames was measured at the rear (S6). All slugs had steady temperatures after the arc because there was no ensuing fire.

The left side slugs (S1 to S3) responded quickly due to the arc breaking through the top left panel causing hot gases and plasma to exit directly to the slugs.

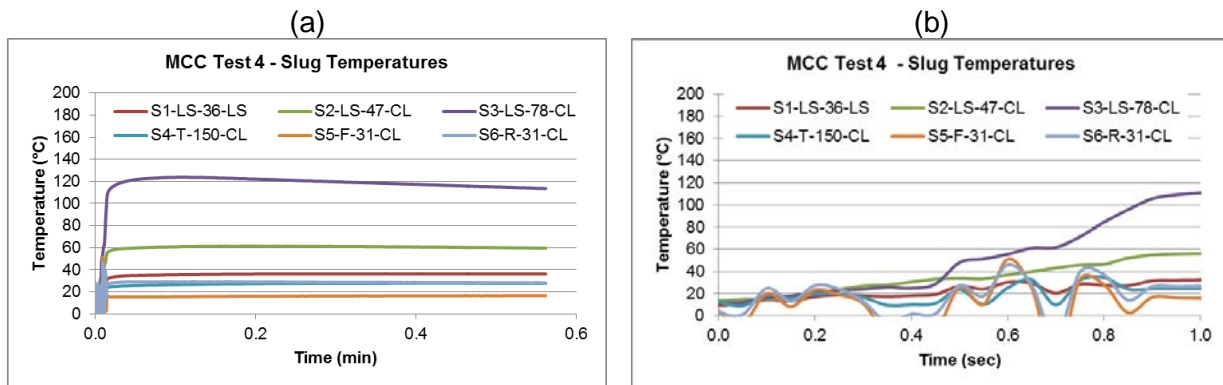


Figure 3.10-5. MCC Test 4 Calorimetry Data

Table 3-9 shows the flux results based on the ASTM F1959 method in Appendix A using the change in temperature (ΔT) between the start and end of the arc. The maximum valid flux of 65 kW/m² was measured at 1.5 m (5 ft) above the cabinet (S4). The bottom rear (S6) had a higher flux but was closer to the cabinet than the 0.91 meters. The maximum slug temperatures are also shown to indicate the maximum temperature a metal object could reach.

Table 3-9. MCC Test 4 Flux Results.

Slug	ΔT (°C)	Flux (kW/m ²)	Max T (°C)
S1-LS-36-LS	18.7	121*	36
S2-LS-47-CL	42.3	274*	61
S3-LS-78-CL	95.8	626*	124
S4-T-150-CL	10.0	65	28
S5-F-31-CL	2.5	16	17
S6-R-35-CL	12.5	81**	29

* Contacted by flames, result not valid, see Appendix A, Section A.1.

** S6 was closer to the cabinet than the 0.91 meter ZOI

3.10.2 MCC Test 4 Temperature Data

The temperatures measured by TC1 and TC2 are shown in the Figure 3.10-6. Table 3-10 shows the maximum temperature results. TC1 failed at 0.5 seconds, as indicated by the rapid temperature recovery from the maximum and by data that was intermittent thereafter; the TC1 temperature reported is the maximum before the failure. The thermocouple maximum temperature is a general indication of the air temperature 15.2 cm (3 in) from the cabinet and as expected, TC1 at the rear top where near the final arc location measured the highest temperature. The TCs cannot practically be used to estimate flux.

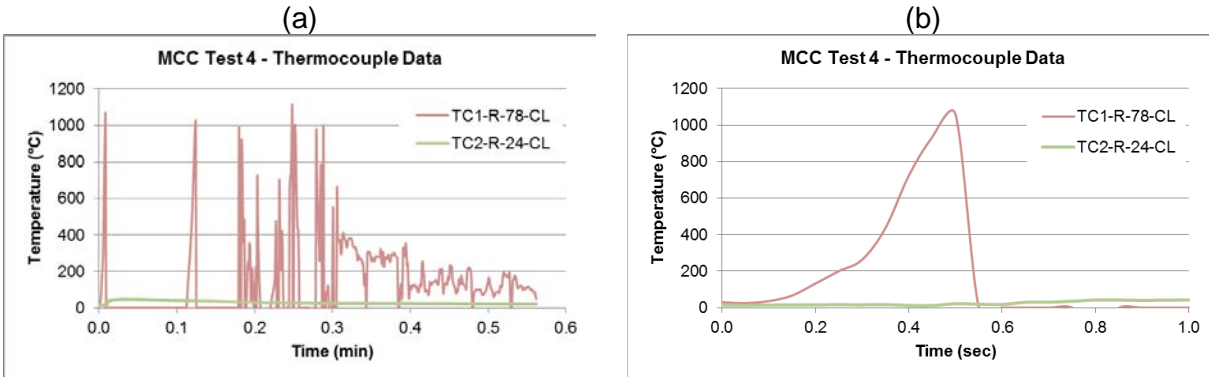


Figure 3.10-6. MCC Test 4 Thermocouple Data

Table 3-10. MCC Test 4 TC Results.

TC	Max T (°C)
TC1-R-78-CL	1045*
TC2-R-24-CL	49
TC3-LS-24-R	**
TC4-LS-24-F	**
TC5-RS-24-CL	**

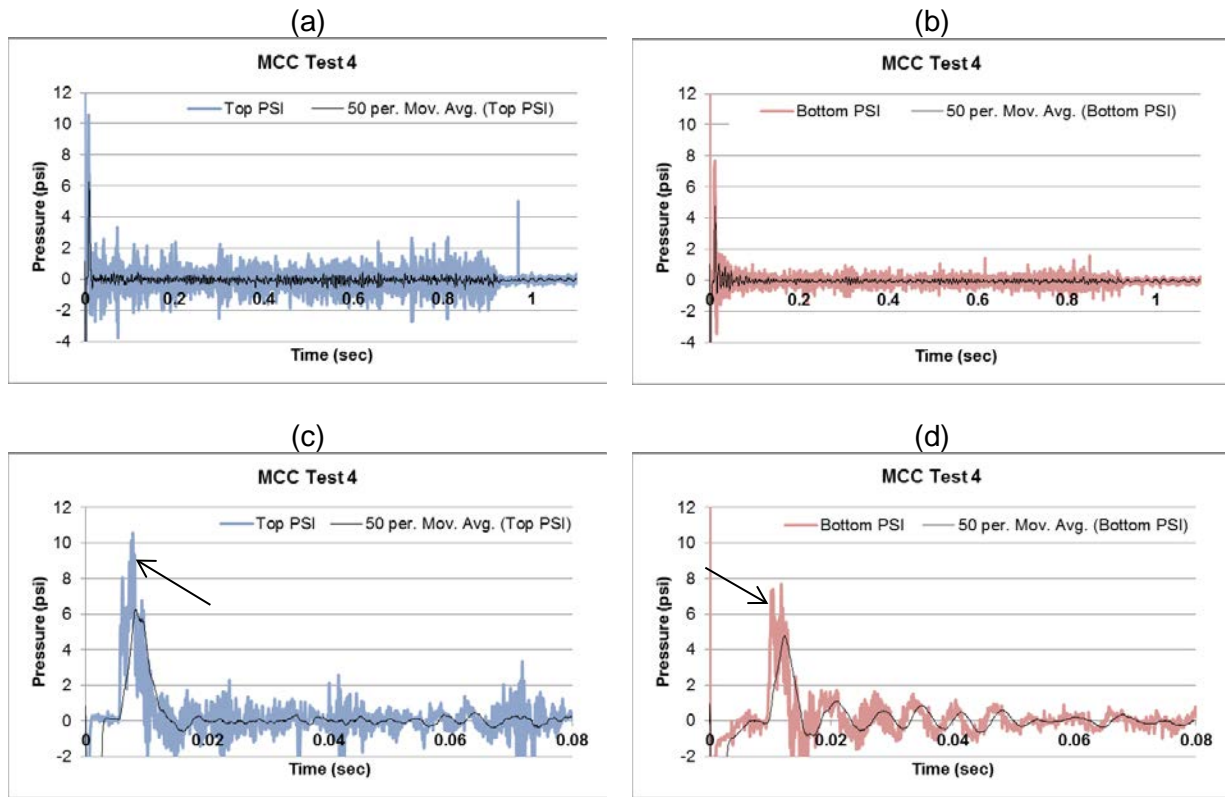
*Maximum reading before TC failed

**Data was corrupt

3.10.3 MCC Test 4 Pressure Data

The pressures during the arc are seen in Figure 3.10-7. The results for the top pressure near the arc has a little more noise than at the bottom. There was a noise spike near the end of the arc on the top. The top pressure, measured closer to the arc, had a higher maximum and occurred earlier than the bottom pressure, which was measured further from the arc. The maximum pressures are indicated by the arrows in Figure 3.10-7(c) and (d). These pressures are higher than the other MCC tests. The bus bar at the top is much thicker and larger than the bus bars at the bottom. Perhaps this caused a strong initial arc pressure wave that caused higher pressures. The bus bars in Tests 1 through 3 were thin and bent quickly, causing a weaker arc that extinguished. The top left panel at the arc burned through very quickly and this caused a rapid drop in pressure.

The pressure analysis methods are in Appendix A and involved picking the maximum near the start of the arc then including a nominal uncertainty for the noise in the signal just before the arc.



Test 4 Pressure 1 Top
 63.4 ± 1.4 kPa (9.2 ± 0.2 psi)
@ 0.0078 s

Test 4 Pressure 2 Bottom
 45.5 ± 1.4 kPa (6.6 ± 0.2 psi)
@ 0.0105 s

Figure 3.10-7. MCC Test 4 Pressure Data

3.10.4 MCC Test 4 Arc Energy

The arc duration was 0.922 seconds with total energy of 17.6 MJ, as seen in Figure 3.10-10. The energy analysis methods are in Appendix A. The “Energy” is calculated as volts multiplied current multiplied by the time step and each time step is shown. “Energy Total” is the cumulative sum of the energy in each time step.

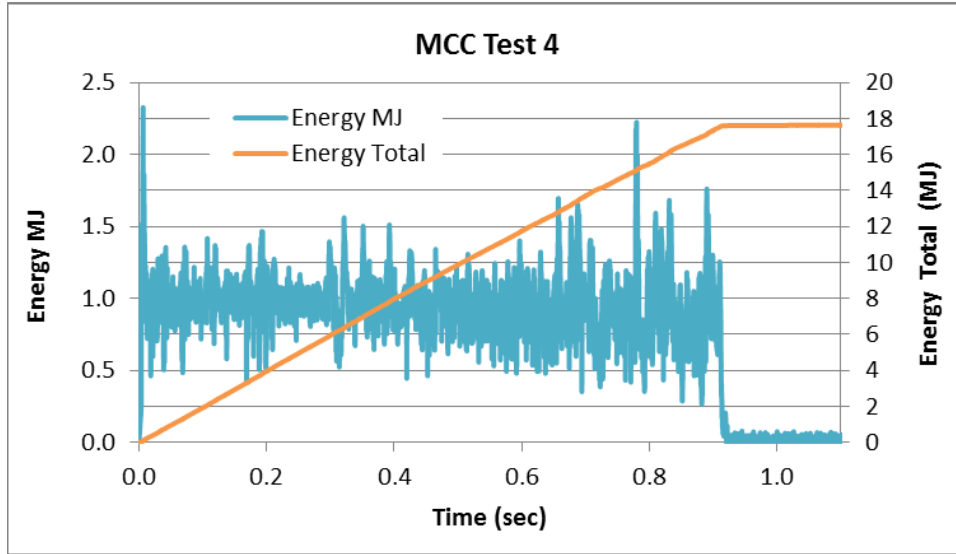


Figure 3.10-8. MCC Test 4 Arc Energy

3.11 MCC Tests 1 through 4: Electrical Conditions

Table 3-11 shows the electrical conditions measured by KEMA.

Table 3-11. MCC Test 1 through 4 Electrical Results (1).

Test	Arc Location	OCV (V)	Phase	Sym (kA)	Peak (kA)	Sym @End (kA)	Curr. Dur. (sec)	Arc Energy (MJ)	Freq @End (Hz)	Phase Arc Volts
1	Bottom of bus bars	484	A	22.7	34.3	10.5	0.145	0.7	50	A-N 260
			B	19.2	37.3	14.9		0.5		B-N 256
			C	22.2	45.9	10.1		0.5		C-N 233
			AVG	21.4	39.17	11.2		Σ2		AVG L-L 432
2	Bottom of bus bars	492	A	42.5	80.3	34.9	0.952	6	50	A-N 221
			B	29.3	61.6	14.5		5		B-N 229
			C	30.4	63.5	26.1		6		C-N215
				34.1	68.47	25.2		Σ17		AVG L-L 384
3	Bottom of bus bars	492	A	43.1	65.3	27.9	0.256	2	50	A-N 2209
			B	38.5	67.7	33.0		1		B-N 218
			C	39.6	67.5	19.6		1		C-N 215
			AVG	40.4	66.83	26.8		Σ 4		AVG L-L 384
4	Top horizontal bus bar neat left wall	492	A	47.6	87.6	22.4	0.922	6	50	A-N 215
			B	47.4	76.1	48.0		6		B-N 225
			C	44.1	91.0	40.6		6		C-N 206
			AVG	46.4	84.90	37.0		Σ18		AVG L-L 374

(1) See Table 2-16 for abbreviations and acronyms used in this table.

3.12 MCC Tests 1 through 4 Qualitative Summary

1. Ensuing Fire: There were no ensuing fires for any of the tests. The damage to the internal cables suggests that slightly more energy may have led to an ensuing fire in Test 2. In Test 4 there was a small fire metal fire at the top bus bars but is not considered an ensuing fire since none of the internal combustibles ignited.
2. Damage: In all of the tests, part of the bus bar was consumed during the arc. In Tests 1 the bus bars burned upwards but since the arc was obstructed by arc chutes, the bus bars were not consumed as much in the following tests. In Tests 2 and 4, the bus bars were consumed up to where the support strut is located. The bus bars bent away from each other in Tests 2 and 3.

Cabinet damage varied between the tests: Tests 1 and 3 resulted in minor damage to the cabinet. Tests 2 and 4 resulted in significant damage to the cabinet; the arc burned through the top panel. The internal cables were not significantly damaged in any MCC test. Test 4 also resulted in panels being blown off. There was no major deformation in these panels; the panels detached instead of deforming.

3. Calorimetry: The maximum measured flux varied between the tests. Tests 1 and 3 showed the maximum heat flux in the same location: at the bottom left side of the cabinet as expected for the arc position in the bottom of the cabinet. There was some impingement of flames on the slug calorimeters in Tests 2 and 4, reducing the number of valid flux results. The maximum valid flux for Test 2 was measured at the bottom rear as expected for an initial arc at the bottom of the cabinet that traveled to the top of the cabinet. In Test 4, the maximum flux was above the cabinet as expected because the arc was just below the top panel.
4. Temperature: The maximum air temperatures were measured in the same location, the top rear, in Tests 1, 2 and 4. The maximum for Test 3 was measured at the bottom rear. The thermocouples are indicative of the air temperature about 15.2 cm (3 in) from the cabinet.
5. Pressure: As expected, the maximum pressure was measured near the arc location. In Tests 2 and 4, the arc burned through the panel or a panel detached, causing a quick drop in pressure. The pressures measured in Test 4 were higher than the other tests possibly because the fraction of the initial energy burst related to the initial shock wave on the large bus bars at the top was larger than at the small, thin bus bars at the bottom where some energy was lost to deformation.
6. Arc Energy: In all tests the total energy was proportional to the arc duration for the given electrical testing conditions. The arc durations for all tests were less than 1 second so energies were very low. Tests 1 and 4 showed a smooth increase of the total energy during the arc indicating stable but short lived arc conditions. Test 2 showed the energy stopped increasing during the time the arc moved from the bottom of the cabinet to the top of the cabinet but the arc was stable before and after the transition. Test 3 showed some rapid changes in energy and signs of instability during the last part of the arc probably caused by the severe bending and spreading of the bus bars as the arc progressed.

4 Switchgear HEAF Tests 1 through 3, Single Arc Tests – KEMA (June 2013)

4.1 SWGR Tests 1 through 3 Overview

The purpose of these tests is to obtain the basic HEAF data for Switchgear (SWGR) such as duration, energy, flux, temperatures, pressures, and ensuing fire effects. There were three (3) tests at KEMA conducted June 17-19, 2013. The tests were in a SWGR lineup of five cabinets (numbered 6-10 to match Onagawa) with the arc initiated in Cabinet 8 in the center.

4.2 SWGR Tests 1 through 3 Summary of Results

The key test parameters and results are in the table below. The tests were single arc events; the target test voltage was nominally 6.9 kV and the target test current was 23 kA (symmetrical, sym.). The original plan was for a 2 second arc but this was increased to 3 seconds after Test 1 to provide more energy to evaluate the impact of duration on the potential for ensuing fires.

Table 4-1. SWGR Tests 1 through 3 Summary of Results.

Test	Volt (kV) (1) Curr (kA) (2)	Test Peak Current (kA) (3)	Arc Duration (sec) (4)	Arc Energy (MJ)	Internal Max Press (kPa/psi) (6)	Ext Max Flux (5) (kW/m ²)	Ensuing fire? Key Observations
1	7.1 / 0.609 29.5 / 22.6	58.4	2.0 2.048	42.6	4.8 ± 1.4 0.7 ± 0.2 (6)	52	No. The energy was too low to cause the fire.
2	7.1 / 0.608 30.5 / 23.5	59.5	3.0 2.957	58.2	16.5 ± 1.4 2.4 ± 0.2	71	Yes. Full duration ensuing fire.
3	7.1 / 0.633 29.8 / 22.6	58.9	3.0 2.911	64.2	13.5 ± 1.4 2.0 ± 0.2	107	Yes. Ensuing fire extinguished after 4 minutes.

Notes:

- (1) The voltage is shown as the target voltage / arc Line-to- Line (L-L) voltage (L-L is the “arc voltage”)
- (2) The symmetric arc current slowly drops during the test as the arc impedance increases. This shows the *test start current / test end current*. These are average currents of all 3 phases.
- (3) This is the peak current for any phase or time, usually the asymmetric current at the start
- (4) The duration is shown as the target duration and the actual test duration below it.
- (5) The maximum heat flux was at the slug calorimeter located at the 1.5 m (5 ft) above the cabinet.
- (6) Maximum pressure is one cabinet away from the cabinet with the arc, the pressure transducer failed in the cabinet with the arc. In other tests, the cabinet with the arc had the maximum pressure.

Test 1 did not have an ensuing fire with a 2 second arc. The arc duration was increased to 3 seconds for Tests 2 and 3. Test 2 developed into a full ensuing fire that was allowed to completely burn the cables in the cabinet with the arc and one adjacent cabinet on each side in about 20 minutes. Cables in the end cabinets were only partially burned when the fire was extinguished. Test 3 showed similar results and had an ensuing fire but the ensuing fire was extinguished after 4 minutes for safety concerns. The arc and electrical results of Test 2 and 3 are similar. The key results from the June 2013 SWGR tests at KEMA were:

- The tests at KEMA did not duplicate the 2011 Onagawa damage conditions. It is believed the actual 2011 Onagawa event also was subjected to higher energy levels from possibly longer arc duration (the actual duration is unknown) and from the oxidation (burning) of the aluminum bus bars, as discussed in Chapter 7. It is also possible that there were two separate arcs in the Onagawa event.
- The SWGR were well-ventilated cabinets, like the Onagawa cabinets. The highest external flux measured was a momentary 107 kW/m² at 1.5 m (5 ft) above the cabinet, indicating that heat escaped through the vent on the top of the cabinet and flames spread over the roof of the cabinet. However, the high flux was a short duration, and did not damage the cable samples at the flux measurement point.
- Based on all the SWGR tests, an energy of about 60 MJ was needed to ignite an ensuing fire in the KEMA SWGR tests. One observation on MCC and DP tests was that the ensuing fire usually required an energy of around 25 MJ or greater to ignite. There is likely more heat loss through the vents in the SWGR, requiring a higher energy (60 MJ) to cause an ensuing fire within the cabinet. Cabinets with vents and the vent location will be an important consideration in heat damage effects from HEAF.
- The resultant pressures in the SWGR tests were lower than the DP and MCC tests because the pressure escaped through the large vent above the arc in Cabinet 8. Cabinet 7 pressures are higher than Cabinet 8, as expected, because the pressure transducer is located closer to the arc.

4.3 SWGR Tests 1 through 3 Cabinet Configuration

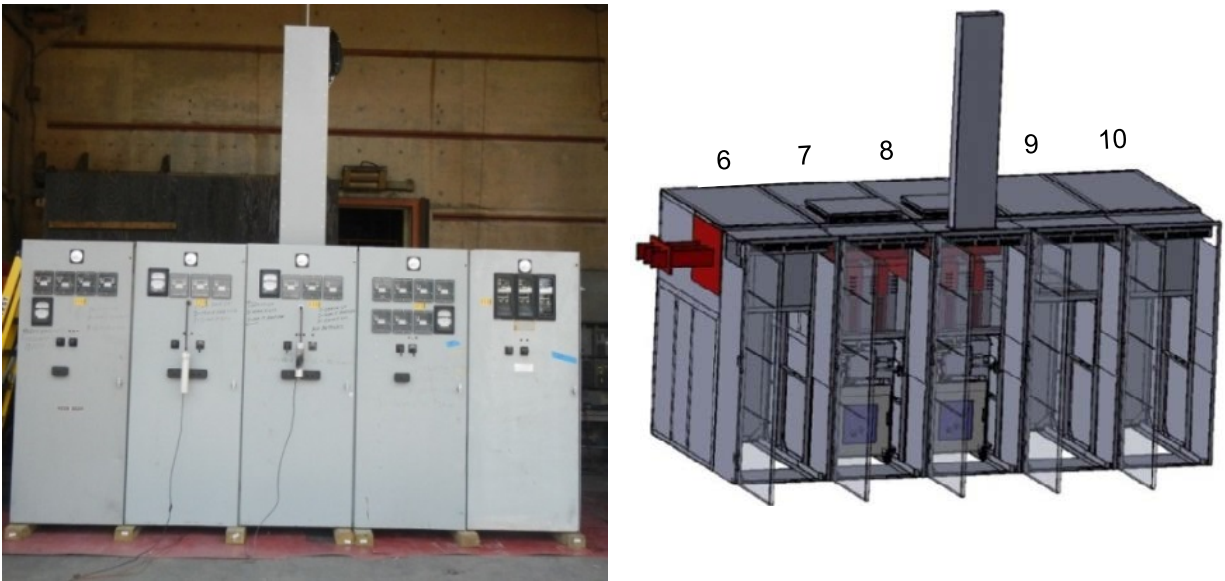
The test configuration is shown in Figure 4.3-1. Actual SWGR and cabinets from Onagawa were not available to test. GE Magneblast SWGRs built in the 1970's are the closest U.S. SWGR to the Onagawa design. The SWGR was nominally 91.4 cm wide by 228.6 cm high by 114 cm deep (36 in wide by 90 in high by 45 in deep). However, the GE SWGR and cabinets are not identical to Onagawa; Figure 4.3-2 that shows the differences in internal partition configuration and the bus bar configuration. The Onagawa cabinet also has a large vent on the top.

The GE Magneblast SWGRs were modified, as shown in Figure 4.3-3 through Figure 4.3-5. The interior volume in the cabinets around the arc and any vents in the cabinets are very important. The bus bars, interior SWGR partitions, interior SWGR wire duct, and bus bar partitions between cabinets were relocated similarly to the Onagawa SWGR. The U.S. cabinet is 91.4 cm (36 in) wide, whereas the Onagawa cabinet is 100 cm (39 in) wide; this could not be changed. As shown in Figure 4.3-4, the volume formed by Plates A-B-C-D-E-F and the top is similar to the volume of the Onagawa SWGR where the arc occurred. The volume in the top front is similar to the 0.30 m by 0.41 m (11.8 in by 16.1 in) wire duct at the top front of the

Onagawa SWGR. A rectangular vent area was added on the top to match the Onagawa vent. Panel B in front of the primary insulators had vents to match Onagawa because these vents were the postulated path for the arc plasma to ignite cables in the front of the cabinet during the Onagawa event. As shown in Figure 4.3-5, the aluminum bus bars were covered by a polymer coating which were considered a negligible part of the combustible load and were supported by phenolic panels, similar to the Onagawa design.

In the June 2013 tests, “dummy” SWGR breakers were used to simulate the cabinet configuration and combustible load present at Onagawa in Cabinets 7 and 8. Cabinets 6, 9, and 10 did not have any breakers in them. Cabinets 6, 9, and 10 were included to provide the cable loads and cabinet configuration similar to Onagawa.

(a) Front Views



(b) Side View showing arc on primary side of breaker

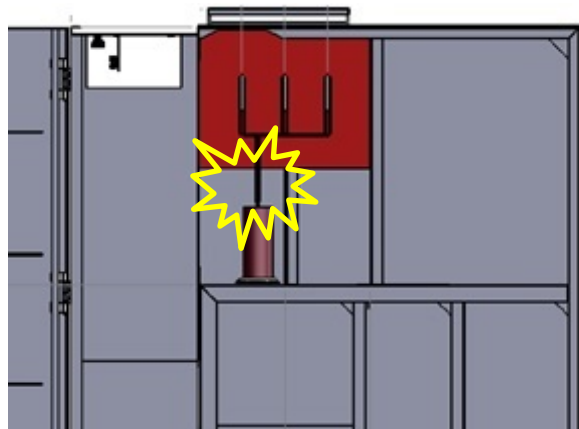


Figure 4.3-1. SWGR 5-Cabinet Test Configuration

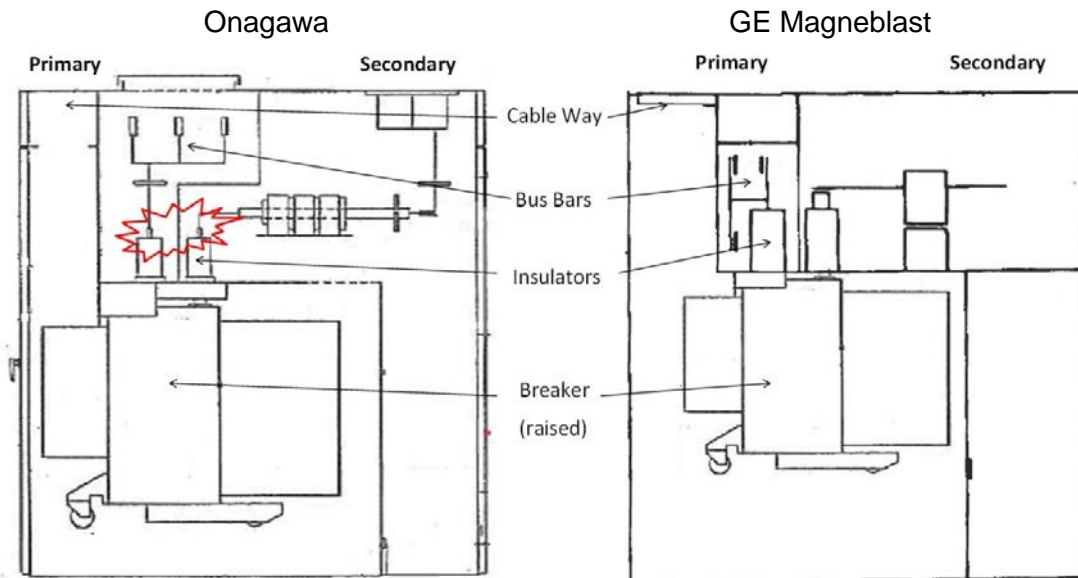


Figure 4.3-2. Onagawa SWGR and GE Magneblast SWGR

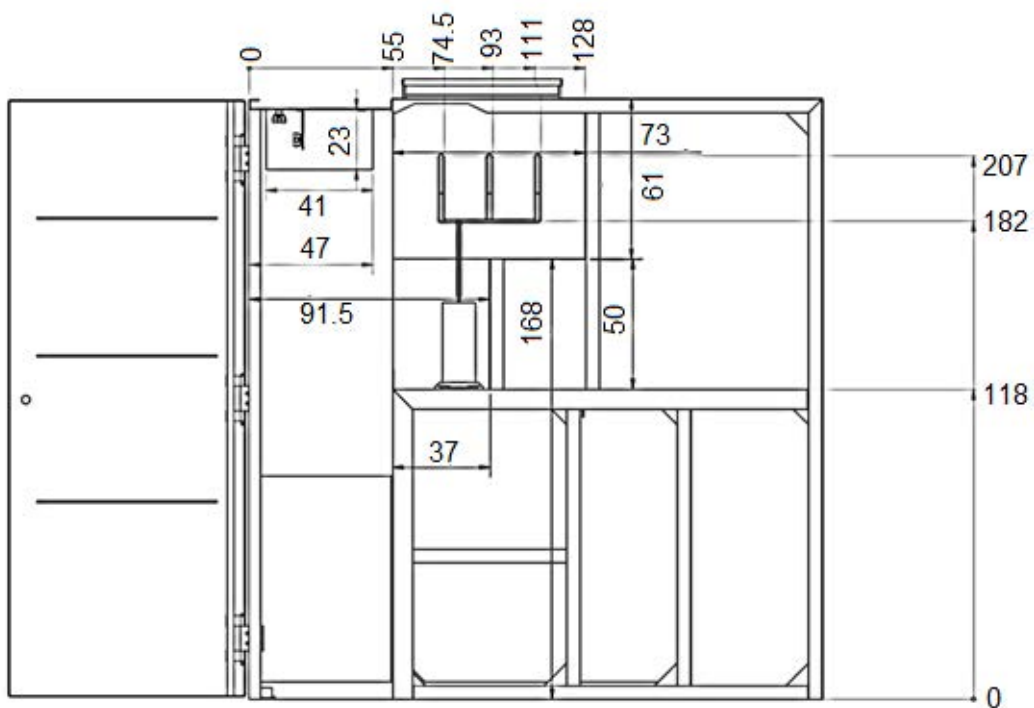


Figure 4.3-3. Modified GE Magneblast Dimensions (in cm)

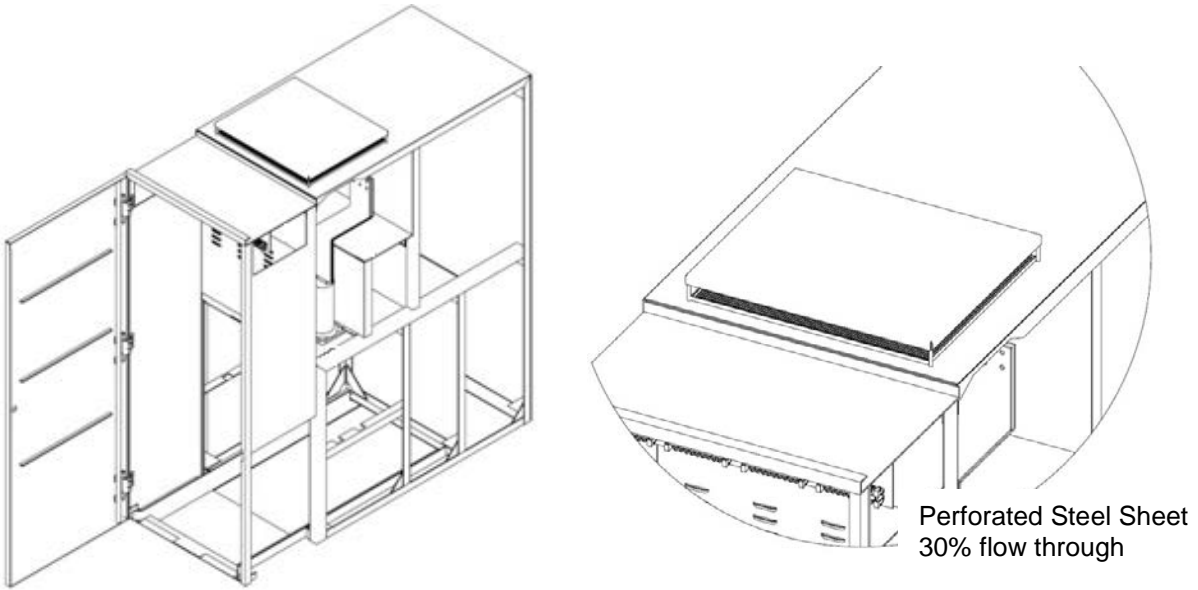


Figure 4.3-4. SWGR Cabinet Configuration Cabinets 7 and 8

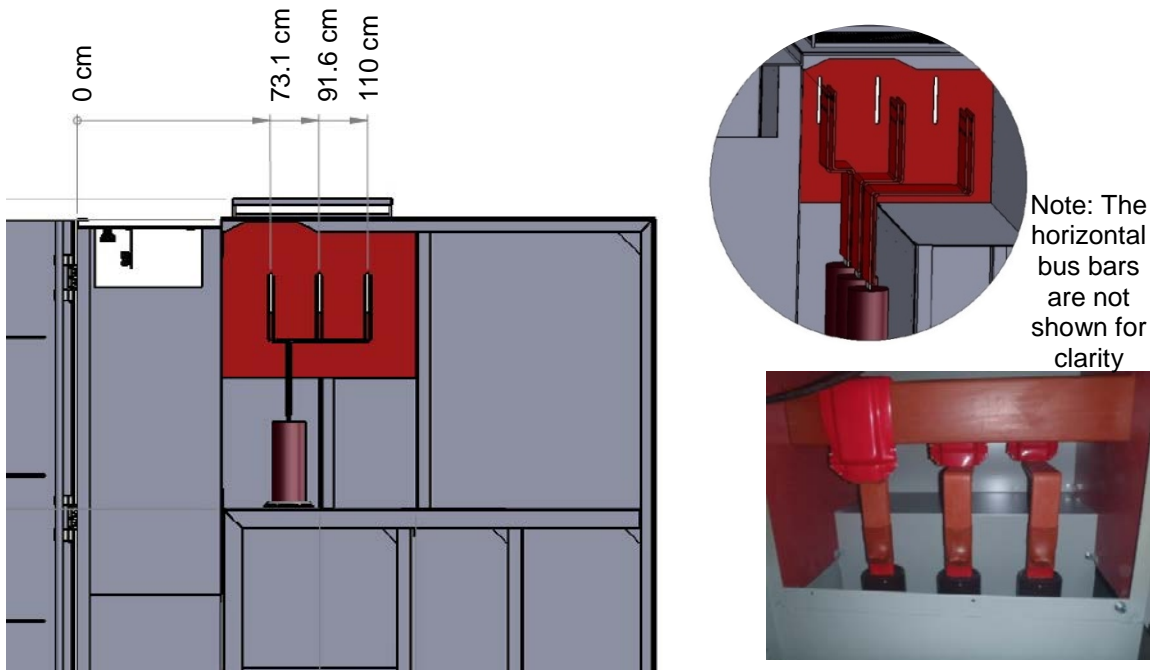
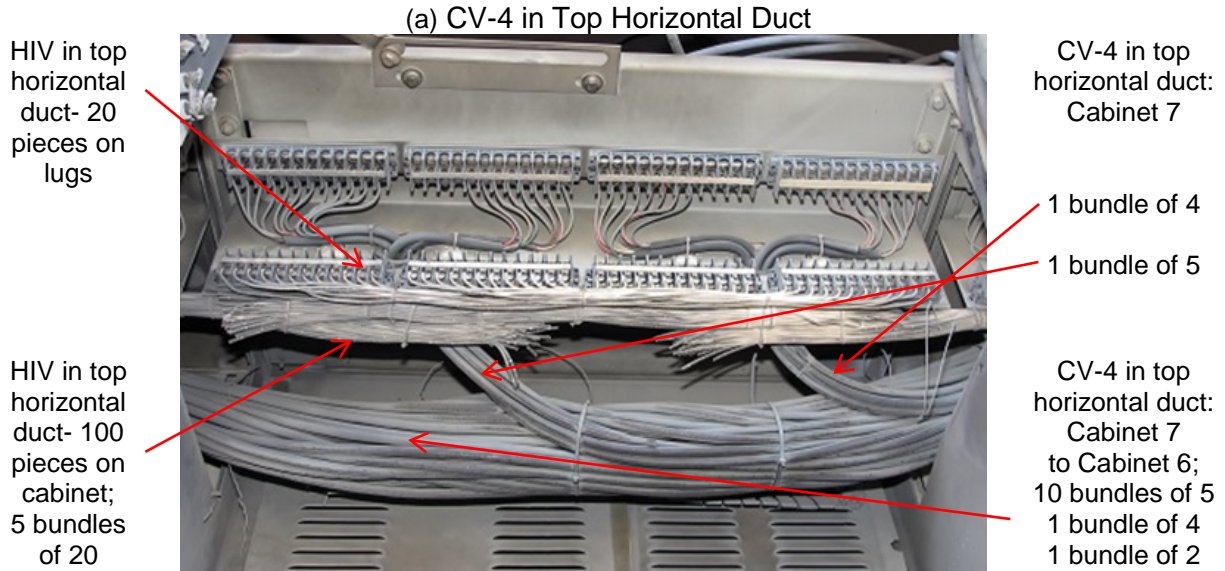


Figure 4.3-5. SWGR Bus Bar Configuration

4.4 SWGR Tests 1 through 3 Cable Combustible Loading

Cables, wires, and wire ways were added to the cabinet to give a combustible load similar to the cabinets in Onagawa, as shown in Figure 4.4-1. Japanese CV-4 PVC/XLPE type cable and HIV PVC single wire instrument wires were used in the front of the cabinets as in Figure 4.4-1(b). Three, 1.5 m (5 ft) lengths of Japanese 6 kV-CHSVT single conductor, 28 mm (1.1 in) diameter, PVC, power cables were installed in the rear of Cabinets 7 and 8.



(b) HIV in Cabinets



(c) In Vertical Duct

92 CV-4 cables (after burning)

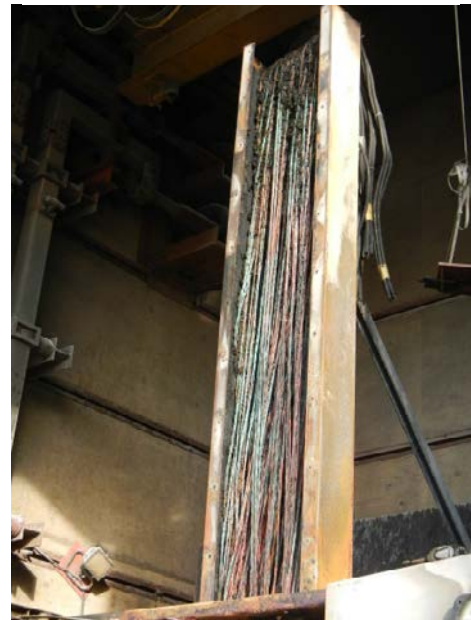


Figure 4.4-1. SWGR Cabinet Combustible Load

(d)

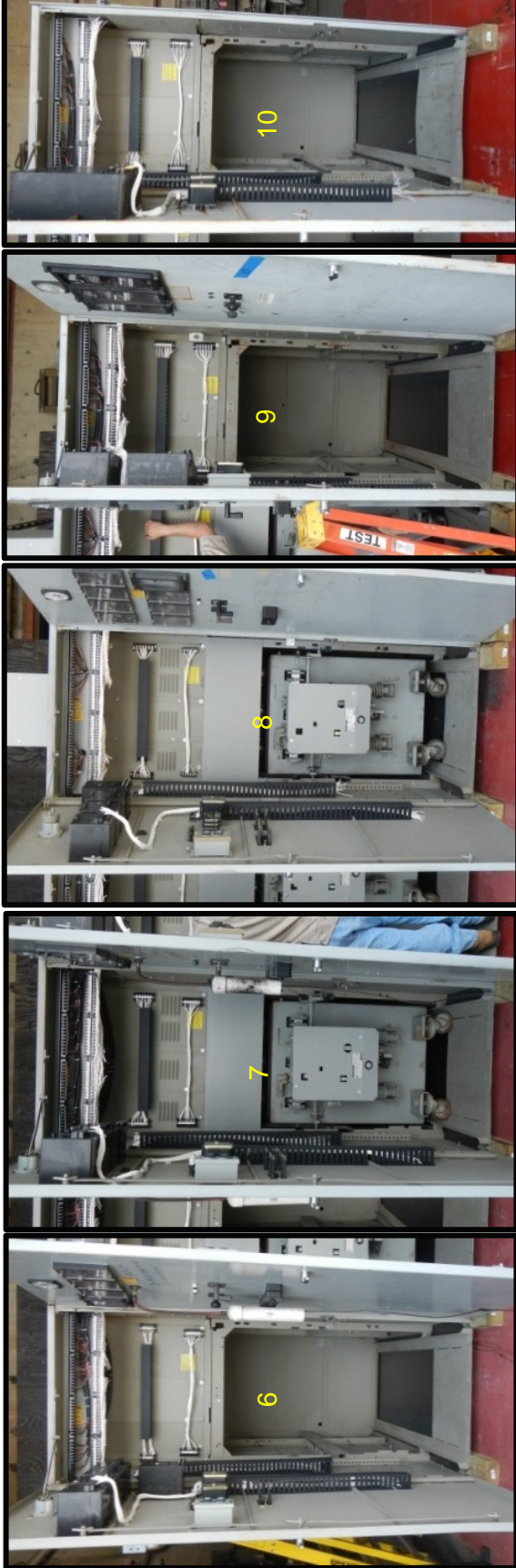


Figure 4.4-1. SWGR Cabinet Combustible Load, continued

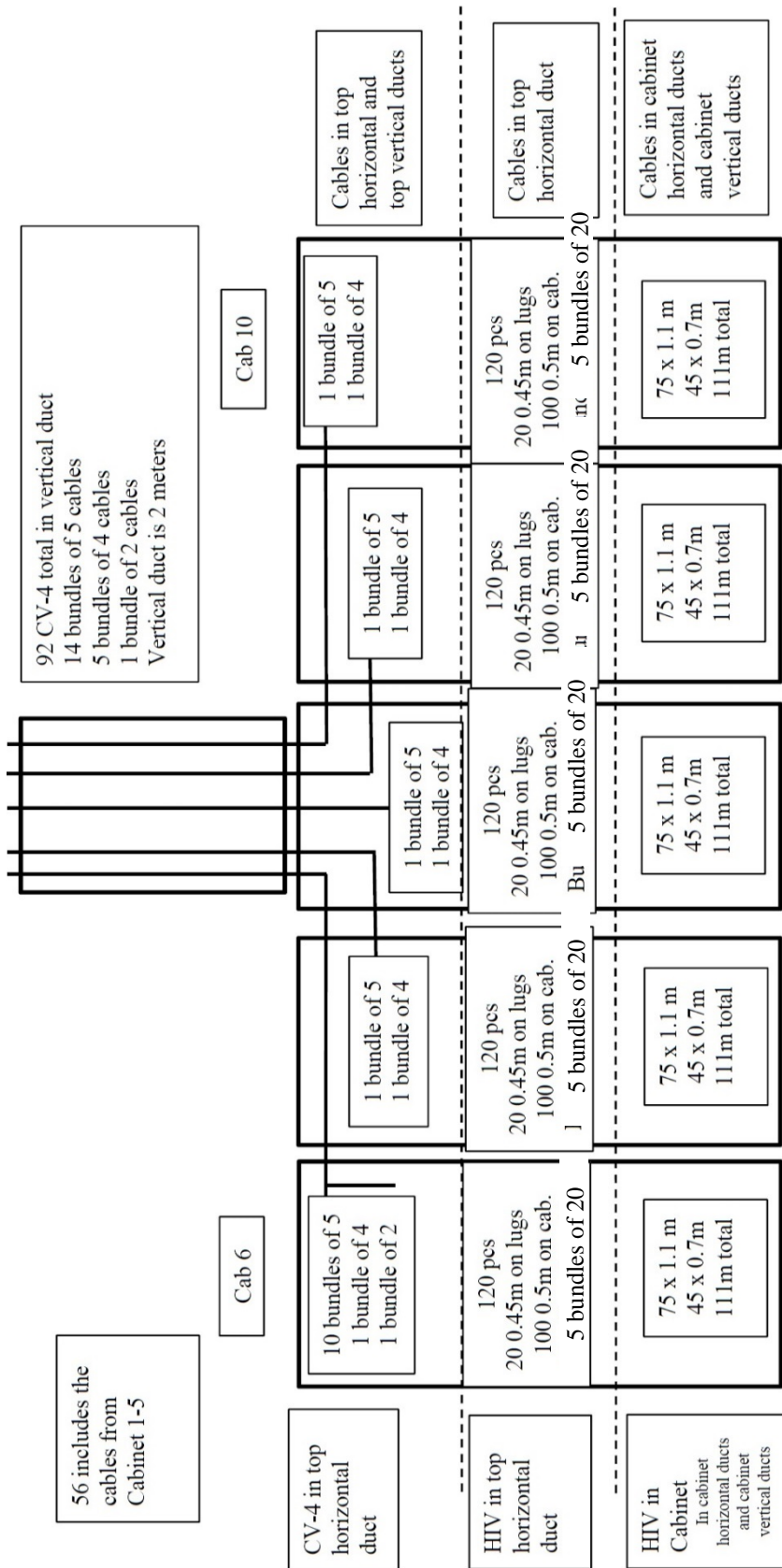


Figure 4.4-2. SWGR Test Cable Combustible Load

4.5 SWGR Tests 1 through 3 Temperature and Heat Flux Instrumentation

Thermocouples (Type K) were used to measure the temperatures during each test. For electrical independence from the KEMA measurement systems and safety concerns, TCs are not in contact with the metal cabinet to prevent possible electrical shorting. The TCs are about 15 cm (6 in) from the cabinet to measure the air temperatures. The air temperatures are likely much lower than the actual metal temperature. Therefore, the temperatures are only a qualitative measure of thermal and fire behavior.

ASTM F1959 slug calorimeters were also used for heat flux. The TC and slug locations are in Figure 4.5-1 and Table 4-3. Flux calculation methods are in Appendix A.

Table 4-2. Calorimeter and TC Locations SWGR Tests 1 through 3.

Slug or TC	From Floor cm (in)	Position	Slug or TC Name
S1	178 (70)	Front (F)	S1-F-70-Cab7
S2	178 (70)	Front	S2-F-70-Cab8
S3	91 (36)	Front	S3-F-36-Cab8
S4	178 (70)	Rear (R)	S4-R-70-Cab8
S5	381 (150)	Top (T)	S5-T-150-Cab8
TC1	178 (70)	Front	TC1-F-70-Cab6
TC2	178 (70)	Front	TC2-F-70-Cab7
TC3	178 (70)	Front	TC3-F-70-Cab8
TC4	178 (70)	Front	TC4-F-70-Cab9
TC5	422 (166)*	Vertical Duct (V)	TC5-V-Cab8

*TC5 is 7.62 cm (3 in) from the top of the vertical duct.

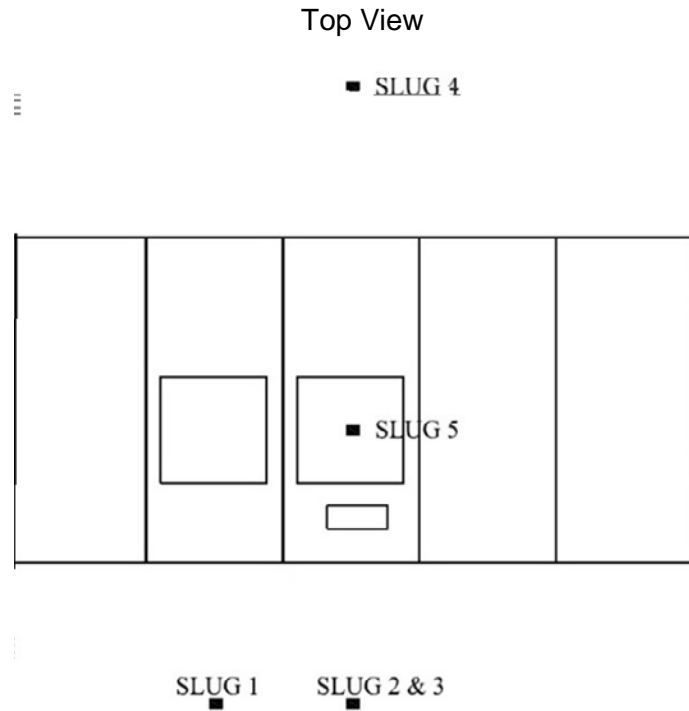
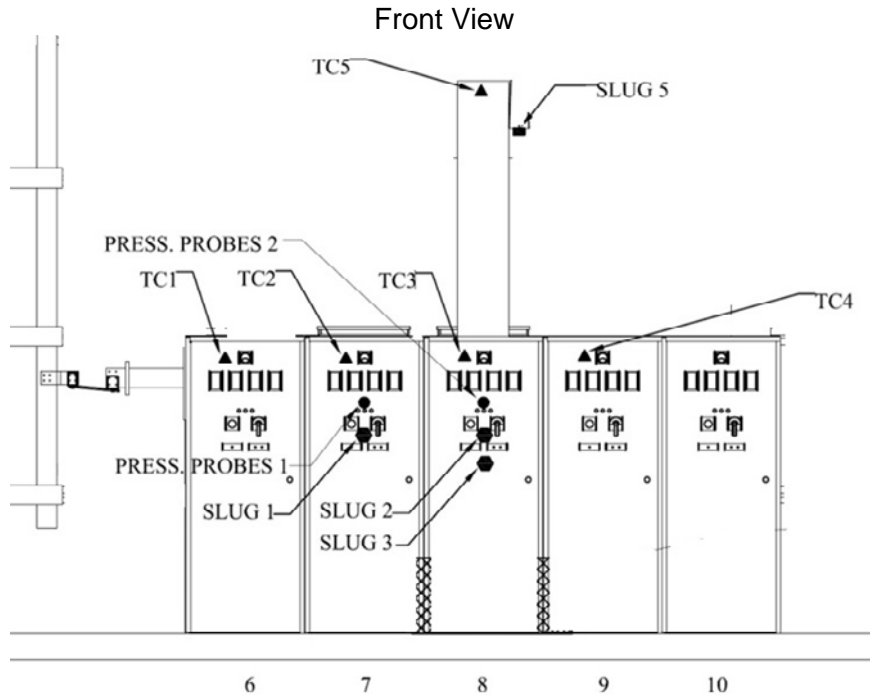


Figure 4.5-1. SWGR Tests 1 through 3 Instrument Locations

4.6 SWGR Tests 1 through 3 Pressure Instrumentation

Two Dynisco PT150-50 strain-gauge type pressure transducers (PRT) were used. See Appendix A for the analysis method. The pressure probe positions are in Figure 4.5-1.

4.7 SWGR Test 1 Key Observations

Test 1 was initiated at 7.1 kV and 29.5 kA with a target arc duration of 2 seconds that was achieved with a total energy of 42.6 MJ. The arc progression is seen in Figure 4.7-1. The energy was too low to start an ensuing cable fire. The maximum external cabinet temperature as indicated by the IR thermal image, seen in Figure 4.7-2(a) was much lower than 750 °C (1382 °F) immediately after the arc. At this time the FLIR was set to the maximum 750 °C so the video after the initial arc showed no colors. Ten minutes after the arc, the FLIR was set to auto scale as shown in Figure 4.7-2(b). The exterior cabinet temperatures were less than 90 °C (194 °F) indicating residual heat at the bottom of the vertical duct and no internal cable fire in the top front of the cabinets.

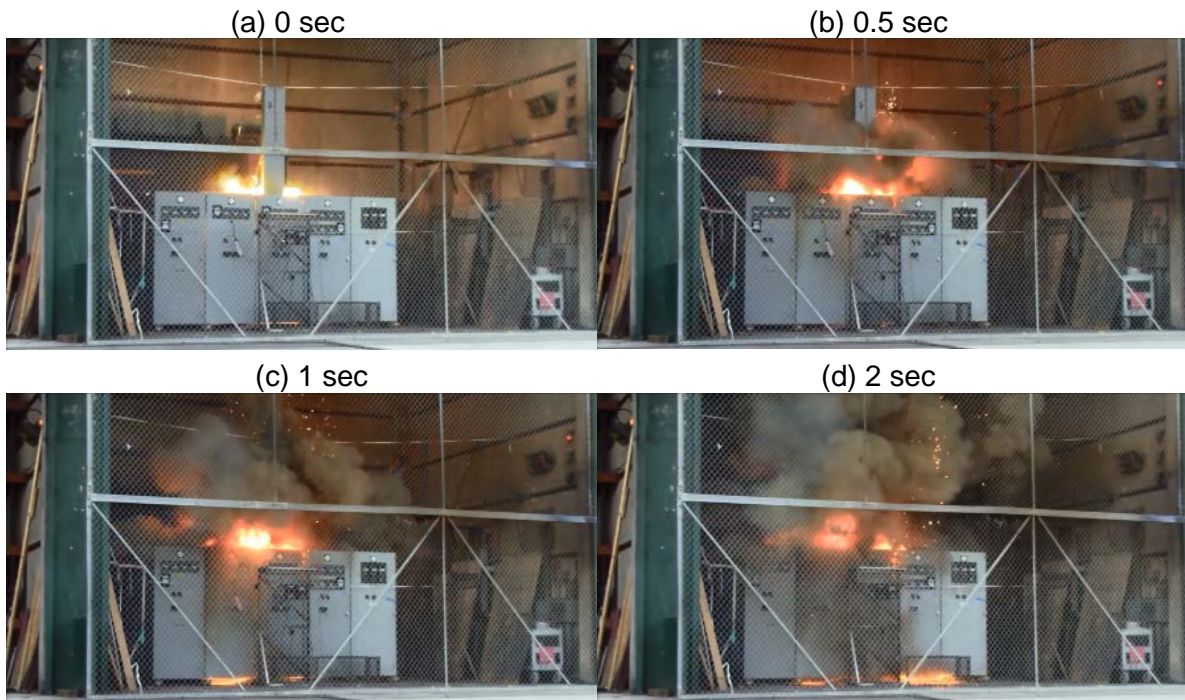


Figure 4.7-1. SWGR Test 1 Arc

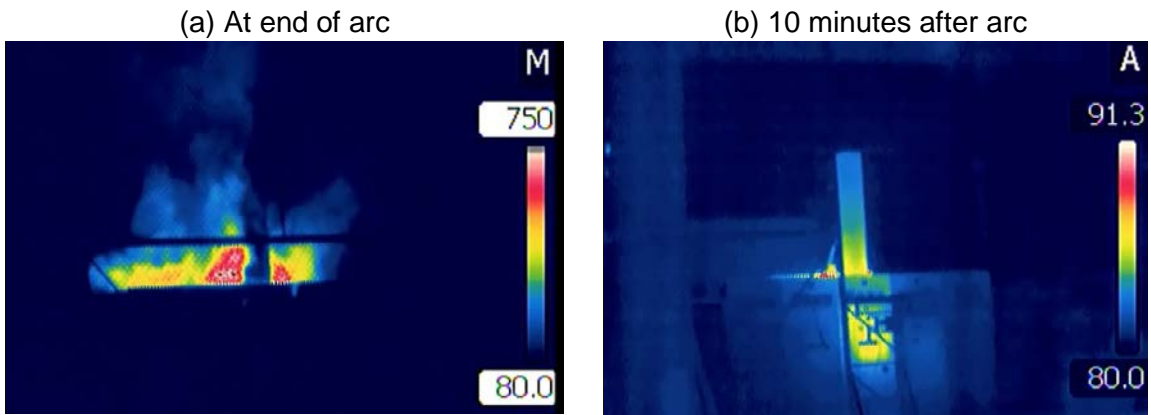


Figure 4.7-2. SWGR Test 1 Thermal Image at Arc Extinction

The exteriors of the cabinets were not damaged since there was not a large fire, as seen in Figure 4.7-3. There is a little soot at the bottom of the vertical duct. The top had some soot deposits and minor scorching where the arc discharged through the top vent.

(a) Front View Cabinets 6-10



Figure 4.7-3. SWGR Test 1 Exterior Damage

(b) Top of Cabinets 6-10



Figure 4.7-3. SWGR Test 1 Exterior Damage, continued

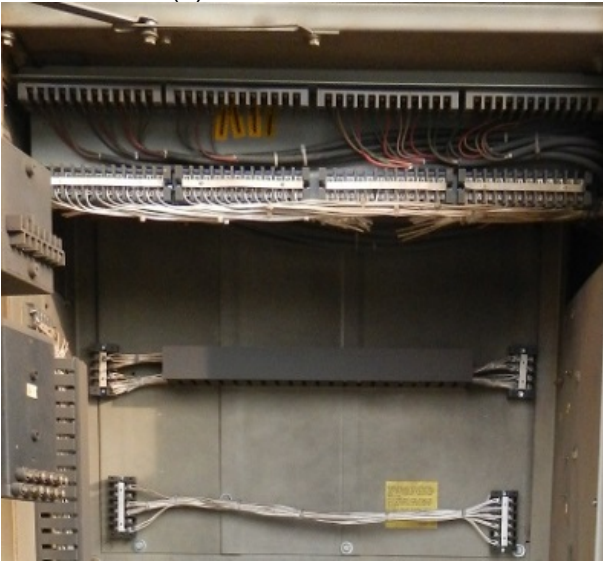
As shown in Figure 4.7-4, the cabinet interior damage was minor; details of the interiors are in Figure 4.7-5. Cabinet 7 and 8 had some scorching and orange discoloration from high heat on the interior panels at the arc level. Cabinets 6, 9, and 10 mainly had soot damage. The interior of the cabinet had some cable scorching in Cabinet 8. In Cabinet 7 and 9 there were some soot deposits on the cables. In Cabinets 6 and 10 the cables were virtually undisturbed. As shown in Figure 4.7-5(c), Cabinet 8 interior had some scorching in the front area but other areas only had very light soot deposits in the rear of the cabinet.

Cabinets 6-10



Figure 4.7-4. SWGR Test 1 Interior Damage

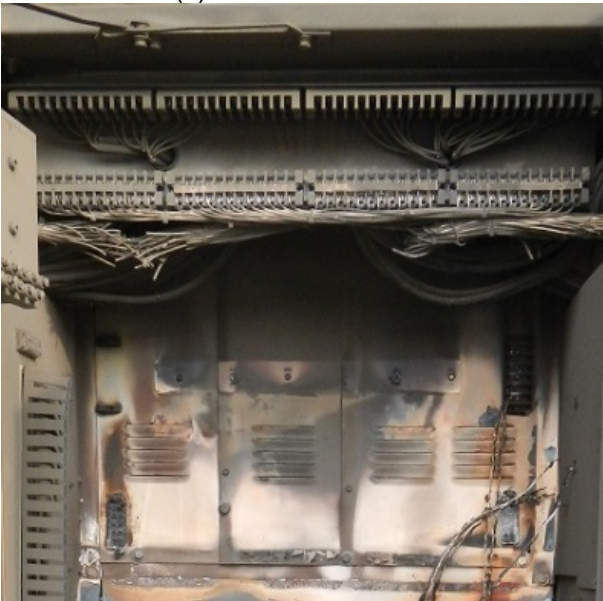
(a) Cabinet 6 Cables



(b) Cabinet 7 Cables



(c) Cabinet 8 cables



(d) Cabinet 9 Cables

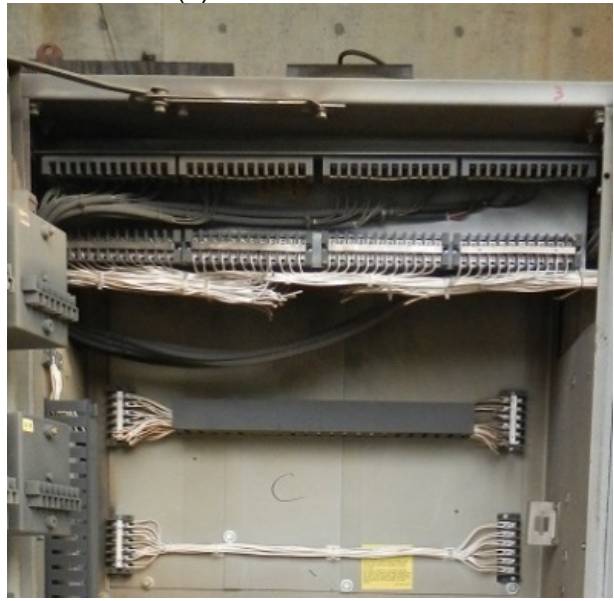
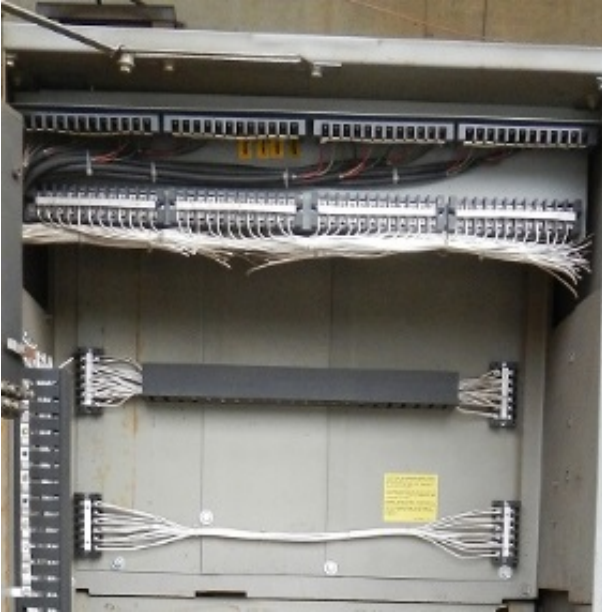


Figure 4.7-5. SWGR Test 1 Interior Damage, Detailed

(e) Cabinet 10 Cables



(f) Cabinet 8 Interior



Figure 4.7-5. SWGR Test 1 Interior Damage, Detailed, continued

The vertical bus bars above the insulators were not heavily oxidized, as shown in Figure 4.7-6, because the arc was short. The orange bus bar insulation was not burned, indicating a low temperature and heat flux within the cabinet. The horizontal bus bars had some bending but much less than Onagawa where the bars bent and touched. The insulators were destroyed.

(a) Cabinet 7



(b) Cabinet 8



Figure 4.7-6. SWGR Test 1 Insulator and Bus Bar Damage

The Cabinet 8 breaker was not destroyed during the arc, however, the insulators were destroyed and the debris fell onto the top of the breaker. The Cabinet 7 breaker did not have any damage just some soot, as seen in Figure 4.7-7.

(a) Cabinet 8 breaker with insulator debris



(b) Cabinet 8 breaker with insulator debris



(c) Cabinet 7 breaker



Figure 4.7-7. SWGR Test 1 Breaker Damage

4.7.1 SWGR Test 1 Calorimetry Data

Temperatures measured at the slug locations are shown in Figure 4.7-8. The arc quenched at 2.048 seconds. Several slugs had high noise during the arc probably due to EMI; the power supply was directly next to the slug calorimeters. The highest temperature at the end of the arc was seen at the top of the cabinet (S5) above where the hot gases escaped through the roof vent. All slugs had steady temperatures after the arc because there was no ensuing fire.

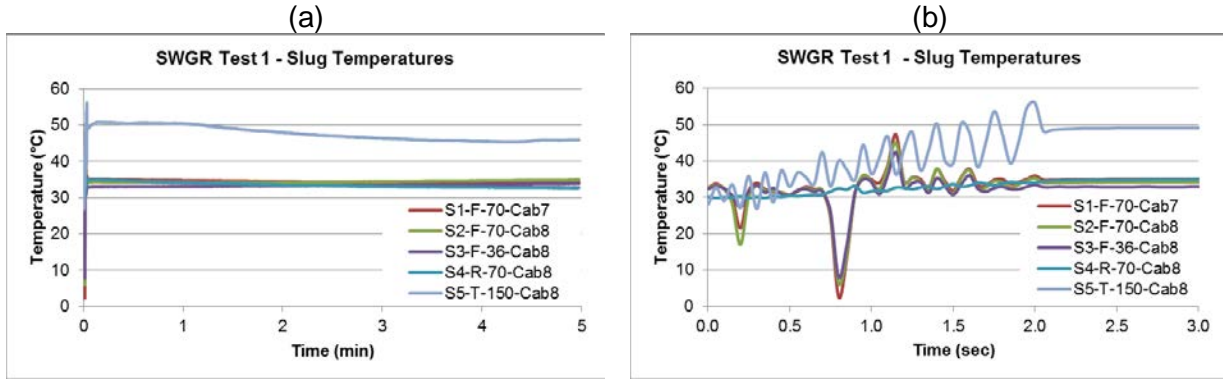


Figure 4.7-8. SWGR Test 1 Calorimetry Temperature Data

Table 4-3 shows the flux results based on the ASTM F1959 method in Appendix A using the change in temperature (ΔT) between the start and end of the arc. The maximum flux of 52 kW/m² was measured at the top (S5). The maximum slug temperatures are also shown to indicate the maximum temperature a metal object could reach.

Table 4-3. SWGR Test 1 Flux Results.

Slug	ΔT (°C)	Flux (kW/m ²)	Max T (°C)
S1-F-70-Cab7	2.3	7	34
S2-F-70-Cab8	1.8	5	35
S3-F-70-Cab8	0.6	2	34
S4-R-70-Cab8	4.4	13	33
S5-T-150-Cab8	17.1	52	48

4.7.2 SWGR Test 1 Temperature Data

The temperatures measured by the TCs are shown in the Figure 4.7-9. Table 4-4 shows the maximum temperature results. The thermocouple maximum temperature is a general indication of the air temperature 7.62 cm (3 in) from the cabinet. The highest temperature was likely at the vertical duct (TC5), however, it appears the TC failed. The TCs cannot practically be used to estimate flux. Noise during the arc is from EMI.

For TC3, the fluctuating response after the arc does not appear to be noise. TC3 was located in front of Cabinet 8 and is detecting the residual heat escaping from the cabinet.

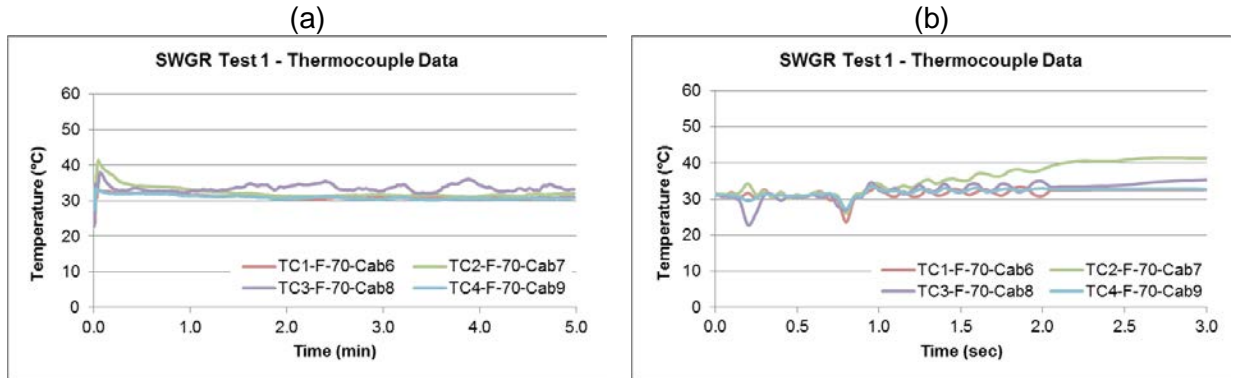


Figure 4.7-9. SWGR Test 1 Thermocouple Data

Table 4-4. SWGR Test 1 TC Results.

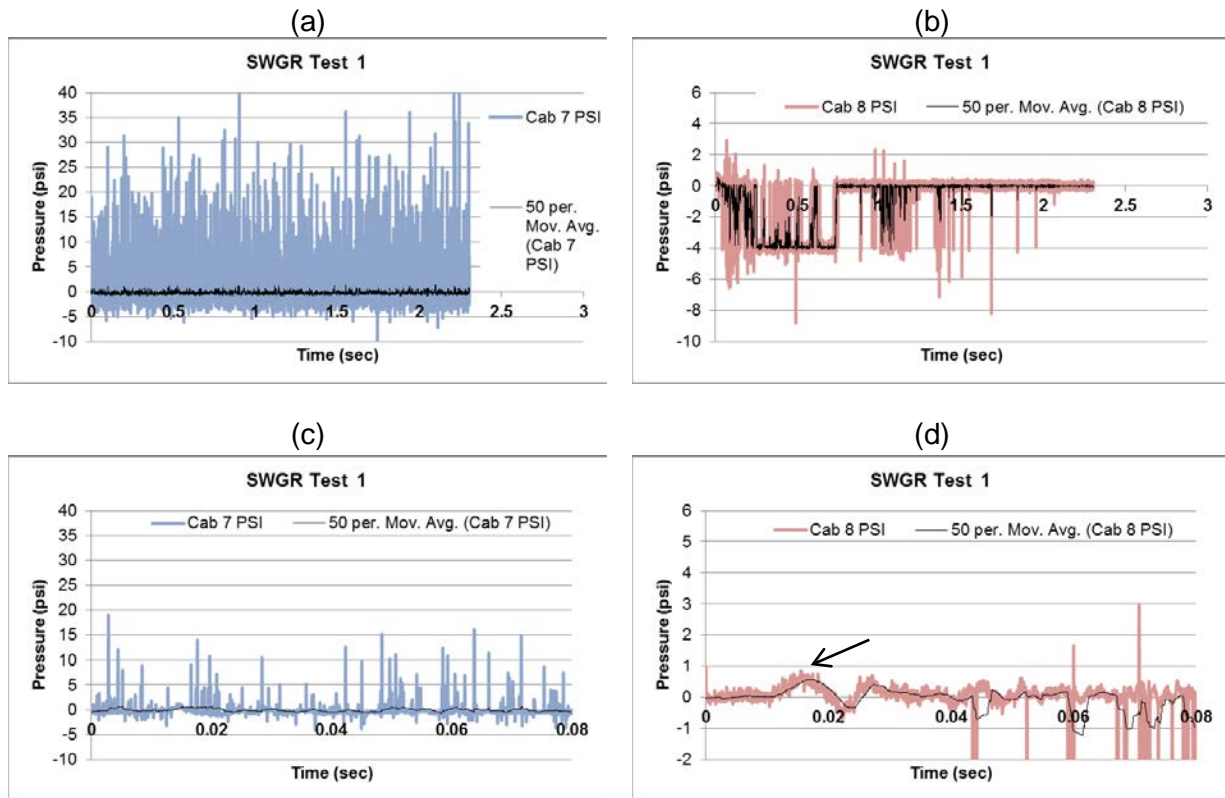
TC	Max T (°C)
TC1-F-70-Cab6	31
TC2-F-70-Cab7	32
TC3-F-70-Cab8	36
TC4-F-70-Cab9	31
TC5-V-Cab8	*

*Data was corrupt

4.7.3 SWGR Test 1 Pressure Data

The pressure curves are shown in Figure 4.7-10. The data signal for Cabinet 7 showed noise during the arc that could not be treated with the method in Appendix A, so the data is not reported. The Cabinet 8 signal data showed the zero base line changed from 0.04 to 0.8 seconds, recovered, and then had numerous negative spikes. There was considerable noise after 0.04 seconds but the data for the initial pressure spike looks reasonable, and is evaluated. The maximum pressure for Cabinet 8 is indicated by the arrows in Figure 4.7-10(d).

The pressure analysis methods are in Appendix A and involved picking the maximum near the start of the arc then including a nominal uncertainty for the noise in the signal just before the arc.



Test 2 Pressure 1 Cab. 7
No data reported

Test 2 Pressure 2 Cab. 8
 4.8 ± 1.4 kPa (0.7 ± 0.2 psi)
@ 0.0154 s

Figure 4.7-10. SWGR Test 1 Pressure Data

4.7.4 SWGR Test 1 Arc Energy

The arc duration was 2.048 seconds with total energy of 42.6 MJ, seen Figure 4.7-11. The energy analysis methods are in Appendix A. The “Energy” is calculated as volts multiplied current multiplied by the time step and each time step is shown. “Energy total” is the cumulative sum of the energy in each time step. The energy was smooth and steady with no-restrikes that were typical of the medium voltage SWGR Tests 1 through 4.

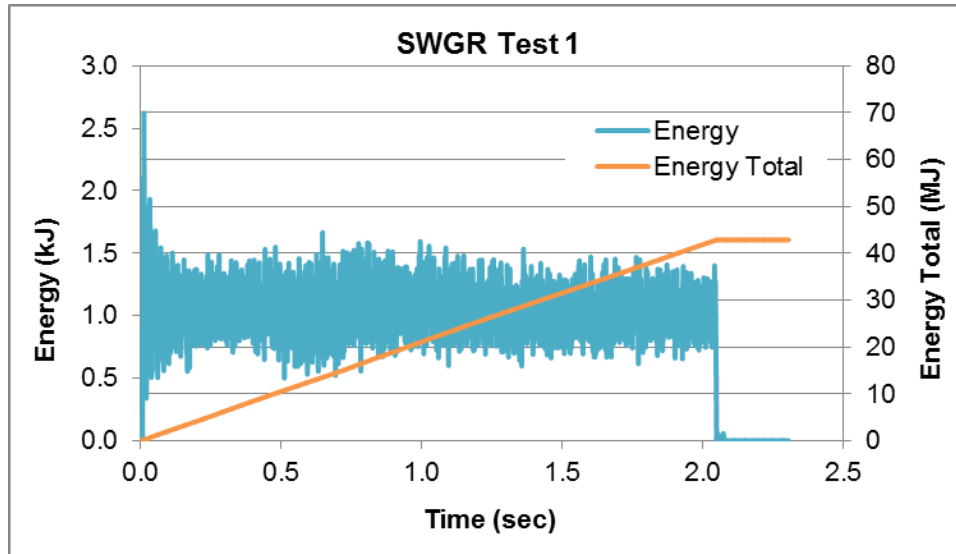


Figure 4.7-11. SWGR Test 1 Arc Energy

4.8 SWGR Test 2 Changes

Based on the results of Test 1, the changes and key set up items for Test 2 and all future SWGR tests were:

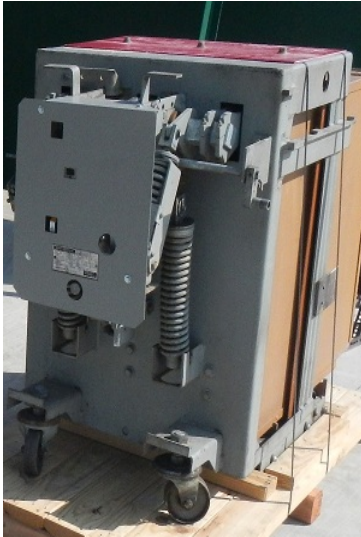
1. Increased the energy from Test 1 (no cable fire) by 50% by increasing the arc duration from 2 seconds to 3 seconds (results show an energy increase from 43 to 58 MJ).
2. The shorting wire configuration was changed to use two wires toward the front of the cabinet to bring the arc forward in the cabinet in Tests 2 and 3, see Figure 4.8-1. In Test 1 the arc was toward the back through Panel C and this did not happen at Onagawa. Moving the arc forward should increase the heat in the front of the cabinet and cause a cable fire. A sheet of red board was added on the front of panel C to protect it from the arc. However, this resulted in an arc in the front of the cabinet, causing the arc to leak into Cabinet 7 in Tests 2 and 3.



Figure 4.8-1. SWGR Test 2 Shorting Wire Changes

3. Test 1 used a red board on the top of the breaker to direct the energy into the cabinet but there was no damage on the breaker secondary side. In Test 2 this red board was removed to direct more energy to the breaker side. But there was still no major fire damage on the breaker secondary side.

(a) Red board in Test 1



(b) Red board removed for Test 2

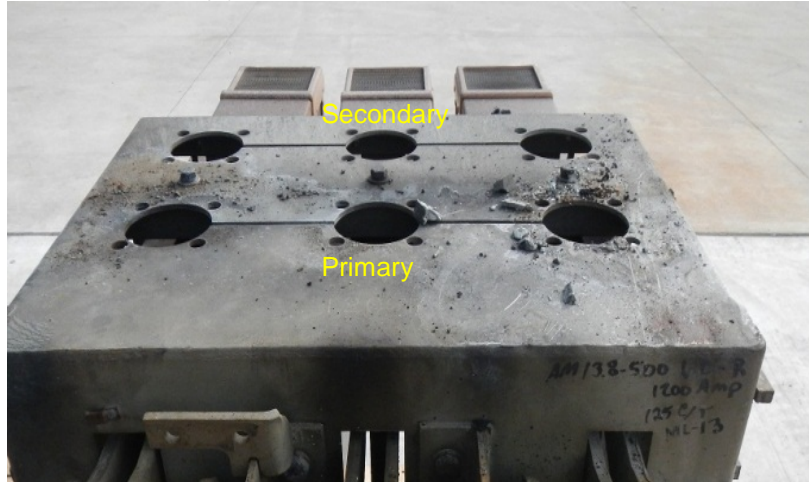


Figure 4.8-2. SWGR Test 2 Breaker Changes

4. More brackets and supports were added for the cables because they fell off in Test 1.

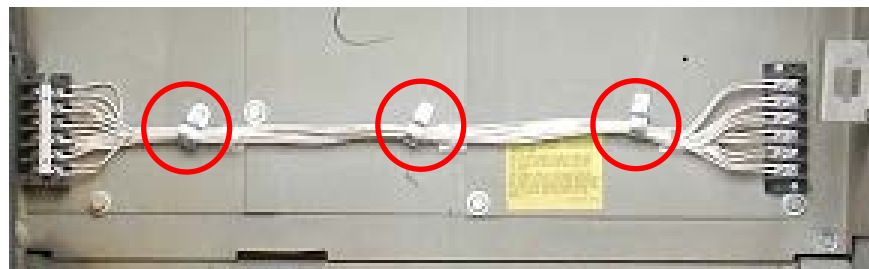


Figure 4.8-3. SWGR Test 2 Wiring Changes

- Two metering devices were removed from the front door to simulate the openings created during Onagawa event when some meters blew off. In all future SWGR tests, two rectangular openings were created by removing these meters on the front doors.

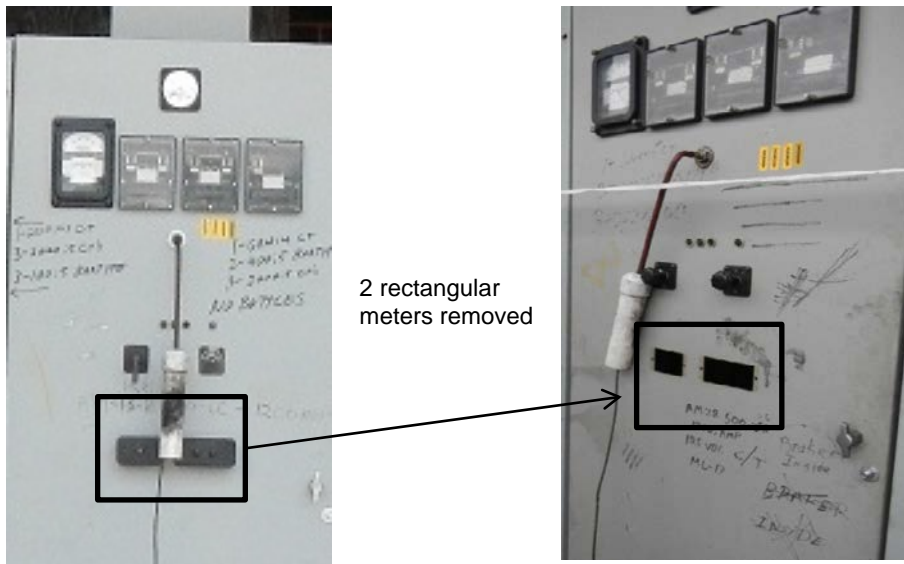


Figure 4.8-4. SWGR Test 2 Front Door Meter Changes

4.9 SWGR Test 2 Key Observations

This test was initiated at 7.1 kV and 30.5kA with a target duration of 3 seconds with a total energy of 58.2 MJ. The target of 3 seconds was achieved. The arc flames died quickly and no flames were visible until the 7 minute mark where flames were seen in the vertical duct. Manual extinguishment was attempted at 12.5 minutes for two minutes but was unsuccessful. The fire then returned to full intensity by 15.5 minutes with flames exiting at the top of the vertical duct. Finally, water was applied for about 5 minutes and the fire was extinguished, largely because the cables in the vertical duct were completely burned.

The ensuing fire observed during Test 2 and associated cable damage was similar to the Onagawa event but the fire did not spread as far and cables were burned two cabinets away from the arc points at Onagawa. For Test 2, only the cables on the adjoining Cabinet 7 and 9 were burned.

The arc sequence and ensuing fire are shown in Table 4-5 and Table 4-6. The first 3 seconds is the actual arc. It appears that the arc in Cabinet 8 created a hole in the wall to Cabinet 7 and the hot gas and plasma entered Cabinet 7 causing ensuing fires and heavy damage in Cabinet 7.

Table 4-5. Arc Sequence SWGR Test 2.




Image	Time	Description
	0	Arc initiated.
	0.2 seconds	Fireball develops.
	0.3 seconds	Fireball expands; flame spreads across the top, see next figure.

Table 4-5. Arc Sequence SWGR Test 2, Continued.




Image	Time	Description
	1 second	Flames emerge from top vents in Cabinets 7 and 8, fire spreads down the wire duct and travels to Cabinet 10.
	1.5 seconds	Fire continues in wire duct and escapes from cabinets.
	2 seconds	Fire continues to evolve, sparks escaping at the bottom of the cabinet.

Table 4-5. Arc Sequence SWGR Test 2, Continued.




Image	Time	Description
	<p>2.5 seconds</p>	<p>Flame and sparks between Cabinets 6 and 7 indicate the arc plasma leaking from Cabinet 8 to Cabinet 7.</p>
	<p>2.8 seconds</p>	<p>The plasma leak into Cabinet 7 continues with more flames between Cabinets 6 and 7. There are additional flames at the Cabinet 7 vent.</p>
	<p>3 seconds</p>	<p>The arc quenches.</p>

Table 4-5. Arc Sequence SWGR Test 2, Continued.




Image	Time	Description
	<p>4 seconds</p>	<p>The fire ball quickly extinguishes at the top after the arc. Sparks and flames remain at the cabinet bottom.</p>
	<p>5 seconds</p>	<p>Flames are mostly gone.</p>
	<p>6 seconds</p>	<p>This is the last time small flames are visible until 7 minutes. These are around the Cabinets 7 and 8 top vent areas.</p>

Table 4-6. Ensuing Fire Sequence SWGR Test 2.

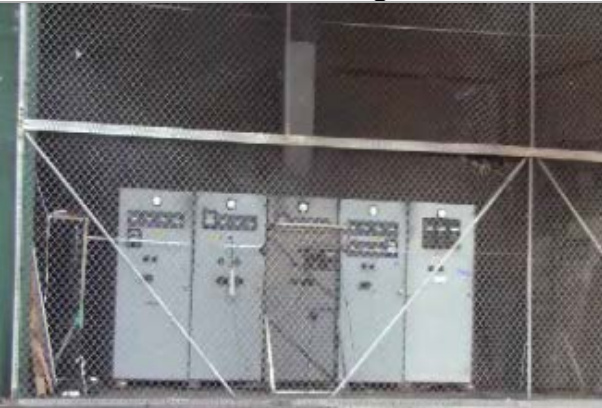


Image	Time	Description
	3 minutes	Still no flames visible, but smoke from cabinets increases.
	7 minutes	The flames from the vertical duct cables emerge.
	11 minutes	The fire was large because the duct acted like a stack pulling oxygen into all cabinets. Flames were 1 to 2 meters high.

Table 4-6. Ensuing Fire Sequence SWGR Test 2, Continued.






Image	Time	Description
	12.5 minutes	Manual extinguishment with water/baking soda started. Later water was applied.
	15.5 minutes	The water was not adequate to cool the fire and extinguishment stopped after 1.5 minutes. Fire re-grew to the original intensity.
	21 minutes	The cables in the vertical duct were mostly consumed and after 5 minutes of applying water, the fire was mostly out.

Table 4-6. Ensuing Fire Sequence SWGR Test 2, Continued.

Image	Time	Description
	<p>51 minutes</p>	<p>Cabinet 7 was opened, some CV-4 cables were still on fire.</p>
	<p>Final State</p>	<p>Cabinets 7 and 8 are heavily damaged. Propagation of fire into Cabinets 6 and 9. Cabinet 10 showed less damage.</p>

The fire was allowed to burn completely, providing the longest time-temperature data to study in the tests within this report. Table 4-7 shows the IR image sequence. The FLIR camera was set on “auto scale” to make the color spectrum distinct over the large range of temperatures and make it easy to see the fire spread. The fire visually appeared to reach its peak intensity at approximately 11 to 12 minutes. Although the HEAF was an intense ignition source, the fire behaved as expected for a typical cabinet fire.

Table 4-7. Thermal Image of Ensuing Fire SWGR Test 2.


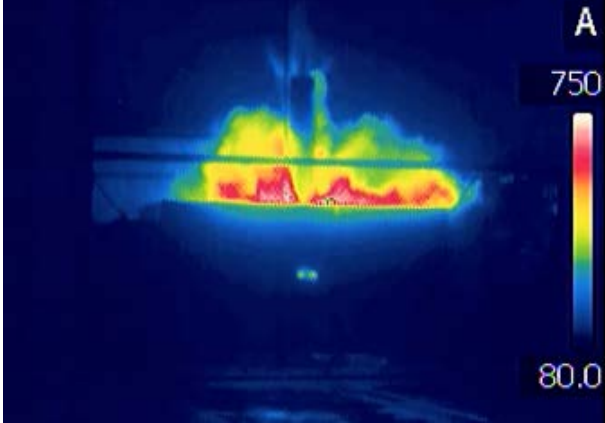
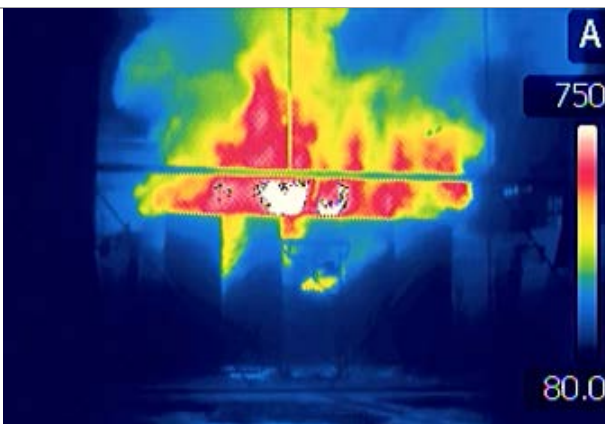
Image	Time	Description
	0	Arc Initiated.
	0.38 seconds	Fire expands.
	2.8 seconds	The flame between Cabinets 6 and 7 is from the plasma from Cabinet 8 leaking into Cabinet 7.

Table 4-7. Thermal Image of Ensuing Fire SWGR Test 2, Continued.

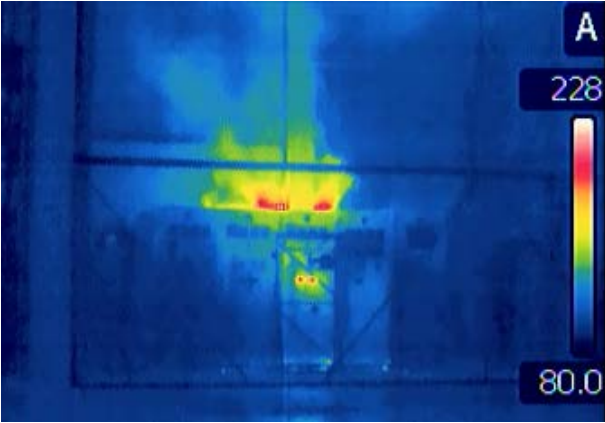
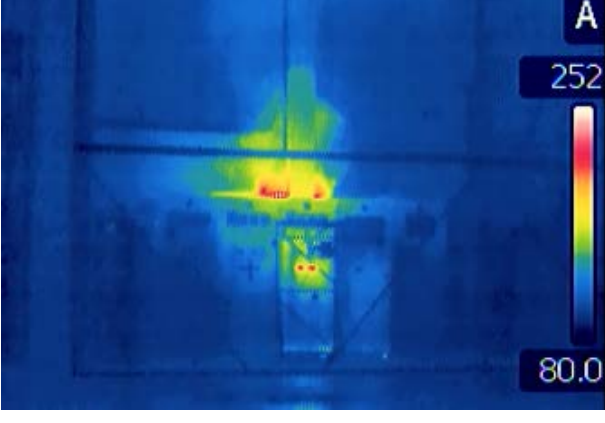
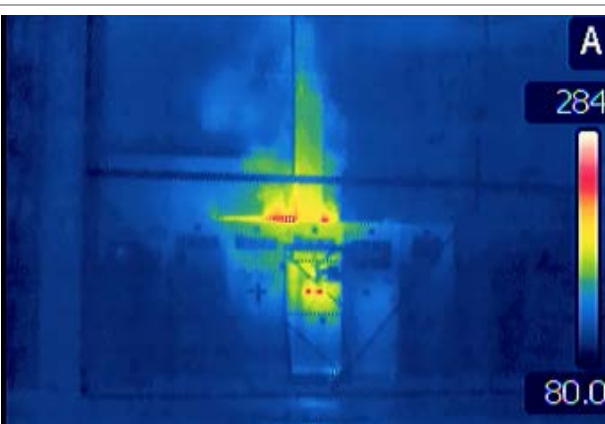
Image	Time	Description
	30 seconds	FLIR re-scaled for the much cooler fire.
	1 minute	Fire intensified as indicated by the FLIR temperature measurement.
	2 minutes	Fire continues to expand and intensify across the top front of the cabinets and up the vertical duct.

Table 4-7. Thermal Image of Ensuing Fire SWGR Test 2, Continued.

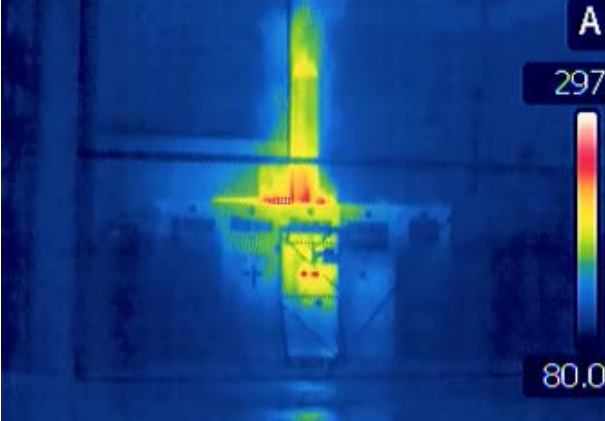
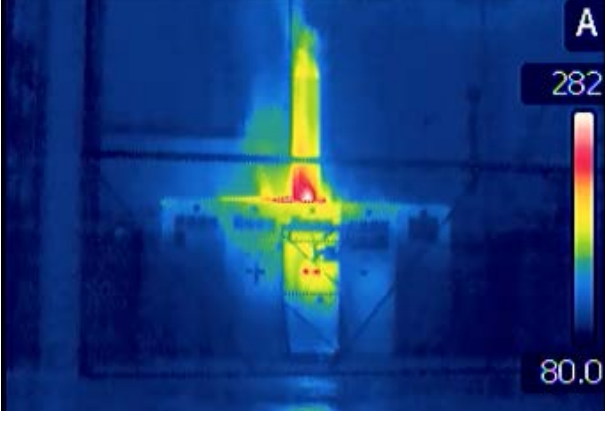
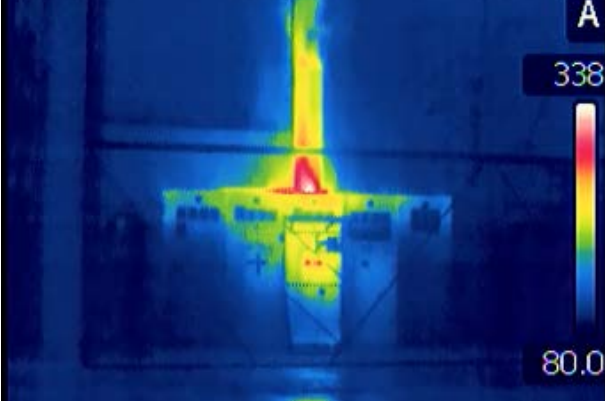
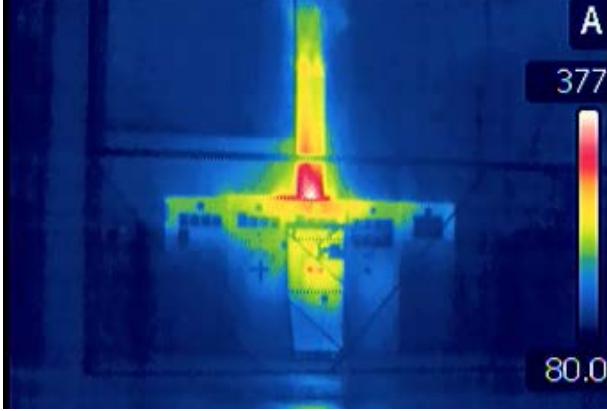
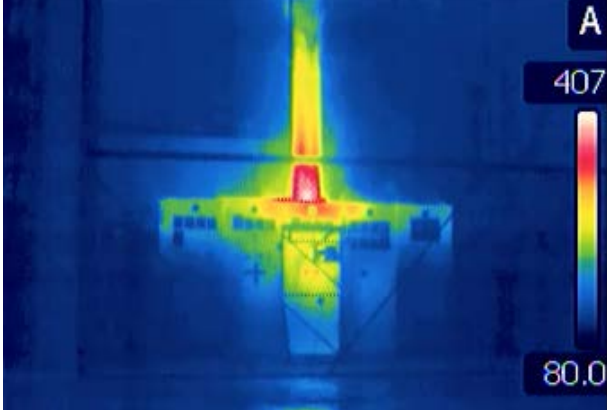
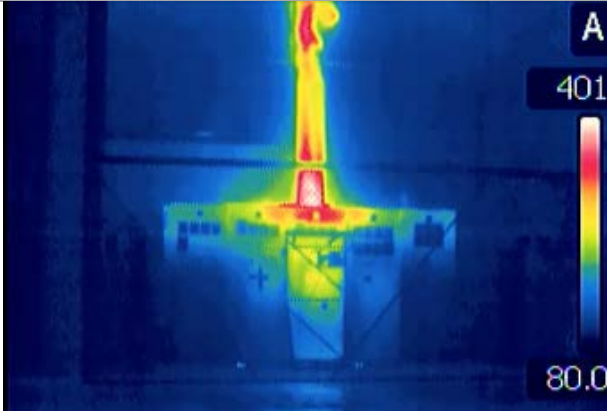
Image	Time	Description
	3 minutes	Fire continues to spread and intensify.
	4 minutes	Fire continues to spread but maximum temperature decreases slightly.
	5 minutes	Fire continues to spread and intensify.

Table 4-7. Thermal Image of Ensuing Fire SWGR Test 2, Continued.

Image	Time	Description
	6 minutes	Fire continues to spread and intensify.
	7 minutes	Just before flame was seen out of vertical duct.
	8 minutes	Flame out of vertical duct.

The SWGR cabinet outer walls did not have major deformation like the DP and MCC. The SWGR cabinet outer walls are thicker and the large vent allowed for pressure relief. The cabinet exteriors were slightly charred from the ensuing fire, but not as severely as at Onagawa which was not extinguished for 7 hours (see Chapter 6.10.4 for more detail). The vertical stack was heavily scorched and discolored from the intense stack fire. The orange color was also observed in the Onagawa event. The cables in the vertical duct (shown with cover removed) were completely burned.

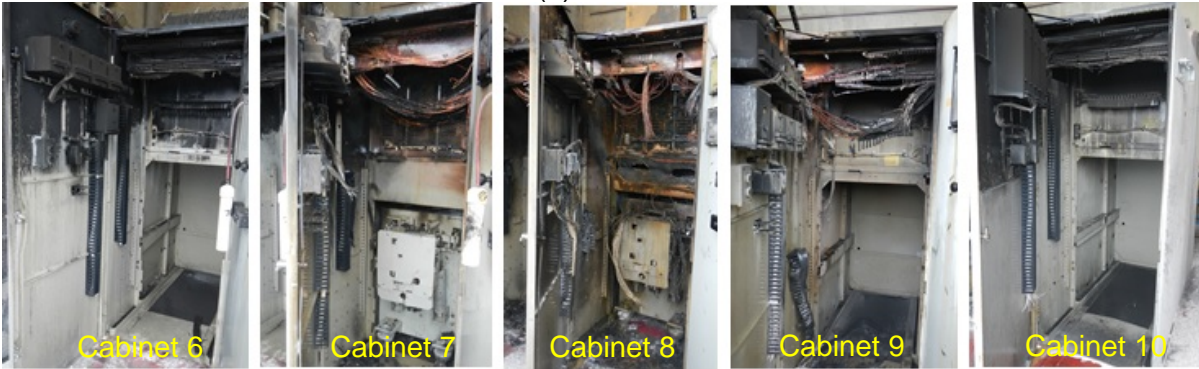


Figure 4.9-1. SWGR Test 2 Exterior Damage

The interior primary side was heavily damaged from the large and ensuing fire. Some cables burned in all cabinets except cabinet 10 on the far right, which only showed soot damage. There was heavy soot damage in Cabinets 6 through 8 and lighter soot damage in Cabinets 9 and 10. See Figure 4.9-2 for damage.

In Cabinet 6, about 50 percent of the cables burned in place but in Cabinets 7 and 8, the cables detached from the cabinet, slumped down, and were completely burned. The pressure and violence of the arc and associated leaking plasma most likely contributed to the detachment and disarray. In Cabinet 9, about 80 percent of the cables burned and there was also detachment and slumping of the cable bundle that was attached to the ceiling. The cables in Cabinet 10 did not burn.

(a) All cabinets



(b) Cabinet 6 Cables



(c) Cabinet 7 Cables



(d) Cabinet 8 Cables

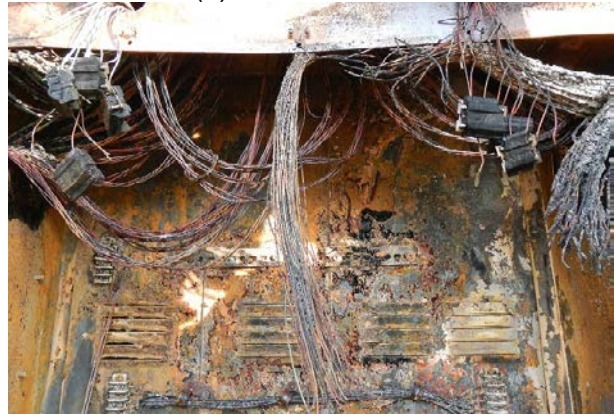
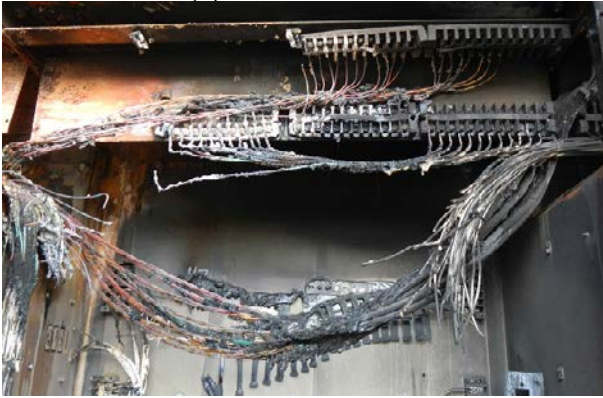


Figure 4.9-2. SWGR Test 2 Interior Damage, Continued

(e) Cabinet 9 Cables



(f) Cabinet 10 Cables



Figure 4.9-2, continued. SWGR Test 2 Interior Damage

Cabinet 7, Insulator 3 (on the right side of the cabinet) was damaged by the arc plasma coming from Cabinet 8, Insulator 1. The Cabinet 8 arc made a hole in the wall to Cabinet 7 as shown in the figure and the arc plasma spread. The vertical bus bars in Cabinet 8 were oxidized by the arc, as seen in Figure 4.9-3. The insulators in Cabinet 8 were destroyed, as expected and similar to Onagawa.

(a) Cabinet 7



(b) Cabinet 8



Figure 4.9-3. SWGR Test 2 Insulator and Bus Bar Damage

Breaker 8 had damage at the top primary side under the arc position but the secondary side was not damaged- only some soot was observed. There was some front panel discoloration from the heat and the control cable bundle on the front left burned. Breaker 7 only had some soot covering as shown in Figure 4.9-4.

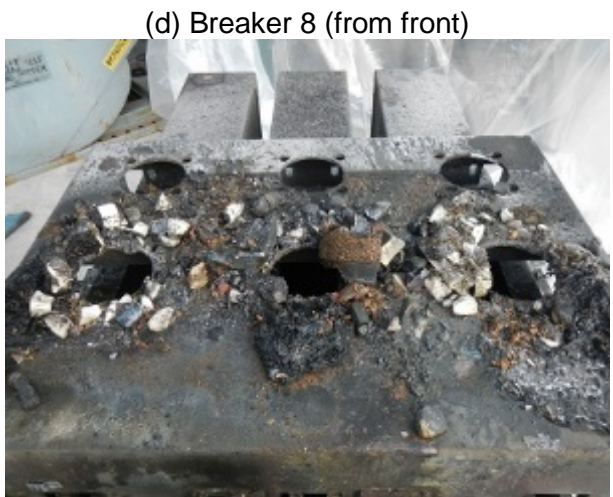
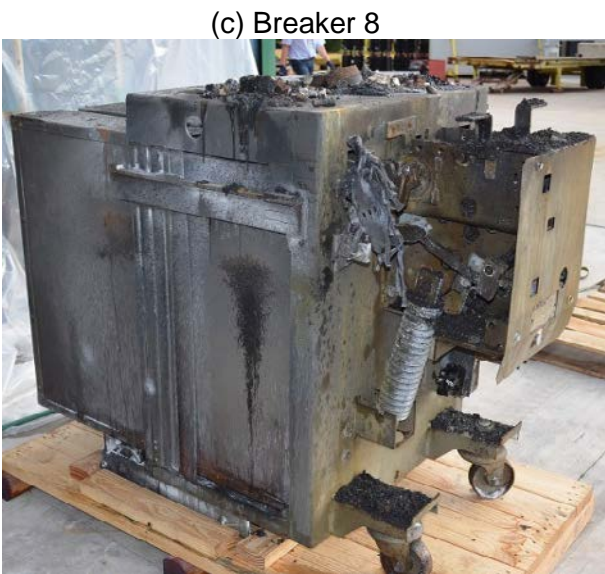
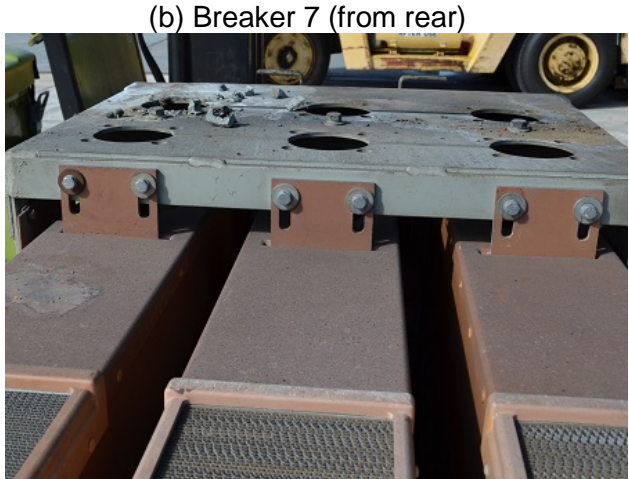
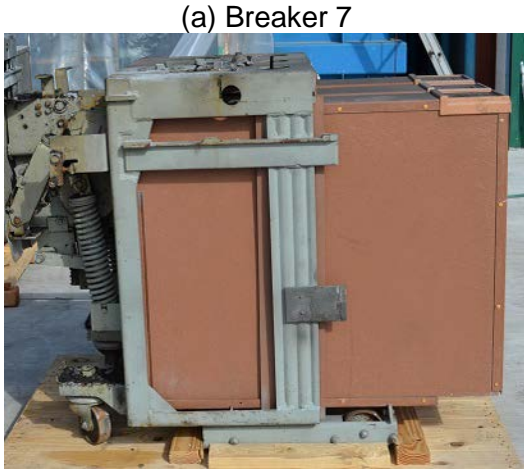


Figure 4.9-4. SWGR Test 2 Breaker 7 and 8 Damage

4.9.1 SWGR Test 2 Calorimetry Data

Temperatures measured at the slug locations are shown in Figure 4.9-5. The arc quenched at 2.957 seconds. Several slugs had significant noise during the arc, probably due to EMI; the power supply was directly next to the slug calorimeters. As in Test 1 the highest temperature at the end of the arc was above the cabinet (S5), hot gases were escaping through the roof vent. The ensuing fire produced a smooth and linear slug temperature rise from about 3 minutes to 12 minutes. At 12 minutes all of the slugs showed a temperature decrease as firefighting was started but subsequently all slugs showed when the firefighting efforts failed. The highest post-arc temperature response as the heat from the fire rose up was measured at the top (S5).

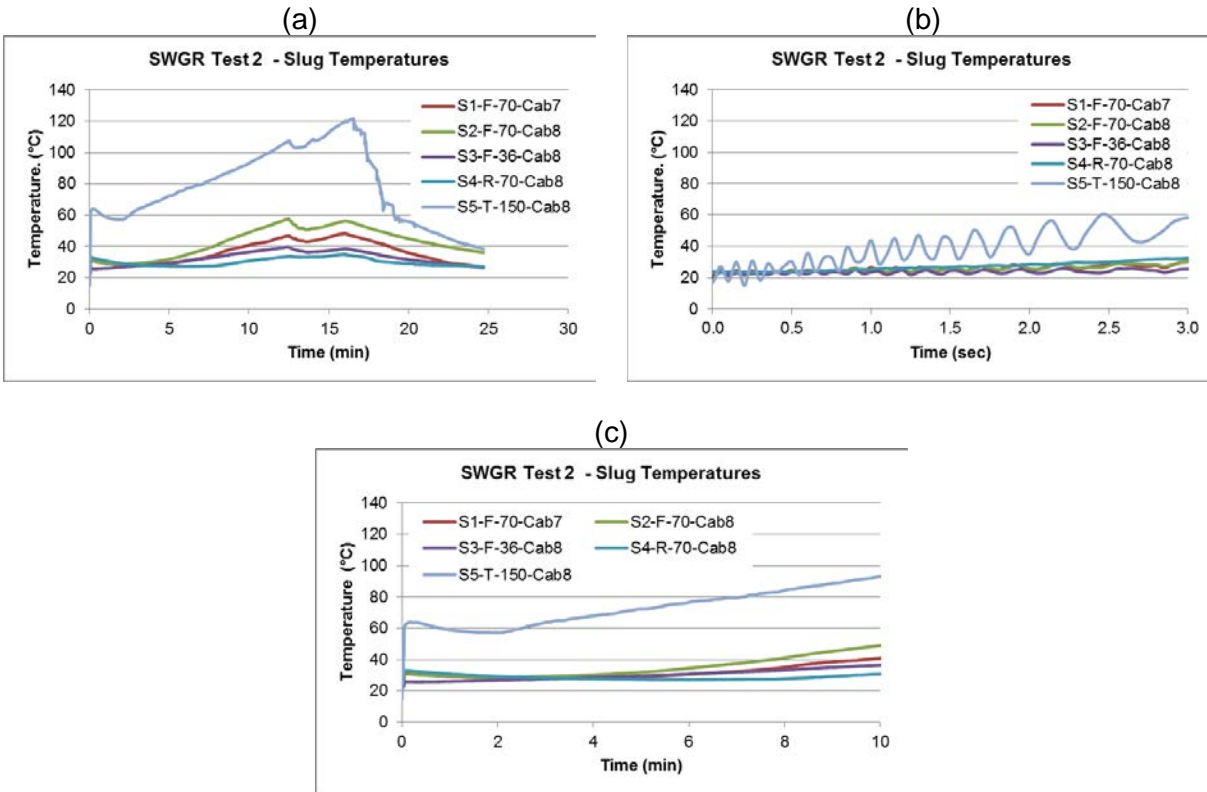


Figure 4.9-5. SWGR Test 2 Slug Calorimeter Temperature Data

Table 4-8 shows the flux results based on the ASTM F1959 method in Appendix A using the change in temperature (ΔT) between the start and end of the arc. Like Test 1, the maximum flux of 71 kW/m² is reported at the top (S5). The maximum slug temperatures are also shown to indicate the maximum temperature a metal object could reach during the arc.

Table 4-8. SWGR Test 2 Flux Results.

Slug	ΔT (°C)	Flux (kW/m ²)	Max T (°C)
S1-F-70-Cab7	6.8	14	48
S2-F-70-Cab8	6.9	14	58
S3-F-70-Cab8	2.6	5	40
S4-R-70-Cab8	8.9	18	35
S5-T-150-Cab8	34.7	71	122

4.9.2 SWGR Test 2 Temperature Data

The temperatures measured by the TCs are shown in the Figure 4.9-6. Table 4-9 shows the maximum temperature results. The only reliable data based on analysis was for TC1 and TC 2. The thermocouple maximum temperature is a general indication of the air temperature 15.2 cm (6 in) from the cabinet. Temperatures stayed low in the front of Cabinet 6 (TC1) and Cabinet 7 (TC2). Temperatures slowly increased during the ensuing fire from 6 to 12 minutes then became erratic during firefighting efforts. The TCs cannot be used to estimate flux.

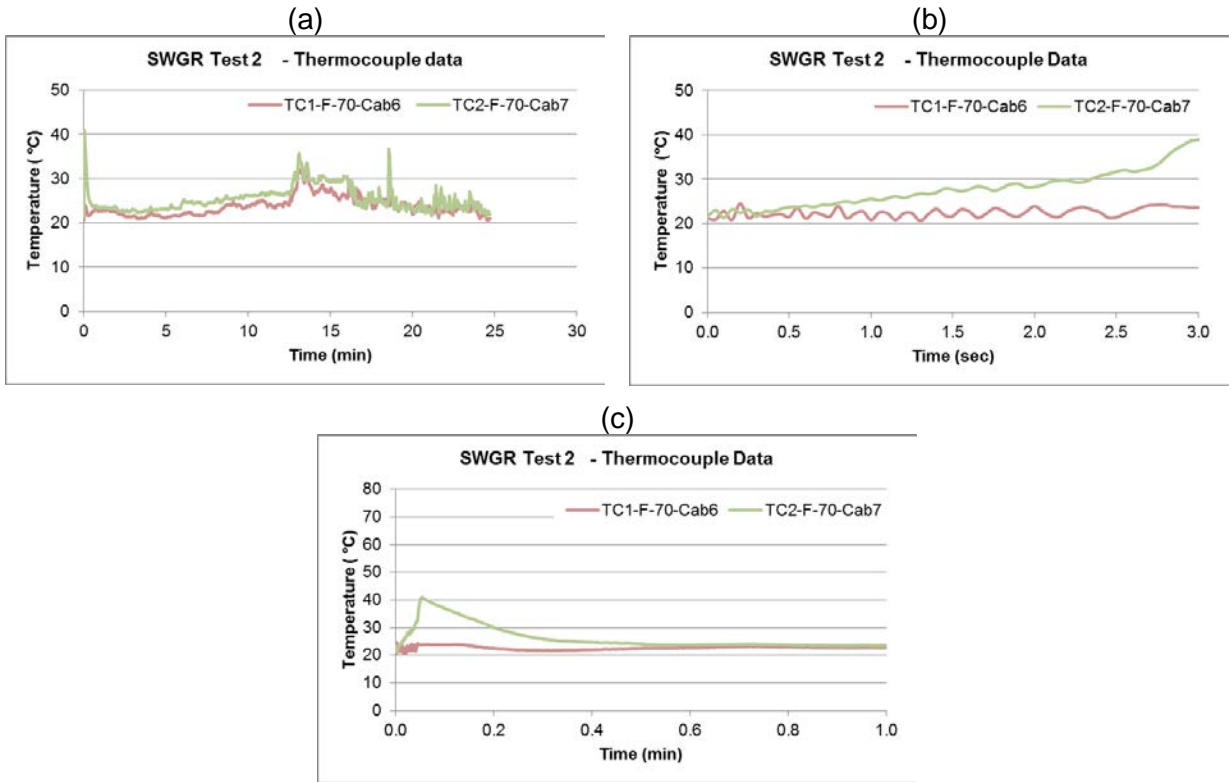


Figure 4.9-6. SWGR Test 2 Thermocouple Data

Table 4-9. SWGR Test 2 TC Results.

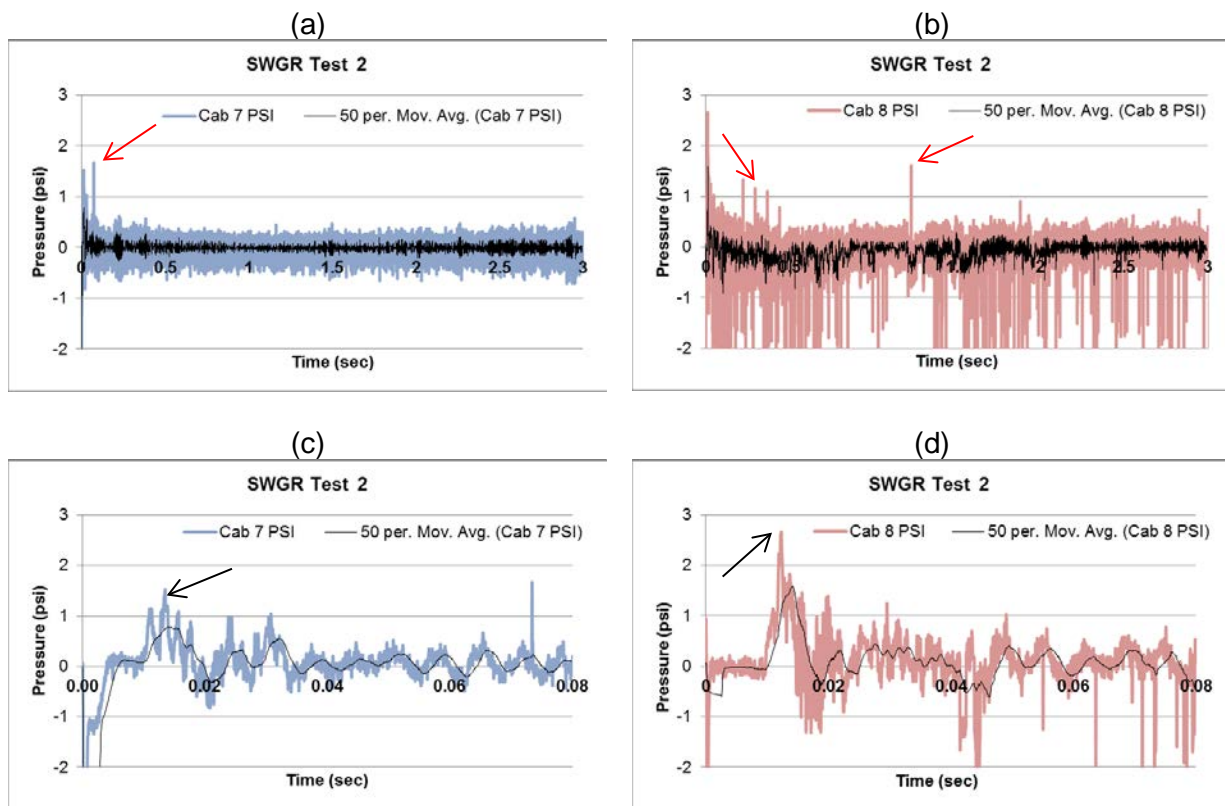
TC	Max T (°C)
TC1-F-70-Cab6	32
TC2-F-70-Cab7	41
TC3-F-70-Cab8	*
TC4-F-70-Cab9	*
TC5-V-Cab8	*

*Data was corrupt

4.9.3 SWGR Test 2 Pressure Data

The pressures during the arc are shown in Figure 4.9-11. There were noise spikes in the data at 0.07 seconds for Cabinet 7 and several around 0.4 seconds and at 1.22 seconds for Cabinet 8 (denoted by the red arrows in Figure 4.9-11(a) and (b)). Cabinet 8 also had numerous large negative spikes that do not have a known cause; it may be due to noise or sensor failure. The Cabinet 8 pressure closer to the arc had a higher maximum and occurred slightly earlier than the Cabinet 7 pressure that was further from the arc. The maximum pressures are indicated by the arrows in Figure 4.9-7(c) and (d). The pressures were low because the vents at the top of Cabinets 7 and 8 allowed the pressure to escape.

The pressure analysis methods are in Appendix A and involved picking the maximum near the start of the arc then including a nominal uncertainty for the noise in the signal just before the arc.



Test 2 Pressure 1 Cab. 7
 8.3 ± 1.4 kPa (1.2 ± 0.2 psi)
@ 0.0135 s

Test 2 Pressure 2 Cab. 8
 16.5 ± 1.4 kPa (2.4 ± 0.2 psi)
@ 0.0123 s

Figure 4.9-7. SWGR Test 2 Pressure Data

4.9.4 SWGR Test 2 Arc Energy

The arc duration was 2.957 seconds with total energy of 58.2 MJ, seen in Figure 4.9-8. The energy analysis methods are in Appendix A. The “Energy” is calculated as volts multiplied current multiplied by the time step and each time step is shown. “Energy Total” is the cumulative sum of the energy in each time step.

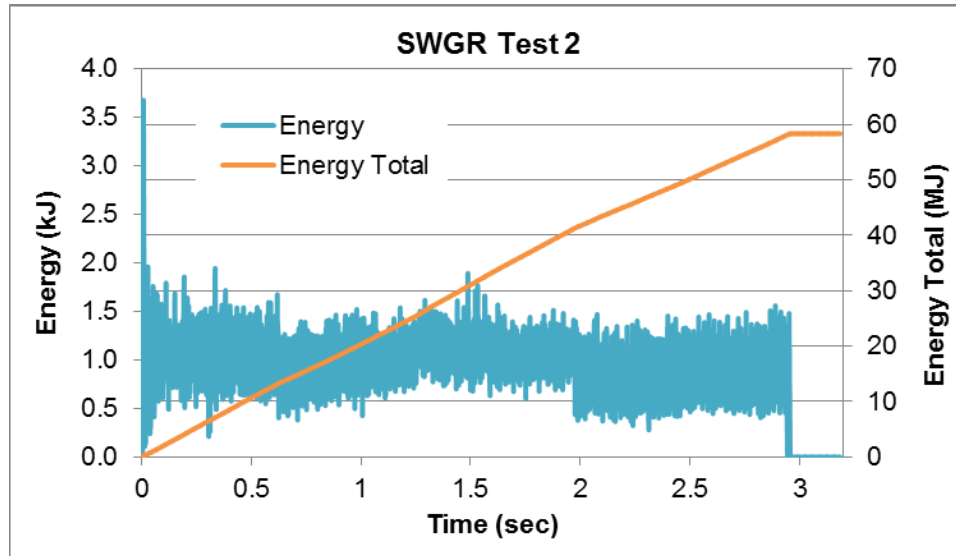


Figure 4.9-8. SWGR Test 2 Arc Energy

4.10 SWGR Test 3 Key Observations

This test was initiated at 7.1 kV and 29.8 kA and a target arc duration of 3 seconds with a total energy of 64.2 MJ. The arc duration of 3 seconds was achieved. The arc progression can be seen in Figure 4.10-1. Although there was an ensuing fire, it was manually extinguished quickly for safety reasons.

In this test, two 10.1 cm (4 in) circular openings were added at 30.5 cm (12 in) and 61 cm (24 in), centered from the bottom of the vertical duct to provide a way to inject water for fire suppression. This was done as a precautionary measure for facility safety based on the fire intensity of Test 2.

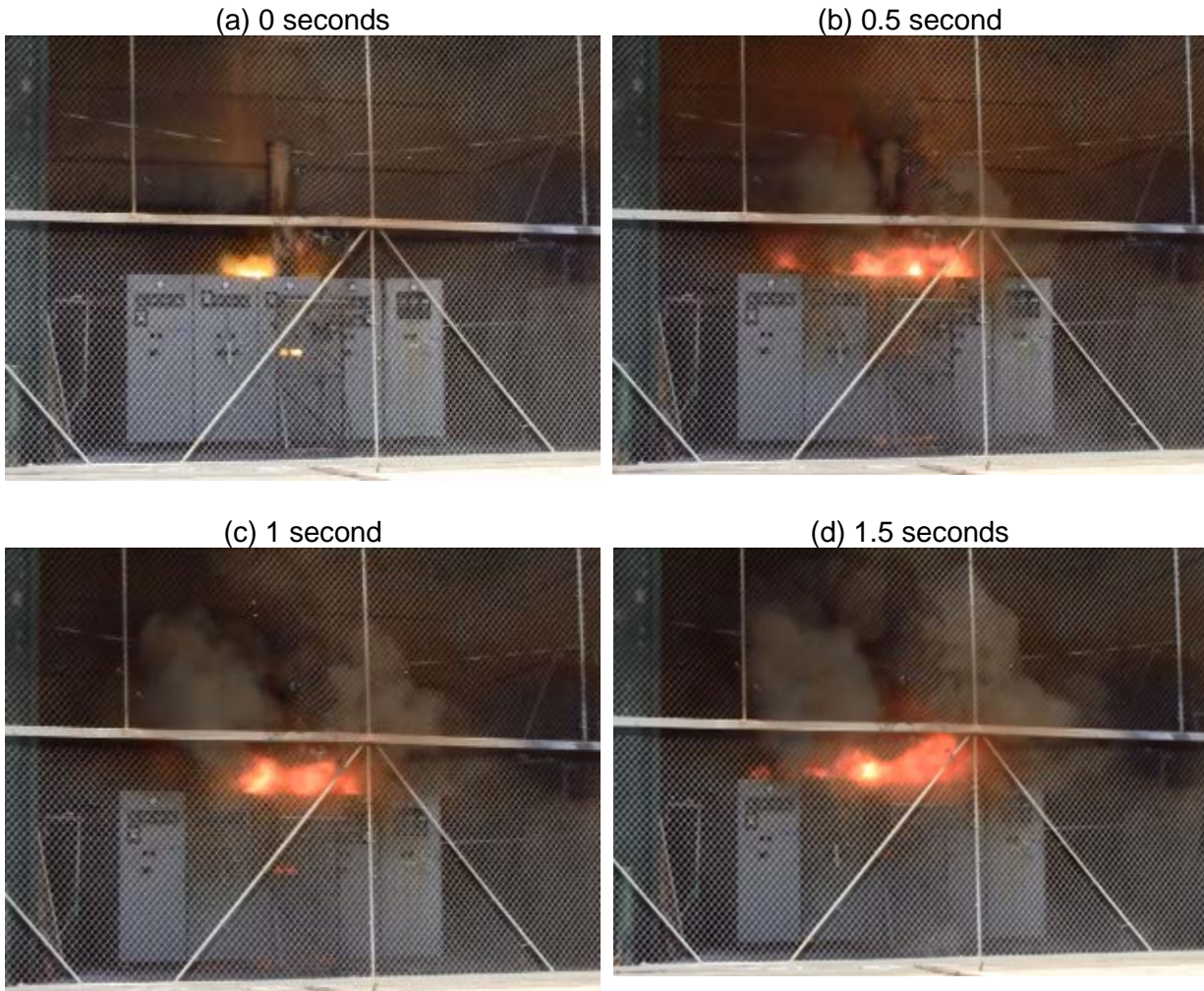


Figure 4.10-1. SWGR Test 3 Arc



Figure 4.10-1. SWGR Test 3 Arc, continued

Figure 4.10-2 shows the ensuing internal fire (noted by the arrows). No large flames were visible; the only visible flames were through the holes in the vertical duct and in the front door of the cabinet shown by the arrows. The FLIR camera failed in this test so there are no IR thermal images.

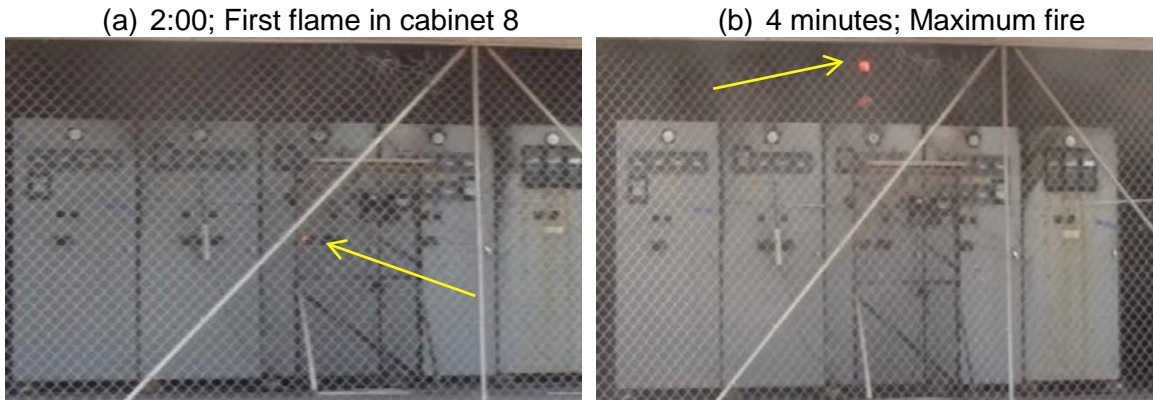


Figure 4.10-2. SWGR Test 3 Ensuing Fire

Exterior cabinet damage was small since the fire was extinguished quickly, as seen in Figure 4.10-3. There was no major scorching or charring on the front of the cabinets. There was light soot that leaked from behind the instruments and at the door joints at the very top of Cabinets 6, 7, and 8. The yellowish water streaks from the instruments to the bottom of the cabinet front doors were there before the tests (probably from long-term outdoor storage of the cabinets at the used electrical equipment vendor).

(a) Cabinets 6, 7, and 8



(b) Cabinets 9, 10



Figure 4.10-3. SWGR Test 3 Exterior Damage

Figure 4.10-4 shows the interior damage; Figure 4.10-5 shows detailed damage. Cabinets 7 and 8 showed heavy soot damage and orange discoloration from the high temperatures. Figure 4.10-5(f) shows the soot was throughout the interior of Cabinet 8.

Some cables burned in all cabinets except Cabinet 10, which only showed soot damage, in Figure 4.10-4. There was heavy soot damage in all cabinets. In Cabinet 6, only a few centimeters of the cables burned where they entered from Cabinet 7. The Cabinet 7 upper cables were completely burned, and had detached from the cabinet and slumped down. The Cabinet 8 upper cables were mostly burned and remained in place and attached. In Cabinet 9, a small amount of the upper cables burned where the cables entered from Cabinet 8, and the cables detached and slumped. This fire was quickly extinguished by KEMA personnel to avoid the large fire that occurred during Test 2.

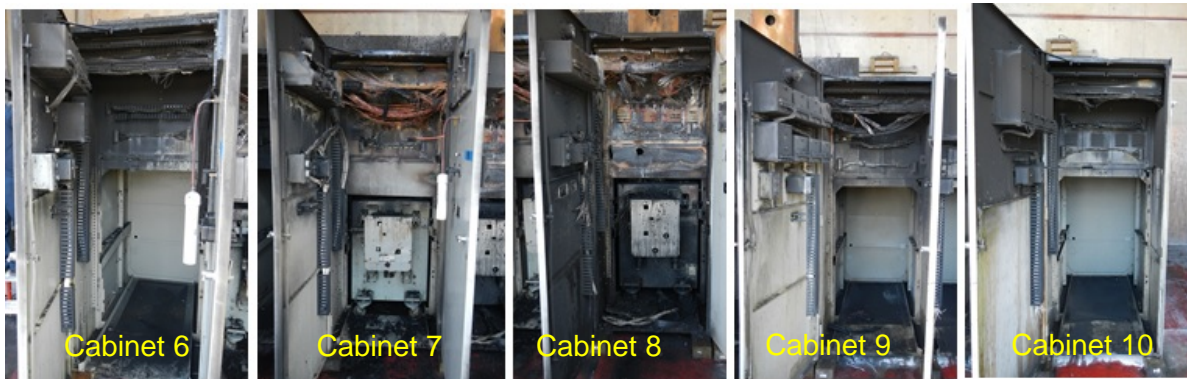
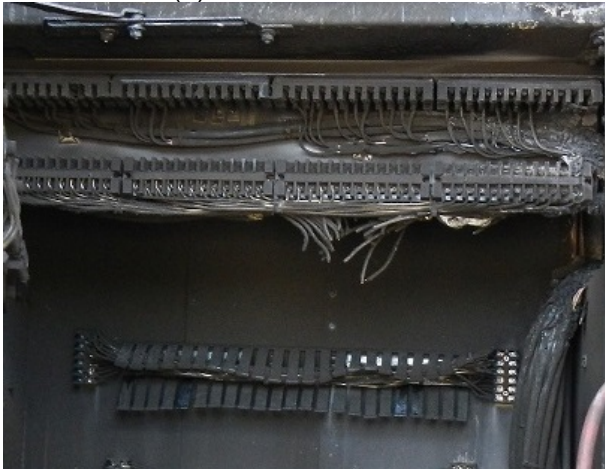
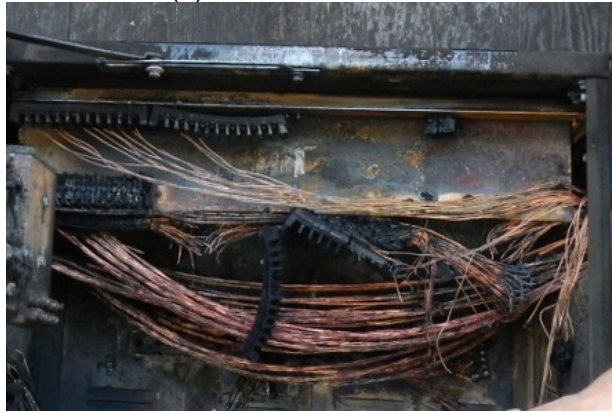


Figure 4.10-4. SWGR Test 3 Interior Damage

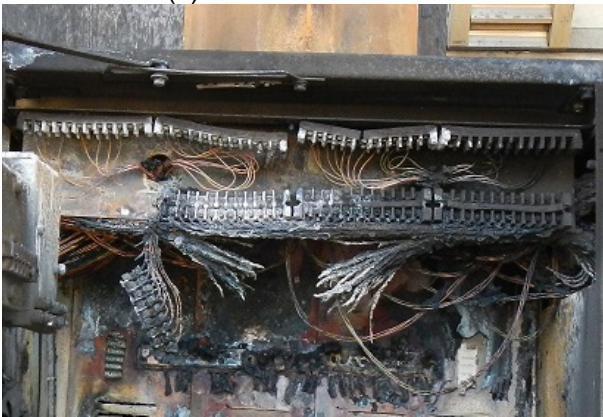
(a) Cabinet 6 Cables



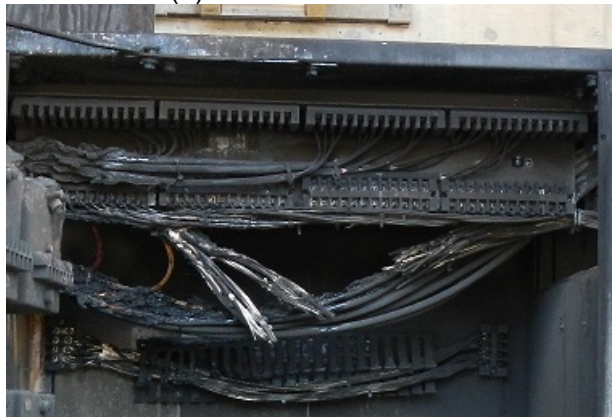
(b) Cabinet 7 Cables



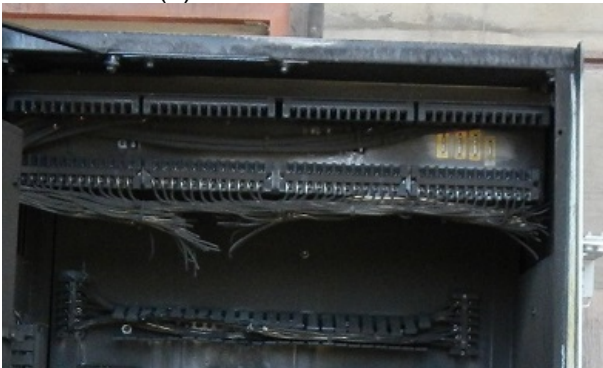
(c) Cabinet 8 Cables



(d) Cabinet 9 Cables



(e) Cabinet 10 Cables



(f) Cabinet 8 Side View



Figure 4.10-5. SWGR Test 3 Interior Damage, Detailed

The bus bar damage was very similar to Test 2, and is shown in Figure 4.10-6. Cabinet 7, Insulator 3 (on the right side of the cabinet) was damaged by the arc plasma coming from Cabinet 8, Insulator 1. The Cabinet 8 arc made a hole in the wall to Cabinet 7 as shown in the figure and the arc plasma spread. The vertical bus bars in Cabinet 8 were oxidized by the arc. The insulators in Cabinet 8 were destroyed, as expected, similar to Onagawa.



Figure 4.10-6. SWGR Test 3 Insulator and Bus Bar Damage

Figure 4.10-7 shows the breaker damage. Breaker 8 had damage at the top primary side under the arc position but the secondary side was not damaged - only some soot was observed. There was no front panel discoloration and the control cables on the front were not burned. Breaker 7 only had some minor soot at the top of the breaker.

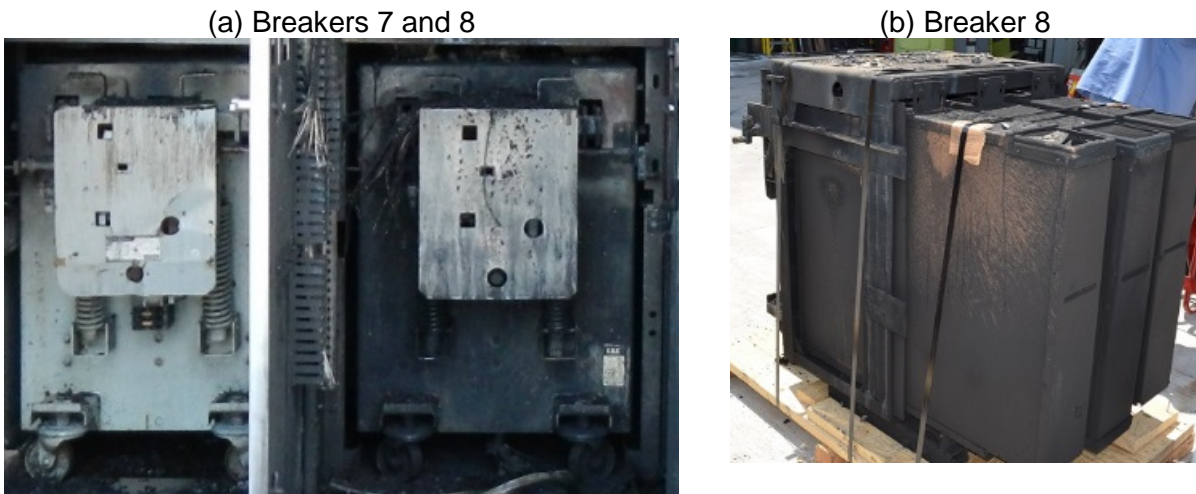


Figure 4.10-7. SWGR Test 3 Breaker Damage

4.10.1 SWGR Test 3 Calorimetry Data

Temperatures measured at the slug locations are shown in Figure 4.10-8. The arc quenched at 2.911 seconds. Several slugs had high noise during the arc probably due to EMI; the power supply was nearby. The highest temperature at the end of the arc was at the top of Cabinet 8 (S5), probably because hot gases escaped through the roof vent as in Tests 1 and 2. All of the slugs except S4 on the rear showed increasing temperature as the ensuing fire began to build. At 4.2 minutes all of the slugs showed temperature decreases as firefighting was started and the fire was extinguished.

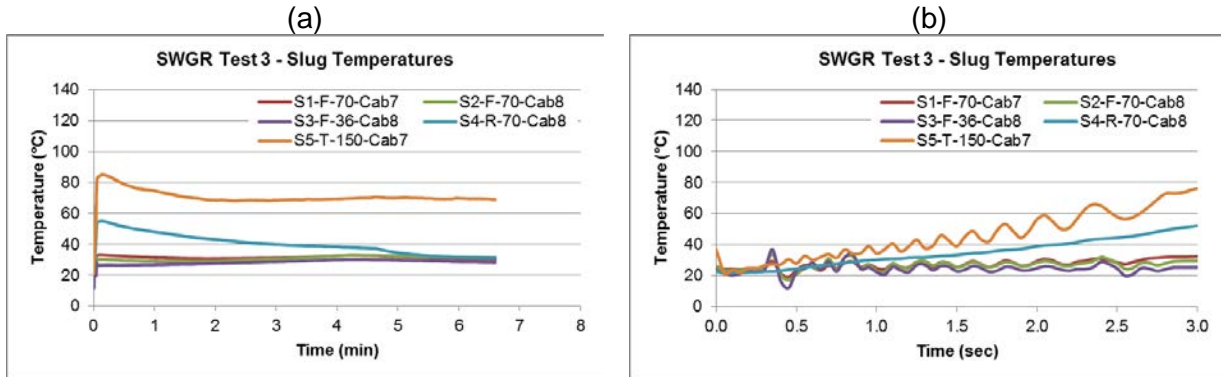


Figure 4.10-8. SWGR Test 3 Calorimetry Temperature Data

Table 4.10-1 shows the flux results based on the ASTM F1959 method in Appendix A using the change in temperature (ΔT) between the start and end of the arc. The maximum flux of 107 kW/m² was measured at the top (S5). The maximum slug temperatures are also shown to indicate the maximum temperature a metal object could reach.

Table 4-10. SWGR Test 3 Flux Results.

Slug	ΔT (°C)	Flux (kW/m ²)	Max T (°C)
S1-F-70-Cab7	7.6	16	33
S2-F-70-Cab8	5.1	11	34
S3-F-70-Cab8	1.9	4	37
S4-R-70-Cab8	29.7	62	55
S5-T-150-Cab8	51.2	107	85

4.10.2 SWGR Test 3 Temperature Data

The temperatures measured by the TCs are shown in the Figure 4.10-9. Table 4-11 shows the maximum temperature results. Only TC1 and TC 2 had valid data. The thermocouple maximum temperature is a general indication of the air temperature 15.2 cm (6 in) from the cabinet. Temperatures stayed low in the front of Cabinet 6 (TC1) and Cabinet 7 (TC2). Temperatures did not increase during the ensuing fire because the fire was extinguished quickly.

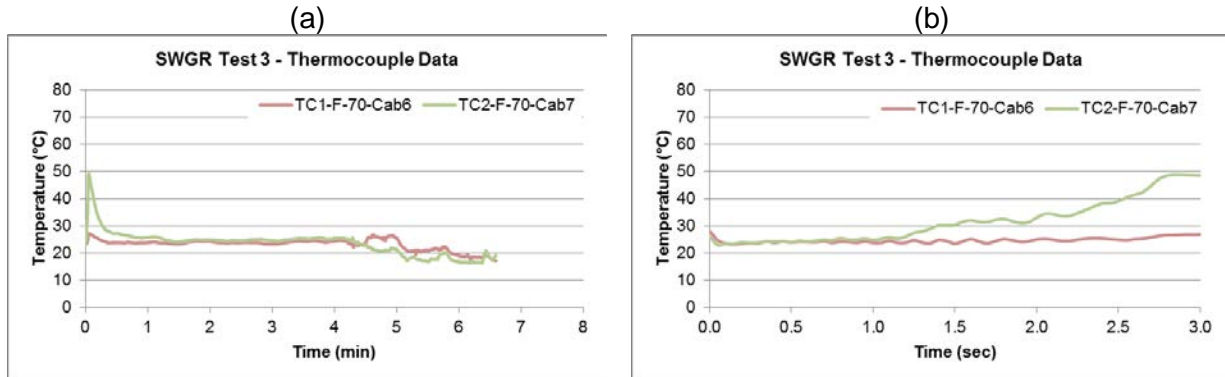


Figure 4.10-9. SWGR Test 3 Thermocouple Data

Table 4-11. SWGR Test 3 TC Results.

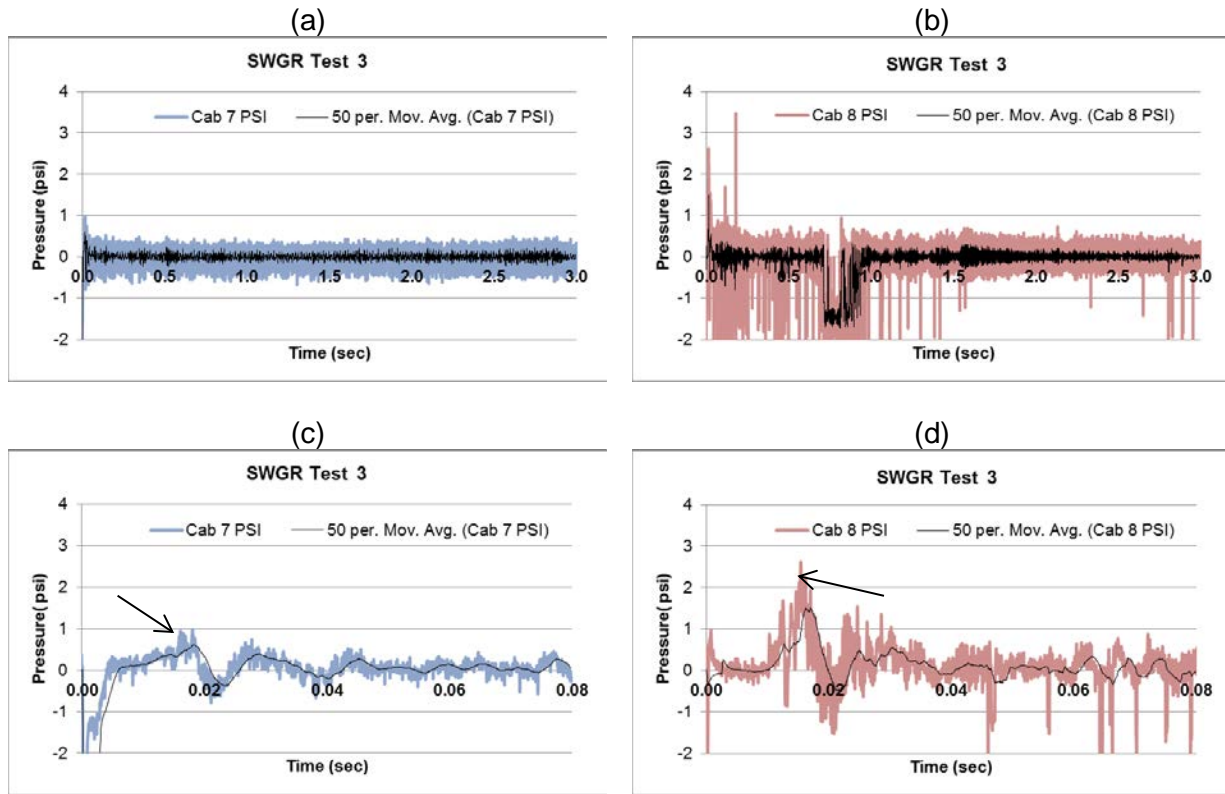
TC	Max T (°C)
TC1-F-70-Cab6	28
TC2-F-70-Cab7	49
TC3-F-70-Cab8	*
TC4-F-70-Cab9	*
TC5-V-Cab8	*

*Data was corrupt

4.10.3 SWGR Test 3 Pressure Data

The pressures during the arc are shown in Figure 4.10-10. Cabinet 8 had positive noise spikes at 0.116 and 0.180 seconds and numerous negative noise after 0.04 seconds that do not have a known cause. The Cabinet 8 response also had a base line zero shift from 0.7 to 0.9 seconds (similar to SWGR Test 1) and at the start of the arc that was considered in the analysis. The Cabinet 8 pressure closer to the arc had a higher maximum and occurred earlier than the Cabinet 7 pressure that was further from the arc. The pressures were low because the vents at the top of Cabinets 7 and 8 allowed for significant pressure relief. The maximum pressures are indicated by the arrows in Figure 4.10-10(c) and (d).

The pressure analysis methods are in Appendix A and involved picking the maximum near the start of the arc then including a nominal uncertainty for the noise in the signal just before the arc



Test 3 Pressure 1 Cab. 7
 5.5 ± 2.1 kPa (0.8 ± 0.2 psi)
 @ 0.016 s

Test 3 Pressure 2 Cab. 8
 13.8 ± 1.4 kPa (2.0 ± 0.2 psi)
 @ 0.0155 s

Figure 4.10-10. SWGR Test 3 Pressure Data

4.10.4 SWGR Test 3 Arc Energy

The arc duration was 2.911 seconds with total energy of 64.2 MJ, seen in Figure 4.10-11. The energy analysis methods are in Appendix A. The “Energy” is calculated as volts multiplied current multiplied by the time step and each time step is shown. “Energy Total” is the cumulative sum of the energy in each time step.

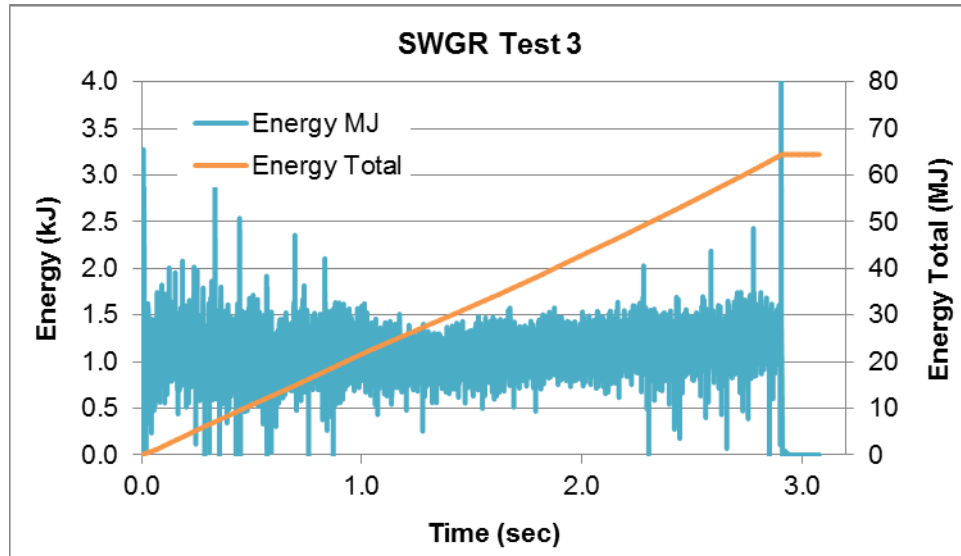


Figure 4.10-11. SWGR Test 3 Arc Energy

4.11 SWGR Tests 1 through 3: Summary of Electrical Conditions

Table 4.11-1 shows the electrical conditions measured by KEMA.

Table 4-12. SWGR Tests 1 through 3 Electrical Results (1).

Test	OCV (KV)	Phase	Sym (kA)	Sym @End (kA)	Peak (kA)	Curr. Dur. (sec)	Arc Energy (MJ)	Freq @End (Hz)	Phase Arc Volts
1	7.1	A	33.7	22.8	58.4	2.044	13	45	A-N 330
		B	22.9	22.6	36.4		15		B-N 375
		C	31.8	22.5	53.8		14		C-N 349
		AVG	29.5	22.6	49.5		Σ42		AVG L-L 609
2	7.1	A	34.3	22.9	59.5	2.957	22	40.8	A-N 359
		B	25.8	25.4	37.9		25		B-N 435
		C	31.5	22.2	53.5		11		C-N 259
		AVG	30.5	23.5	50.3		Σ58		AVG L-L 608
3	7.1	A	34.0	22.6	58.9	2.911	22	40.8	A-N 365
		B	23.3	22.9	36.7		23		B-N 412
		C	32.1	22.4	54.1		19		C-N 320
		AVG	29.8	22.6	49.9		Σ64		AVG L-L 633

(1) See Table 2-16 for abbreviations and acronyms used in this table.

4.12 SWGR Tests 1 through 3 Qualitative Summary

Although the configuration was slightly changed from Test 1 for Tests 2 and 3, there were many similarities in the test results. However, the increase in arc duration produced some differences in the tests, too.

1. **Ensuing Fire:** An ensuing fire occurred after the configuration and test conditions were changed between Test 1 and Test 2. The extra one second of arc duration in Tests 2 and 3 provided enough heat to ignite the internal cables. The ensuing fire was allowed to burn in Test 2, providing new long-term data on the ensuing fire and showed fire spreading to all cabinets. In Test 3 (and future SWGR tests) the fire was extinguished after a few minutes.
2. **Damage:** In all of the tests, there was oxidation of the aluminum bus bars and the associated heat release during the arc. The vertical bus bars in Cabinet 8 in Tests 2 and 3 were oxidized and melted by the arc; Test 1 only resulted in minor bus bar oxidation. Bus bar oxidation in Test 2 and 3 likely contributed to the ignition of the ensuing fire.

There was a variety of damage to the cabinets and internal cables. Since there was no internal or ensuing fire in Test 1, there was minor damage; mostly soot deposits, and discoloration, and no damage to the internal breakers. Tests 2 and 3 resulted in severe internal cable consumption but with minor external damage.

The SWGR cabinet outer walls did not have major deformation like the DP and MCC cabinets. The cabinet outer walls are thicker and the large vent on the top directly above the arc kept the pressure low. Additionally, the arcs in SWGR Tests 1 through 3 were not directly inside an outer cabinet wall so external wall damage was minimal. There was significant bending, deformation, or burn-through of the internal walls directly exposed to the arc.

3. Calorimetry: In all three tests, the resultant maximum heat flux occurred at 1.5 m (5 ft) above the cabinets because the flux from the arc travels through the single steel plate above the arc to the slug calorimeter. At other locations, the heat passes through an internal wall and external panels to reach the calorimeters. Also, the top slug calorimeter can view the flames and plasma that spread across the top of the cabinet as they exit the roof vent.
4. Temperature: During these tests, many of the thermocouples failed for various reasons. Of the remaining valid measurements, it was evident that the temperatures increased in Tests 2 and 3, as compared to Test 1, as expected.
5. Pressure: The measured pressures for Tests 1 through 3 were very low since there were vents at the top of the tested cabinets (Cabinets 7, 8). For Tests 2 and 3 the pressures were highest in Cabinet 8 where the arc occurred, as expected (there was no Cabinet 7 data to compare for Test 1).
6. Arc Energy: In all tests the total energy was proportional to the arc duration for the given electrical testing conditions. All tests showed a smooth increase of the total energy during the arc indicating stable arc conditions and the target arc durations were achieved in all the tests. Based on the occurrence of ensuing fires, the electrical energy threshold for an ensuing internal cable fire was about 60 MJ. This is likely higher than what was sufficient to ignite an ensuing fire in the DP tests because heat was lost through the vent above the arc.

5 Switchgear HEAF Tests 4 through 6, Two Arcs Tests - KEMA (March 2014, March 2015)

5.1 SWGR Tests 4 through 6 Overview

The purpose of these tests was to obtain the basic data for SWGR like the June 2013 tests. However, the tests presented in this section, conducted in March 2014 and March 2015, used two arcs, one in Cabinet 7 and one in Cabinet 8, to be more like the assumed condition of the Onagawa event.

5.2 SWGR Tests 4 through 6 Summary of Results

The key test parameters and results are in the table below; two arcs were initiated for each test. Tests 4 and 5 were conducted at the same parameters: Arc 1 target test voltage was nominally 6.9 kV and the target test current was 23 kA (symmetrical, sym) for 2.5 seconds, Arc 2 was also nominally 6.9 kV but with a test current of 35 kA for 3 seconds for Tests 4 and 5. Test 6 had target durations of 1 second for Arc 1 and 3 seconds for Arc 2.

Table 5-1. SWGR Tests 4 through 6 Summary of Results.

Test	Arc	Volt (kV) (1) Curr (kA) (2)	Test Peak Current (kA) (3)	Arc duration (sec) (4)	Arc Energy (MJ)	Internal Max Press (kPa/psi)	Ext Max Flux (kW/m ²)	Ensuing fire? Key Observations
4	1	7.0/0.726 24.5/24.4	51.3	2.5 2.354	64.6	23.4 ± 0.7 3.4 ± 0.1	46 (5)	Yes. Small fire after Arc 1 and large fire after Arc 2 from aluminum oxidation.
	2	7.0/0.727 34.1/33.3	74.8	2.0 2.081	78.4	12.4 ± 0.6 1.8 ± 0.1	220 (6)	
5	1	7.0/0.639 24.4/25.7	50.1	2.5 2.316	57.2	17.9 ± 0.7 2.6 ± 0.1	37 (5)	Yes. Small fire after Arc 1 and small fire after Arc 2.
	2	7.0/0.603 33.9/33.3	60.3	2.0 2.071	62.0	13.1 ± 0.7 1.9 ± 0.1	113 (5,7)	
6	1	7.0/0.882 24.6 / 21.4	56.2	1.0 1.129	26.5	12.4 ± 1.4 1.8 ± 0.2	- (8)	No. Energies including aluminum oxidation were too low.
	2	7.0/1.007 33.1 / 33.5	75.5	3.0 0.568	21.1	9.0 ± 1.4 1.3 ± 0.2	53 (9)	

Notes:

- (1) The voltage is shown as the target voltage / arc Line-to- Line (L-L) voltage.
- (2) The symmetric arc current slowly drops during the test as the arc impedance increases. This shows the *test start current / test end current*. These are average currents of all 3 phases.
- (3) This is the peak current of for any phase or time, usually the asymmetric current at the start
- (4) The duration is shown as the target duration and the actual test duration below it.
- (5) The maximum flux was measured at the top, 1.5 m (5 ft) above Cabinet 8 (S5).
- (6) The highest flux was measured 0.91 m (3 ft) in front of Cabinet 7 (S1), which had the large horizontal bus bar arc and aluminum oxidation. This was the highest flux in all NRA tests.
- (7) A high flux of 67 kW/m² was measured at 0.91 m (3 ft) from the rear of Cabinet 8, indicating a strong arc in the secondary side of Cabinet 8, as planned.

- (8) There was no slug calorimeter data for Arc 1 because the data trigger failed.
- (9) The maximum flux was measured at 0.91 m (3 ft) from the top rear of Cabinet 8 (S10).

The key results from the SWGR 2-arc tests at KEMA were:

- Test 4, Arc 2 had severe horizontal bus bar arcing, which was similar to the assumed second arc in the 2011 Onagawa event scenario. The arc energy progressed to a significant fire and extensive damage on the front of Cabinet 7, similar to Onagawa. This test confirms that the aluminum bus bar oxidation probably contributed to the large ensuing fire at Onagawa.
- In Arc 2 of Tests 5 and 6, there were strong arcs in the secondary (rear) of Cabinet 8, as planned. However, the damage to the circuit breaker was not as severe as the event at Onagawa. In Test 5 Arc 2, the hot gas and plasma were expelled up through the roof and out the vent rather than down toward the breaker. In Test 6 Arc 2, the hot gas and plasma remained in the rear of the cabinet but the damage to the breaker was still minor.
- The energies for the arcs were greater than 60 MJ in SWGR Tests 4 and 5, resulting in ensuing fires. This is similar to the result in SWGR Tests 1 through 3. The energies in Test 6 were not adequate for an ensuing fire because a shorter Arc 1 was planned (1 second versus 2 seconds) and the second arc was extinguished by a hot short that opened the Cabinet 8 breaker carrying the arc current from the KEMA source.
- These tests had higher total energies than Tests 2 and 3 because there were two electrical arcs and much more aluminum oxidation, especially in the case of Test 4, Arc 2. The fire in Test 4 quickly spread to the other cabinets. The cables were pre-heated by Arc 1 so the cable fire spread was very rapid in Test 4, Arc 2.
- Test 4, Arc 2 showed the highest external flux in any NRA test. None of the cables in the test cable trays on the top of the SWGR ignited but there was some fire damage; there was localized burning where the cables were in contact with the tray rungs, and charring.
- Test 6, Arc 2 demonstrated the important behavior that arcs can move from the initial ignition point because the arc ignited at the insulator but moved to the end of the bus bars along the path of the current. This also demonstrates that arc behavior is difficult to predict because in an identical test configuration in SWGR Test 5, Arc 2 stayed at the initial ignition point.

5.3 SWGR Tests 4 through 6 Cabinet Lineup and Combustible Load

The configuration was very similar to SWGR Test 1 through 3 tests except a working breaker was used in Cabinet 8 to allow two arcs. Arc 1 was initiated in the primary side of Cabinet 7 with the breaker open and Arc 2 was initiated in the secondary side of Cabinet 8 with the breaker closed. The bus bars were modified for the working breakers. The bus bars in Cabinet 7 were moved up (this makes the vertical bus bars much longer than in the June 2014 tests), as seen in Figure 5.3-1. Insulator bushings were added to the secondary side of Cabinet 8 at the arc location. Cabinet 8 was modified for a working circuit breaker so the primary insulators were moved higher in the cabinet and secondary insulators were added, as seen in Figure 5.3-2. The shorting wires to start the arc were on the primary side of Cabinet 7 and secondary side of Cabinet 8, as seen in Figure 5.3-4. Cabinets 6, 7 and 10 were the same as in the previous

SWGR tests. Tests 4 and 5 were 5-cabinet line-ups and Test 6 was a 3-cabinet line-up without Cabinets 9 and 10 to enable a fit under a hood calorimeter.

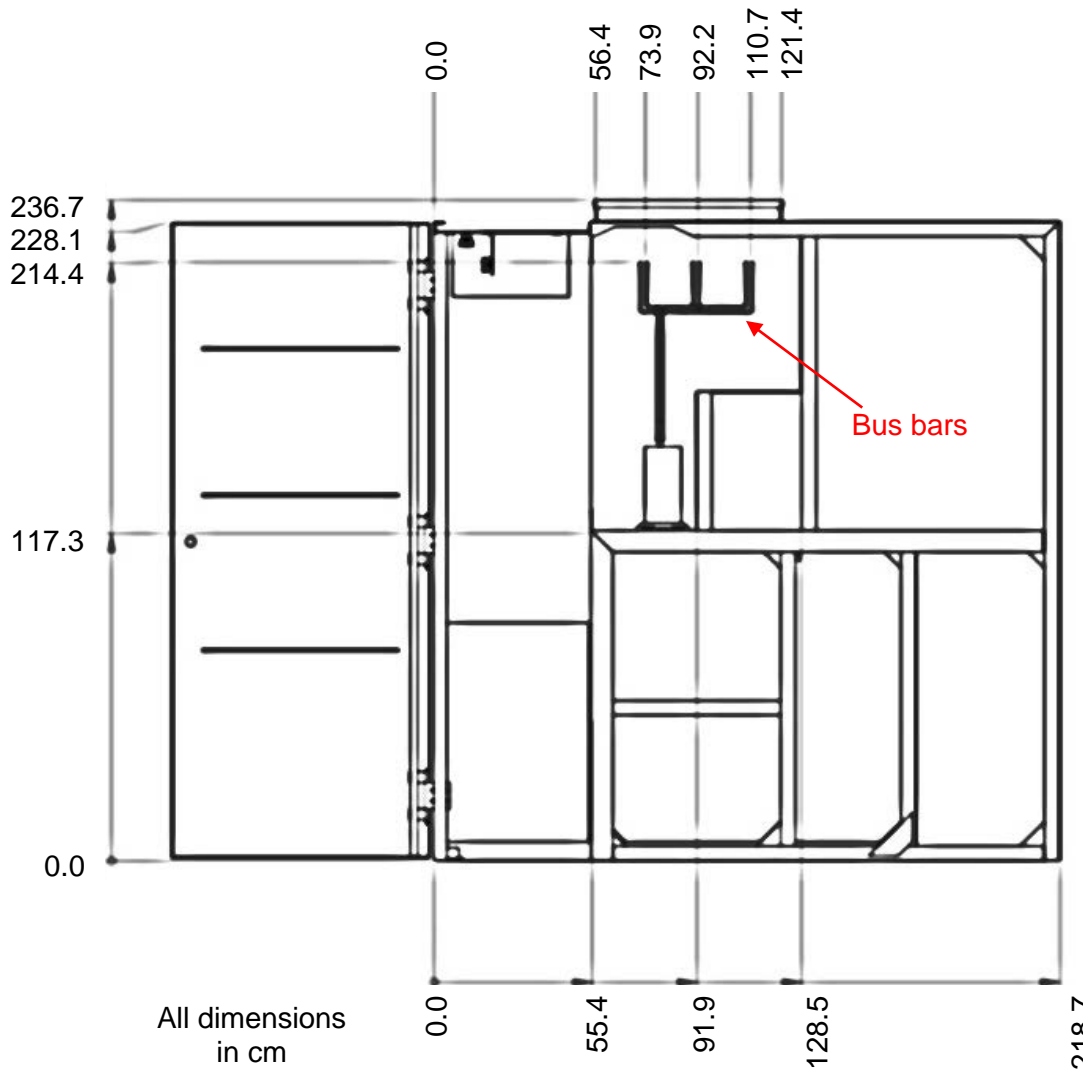


Figure 5.3-1. SWGR Tests 4 through 6: Cabinet 7

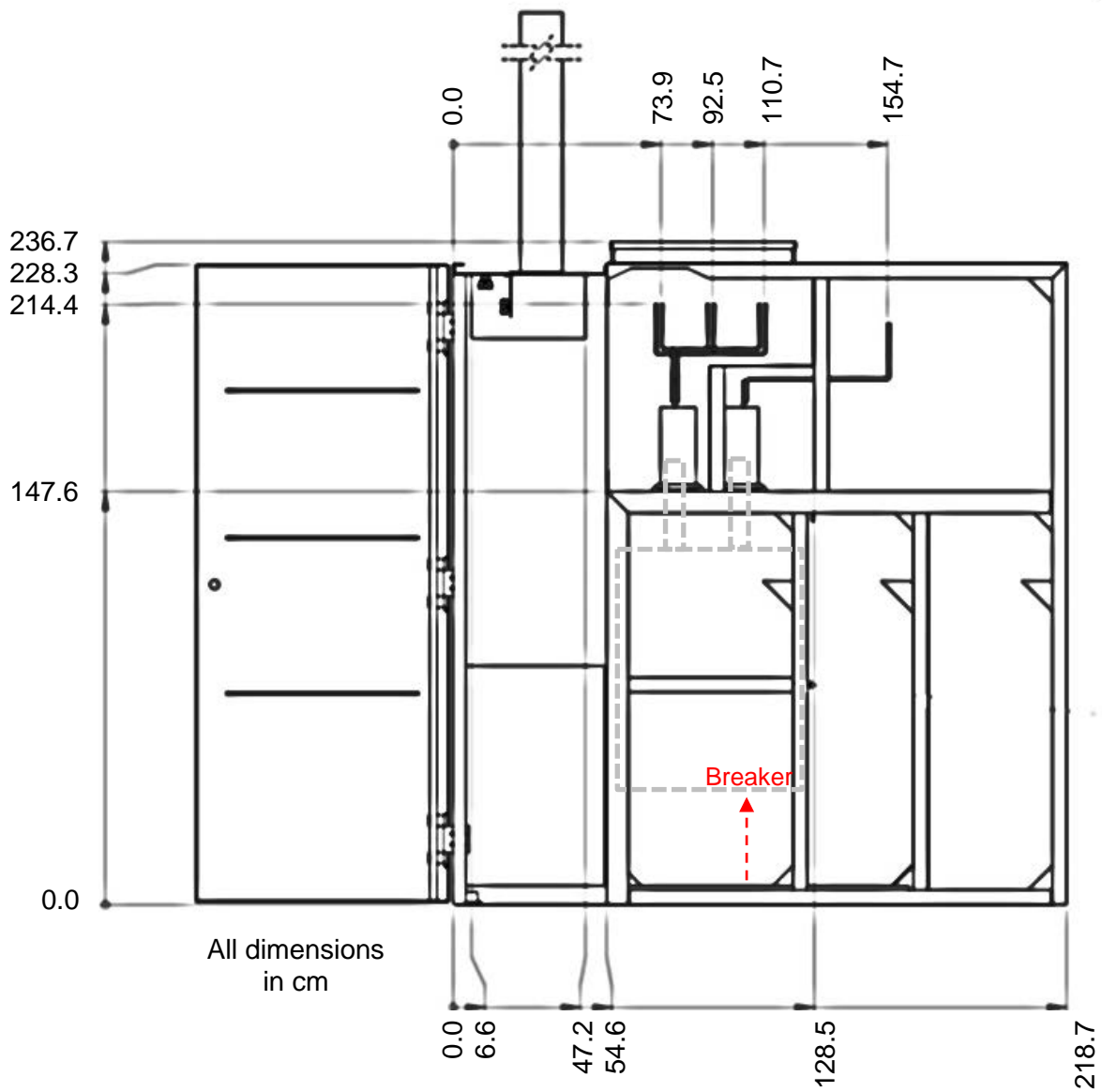


Figure 5.3-2. SWGR Tests 4 through 6: Cabinet 8

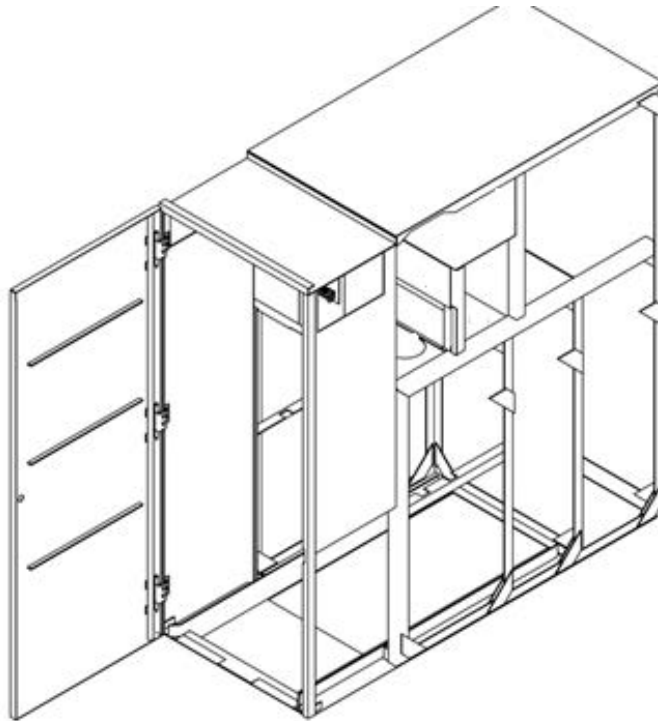


Figure 5.3-3. SWGR Tests 4 through 6: Schematic of Cabinets 6, 9, and 10

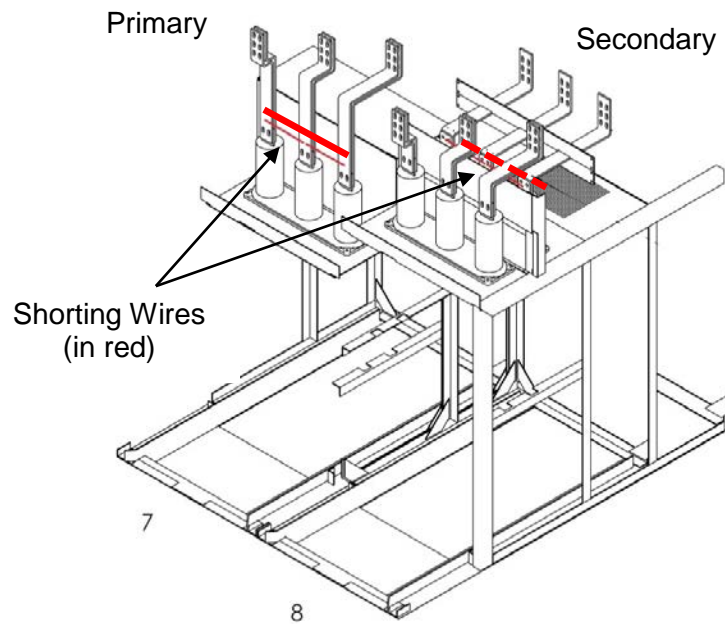


Figure 5.3-4. SWGR Tests 4 through 6 Cabinets 7 and 8 Shorting Wire Locations

5.3.1 Internal Combustible Load

The combustible loads were the same as Tests SWGR Tests 1 through 3 except the cables in Cabinets 9 and 10 were not needed for Test 6, 3-cabinet test.

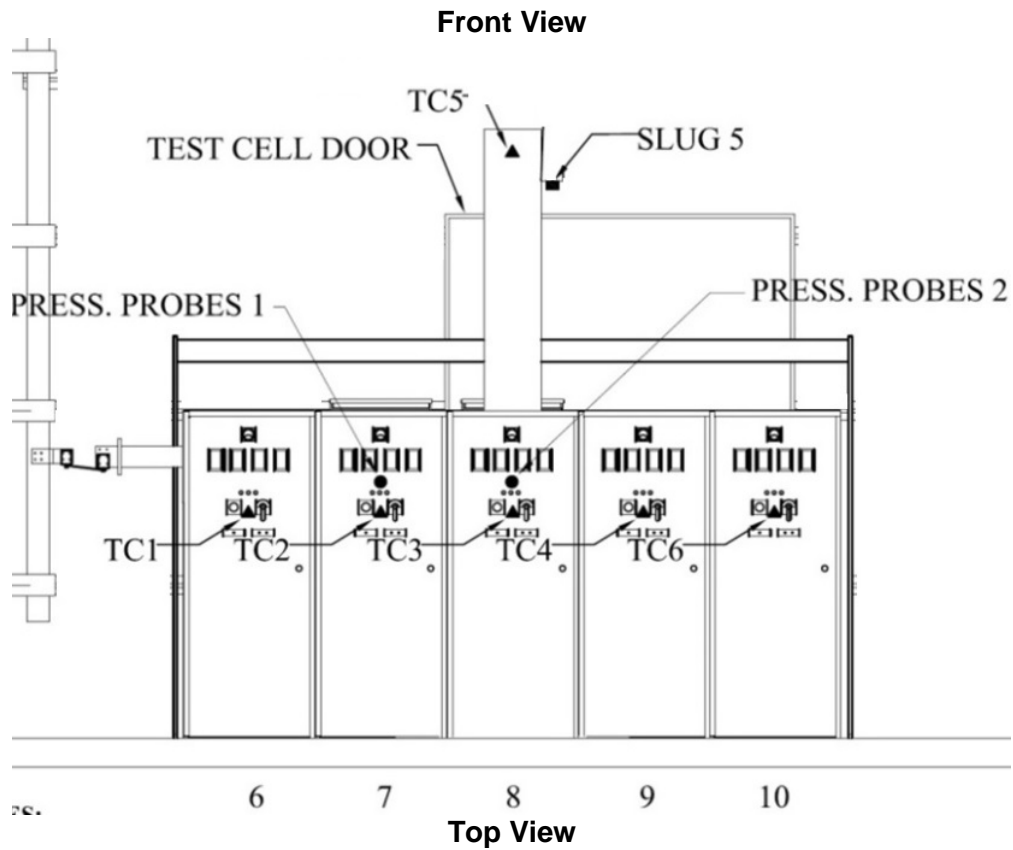
5.3.2 External Combustible Load

In SWGR Tests 4 through 6, a cable tray, loaded with cable was installed 46 cm (18 in) above the cabinet. In each test, the tray was loaded with 44 CV-2 cables, each 1.02 m long plus 16 CV-4 cables, each 1.02 m long.

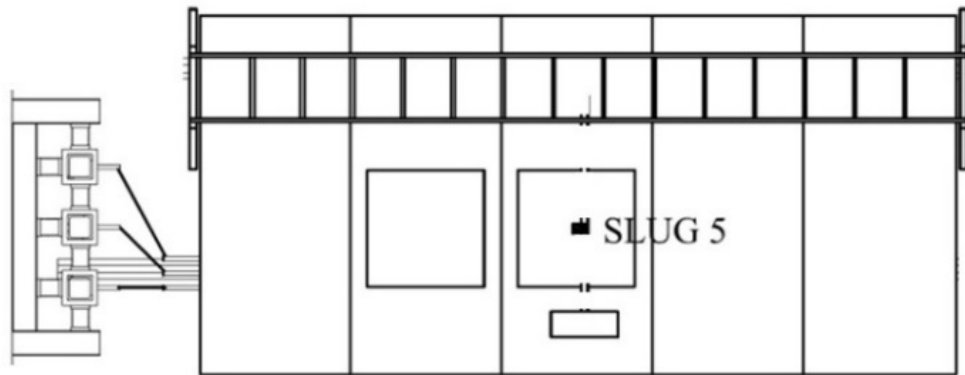
5.4 SWGR Tests 4 through 6 Temperature, Heat Flux and Pressure Instrumentation

The SWGR Tests 4 and 5 had instrumentation similar to SWGR Tests 1 through 3. The instrumentation locations are in Figure 5.4-1. SWGR Test 6 had similar instrumentation but also included a portable oxygen calorimeter and PTs provided by NIST as shown in Figure 5.4-2 (see References [7, 11] for more information on the NIST instruments). A cable tray was added as an ignition test target on the top of the SWGR.

Slugs 1, 2, 3, 4, and 7 are 0.91 m (3 ft) from the cabinet. Slug 5 is 1.5 m (5 ft) above the cabinet. The bare TCs were 15.2 cm (6 in) in front of the cabinets in Tests 4 and 5 only. PTs were added to the cable tray only in Test 6. Left side slug calorimeters are not used because the left side is far away from the arcs and heat.



SLUG 4 & 7



SLUG 1 & 6 SLUG 2 & 3

Figure 5.4-1. SWGR Tests 4 and 5, Instrument Locations

Table 5-2. SWGR Test 4 and 5 Calorimeter and TC Locations.

Slug or TC	From Floor (cm/in)	Position	Slug or TC Name
S1	178 (70)	Front (F)	S1-F-70-Cab7
S2	178 (70)	Front	S2-F-70-Cab8
S3	91 (36)	Front	S3-F-36-Cab8
S4	178 (70)	Rear (R)	S4-R-70-Cab8
S5	381 (150)	Top (T)	S5-T-150-Cab8
S6	91 (36)	Front (F)	S6-F-36-Cab7
S7	91 (36)	Rear (R)	S7-R-36-Cab8
TC1	178 (70)	Front	TC1-F-70-Cab6
TC2	178 (70)	Front	TC2-F-70-Cab7
TC3	178 (70)	Front	TC3-F-70-Cab8
TC4	178 (70)	Front	TC4-F-70-Cab9
TC5	422 (166)*	Vertical Duct	TC5-V-Cab8
TC6	178 (70)	Front	TC6-F-70-Cab10

* Located near the top of the duct on the side 6 inches from the duct.

Table 5-3. SWGR Test 6 Calorimeter Locations.

Slug or TC	From Floor cm (in)	Position	Slug Name
S1	178 (70)	Front (F) 7	S1-F-70-Cab7
S2	91 (36)	Front 7	S2-F-36-Cab 7
S3	41 (16)	Front 7	S3-F-16-Cab7
S4	178 (70)	Front 8	S4-F-70-Cab8
S5	91 (36)	Front 8	S5-F-36-Cab8
S6	41 (16)	Front 8	S6-F-16-Cab8
S7	178 (70)	Right Side (RS)	S7-RS-70-Cab8
S8	91 (36)	Right Side	S8-RS-36-Cab8
S9	178 (70)	Rear (R)7	S9-R-70-Cab7
S10	178 (70)	Rear 8	S10-R-70-Cab8

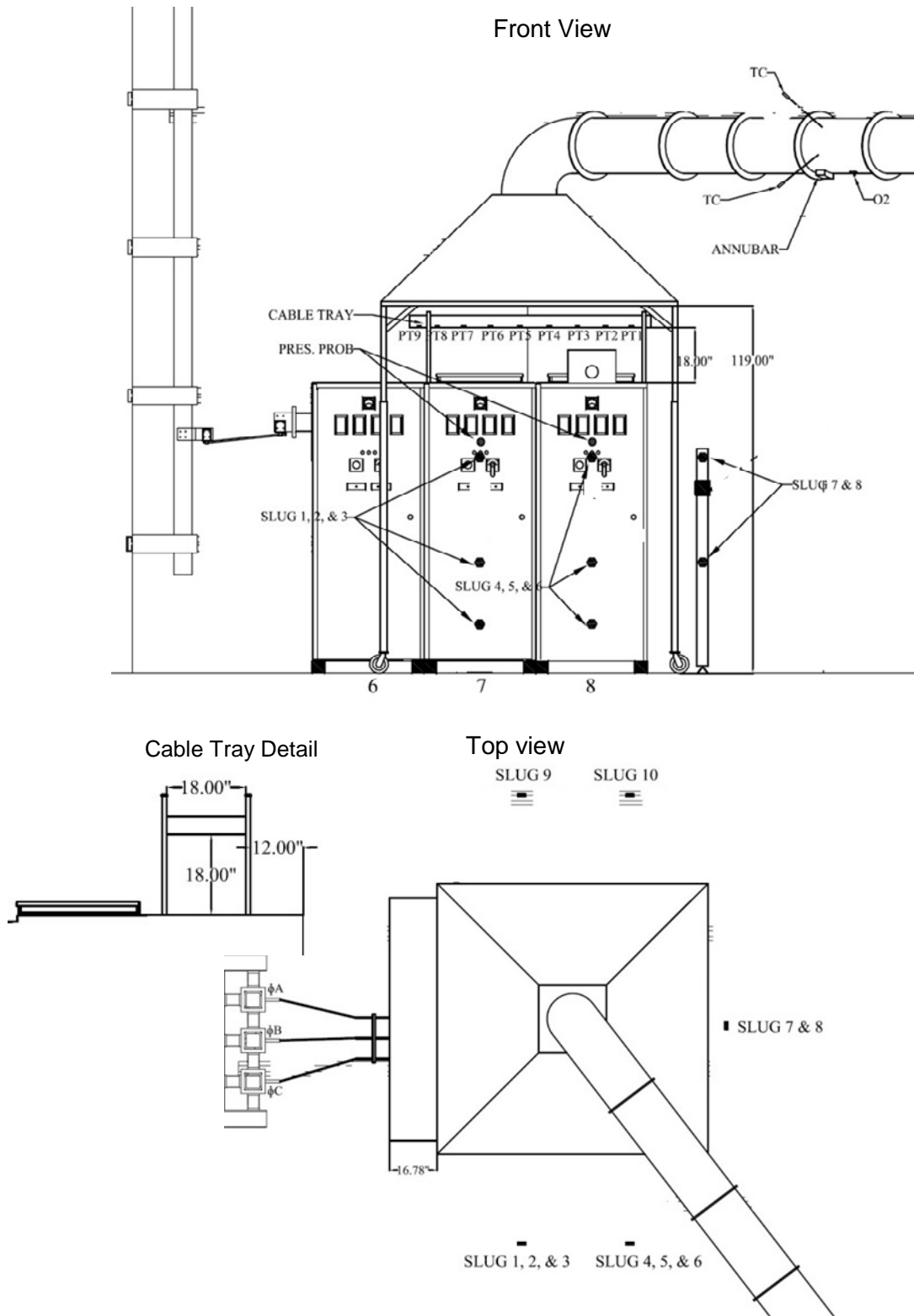


Figure 5.4-2. SWGR Test 6 Instrument Locations

5.5 SWGR Test 4 Key Observations (March 2014)

Two arcs were initiated in this test; the first at 7 kV at 24.5 kA with a target duration of 2.5 seconds, and the second arc was initiated 3.7 minutes later at 7 kV and 34.1 kA with a target duration of 2.0 seconds, see Figure 5.5-1. The target arc durations were nominally achieved; Arc 1 had an energy of 64.6 MJ and Arc 2 had an energy of 78.5 MJ. Although the second arc was initiated in Cabinet 8, the resultant arc was at the Cabinet 7 top horizontal bus bar (as in the assumed Onagawa event) because the current drawn by the second arc on the secondary side of Cabinet 8 was very large. The high current caused the horizontal bus bars in Cabinet 7 to flex and contact each other, causing a very large arc and disrupting additional current to Cabinet 8, quickly extinguishing the initial arc in Cabinet 8. Therefore, the Cabinet 8 breaker secondary side had little damage. The first arc in Cabinet 7 resulted in high energy because there was high aluminum bus bar oxidation, causing an ensuing fire after Arc 1. The arrow in Figure 5.5-1(c) shows the direction that the Cabinet 8 door opened at about 0.037 seconds when the arc moved from Cabinet 8 to Cabinet 7.

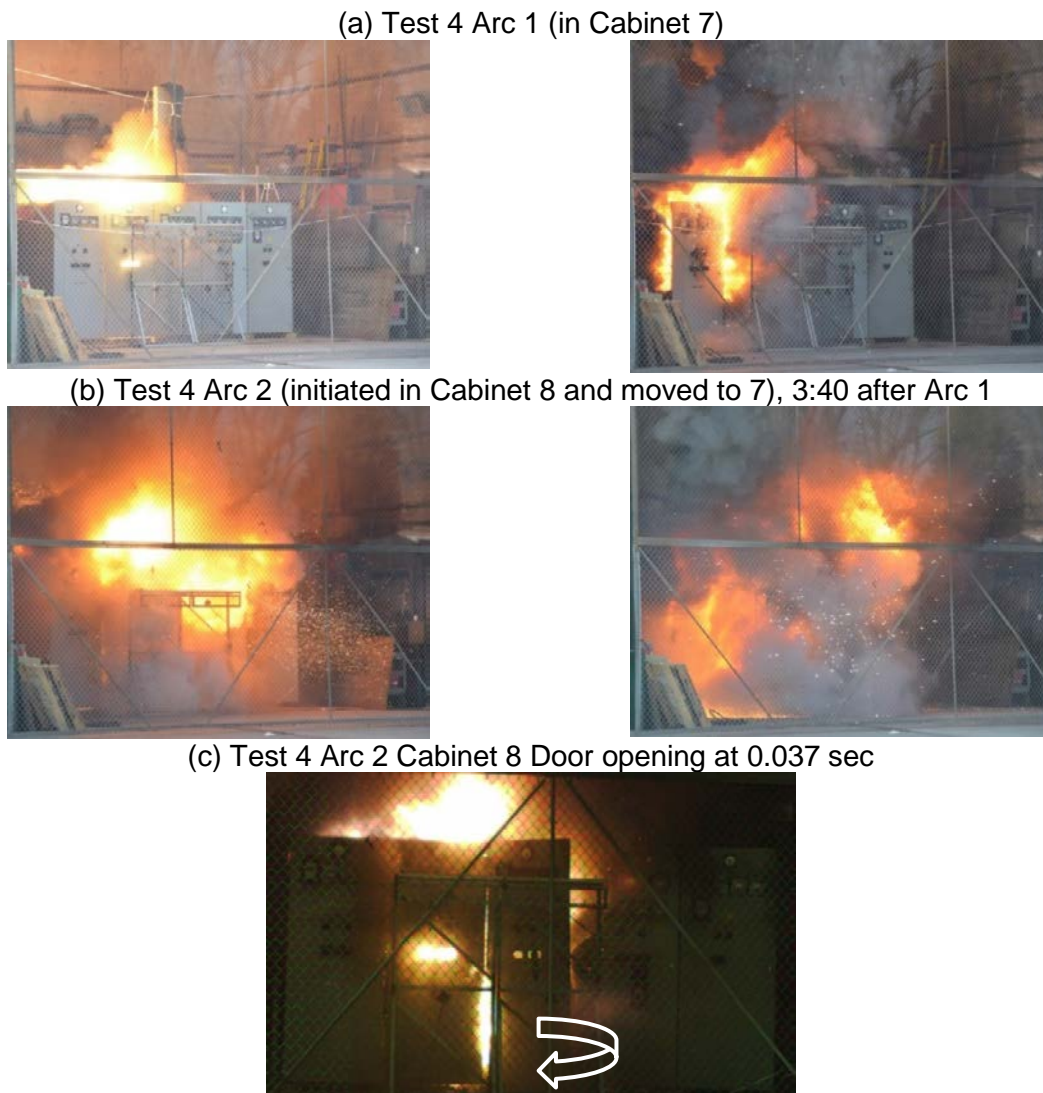


Figure 5.5-1. SWGR Test 4 Arcs

An ensuing fire occurred after Arc 1, and remained in Cabinet 7 and at the bottom of the vertical duct before Arc 2 was initiated. Figure 5.5-2(a) shows thermal images of the SWGR before the second arc. Figure 5.5-2(b) shows the ensuing fires after the Arc 2, just before the fire was manually extinguished. At the time the fire was extinguished the fire had spread into Cabinets 6 and 8 but Cabinets 9 and 10 had no fire.

(a) Before Second Arc at 3:40 after Arc 1



(b) Maximum after Second Arc at 2:33 after Arc 2



Figure 5.5-2. SWGR Test 4 Thermal Image Ensuing Fire

There was heavy damage at the top of Cabinet 7 from the ensuing fires and aluminum bus bar oxidation as shown in Figure 5.5-3. As shown in Figure 5.5-3(a) the front of Cabinet 7 had showed charring like Onagawa from high heat from aluminum bus bar oxidation. Some of the soot was washed off by firefighting.

As shown in Figure 5.5-3(b) the cable tray 45.72 cm (18 in) above the cabinet had some scorching on the side but the cables did not ignite and only had some minor scorching. SWGR Test 4 had the largest amount of fire and plasma that escaped the top vent that was deflected toward the cable tray by the vent cover plate. Yet, in these harsh conditions, the cables did not ignite. The cables did scorch where they crossed the bus bars as shown in Figure 5.5-3(c). Figure 5.5-3(d) shows the cables in the vertical duct were completely burned.

(a) Cabinets 6-10



(b) Cabinet 7 top



(c) Cable Tray (from bottom)



(d) Vertical Duct



Figure 5.5-3. SWGR Test 4 Exterior Damage

Figure 5.5-4 shows the interior damage, the heavy soot damage, and orange discoloration from high temperatures. Figure 5.5-5 (a) through (f) shows cable fire damage in all the cabinets. Some cables burned in all cabinets except Cabinet 10. In Cabinet 6, a few centimeters of the cables burned where they entered from Cabinet 7. The Cabinet 7 upper cables were completely burned and had detached from the cabinet and slumped down. The Cabinet 8 upper cables were mostly burned and remained in place and attached. In Cabinet 9 about 10 percent of the upper cables burned where the cables entered from Cabinet 8 and the cables detached and slumped. The cables in Cabinet 10 did not burn. Figure 5.5-5 (d) shows the soot was throughout the interior of Cabinet 8.



Figure 5.5-4. SWGR Test 4 Interior Damage

(a) Cabinet 6 Cables



(b) Cabinet 7 Cables



.5

(c) Cabinet 8 Front Cables



(d) Cabinet 8 Rear Cables



(e) Cabinet 9 Cables



(f) Cabinet 10 Cables

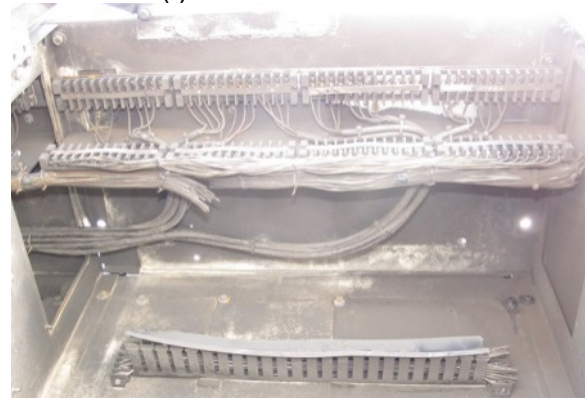


Figure 5.5-5. SWGR Test 4 Interior Damage, Detailed

Figure 5.5-6 shows the insulator and bus bar damage. Figure 5.5-6(a) and (b) show that the front horizontal aluminum bus bar was completely destroyed as were the vertical bus bars; the white dashed lines show the initial location of the front bus bar. The middle, horizontal aluminum bus bar was bent from the strong arcing current contacted the front bus bar, shorted, and the front bus bar oxidized.

Figure 5.5-6(c) shows that most of the vertical bus bars were destroyed, caused by energy released from the aluminum exothermic reaction and electrical energy in Arc 1 and Arc 2. This almost complete destruction did not happen in SWGR Tests 1 through 3 (only partial oxidation) or in Tests 5 and 6. Only part of the vertical bus bars burned in Test 5 even though the planned test conditions were the same.

Figure 5.5-6(d) shows light to moderate damage on the Cabinet 8 insulators. Figure 5.5-6(e) shows the Cabinet 8 front (primary) insulators stayed fairly intact but did crack and have some damage. There is a small hole burned in the left wall probably from Arc 1 on the right connection in Cabinet 7 that burned through the wall toward Cabinet 8 and the plasma exiting this hole caused most of the damage.

Figure 5.5-6(f) shows that the Cabinet 8 secondary insulators had minor damage (less than 5 mm was oxidized) from the short duration arc that occurred because the shorting current was stopped by the Cabinet 7 horizontal bus bar short and the Cabinet 8 arc extinguished.

(a) Cabinet 7 Horizontal Bus Bars



(b) Cabinet 7 Horizontal Bus Bars



(c) Cabinet 7 Vertical Bus Bar Location



(d) Cabinet 8 Bus Bars (Front and Rear)



(e) Cabinet 8 Bus Bars (Front)



(f) Cabinet 8 Bus Bars (Rear)



Figure 5.5-6. SWGR Test 4 Insulator and Bus Bar Damage

Breaker 8 only had some soot covering as shown in Figure 5.5-7(b) with some minor debris on the primary side from the damage to the primary insulators. Breaker 7 had damage at the top primary side under the arc position but the secondary side was not damaged - only some soot was observed. There was some front panel discoloration of Circuit Breaker 7 from the heat and the control cable bundle on the front left burned. This damage was much less severe than the damage observed in the Onagawa event.

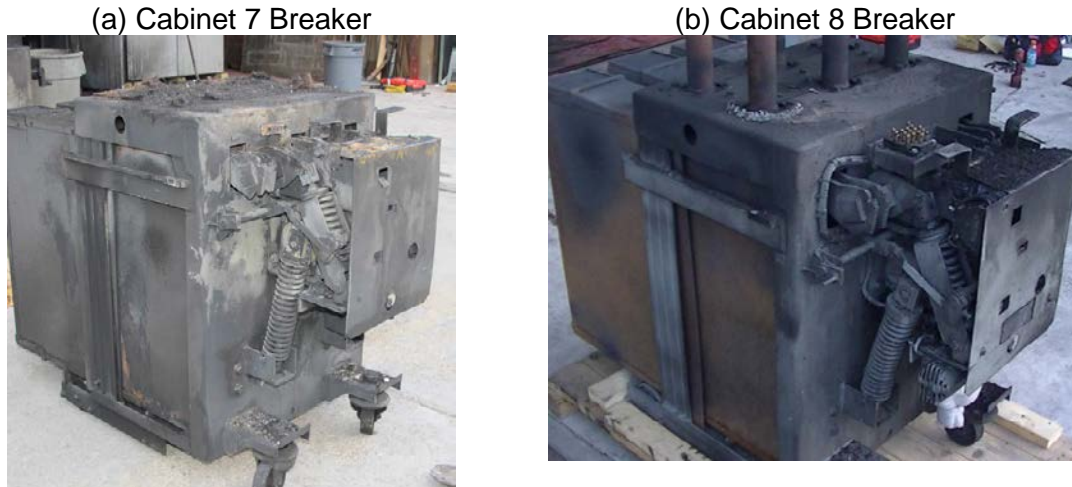


Figure 5.5-7. SWGR Test 4 Breaker Damage

5.5.1 SWGR Test 4 Calorimetry Data

Temperatures measured at the slug locations are shown in Figure 5.5-8. Arc 1 was intentionally extinguished at 2.354 seconds and Arc 2, occurring 3 minutes 40 seconds later, was intentionally extinguished at 2.081 seconds, as planned. Most of the slugs had high noise during the arc, probably due to EMI. The highest temperature at the end of Arc 1 was at the top (S5) that was detecting the hot gas and flames escaping from the top vent. Slug 1, in front of Cabinet 7 where the arc was located also measured a high temperature.

Slug 5 fell from position at the end of Arc 1 (the supporting line burned and broke; the line supporting the TC in the front of the cabinets also burned and fell as discussed later) so the S5 temperature data after 3 seconds is taken with the slug calorimeter laying top of Cabinet 8 with the copper disk facing the top of the cabinet. S5 data cannot be analyzed for flux after Arc 1.

The highest temperature at the end of Arc 2 was at the top front of Cabinet 7 (S1), probably because the high heat from the horizontal bus bar oxidation in Cabinet 7.

Decreasing temperatures between Arc 1 and Arc 2 show that all slug calorimeters were cooling. For S1 and S6 in the front of Cabinet 7, the temperatures were increasing slightly after 2 minutes indicating some heat was probably escaping a small fire in Cabinet 7 or residual heat from Arc 1. After Arc 2, Slugs 1, 2, 6, and 3 showed slightly increasing temperatures after 5 minutes probably from the ensuing fire. The large ensuing fire observed in Test 2 was not allowed to grow in Test 4 and the fire was manually extinguished at 7.5 minutes.

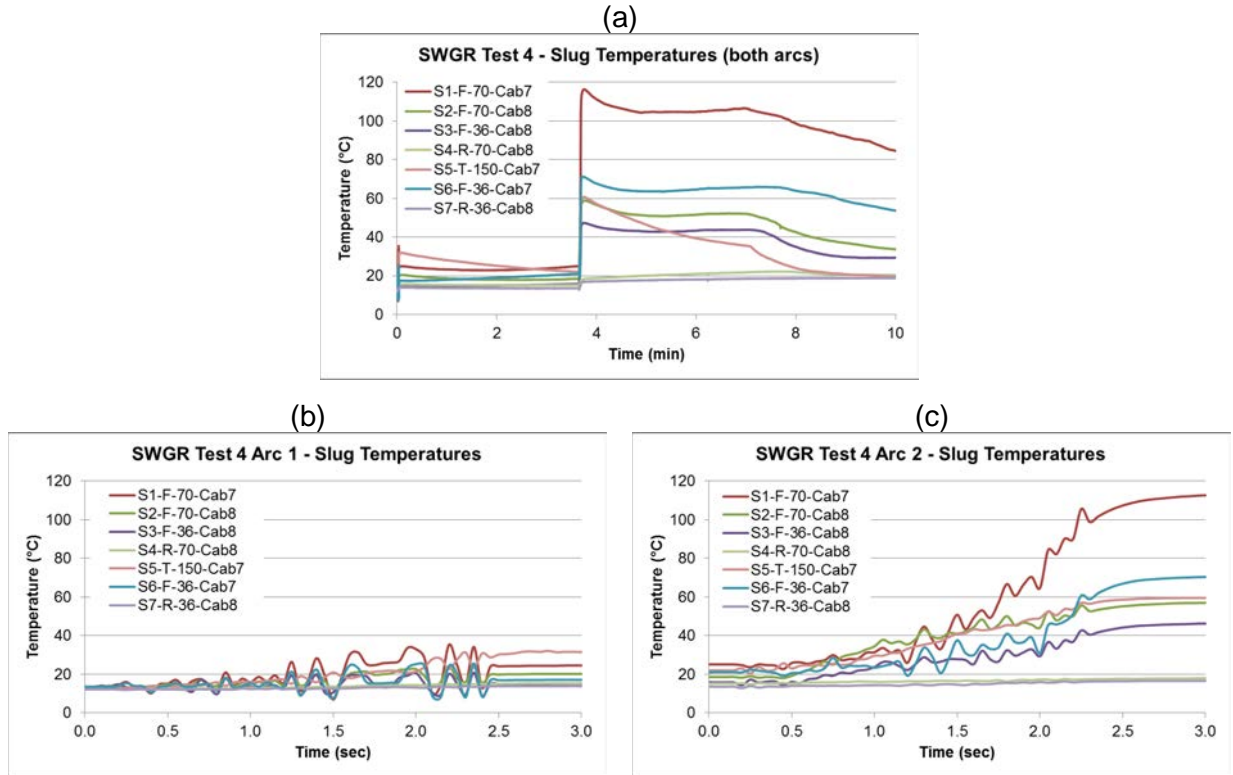


Figure 5.5-8. SWGR Test 4 Calorimetry Data: Temperature

Table 5-4 shows the flux results based on the ASTM F1959 method in Appendix A using the change in temperature (ΔT) between the start and end of the arc. The maximum flux was measured to be 46 kW/m² at 1.5m (5 ft) from the top of the cabinet (S5), similar to Tests 1 through 3. For Arc 2, the maximum flux of 220 kW/m² was measured at the front of Cabinet 7 near the height of the oxidizing horizontal bus bar (S1). This was the highest flux reported in any of the HEAF tests in this report. High fluxes were also measured in front of the cabinet (S2, S3, and S6). Arc 2, which was a very short duration, was initiated in the rear of Cabinet 8 resulting in very low fluxes at that location (S4, S7). The maximum slug temperatures are also shown to indicate the maximum temperature a metal object could obtain during the arc.

Table 5-4. SWGR Test 4 Flux Results.

Slug	Arc 1			Arc 2		
	ΔT (°C)	Flux (kW/m ²)	Max T (°C)	ΔT (°C)	Flux (kW/m ²)	Max T (°C)
S1-F-70-Cab7	10.6	28	116	73.8	220	116
S2-F-70-Cab8	6.4	17	59	36.3	107	59
S3-F-70-Cab8	2.0	5	47	27.2	80	47
S4-R-70-Cab8	2.5	6	22	2.3	7	22
S5-T-150-Cab8	17.6	46*	61*	35.9	*	*
S6-F-36-Cab7	3.4	9	71	45.0	133	71
S7-R-36-Cab8	1.7	4	19	2.8	8	19

*For first 2 seconds of Arc 1 only.

** S5 fell and was not measuring flux after 2 seconds of Arc 1.

5.5.2 SWGR Test 4 Temperature Data

The temperatures measured by the TCs are shown in Figure 5.5-9. Table 5.5-2 shows the maximum temperature results. Thermocouples T1 through TC4 and TC6, in the front of the cabinets fell to the floor during Arc 1, consequently, the TC measurements were of the floor and the exact positions are not known so the data is not useful after Arc 1. For Arc 1, the highest temperature, 59 °C (138 °F), was measured at the front of Cabinet 7 (TC2) where the arc occurred. The only valid data after Arc 1 was for in the vertical duct (TC5), which showed increasing temperatures during the arcs and in the ensuing fire as expected with a maximum temperature of 160 °C (320 °F). The TCs cannot practically be used to estimate flux.

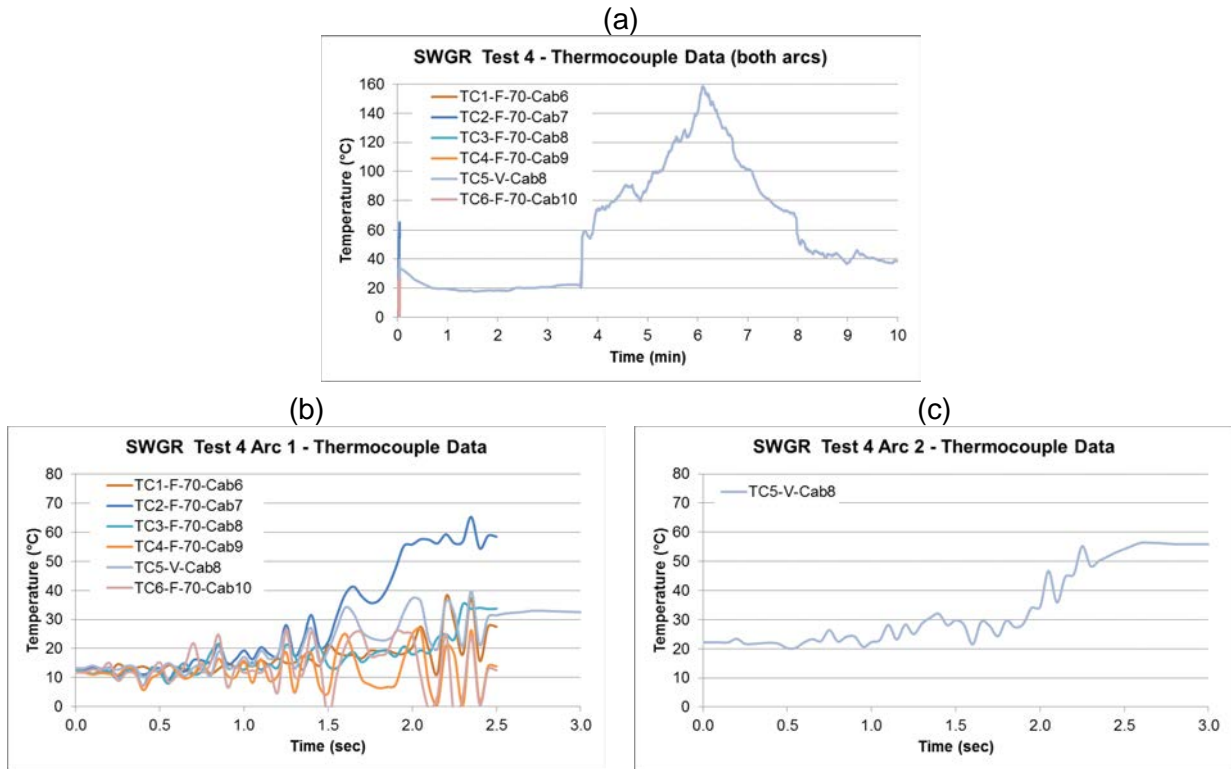


Figure 5.5-9. SWGR Test 4 Thermocouple Data

Table 5-5. SWGR Test 4 TC Results.

TC	Arc 1* Max T (°C)	Post Arc 1 Max T (°C)	Arc 2* Max T (°C)	Post Arc 2 Max T (°C)
TC1-F-70-Cab6	28	**	**	**
TC2-F-70-Cab7	59	**	*	**
TC3-F-70-Cab8	34	**	**	**
TC4-F-70-Cab9	14	**	**	**
TC5-V-Cab8	31	33	55	159
TC6-F-70-Cab10	13	**	**	**

*To allow for noise, the maximum temperature is the measured value at the end of the arc.

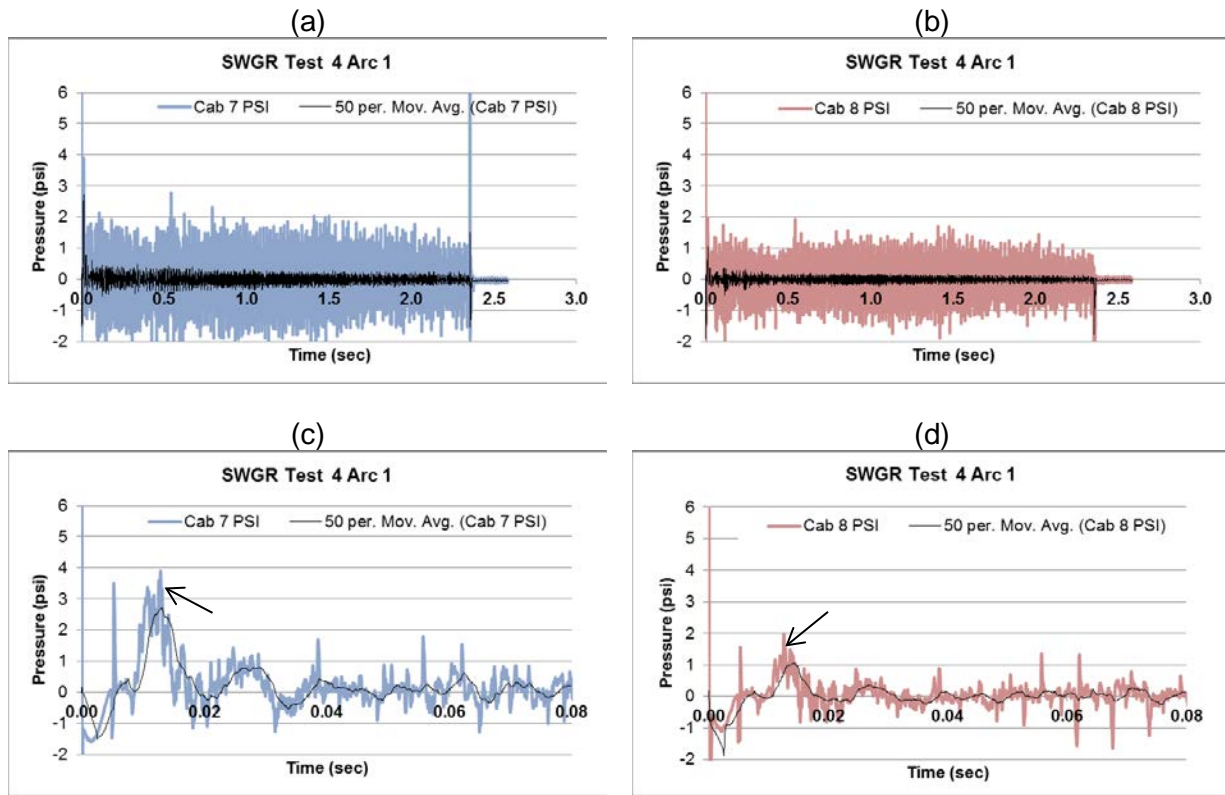
**The TC support burned and fell during Arc 1 so data is not valid.

5.5.3 SWGR Test 4 Pressure Data

The pressures during the arc are shown in Figure 5.5-10 and Figure 5.5-11. The pressures for both arcs were higher than SWGR Tests 1 through 3 but lower than the MCC and DP tests low because the vents at the top of Cabinets 7 and 8 allowed the pressure to escape.

The pressure analysis methods are in Appendix A and involved picking the maximum near the start of the arc, then including a nominal uncertainty for the noise in the signal just before the arc.

For Arc 1, there were numerous noise spikes for Cabinet 7 and Cabinet 8 and both had a noise spike at 0.005 seconds before the maximum pressures and at the end. Both cabinet pressures had a zero shift at the start of the arc that has been considered in the reported results. The Cabinet 7 pressure closer to the arc had a higher maximum and occurred earlier than the Cabinet 8 pressure that was further from the arc. The maximum pressures are indicated by the arrows in Figure 5.5-10(c) and (d).



Test 4 Pressure 1 Cab. 7 Arc 1
 23.4 ± 0.7 kPa (3.4 ± 0.1 psi)
 @ 0.0129 s

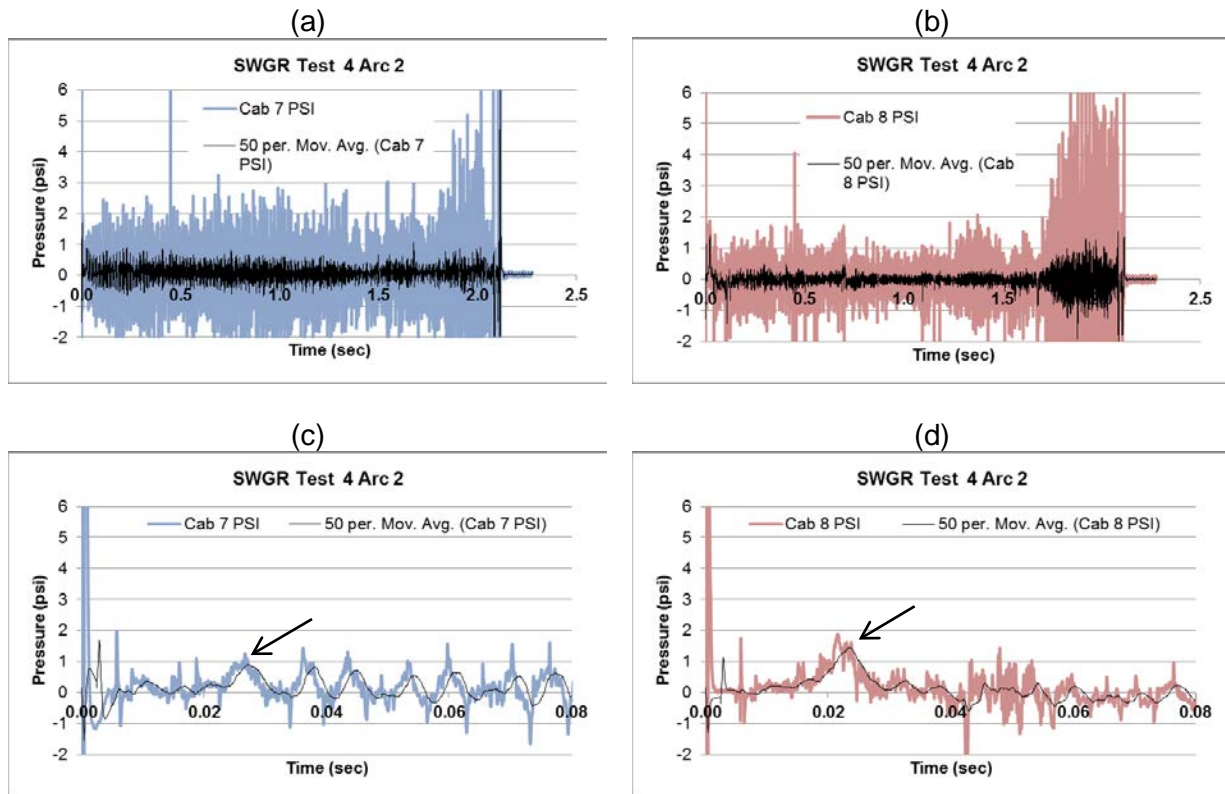
Test 4 Pressure 2 Cab. 8 Arc 1
 12.4 ± 0.7 kPa (1.8 ± 0.1 psi)
 @ 0.0126 s

Figure 5.5-10. SWGR Test 4 Pressure Data, Arc 1

For Arc 2, there were numerous noise spikes for Cabinet 7 and Cabinet 8 and both had noise spikes at 0.005 seconds before the pressure maximums, another at 0.5 seconds, and numerous spikes as the arc terminated probably because the arc in the top horizontal bus bars in Cabinet 7 became unstable and caused high noise. Both cabinet pressures had a zero shift at the start of the arc that is considered in the reported results.

The Cabinet 8 pressure closer to the arc had a higher maximum that occurred earlier than the Cabinet 7 pressure that was further from the arc. The pressure in Cabinet 8 had some small pressure spikes from 0.04 to 0.055 seconds after the door on Cabinet 8 opened when the arc moved from the back of Cabinet 8 to Cabinet 7 about 0.037 seconds after the arc initiation based on high speed film analysis.

The Arc 2, Cabinet 7 pressure had a distinct sinusoidal response for the next four peaks immediately after the maximum peak at 0.0267 seconds that had a frequency of about 140 Hz. The amplitudes of these peaks were about the same as the initial peak. The maximum pressures are indicated by the arrows in Figure 5.5-11(c) and (d). This may have been from pressure waves reflecting within the cabinet.



Test 4 Pressure 1 Cab. 7 Arc 2
 6.9 ± 0.6 kPa (1.0 ± 0.1 psi)
 @ 0.0267 s

Test 4 Pressure 2 Cab. 8 Arc2
 12.4 ± 0.6 kPa (1.8 ± 0.1 psi)
 @ 0.0215 s

Figure 5.5-11. SWGR Test 4 Pressure Data, Arc 2

5.5.4 SWGR Test 4 Arc Energy

The Arc 1 duration was 2.35 seconds with total energy of 64.6 MJ, seen in Figure 5.5-12. Arc 2 was 2.081 seconds with a total energy of 78.4 MJ. The energy analysis methods are in Appendix A. The “Energy” is calculated as volts multiplied current multiplied by the time step and each time step is shown. “Energy Total” is the cumulative sum of the energy in each time step.

SWGR Test 4, Arc 2 showed the highest energy of any arc in the NRA tests in this report probably because the shorted horizontal bus bars provided a longer arc gap at the arc point than the gap in other tests and the arc voltage was nominally 730 V versus 600 V for SWGR Tests 1 through 3.

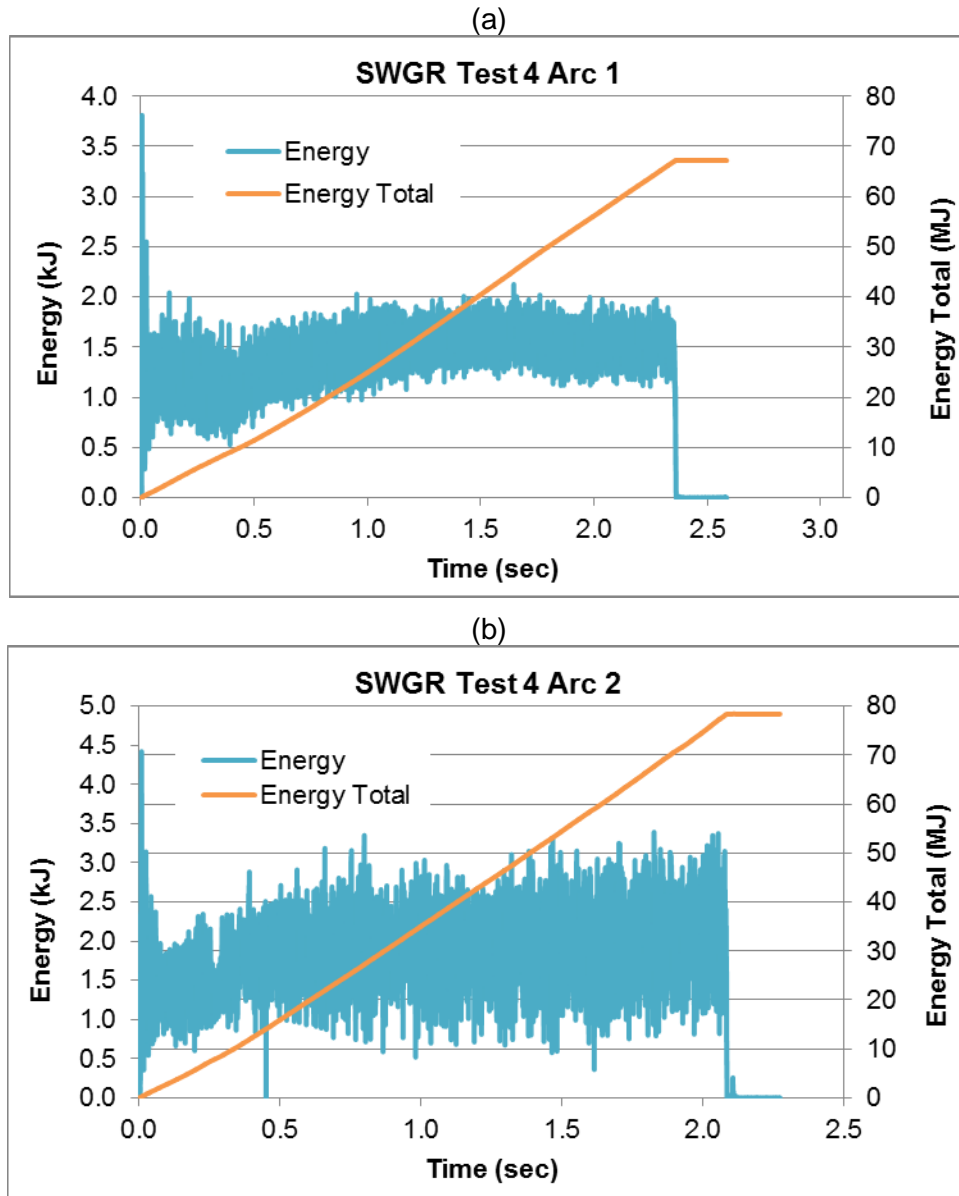


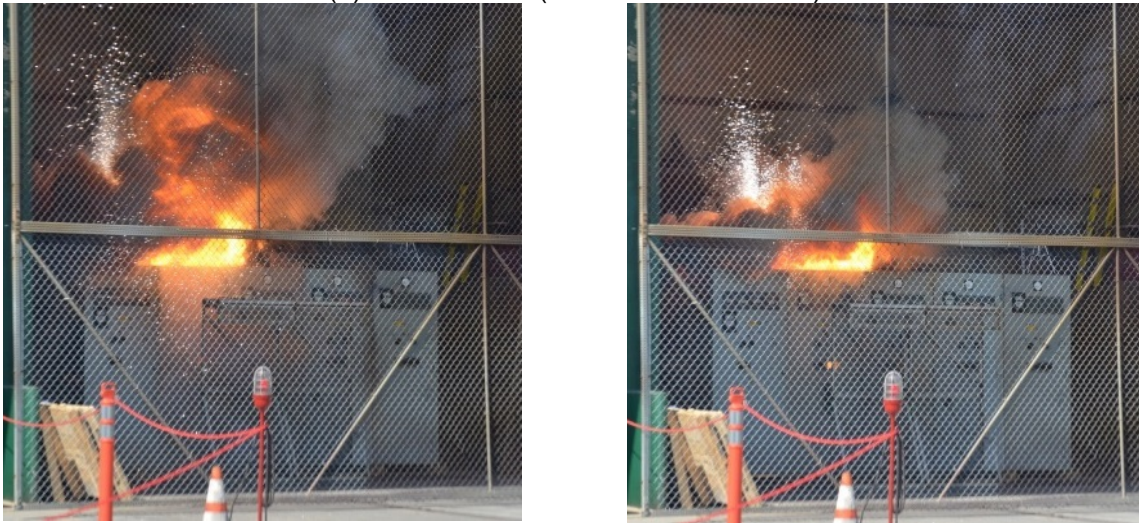
Figure 5.5-12. SWGR Test 4 Arc Energy (both arcs)

5.6 SWGR Test 5 Key Observations (March 2014)

Two arcs were initiated in this test; the first at 7 kV at 24.4 kA with a target duration of 2.5 seconds, and the second arc was initiated 2 minutes and 55 seconds later at 7 kV and 33.9 kA with a target duration of 2.0 seconds (see Figure 5.6-1). The target arc durations were nominally achieved and Arc 1 had an energy of 57.2 MJ and Arc 2 had an energy of 62.0 MJ. The arc conditions and arc wires were very similar to Test 4 but the ensuing fire was smaller and the arcing was different. As in Test 4, two arcs occurred and Arc 1 had adequate energy to ignite an ensuing fire. However, Arc 2 showed the random nature of arc events because the bus bars in Cabinet 7 did not flex and make contact as in Test 1 and instead Arc 2 occurred in the secondary side of Cabinet 8 and remained there as planned.

Figure 5.6-1 shows the arcs at the start and end of each arc. The flames in Arc 2 were much smaller than in Test 4 because the horizontal bus bars in Cabinet 7 did not arc.

(a) Test 5 Arc 1 (initiated in Cabinet 7)



(b) Test 5 Arc 2 (initiated in Cabinet 8); 2:56 after Arc 1



Figure 5.6-1. SWGR Test 5 Arcs

As shown in the thermal images in Figure 5.6-2, an ensuing fire occurred after Arc 1, and before Arc 2. The additional energy from Arc 2 accelerated the ensuing fire as seen in the thermal images before and after the arc.

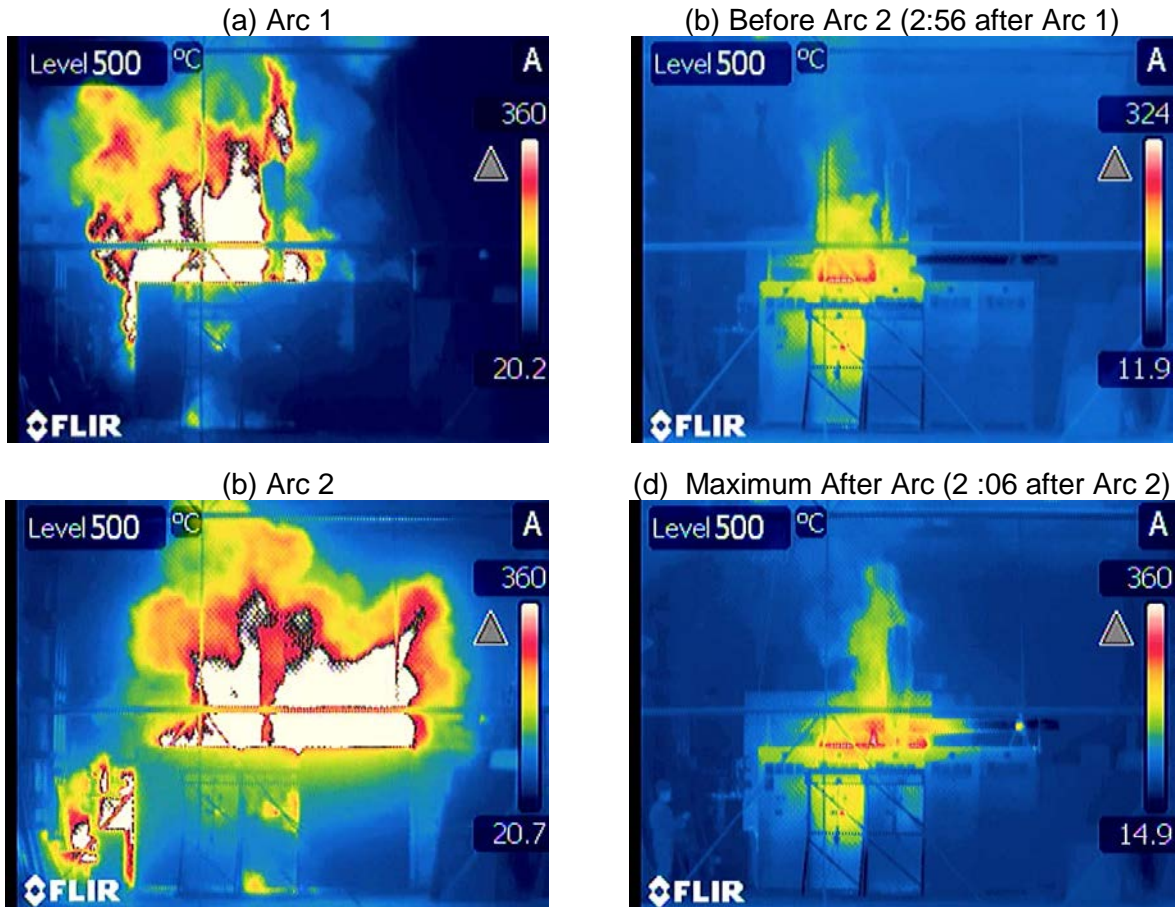


Figure 5.6-2. SWGR Test 5 Thermal Image Ensnuing Fire

The fire was manually extinguished in about 3 minutes after Arc 2 and the fire was not allowed to fully spread as in Test 2. There was no charring of the exterior and very little exterior damage, as seen in Figure 5.6-3(a). There was charring on the exterior of the cable tray. The vertical duct was charred but the same duct was used in Test 4 so this charring is primarily from Test 4. The cables in the vertical duct did not burn. Test 5 had the longest duration of Arc 2 in the rear part of the cabinet for all SWGR tests and this caused the roof to deform as shown in in Figure 5.6-3(d). Figure 5.6-3(c) and (e) show that the exterior cables in the tray did not burn but had slight charring where the cables crossed the support rails of the cable tray.

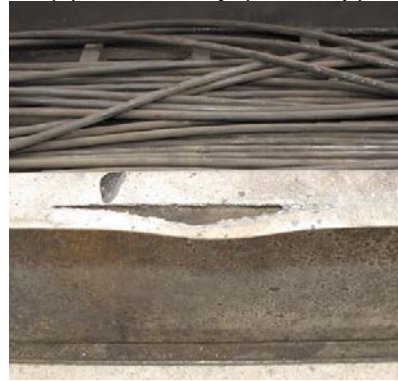
(a) Front Cabinet 6-10



(b) Top of Cabinets (from Cabinet 8 side)



(c) Cable Tray (from top)



(d) Cabinet Top (from rear)



(e) Cables (removed from tray)



Figure 5.6-3. SWGR Test 5 Exterior Damage

As shown in Figure 5.6-4, there was less internal damage than in Test 4 because there was less aluminum bus bar oxidation. The Cabinet 7 internal panels in front of the vertical bus bars bent but did not fall off like in Test 4. Figure 5.6-5(a) through (e) show the cable damage in the cabinet interiors before the fire was extinguished. In Cabinet 6, the first 15.24 cm (6 in) approximately of cable from Cabinet 7 was burned. In Cabinet 7, the cables were completely burned. In Cabinet 8, approximately the first 15.24 cm (6 in) of cable from Cabinet 7 was burned. In Cabinet 9, there was no cable burning but the cover on the plastic wire duct on the internal panel was blown off. In Cabinet 10 there was no burning and little damage

Figure 5.6-5(f) shows the damage at the top inside rear of Cabinet 8 above the Arc 2 location that caused the damage to the roof shown in Figure 5.6-3(d).



Figure 5.6-4. SWGR Test 5 Interior Damage

(a) Cabinet 6 Cables



(b) Cabinet 7 Cables



(c) Cabinet 8 Cables



(d) Cabinet 9 Cables



(e) Cabinet 10 cables



(f) Cabinet 8 Interior



Figure 5.6-5. SWGR Test 5 Interior Damage, Detailed

Figure 5.6-6 shows the damage to the bus bars in Cabinet 7 from Arc 1 and Cabinet 8 from Arc 2. In Cabinet 7, the vertical bus bars did not burn completely in Arc 1 like in Test 4. So, there was less aluminum oxidation energy in Arc 1 for Test 5. The fire was not as big and rapid as Test 4, based on the video and thermal images. The insulators were completely destroyed.

In Cabinet 8, the arc broke through the horizontal panel just above the secondary insulators and arc plasma entered the bus bar compartment then from there went directly up to the vent opening and plate on top of the cabinet. There was also a hole burned through the rear, vertical panel of the bus bar compartment and some damage to the cabinet roof directly behind the bus bar compartment. One of the insulators was partially intact, the other two were destroyed. The damage in the secondary side of the cabinet was much less than at Onagawa.

(a) Cabinet 7 Vertical Bus Bars



(b) Cabinet 7 Insulators 1, 2 and 3 (destroyed)



(c) Cabinet 8 Primary Insulators



(d) Cab. 8 Primary and Secondary Insulators



Figure 5.6-6. SWGR Test 5 Insulator and Bus Bar Damage

Figure 5.6-7 shows the damage to the breakers. Breaker 7 only had some soot covering and no major damage. This was the second test where this particular Breaker 7 was used as a “dummy” so the damage in Figure 5.6-7(a) is in addition to the damage shown in Figure 5.5-7(a) for SWGR Test 4. Breaker 8 had damage at the top secondary side under the arc position but the primary side was not damaged - only some soot was observed. There was some front panel discoloration from the heat. The bushings were not damaged like the bushings at Onagawa that completely shattered.

In Test 5, the hot gas and plasma went up to the cabinet vent. In Onagawa, the hot gas and plasma possibly went into the breaker because the arc may have been inside the insulators. In any case, the breaker damage at Onagawa was much more severe.

(a) Breaker 7



(b) Breaker 8



(c) Breaker 7, side



(d) Breaker 8



Figure 5.6-7. SWGR Test 5 Breaker Damage

5.6.1 SWGR Test 5 Calorimetry Data

Temperatures measured at the slug locations are shown in Figure 5.6-8. Arc 1 was intentionally extinguished after 2.316 seconds and Arc 2, approximately 3 minutes later, was intentionally extinguished after 2.071 seconds, as planned. Most of the slugs had high noise during the arc, probably due to EMI from the nearby power supply. The highest temperature at the end of Arc 1 was measured at 1.5 m (5 ft) above the cabinet (S5), probably because hot gases, flames and plasma escaped through the roof vent as in SWGR Tests 1 through 4.

The highest temperature at the end of Arc 2 was also at the top (S5) but had some unknown malfunction approximately 0.5 seconds after the arc. After that, the response was erratic and decreasing, as if from an unsteady but shrinking fire. Averaging of the data to remove noise showed that the erratic behavior was not noise. As expected, the next highest temperature was measured at the rear of Cabinet 8 where Arc 2 was located (S7). This was the first SWGR test where significantly higher slug temperatures were seen in the rear of the cabinets as expected because previous tests had arcs in the front, primary side compartments.

Decreasing temperatures between Arc 1 and Arc 2 show that all slug calorimeters were cooling except S6 in the front of Cabinet 7. This slug showed a slow increase during the time between the arcs probably from heat escaping a small fire in Cabinet 7 or residual heat from Arc 1. Slug S5, above Cabinet 8 showed the temperatures were increasing slightly after 1.5 minutes. After Arc 2, Slugs 1, 2, 6, and 3 showed slightly increasing temperatures in the first few seconds, then decreasing temperatures until the fire was extinguished at about 10 minutes. The large ensuing fire observed in Test 4 did not appear to be developing based on the decreasing trend and the fire was manually extinguished beginning at about 6 minutes.

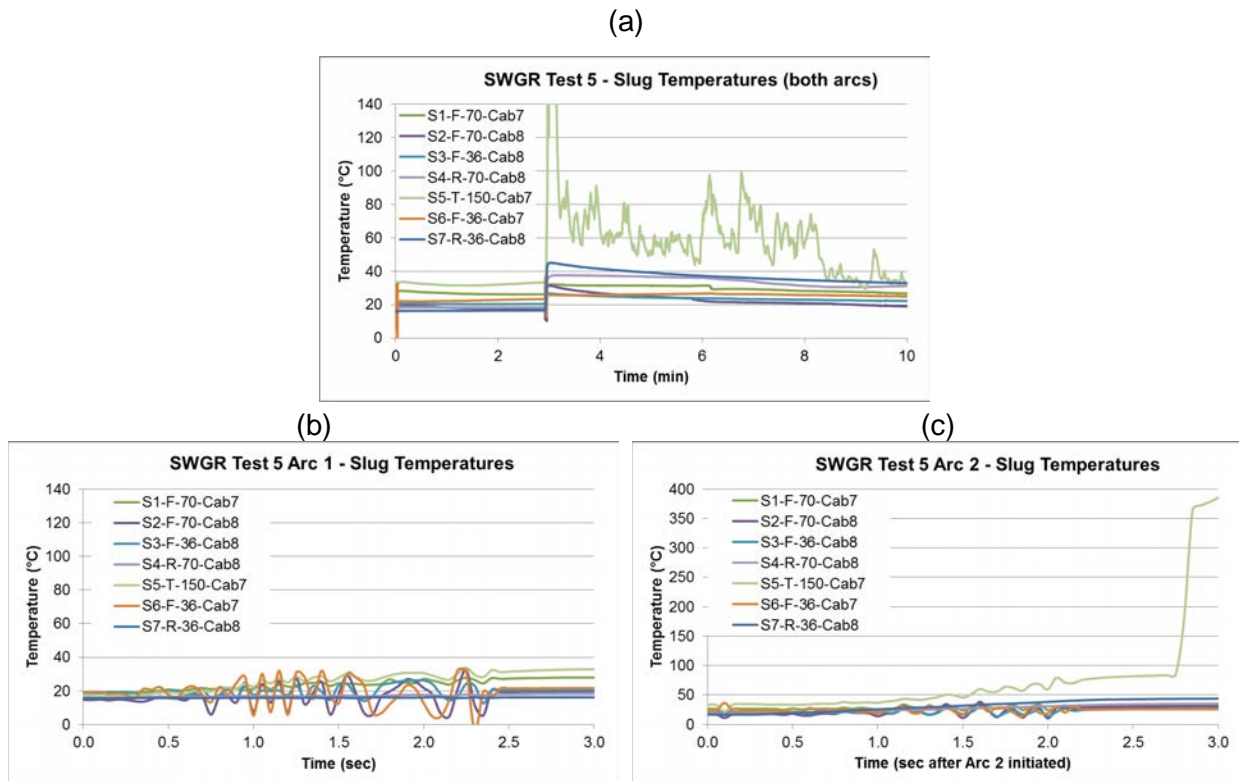


Figure 5.6-8. SWGR Test 5 Slug Calorimeter Temperature Data

Table 5-6 shows the flux results based on the ASTM F1959 method in Appendix A using the change in temperature (ΔT) between the start and end of the arc. For Arc 1, similar to the previous SWGR tests, a maximum flux of 37 kW/m² was measured at 1.5 m (5 ft) from the top of the cabinet (S5). For Arc 2, the maximum was measured to be 113 kW/m² at the same location (S5). This high flux is from the arc plasma entering the bus bar compartment that is directly below the vent and steel plate on top of the cabinet and in direct view of S5. The maximum slug temperatures are also shown to indicate the maximum temperature a metal object could reach. There was also a high flux of 67 kW/m² (S7) as expected for Arc 2 in the rear, secondary side of Cabinet 8.

Table 5-6. SWGR Test 5 Flux Results.

Slug	Arc 1			Arc 2		
	ΔT (°C)	Flux (kW/m ²)	Max T (°C)	ΔT (°C)	Flux (kW/m ²)	Max T (°C)
S1-F-70-Cab7	8.0	21	28	3.2	9	36
S2-F-70-Cab8	4.6	12	32	10.4	31	38
S3-F-70-Cab8	1.5	4	26	0.9	3	29
S4-R-70-Cab8	1.3	3	18	12.9	38	31
S5-T-150-Cab8	13.9	37	34	46.0	113	79*
S6-F-36-Cab7	2.1	6	32	5.8	17	37
S7-R-36-Cab8	0.4	1	16	22.5	67	39

*Approximately 0.5 seconds after the arc, there was a temperature spike to 439°C (822 °F).

5.6.2 SWGR Test 5 Temperature Data

The temperatures measured by the TCs are shown in Figure 5.6-9. Table 5-7 shows the maximum temperature results. The thermocouple maximum temperature is a general indication of the air temperature 15.2 cm (6 in) from the cabinet and, as expected, the highest temperatures were at measured in the Cabinet 8 vertical duct (TC5) as hot gases from residual heat and fires exhausted up the vertical duct.

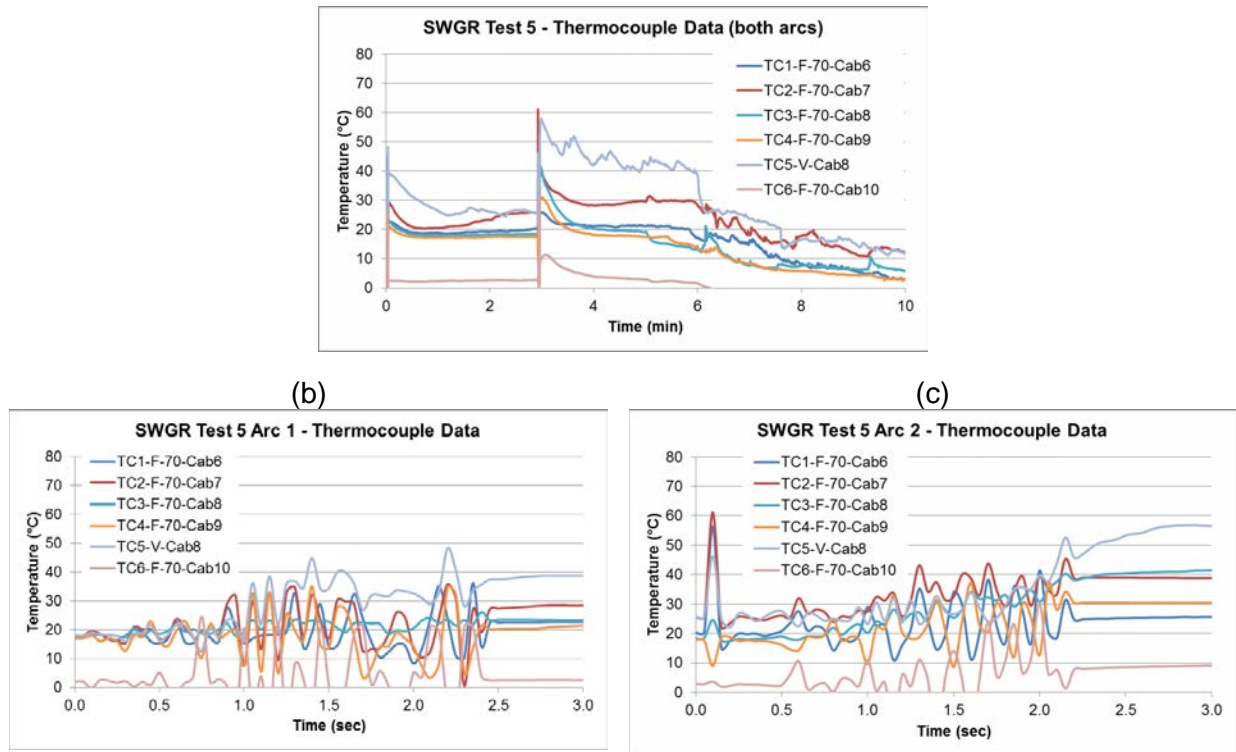


Figure 5.6-9. SWGR Test 5 Thermocouple Data

All TC data were very noisy during the arc, with some major spikes at the start of Arc 2. TC6 appeared to have an additional unidentified instrumentation problem since the temperature dropped to almost zero after Arc 1 and the data after Arc 1 should not be used. The TCs cannot practically be used to estimate flux.

At the end of Arc 1, the maximum temperature of 38 °C (100 °F) was measured in the duct (TC5). TC2 in front of Cabinet 7 where the arc was located, measured 27 °C (81 °F), much lower than the same location in Test 4 (59 °C (138 °F)). This could be because in Test 4, TC2 fell near the end of the arc and may have been subjected to flame and heat escaping from the bottom of the cabinet.

Between the arcs, all TCs were initially measuring cooling similar to the slug calorimeters but TC2 showed increasing temperatures at 1.5 minutes after Arc 1 substantiating there was a small fire in Cabinet 7 after Arc 1. TC1, TC3, and TC5 also indicated some small increases in temperature after 2 minutes.

For Arc 2, the spikes for TC2, TC3, TC4 and TC 5 at the arc start are noise. The highest temperature of 51 °C (124 °F) was measured in the vent (TC5). At the end of Arc 2, TC5 did not

show a large temperature spike like the one observed on S5, which was nearby. This makes the S5 response suspect and perhaps the S5 spike and subsequent erratic signal indicate an instrument problem or some realignment or change in position of S5.

After Arc 2, TC5 on the vertical stack showed an increase for the first minute to a maximum of 58 °C (136 °F; as residual heat and heat from a small fire were exhausting the stack). But 1 minute after Arc 2, TC5 showed a decrease in temperature like the other TCs. This indicates that there was not a major ensuing fire as in Test 4 but there was some fire as indicated by the IR images and the cable damage.

Table 5-7. SWGR Test 5 TC Results.

TC	Arc 1* Max T (°C)	Post Arc 1 Max T (°C)	Arc 2* Max T (°C)	Post Arc 2 Max T (°C)
TC1-F-70-Cab6	22	23	25	32
TC2-F-70-Cab7	27	29	39	45
TC3-F-70-Cab8	23	24	40	42
TC4-F-70-Cab9	20	22	31	34
TC5-V-Cab8	38	39	51	58
TC6-F-70-Cab10	**	**	**	**

*To allow for noise, the maximum temperature is the measured value at the end of the arc.

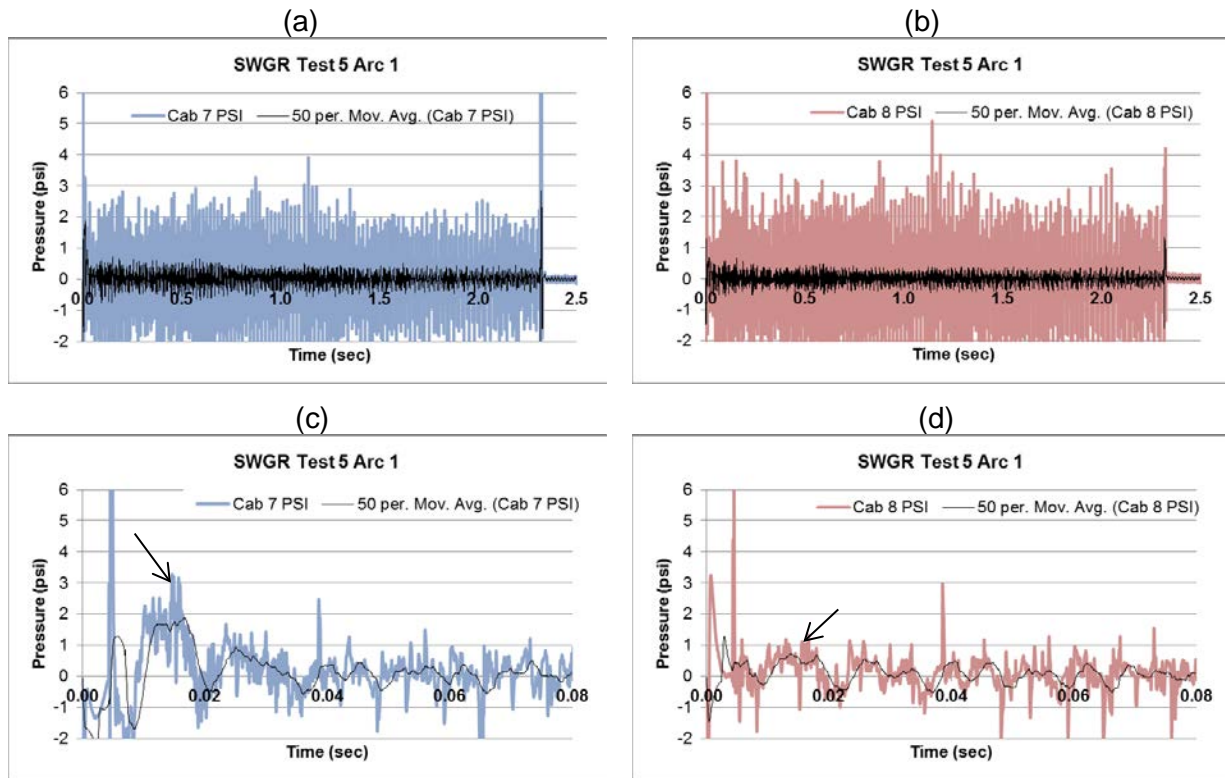
**TC failed during Arc 1.

5.6.3 SWGR Test 5 Pressure Data

The pressures during the arc are shown in Figure 5.6-10 and Figure 5.6-11. The pressures were low because the vents at the top of Cabinets 7 and 8 allowed the pressure to escape.

The pressure analysis methods are in Appendix A and involved picking the maximum near the start of the arc then including a nominal uncertainty for the noise in the signal just before the arc.

For Arc 1, there were numerous noise spikes for Cabinet 7 and Cabinet 8 and both had noise spikes at 0.005 seconds, 0.038 seconds, 1.43 seconds and at the end. During the arc, pressure spikes were virtually continuous and larger magnitude than in previous tests. Both cabinet pressures had a zero shift at the start of the arc that was considered in the analysis. For Arc 1, the Cabinet 7 pressure closer to the arc had a higher maximum and occurred earlier than the Cabinet 8 pressure that was further from the arc. The maximum pressures are indicated by the arrows in Figure 5.6-10(c) and (d).



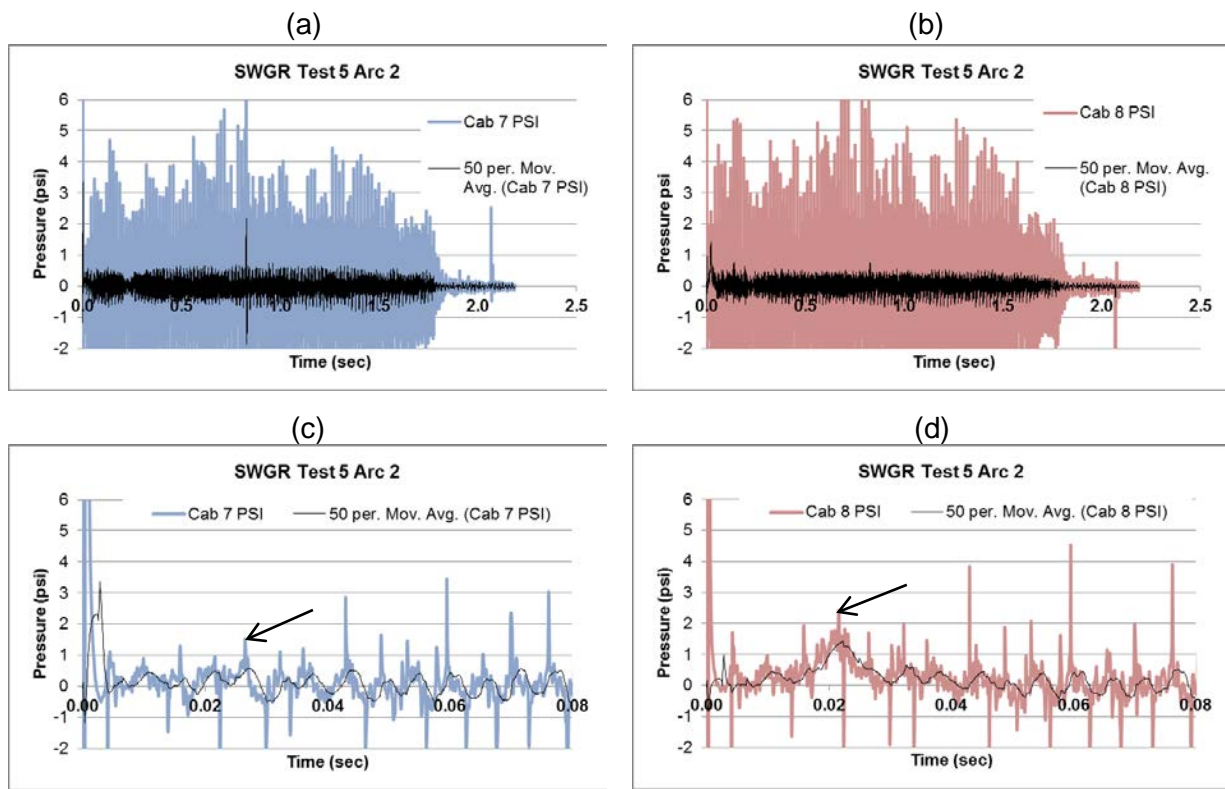
Test 5 Pressure 1 Cab. 7 Arc 1
 17.9 ± 0.7 kPa (2.6 ± 0.1 psi)
@ 0.0150 s

Test 5 Pressure 2 Cab. 8 Arc 1
 8.3 ± 0.7 kPa (1.2 ± 0.1 psi)
@ 0.0167 s

Figure 5.6-10. SWGR Test 5 Pressure Data, Arc 1

For Arc 2, there were numerous noise spikes for Cabinet 7 and Cabinet 8, and both had a large noise spike at 0.001 seconds and several other spikes before the pressure maximums. During the arc, pressure spikes were virtually continuous as in Arc 1. Both cabinet pressures had a zero shift at the start of the arc. The maximum pressures are indicated by the arrows in Figure 5.6-11(c) and (d).

The Arc 2, Cabinet 7 and Cabinet 8 pressures had sinusoidal responses for the next 10 peaks immediately after the maximum peak that had a frequency of about 180-190 Hz. The amplitudes of these peaks were about the same as the initial peak. The noise spikes were superimposed on these sinusoids. This may have been from pressure waves reflecting within the cabinet. However, the frequency is different than the 140 Hz observed in Test 4, which may indicate some other cause. The temperature differences between the runs do not significantly explain the difference on changes in the sonic velocity.



Test 5 Pressure 1 Cab. 7 Arc 2
 6.9 ± 0.7 kPa (1.0 ± 0.1 psi)
 @ 0.0266 s

Test 5 Pressure 2 Cab. 8 Arc 2
 13.1 ± 0.7 kPa (1.9 ± 0.1 psi)
 @ 0.0216 s

Figure 5.6-11. SWGR Test 5 Pressure Data, Arc 2

5.6.4 SWGR Test 5 Arc Energy

The Arc 1 duration was 2.316 seconds with total energy of 57.2 MJ, seen in Figure 5.6-12. Arc 2 was 2.071 seconds with a total energy of 62.0 MJ. The power of Arcs 1 and 2 began to slightly increase after 1.5 seconds as indicated by the rise in the Energy and the increasing slope of Energy Total. The cause is not known but is likely from the arc length from the end of the bus bars to the cabinet increasing as the buses melted causing an increase in the arc voltage.

The energy analysis methods are in Appendix A. The “Energy” is calculated as volts multiplied current multiplied by the time step and each time step is shown. “Energy Total” is the cumulative sum of the energy in each time step.

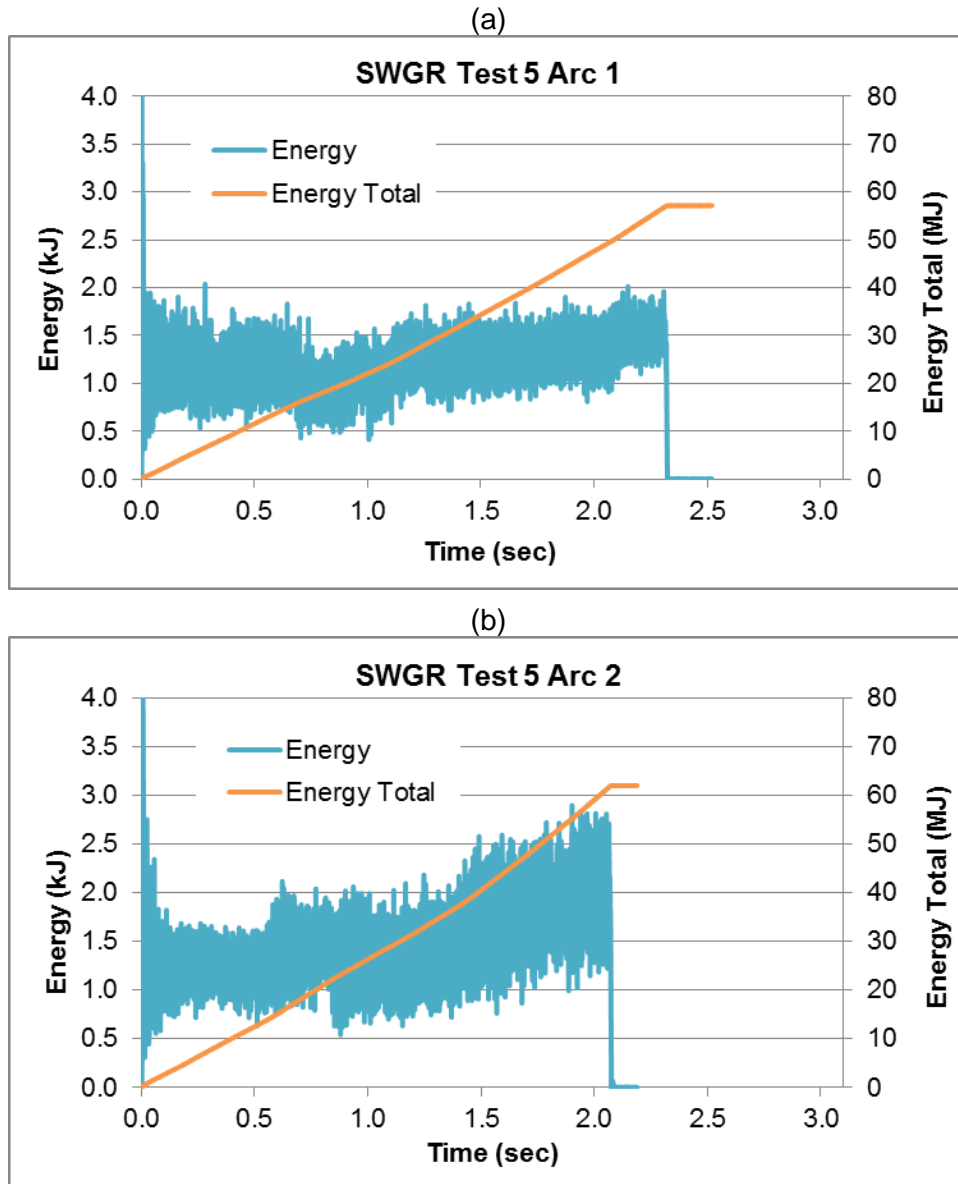


Figure 5.6-12. SWGR Test 5 Arc Energy (both arcs)

5.7 SWGR Test 6 Key Observations (March 2015)

Two arcs were initiated in this test; the first at 7 kV at 24.6 kA with a target duration of 1 second, and the second arc was initiated 4 minutes and 50 seconds later at 7 kV and 33.1 kA with a target duration of 3.0 seconds. These arc durations were recommended by NRA to evaluate effects at lower Arc 1 energies. Arc 1 had a duration of 1.129 seconds and a total energy of 26.5 MJ. Arc 2 in the test was only 0.922 second because of a hot short caused by accidental burning of the control cable to the breaker that caused the breaker to open. Arc 2 had an energy of 21.1 MJ. Although there was some vertical aluminum bus bar oxidation in Cabinet 7, it was not as much as in Tests 4 and 5 because of the shorter Arc 1 duration. There was no ensuing fire and all slug calorimeter locations indicated decreasing temperatures within 5 minutes after Arc 2 so the test was stopped at that time.

Figure 5.7-1 and Figure 5.7-2 shows the high-speed camera images. Flames escaped the rear and right-side panels and reached 0.91 m (3 ft). It appeared there may have been contact with slug calorimeters at the Right Side (RS) top and Rear (R) top but there were no temperature spikes in the temperature data.

There was no major ensuing fire and no visible flames, as seen in the IR thermal images of Figure 5.7-3 and Figure 5.7-4. The temperatures after the arcs were low as indicated by the temperature scale that was set to auto scale. At 5 minutes (300 seconds) after each arc, heat escaped the top vent on Cabinet 8 and the exterior cabinet temperatures were in the 50°C range.

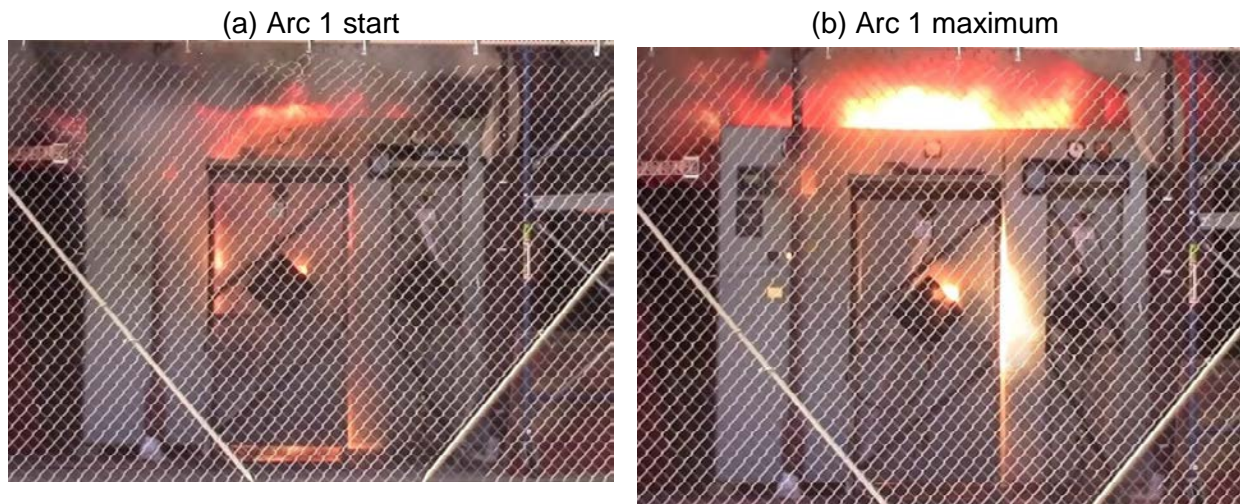


Figure 5.7-1. SWGR Test 6 Arc 1

(a) Arc 2 start

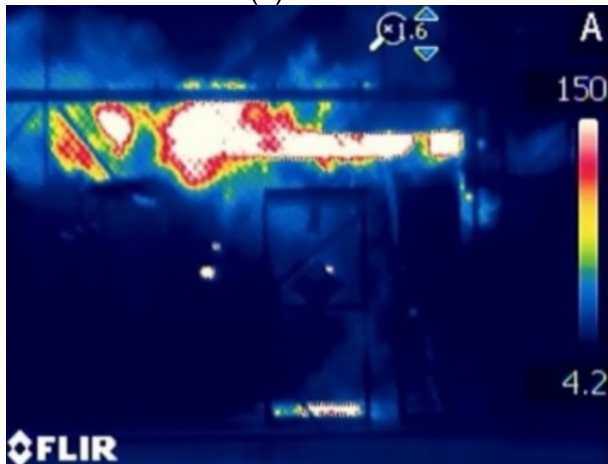


(b) Arc 2 maximum

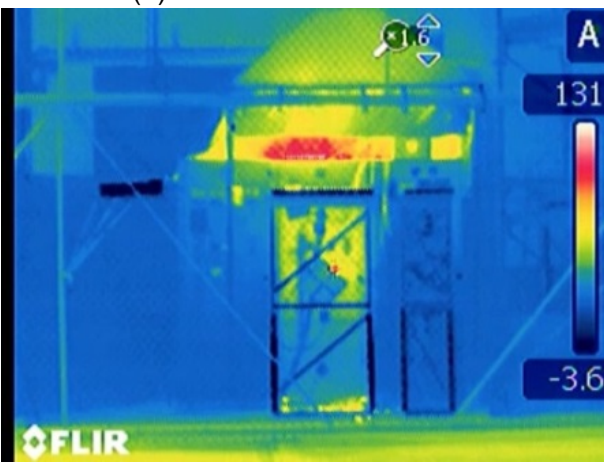


Figure 5.7-2. SWGR Test Arc 2

(a) Arc 1



(b) 10 seconds after Arc 1



(c) 120 seconds after Arc 1



(d) 300 seconds after Arc 1 (just before Arc 2)



Figure 5.7-3. SWGR Test 6 Thermal Image, Arc 1

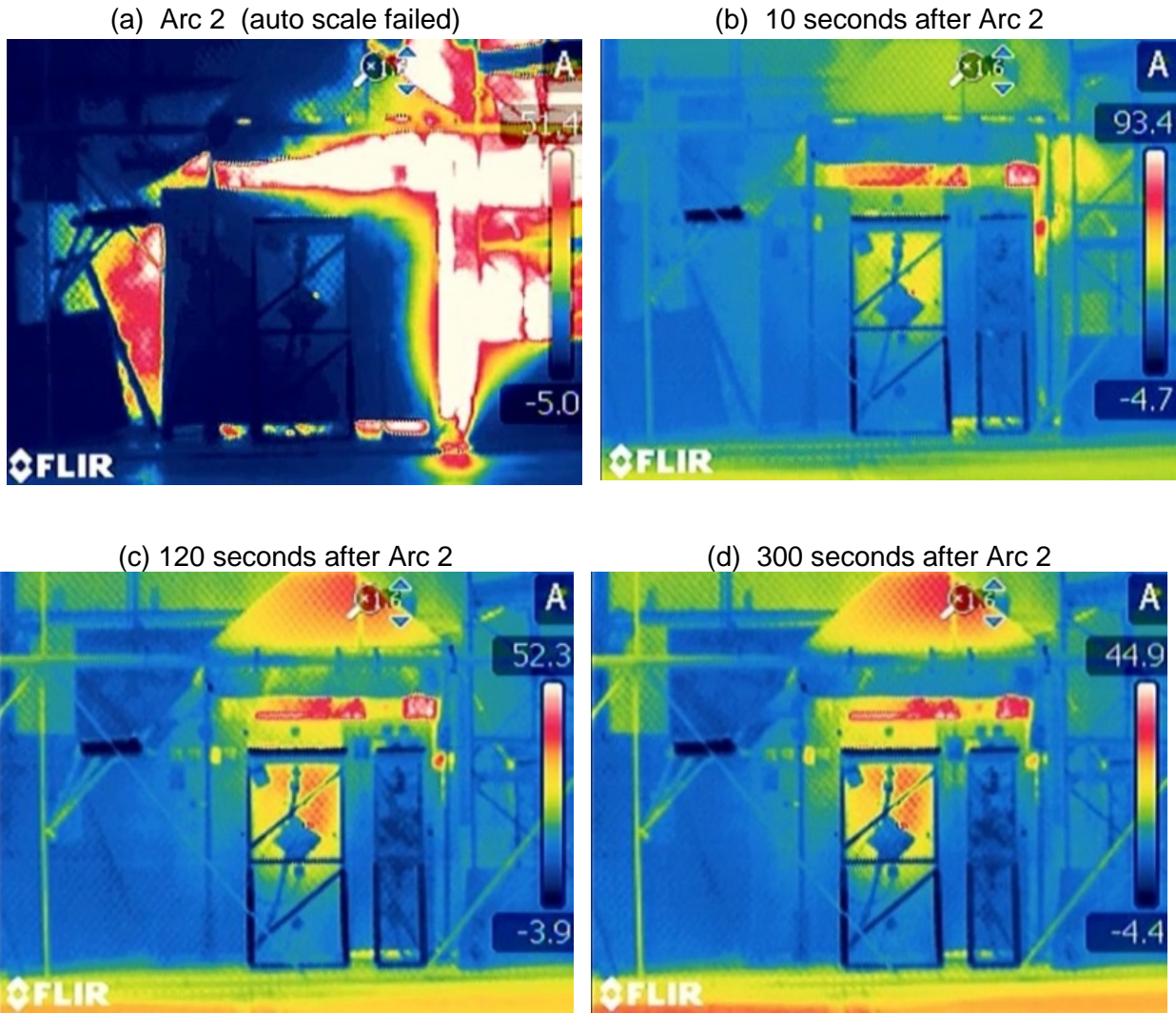
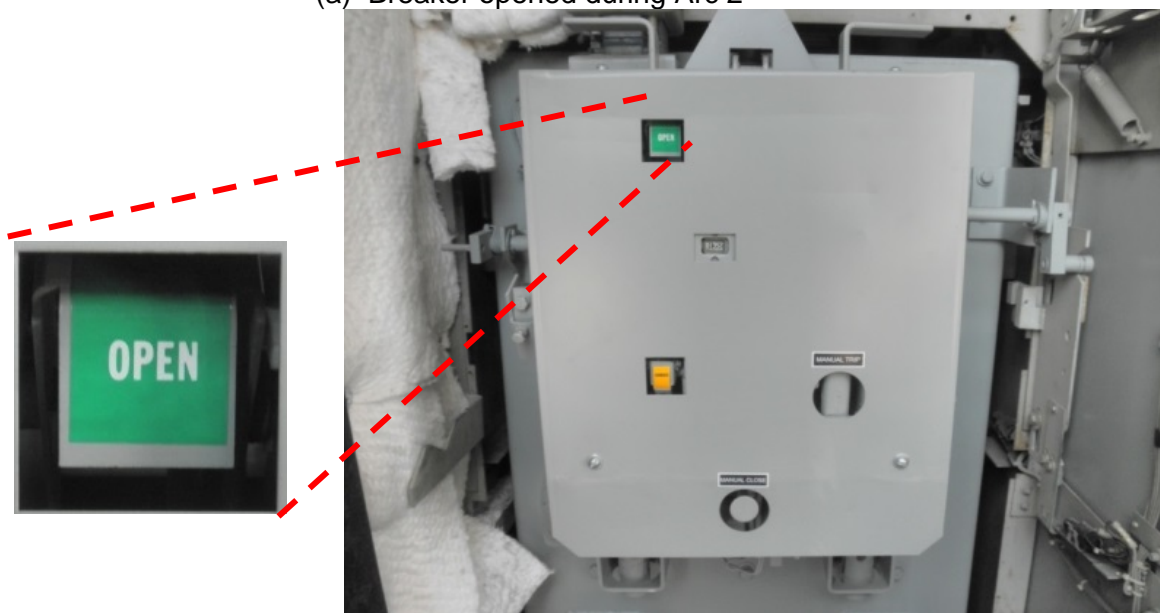


Figure 5.7-4. SWGR Test 6 Thermal Image, Arc 2

Arc 2 caused the control wire for the breaker to hot short within Cabinet 8 and the breaker opened as shown in Figure 5.7-6(a). Additionally, it appears that the internal pressure wave and shock caused the connector for the control cable to unplug as in Figure 5.7-6(b). The wires for AC power to the breaker did not fail so when the hot short occurred AC power was available and the breaker opened resulting in a shorter than planned Arc 2.

(a) Breaker opened during Arc 2



(b) Control cable un-plugged during Arc 2



Figure 5.7-5. SWGR Test 6 Breaker Opened in Arc 2

Because there was no ensuing fire, there was no charring of the front exterior as seen in Figure 5.7-6(a). The panels on the sides and rear of Cabinet 8 were bent and opened by Arc 2 as shown in Figure 5.7-6 (b) and (c). Figure 5.7-6 (d) and (e) show that the cable tray had no soot or charring and the exterior cables in the tray did not char or burn indicating low flux in the cable tray area.

(a) Cabinets 6-8



(b) Side of Cabinet 8



(c) Rear



(d) Cable Tray



(e) Cable Tray Cables



Figure 5.7-6. SWGR Test 6 Cabinet Exterior Damage

The interior damage in all cabinets, shown in Figure 5.7-7(a), was much less than Tests 4 and 5 because of the shorter Arc 1 duration. There was minor discoloration of the front interior panel and light soot on the panel in front to the bus bars in Cabinet 7 where Arc 1 was located. As shown in Figure 5.7-8, none of the cables burned and only had a light soot coating. This was the first SWGR test where all of the cable bundles and cable trays remained intact; the low energy caused little damage. Figure 5.7-8(d) shows heavy soot and some discoloration in the rear of Cabinet 8 where Arc 2 occurred. There was only minor damage in the initial arc location just above the insulators because the arc moved to the end of the bus bars and attached to the ceiling of cabinet, causing discoloration of the top and side panels.

(a) Cabinet Interior Damage - Cabinets 6, 7, 8

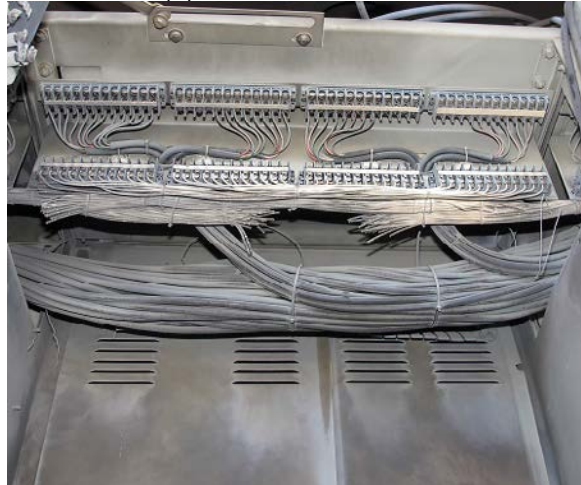


Figure 5.7-7. SWGR Test 6 Cabinet Interior Damage

(a) Cabinet 6 Cables



(b) Cabinet 7 Cables



(c) Cabinet 8 Cables



(d) Cabinet 8 Rear



Figure 5.7-8. SWGR Test 6 Cabinet Interior Damage, Detailed

Figure 5.7-9 shows the deformation of the panel on the right side of Cabinet 8 looking toward the rear. This was about 10 minutes after Arc 2 and there were still small flames from the control wire burning. The wire was well insulated but the insulation blew off. This appears to be the only fire resulting from either of the arcs.



Figure 5.7-9. SWGR Test 6 Cabinet 8 Breaker Control Interior Wire Fire

As shown in Figure 5.7-10(a), there was minor bus bar melting (see additional information in Section 7.2). The arc burned a hole in the right wall of the bus bar compartment toward Cabinet 8 as shown in Figure 5.7-10(b), but the hole was much smaller than observed in other tests because of the short Arc 1 duration.

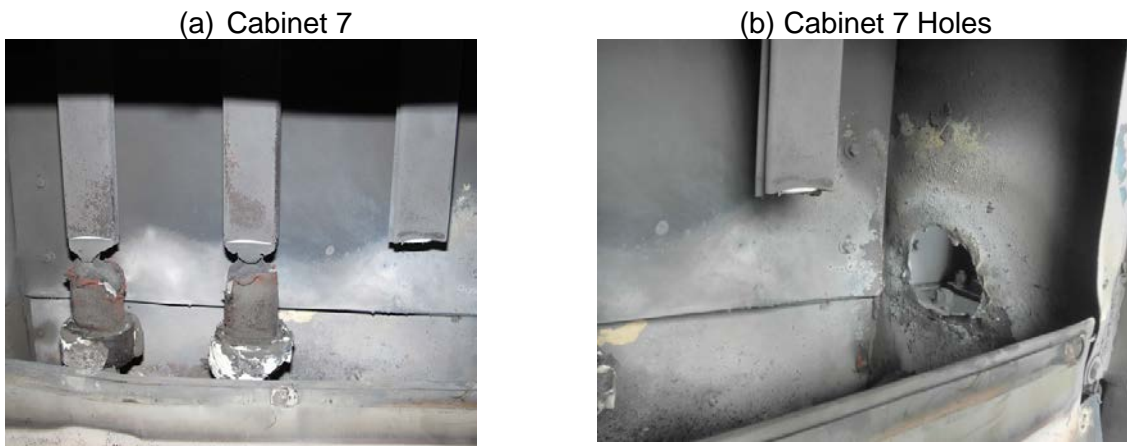


Figure 5.7-10. SWGR Test 6 Arc 1, Cabinet 7 Bus Bar Damage

For Arc 2, the arc moved from the breaker secondary side to the end of the bus bars as shown in Figure 5.7-11. This demonstrated that arcs can move because the arc ignited at the insulator but moved to the end of the bus bars along the path of the current. This also demonstrated that arc behavior is difficult to predict because in an identical test configuration in SWGR Test 4, the arc at this point was interrupted by the short in Cabinet 7 horizontal bus bars and in SWGR Test 5, the arc stayed at the insulators. So, there were three outcomes for the final arc position for the same initial arc position and conditions.

Figure 5.7-11(a) shows only soot damage to the primary side bus bars and insulators that successfully carried the current to the breaker to feed Arc 2. Arc plasma leaking from Cabinet 7 through the wall did not have time to cause major damage in the primary side of Cabinet 8. The side view of the secondary side, rear compartment of Cabinet 8 showed the bus bars remained intact when the arc moved to the final position at the top of the bus bars. Notice that the arc gap between the end of the bus bars and the roof is quite long and this is reflected in the Arc 2 arc voltage that was 1,007 V, much higher than the 603 V observed in SWGR Tests 5.

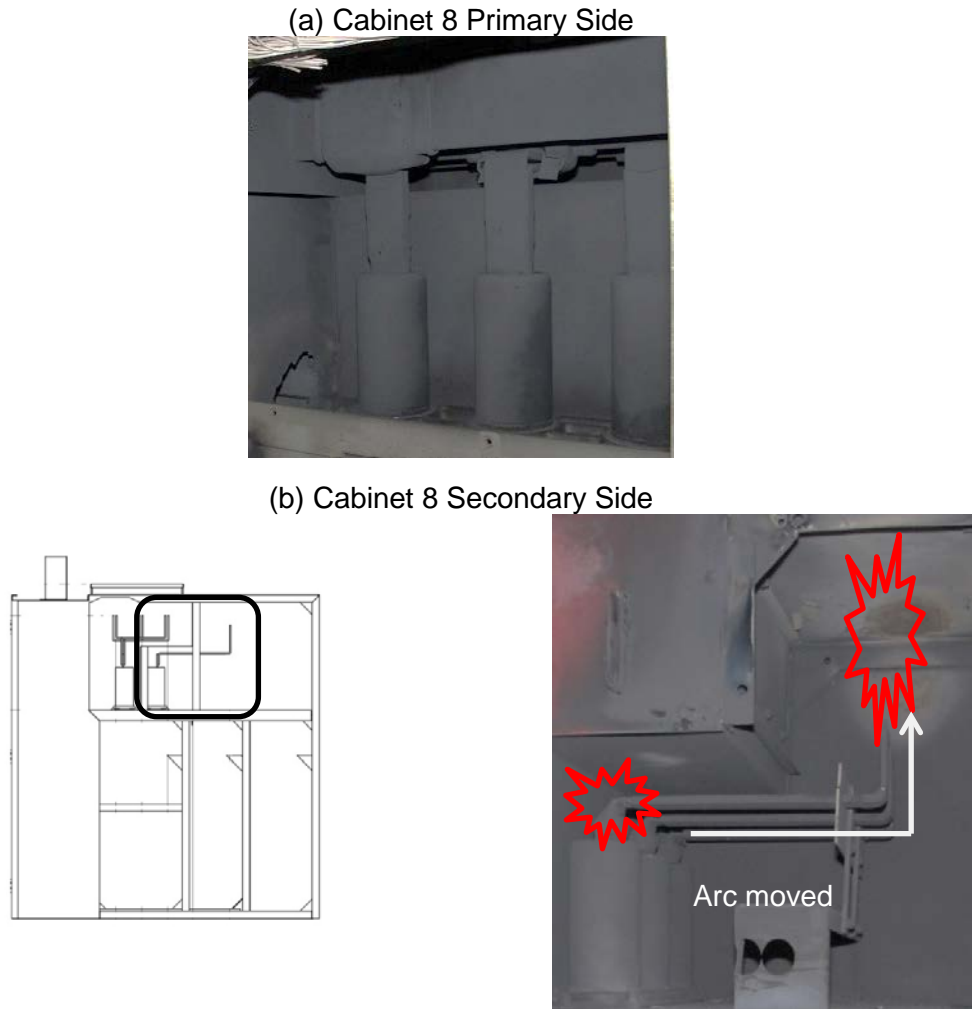


Figure 5.7-11. SWGR Test 6 Arc 2 on Cabinet 8 Damage.

Figure 5.7-12 is a view from the rear showing the damage to the top of the bus bars and the interior roof panel. About 7 cm (2.8 in) were burned off the top of the bus bars (see Section 7.2.5) while the arc was attached from the bus bars to the roof panel. It is likely that if the arc had been the full duration of 2 seconds, the roof panel would have burned through and the damage to the exterior cable tray would have been much worse.



Figure 5.7-12. SWGR Test 6 Arc 2, Breaker Secondary Side Damage

Figure 5.7-13 shows the damage to the breakers. Breaker 7 only had some soot coating. There was no major damage to the Cabinet 8 breaker and the bushings were intact. The full shorting current passed through Breaker 8 but did not cause damage. In the Onagawa event, Breaker 8 was heavily damaged with the bushings almost completely melted and the arc chute covers in the rear were heavily deformed and detached. The test results indicate some other high-energy phenomenon (it could be postulated that the arc passed through the breaker or the arc was very long duration) must have occurred at Onagawa.

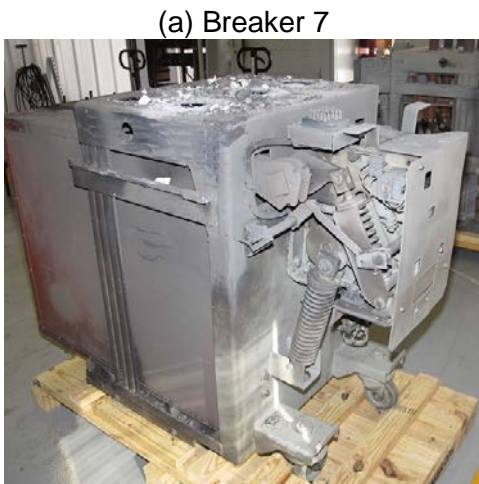


Figure 5.7-13. SWGR Test 6 Breaker 8 Damage

5.7.1 SWGR Test 6 Calorimetry Data

Temperatures measured at the slug locations are shown in Figure 5.7-14 (note the scale change from Tests 4 and 5 results). The Arc 1 slug calorimeter data was not available because the data trigger failed.

For Arc 2, the arc extinguished at 0.568 seconds because the breaker opened. All of the slugs had noise during the arc, probably due to EMI. All the slugs except S6 and S8 have a similar rise in the signal at approximately 0.5 seconds that could be an actual temperature rise when the arc changed positions. However, based on the negligible damage at the original arc point, the arc must have moved much earlier than 0.5 seconds and the rise at 0.5 seconds was attributable to noise common to most of the slugs.

The highest temperature at the end of Arc 2 was measured in the rear of Cabinet 8 near the Arc 2 location (S10). In Cabinet 7, high temperatures were also measured at the rear (S9) and the at right side top position (S7). Both of these locations were exposed to the hot gas and plasma escaping from the openings from the dislodged panels on Cabinet 8. The temperature increases in the slugs in the front of the cabinets were very small because the arc was in the rear of Cabinet 8.

After the arc, slugs on the rear and right side showed increasing temperatures as the heat escaped from the cabinets. All of the slugs showed steady or decreasing temperatures after 2 to 3 minutes, indicating that there was no major ensuing fire.

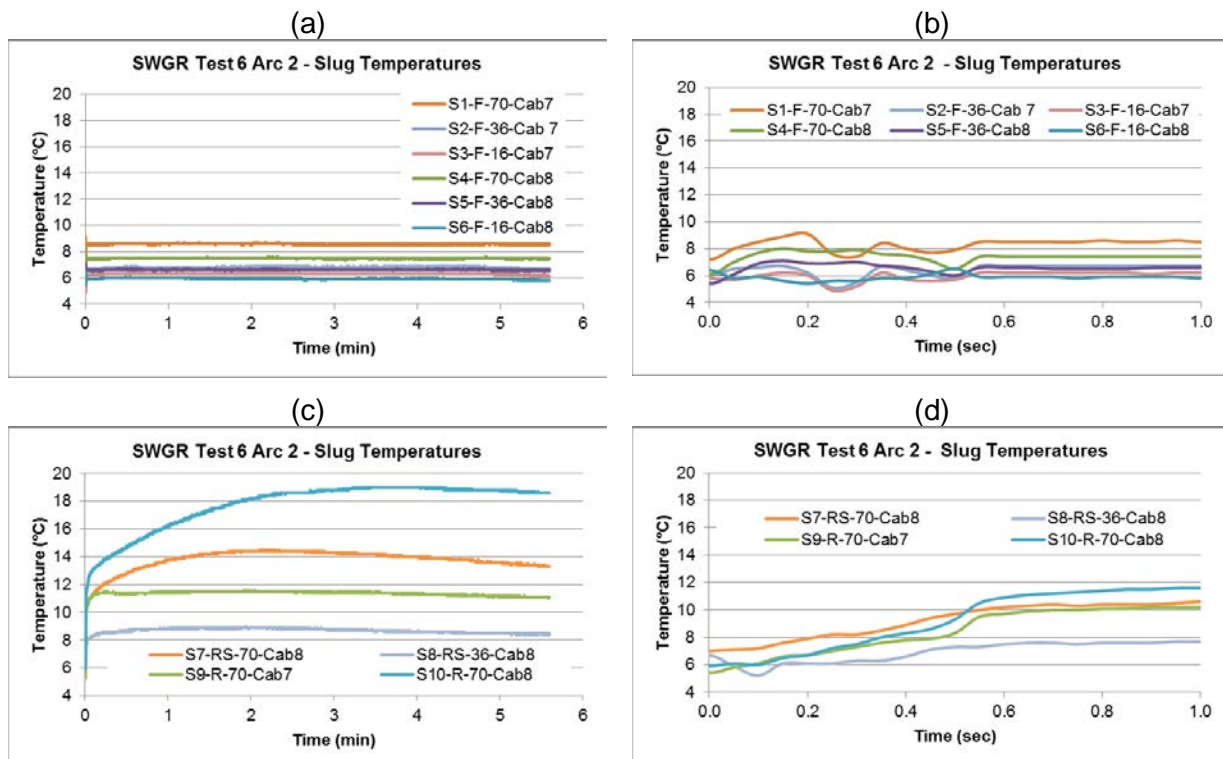


Figure 5.7-14. SWGR Test 6 Calorimetry Data: Temperature

Table 5-8 shows the flux results based on the ASTM F1959 method in Appendix A using the change in temperature (ΔT) between the start and end of the arc. The maximum flux was measured to be 53 kW/m² at the rear of Cabinet 8 (S10). The maximum slug temperatures are also shown to indicate the maximum temperature a metal object could reach.

Table 5-8. SWGR Test 6 Flux Results.

Slug	Arc 1	Arc 2		
		ΔT (°C)	Flux (kW/m ²)	Max T (°C)
S1-F-70-Cab7	*	0.0	0	9
S2-F-36-Cab 7	*	0.0	0	7
S3-F-16-Cab7	*	0.1	1	6
S4-F-70-Cab8	*	0.2	2	8
S5-F-36-Cab8	*	0.1	1	7
S6-F-16-Cab8	*	0.1	1	7
S7-RS-70-Cab8	*	3.6	39	15
S8-RS-36-Cab8	*	1.6	17	9
S9-R-70-Cab7	*	3.7	40	12
S10-R-70-Cab8	*	4.9	53	19

* No data available

5.7.2 SWGR Test 6 Temperature Data

TCs were not used in SWGR Test 6. The temperatures measured by the PTs on the Cable Tray (CT) are seen in Figure 5.7-15. Table 5-9 shows the maximum PT temperatures during the entire 2-arc test and in more detail around the arcs. The PTs indicated the approximate maximum temperature a metal object, with gray surface emissivity of approximately 0.85, located approximately 0.46 m (18 in) above the cabinet rear, could reach.

As expected, for Arc 1 in the center, Cabinet 7, the temperatures in the center of the cable tray were the highest. During Arc 2 in the rear of the right side Cabinet 8, the temperatures on the right side of the cable tray were the highest. For both arcs, the behavior was similar to the DP Tests 4 and 5 where the maximum temperature was about 2 minutes after the arc because the heat escaped from the cabinet. After Arc 1, the heat was in the front of the cabinet and primarily escaped from the top vent about 22 cm (8.7 in) in front of the cable tray. After Arc 2, the heat was in the rear of the cabinet and primarily escaped through the dislocated side panel just below the cable tray right side PTs and also by heating the top panel directly below the right side PTs. Subsequently, the right side PT reached the highest PT temperature in the tests with the cable tray PTs.

Notice that the left side PTs above Cabinet 6 that did not have an arc measured very low temperature increases, as would be expected. Although the temperatures were higher in Arc 2 than other tests, there was still no cable damage as shown earlier.

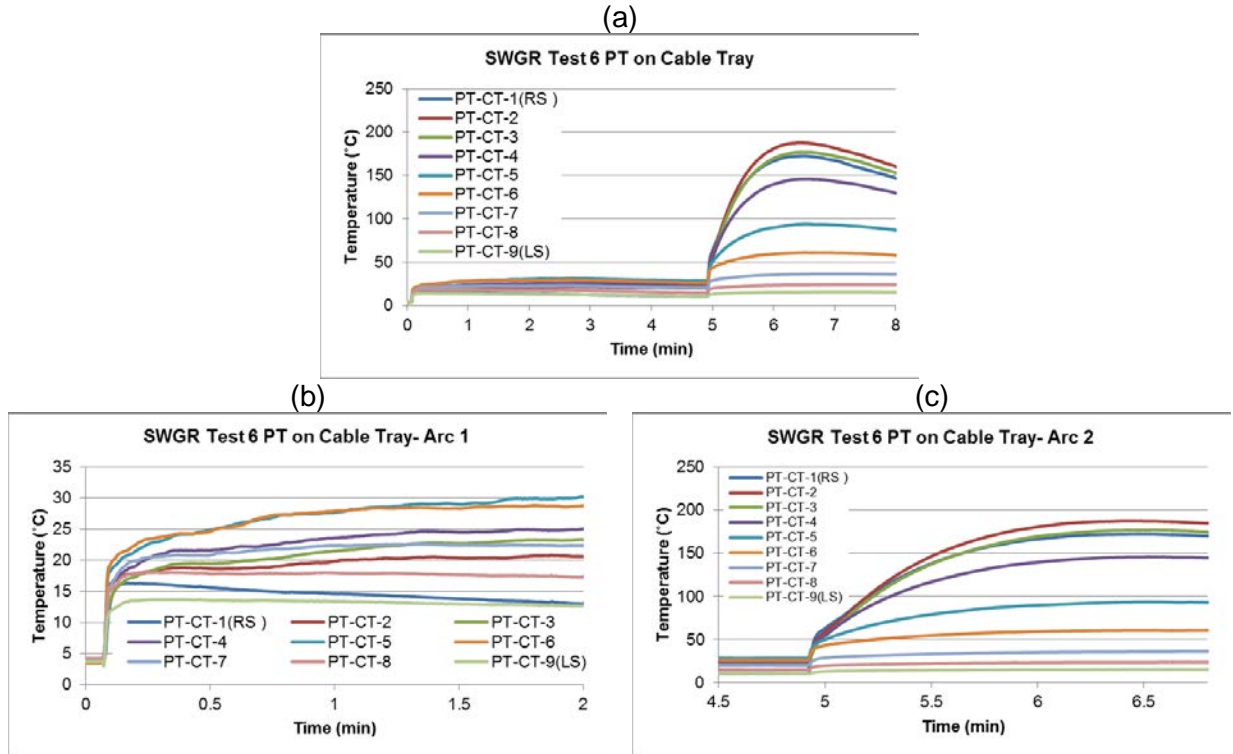


Figure 5.7-15. SWGR Test 6 Cable Tray Plate Thermometer Data

Table 5-9. SWGR Test 6 Plate Thermometer Results.

PT	Arc 1 to Arc 2 Max T (°C)	After Arc 2 Max T (°C)
PT-CT-1(RS)	16	172
PT-CT-2	21	188
PT-CT-3	24	177
PT-CT-4	26	146
PT-CT-5	31	94
PT-CT-6	30	61
PT-CT-7	23	36
PT-CT-8	18	24
PT-CT-9(LS)	14	15

5.7.3 SWGR Test 6 Pressure Data

The pressures during the arc are shown in Figure 5.7-16 and Figure 5.7-17. The pressures were low because the vents at the top of Cabinets 7 and 8 allowed the pressure to escape.

The pressure analysis methods are in Appendix A and involved picking the maximum near the start of the arc then including a nominal uncertainty for the noise in the signal just before the arc.

For Arc 1, there were numerous noise spikes for Cabinet 7 and Cabinet 8 and both had noise spikes at 0.007, 0.014 and 0.017 seconds. During the arc, pressure spikes were virtually continuous as in Test 5 but at slightly lower magnitude. Both cabinet pressures had a zero shift at the start of the arc that is considered in the analysis.

For Arc 1, the Cabinet 7 pressure closer to the arc had a higher maximum and occurred earlier than the Cabinet 8 pressure that was further from the arc. The Arc 1, Cabinet 7 and Cabinet 8 pressures had rough sinusoidal responses for the next 4 to 5 peaks immediately after the maximum peak that had a frequency of about 180 Hz. The maximum pressures are indicated by the arrows in Figure 5.7-16(c) and (d).

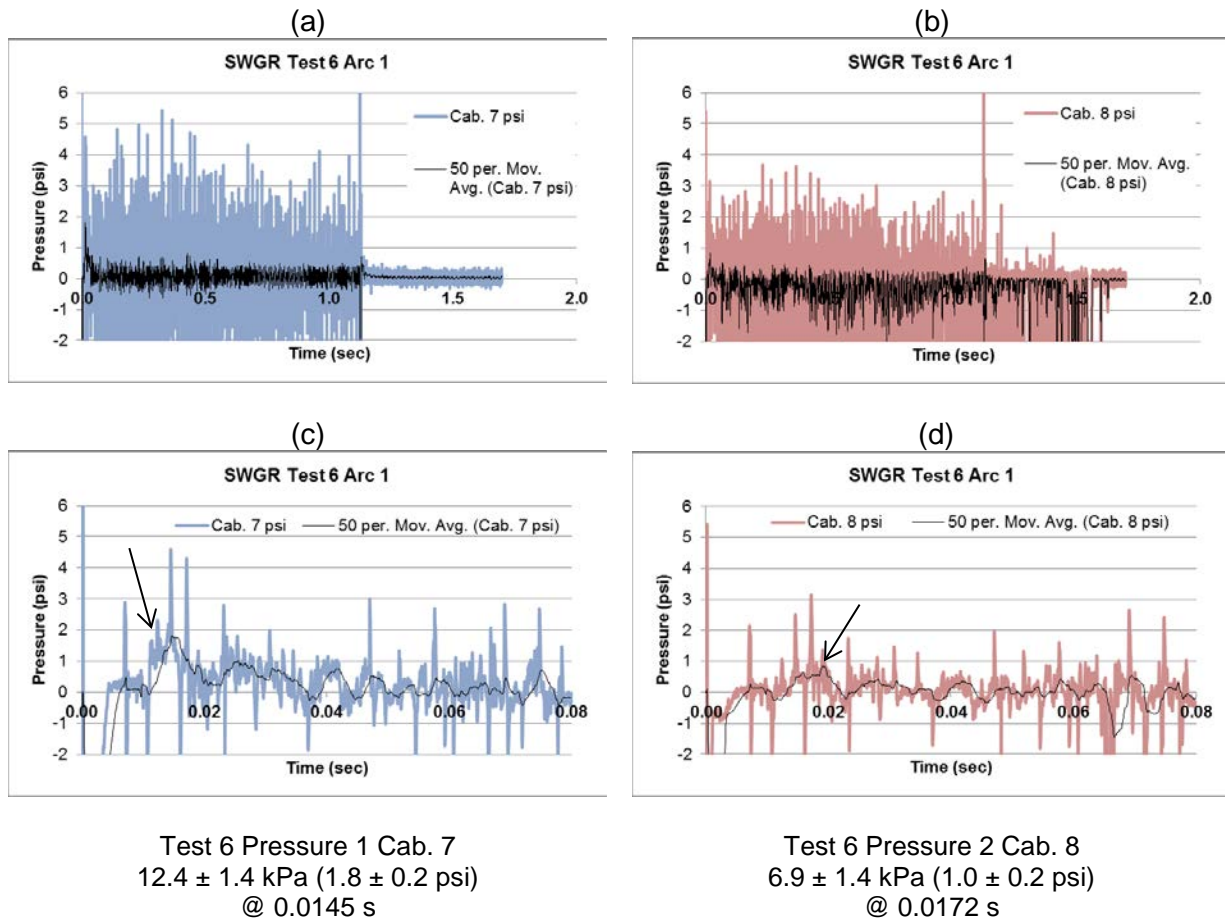


Figure 5.7-16. SWGR Test 6 Pressure Data, Arc 1

For Arc 2, there were numerous noise spikes for Cabinet 7 and Cabinet 8 and both gauges had several spikes before the pressure maximums. During the arc, pressure spikes were virtually

continuous as in Test 5 but at slightly lower magnitude. Both cabinets had very high noise at the end of the arc around 1 second possibly because the arc from the bus bar to the cabinet roof was unstable and EMI increased. Both cabinet pressures had a zero shift at the start of the arc that was considered in the analysis and Cabinet 8 had a large zero shift at the end of the arc. The maximum pressures are indicated by the arrows in Figure 5.7-17(c) and (d).

The Arc 2 Cabinet 7 pressures had sinusoidal responses for the next 10 peaks immediately after the maximum peak that had a frequency of about 190 Hz. The amplitudes of these peaks were about the same as the initial peak. The noise spikes were superimposed on the sinusoids that may have been from pressure waves reflecting within the cabinet.

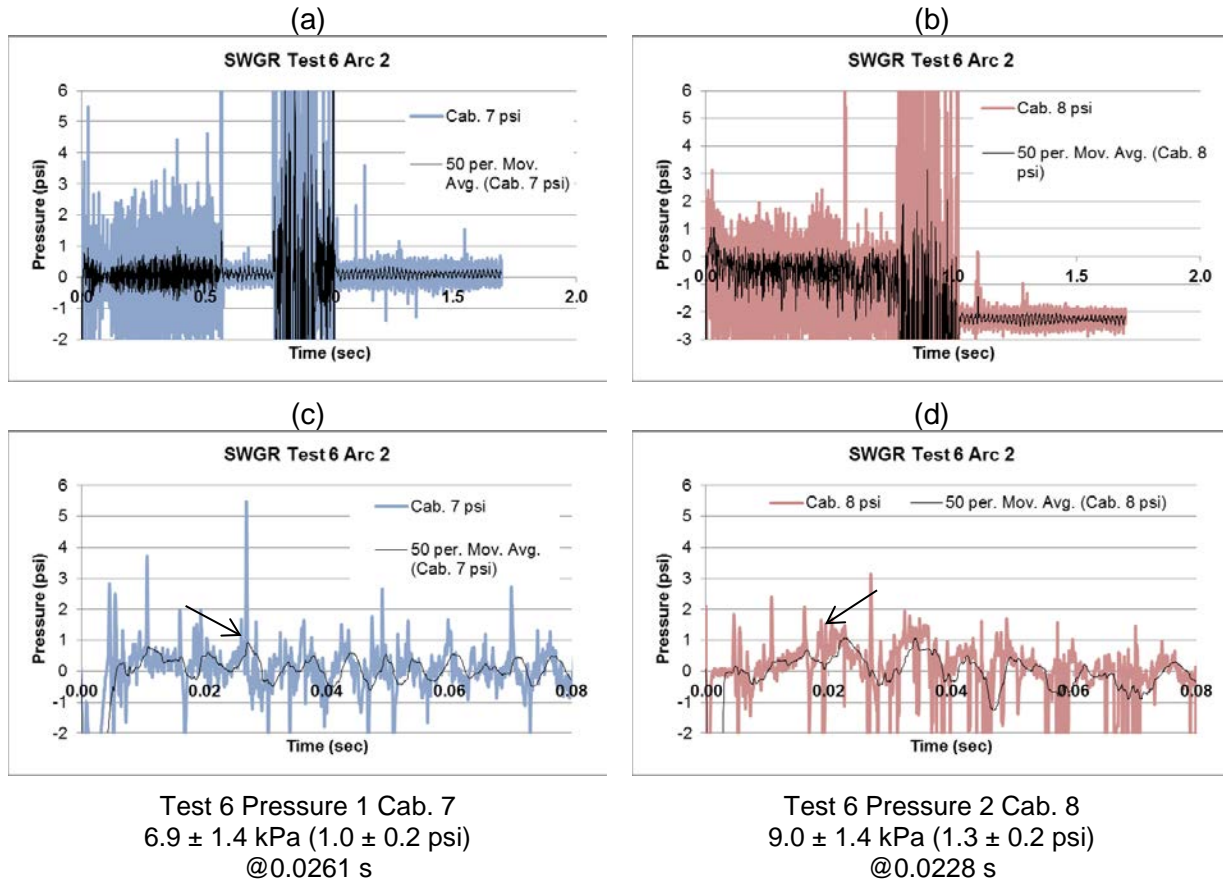


Figure 5.7-17. SWGR Test 6 Pressure Data, Arc 2

5.7.4 SWGR Test 6 Arc Energy

The Arc 1 duration was 1.129 seconds with total energy of 26.5 MJ, seen in Figure 5.7-18. Arc 2 was 0.568 seconds with a total energy of 21.1 MJ. The power of Arc 2 increased during the arc as indicated by the rise in the energy, as seen in Test 5. The cause is not known but is likely from the arc length from the end of the secondary bus bars to the cabinet roof increasing as the buses melted causing an increase in the arc voltage. As mentioned previously, the Arc 2 arc voltage was much higher than in SWGR Tests 4 and 5.

The energy analysis methods are in Appendix A. The “Energy” is calculated as volts multiplied current multiplied by the time step and each time step is shown. “Energy Total” is the cumulative sum of the energy in each time step.

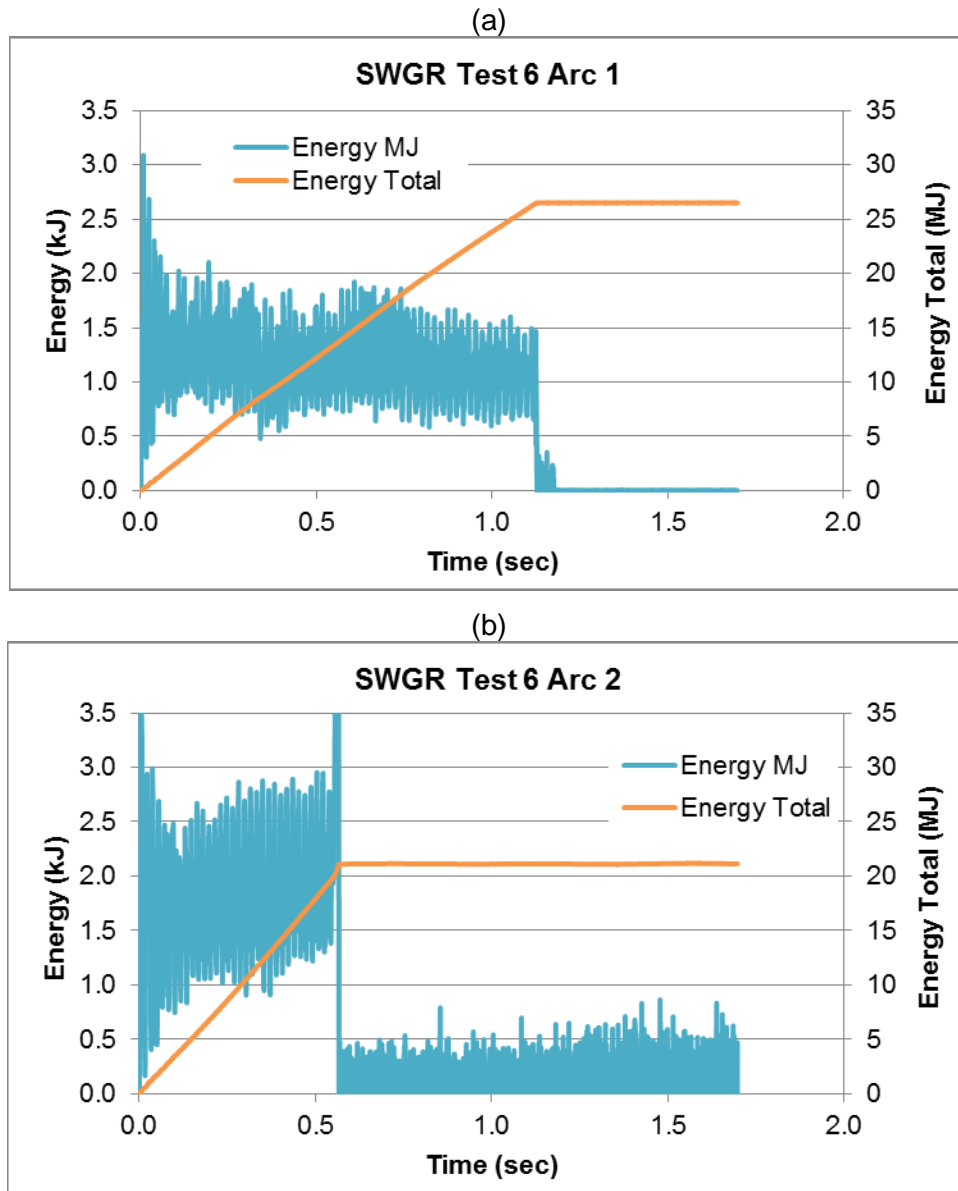


Figure 5.7-18. SWGR Test 6 Arc Energy (both arcs)

5.8 SWGR Tests 4 through 6 Summary of Electrical Conditions

Electrical conditions reported by KEMA are below. For several tests, the KEMA energy results are slightly lower than the results in the previous section and reported as the correct result. The KEMA analyst manually selects the beginning and end of the arc voltage and current waveforms using two cursors on the screen. In this case the cursors were not properly set causing some current and voltage data to be missed, and the energy to be underestimated.

Table 5-10. SWGR Test 4 through 6 Electrical Results (1).

Test	Arc	OCV (KV)	Phase	Sym (kA)	Sym @End (kA)	Peak (kA)	Curr. Dur. (sec)	Arc Energy (2)	Freq @End (Hz) (3)	Phase Arc Volts
4	Arc 1	7.0	A	24.1	24.2	59.6	2.354	21.3	30.7	A-N 410
			B	26.0	24.7	37.8		19.7		B-N 401
			C	23.3	24.4	56.5		23.6		C-N 447
			AVG	24.5	24.4	51.3		Σ64.6		AVG L-L 726
	Arc 2	7.0	A	34.0	34.3	88.2	2.081	24.9	50.5	A-N 404
			B	34.8	33.2	67.1		20.5		B-N 363
			C	33.4	32.5	69.2		30.4		C-N 493
			AVG	34.1	33.3	74.8		Σ75.8		AVG L-L 727
5	Arc 1	7.0	A	24.4	25.3	58.6	2.316	20.0	32.9	A-N 396
			B	25.2	26.2	36.2		17.4		B-N 354
			C	23.8	25.5	55.6		17.5		C-N 354
			AVG	24.4	25.7	50.1		Σ54.9		AVG L-L 639
	Arc 2	7.0	A	34.1	31.8	85.7	2.071	21.1	52.1	A-N 367
			B	34.4	34.8	65.9		24.0		B-N 396
			C	33.2	33.4	67.9		15.2		C-N 282
			AVG	33.9	33.3	73.2		Σ60.3		AVG L-L 603
6	Arc 1	7.0	A	24.5	21.7	51.6	1.129	11.0	49.5	A-N 524
			B	25.0	21.6	51.3		6.9		B-N 480
			C	24.2	20.8	65.7		8.4		C-N 523
			AVG	24.6	21.4	56.2		Σ26.3		AVG L-L 882
	Arc 2	7.0	A	32.8	33.6	71.3	0.568	8.46	57.5	A-N 882
			B	34.4	34.0	68.0		6.09		B-N 626
			C	32.0	32.9	87.2		5.39		C-N 579
			AVG	33.1	33.5	75.5		Σ19.9		AVG L-L 1007

Notes:

- (1) See Table 2-16 for abbreviations and acronyms used in this table.
- (2) As reported by KEMA instruments and results.
- (3) Arc 1 was 50 Hz, Arc 2 was 60 Hz at start of current.

5.9 SWGR Tests 4 through 6 Qualitative Summary

1. Ensuing Fire: Ensuing fires occurred in Tests 4 and 5 and it appears that with an initial arc to preheat the cabinets, that ensuing fires after the second are easier to achieve than with just a single arc. In Test 4, the ensuing fire spread was also accelerated by very high aluminum bus bar oxidation energy caused by an arc on the horizontal bus bars of Cabinet 7. The ensuing fires were extinguished after a few minutes. The electrical energy in Test 6 was too low to initiate an ensuing fire.
2. Damage: The bus bar damage varied widely because the arcs occurred at various locations and various energies. In most tests, several centimeters of bus bars were oxidized greatly increasing the total energy during the arc and causing internal cable fires in Tests 4 and 5. Unlike all the other SWGR tests, the vertical bus bars were mostly destroyed in Test 4 with heavy damage to the horizontal bus bar; only part of the vertical bus bars burned in Tests 2, 3 and 5 even though the conditions were the same. Test 6 resulted in less bus bar damage because the energies were lower from shorter duration arcs but there was still bus bar oxidation from both arcs.

Only Tests 4 and 5 showed internal cable damage; Test 4 had more severe damage due to the high energy from the horizontal bus bar aluminum oxidation that did not occur in Test 5. There was no external cable tray damage in any of the tests.

In Tests 4 and 5 as in SWGR tests 1 through 3 the SWGR cabinet outer walls did not have major deformation like the DP and MCC cabinets. The cabinet outer walls are thicker and the large vent on the top kept the pressure low. Additionally, the arcs in SWGR Tests 1 through 5 were not directly inside an outer cabinet wall so external wall damage was minimal. There was significant bending, deformation, or burn-through of the internal walls directly exposed to the arc. However, in Test 6, because it was a 3-cabinet configuration, the right side wall of Cabinet 8 with Arc 2 was an exterior wall and was directly exposed to Arc 2. So, there was deformation and displacement of the exterior panel in the rear of Cabinet 8 where the arc occurred.

3. Calorimetry: Similar to the previous SWGR tests, Tests 4 and 5 showed the highest resultant heat flux from the first arc at 1.5 m (5 ft) above the cabinets. Test 6 did not have measurements during the first arc. The second arc in these tests resulted in maximum fluxes in different locations, because the arc in Test 6 was in the rear of the cabinet and not under the top vent and the path of the escaping heat to the slug calorimeter was different. As expected, the maximum flux was at the top rear for Test 6.
4. Temperature: In these tests, thermocouples to measure air temperature were only used in Tests 4 and 5, however, almost all of the data for Test 4 is invalid due to the thermocouple support falling during the first arc. Plate thermometers (PT) were used in Test 6 on the cable tray and showed low temperatures (30 °C (86 °F)) for Arc 1 and higher temperatures for Arc 2 (180 °C (356 °F)) because the PTs were directly above the cabinet roof where the arc was attached.
5. Pressure: As with SWGR Tests 1 through 3, the measured pressures for Arc 1 were very low since there were vents at the top Cabinets 7 where the arc occurred. The exception is Test 4, Arc 1, where the pressure was 40 to 50 percent higher than other SWGR tests; the reason is not known. For Arc 2, the pressures were lower because Cabinet 8, where the arc occurred, does not have a direct line of sight to the top vent.

The pressures were higher in the cabinet where the arc occurred (Cabinet 7 for Arc 1 and Cabinet 8 for Arc 2), as expected.

6. Arc Energy: In all tests for both Arc 1 and Arc 2 the total energy was proportional to the arc duration for the given electrical testing conditions. All tests showed a smooth increase of the total energy during the arcs indicating stable arc conditions and the target arc durations were nominally achieved in all the tests except Arc 2, Test 6 where there was an equipment failure. The smooth increases were a little surprising for Test 4, Arc 2 considering that the arc initiated on the secondary side of Cabinet 8 then progressed to the bus bars in Cabinet 7.

6 Switchgear with Rocket Fuel Arc Simulator Fire Test - SwRI (July 2013)

6.1 RFAS Test Overview

The key objective of these tests was to measure the Heat Release Rate (HRR) and other key ensuing fire parameters that could not be measured during the electrical arc tests at KEMA. Specifically, this effort was undertaken to try to achieve temperatures and heat fluxes that would cause cables outside of the cabinet to ignite. The tests used a number of 4 kg (8 lb) Rocket Fuel Arc Simulator (RFAS) slabs to vary the total available energy. The RFAS are slabs consist of aluminum and ammonium-perchlorate based rocket fuel, and were developed to provide short-time high energy bursts similar to electrical arcs.

The initial RFAS tests in SWGR cabinets in January 2013 were in a 1-cabinet configuration and only one RFAS ignition slab was used. These proof-of-concept tests were conducted to show that the RFAS could reliably simulate arc energy in a cabinet configuration with repeatable results. The RFAS tests in July 2013 used two RFAS explosions in Cabinets 7 and 8 of a 5-cabinet SWGR line-up to simulate the two arcs that are assumed to have occurred in Cabinets 7 and 8 in the Onagawa event.

6.2 RFAS Test Summary of Results

The RFAS tests in July 2013 simulated two arcs in the assumed Onagawa event. The plan was to first ignite an RFAS in Cabinet 7, and then ignite a second RFAS in Cabinet 8, nominally 8 minutes later. In Test 1, the 8 minute delay did not occur because RFAS1 also ignited RFAS2. Changes were made for Test 2 to add additional insulation and barriers between Cabinets 7 and 8 to ensure the initial ignition in Cabinet 7 did not ignite the RFAS in Cabinet 8. In Test 2 the delay between RFAS ignitions was successful (7.8 minutes) and the ensuing fire was similar to the KEMA SWGR Test 2. The results are shown in the table below. No useful pressure measurements were made and therefore are not reported.

There was a full ensuing fire in Test 2 that was allowed to burn to self-extinguishment, 90 minutes after ignition. In Test 1 both RFAS charges ignited at the start of the test and there was no major ensuing fire even though the RFAS energy was more than two times the arc energy of KEMA SWGR Test 2 (58 MJ). The cables in Test 1 reached a high temperature during the RFAS ignition but quickly cooled and there was no ensuing cable fire.

Table 6-1. SWGR RFAS Summary of Results.

Test	RFAS Used (#Slabs) (1)	RFAS ignition time (sec)	RFAS Energy (MJ)	Maximum Flux (kW/m ²) (2)	Max Temp. (°C)	Max HRR (kW)	Ensuing Fire? Key Observations
1	RFAS1: 2 RFAS2: 2	RFAS1: 0 RFAS2: 0	140	Front: 3 Top: 14	Door: 97 Cables: 500	RFAS: 3 Fire: N/A	Small. Both RFAS ignited at the same time. High cable temperature was short time
2	RFAS1: 2 RFAS2: 5	RFAS1: 0 RFAS2: 465	RFAS1: 70 RFAS2: 175 Total: 245	Front: 11 Top: 11	Door: 680 Cables: 812	RFAS: 4 Fire: 0.4	Large. Burned for 90 minutes.

Notes:

- (1) RFAS1 slabs were in Cabinet 7 and RFAS2 slabs were in Cabinet 8.
- (2) The flux is measured at the boundaries of the NUREG/CR 6850 ZOI: 1.5 m (5 ft) above the cabinet and 0.91 m (3 ft) from the sides of the cabinet.

The key observations from the July 2013 RFAS SWGR tests at SwRI were:

- The RFAS is a reasonable surrogate to simulate the high energy of a HEAF and obtain more data for the ensuing fires. It was observed that the energy to ignite an ensuing cable fire was 140 to 245 MJ from the RFAS tested at SwRI as compared to 50 to 60 MJ from the electrical test, KEMA SWGR Test 2. Thus, it appears that three to four times more energy is required for ignition using an RFAS heat source than from an electrical arc source. The oxidation of the aluminum bus bars was a candidate source for the additional energy and based on the basic oxidation reaction (see Section 7.2.1) it became the likely additional energy source. The eventual conclusion was aluminum oxidation in addition to the electrical energy was needed to cause the ensuing fires observed in KEMA SWGR Test 2.
- The low pressure and rapid recovery of oxygen in the cabinets after the RFAS ignition indicate that the well-ventilated SWGR cabinets likely quickly lose much of the energy created by a HEAF. The KEMA electrical arc tests also show that the energy to start an ensuing fire is much higher for the SWGR cabinets than for less-ventilated cabinets like the DP, as discussed in other sections of this report.
- In RFAS Test 2, pre-heating from the first RFAS decreased the time to the start of the ensuing fire and accelerated the growth of the ensuing fire to peak temperature. Cabinets without long pre-heating still had an ensuing fire but it took more time to ignite the cables and the fire growth was slower.
- Cabinets isolated from the initial preheat and two cabinets away from the RFAS heat

source like Cabinet 10 did not ignite.

- Even at the higher RFAS Test 2 energies, the damage was not as severe as at Onagawa. The exterior of the cabinet was not as charred and there was no major damage on the secondary side of the SWGR cabinet.

6.3 RFAS 5-Cabinet Test Configuration

Testing was conducted under the 10-MW large scale calorimeter located in Building 222 at SwRI's Fire Technology Department. Each test consisted of five GE Magneblast Switchgear cabinets that contained varying numbers of RFAS slabs, three aluminum bus bars, lengths of 6 kV-CHSVT cable, and bundles of HIV and CV-4 cable, both in the cabinets and horizontal and vertical cableways.

The cabinets and combustible loads were identical to the June 2013 KEMA 5-cabinet tests. Figure 6.3-1 shows the test setup for Test 1; Cabinet 7 is on the left. The cabinets and combustible loads are identical to the June 2013 KEMA SWGR tests (Section 4).

To prevent the RFAS in Cabinet 7 from igniting the RFAS in Cabinet 8 in Test 2, the interior of the RFAS area in Cabinet 7 was insulated with ceramic fiber blanket. Gaps in the cabinets and around the bus bar penetrations were filled with fire-proof materials. Ceramic fiber blanket was also added to the top vent of Cabinet 7 to block any sparks from entering the vent of Cabinet 8 during the first RFAS event. A phenolic composite panel (referred to as "red board") was placed between Cabinet 7 and 8 at the top.



Figure 6.3-1. SwRI 5-Cabinet RFAS Test Setup

Each test used varying amounts of 4 kg (8.82 lb) slabs of aluminum and ammonium-perchlorate-based solid rocket fuel. The RFAS slabs have a 70% Ammonium perchlorate (APCP-oxidizer), 14% aluminum powder (Al-fuel) and 16% binder (common yellow glue). This produces an energy density of 8.72 MJ/kg and a temperature in the range of 7500 °C (13,532 °F). Each set of fuel slabs was arranged so that the sides with the igniters faced each other in pairs to ensure even ignition. The slabs were designed to each release 35 MJ of thermal energy in 2.0 ± 0.5 seconds. The energy content of each fuel batch to make the RFAS slabs was measured and confirmed by bomb calorimetry per International Organization for

Standardization ISO 1716 [9]. The duration of the burn was governed by the thickness of the slabs. Slab thickness was controlled during the fabrication process. Figure 6.3-2 shows two 4 kg (8.82 lb) RFAS slabs with the igniters installed. Several igniters were within each slab to make it burn for approximately 2 seconds. Slabs were 9 mm (0.35 in) thick and had an aluminum foil back that was used in manufacture. The slabs were supported by a stainless steel frame that was reused for all tests.

Figure 6.3-2 also shows the cabinet configuration that was virtually identical to the KEMA SWGR Tests 1 through 3, 5-cabinet configuration. The RFAS slabs were located just below the horizontal bus bars in the cabinet compartment with a vent opening on the top of the cabinet as in the Onagawa cabinets. This location was chosen to simulate the position of the ends of the bus bars and the arcs in the KEMA electrical tests. The top vent was covered with a thin steel plate about 15.2 cm (6 in) above the vent; during RFAS events, the flames exiting the top deflected from this plate and spread over the top of the cabinets in view of the flux measurement instrumentation at 1.5 m (5 ft) above the cabinet.

In this configuration much of the heat was released upwards. The heat also propagated through an interior wall to the right of the RFAS and then through the front door to expose the heat flux meter in front of the cabinet at 0.91 m (3 ft). The wall to the right of the RFAS had some vent louvers which allowed the heat to escape from the RFAS cabinet compartment to the front compartment and ignite the cables at the top of the front compartment. "Dummy" circuit breakers with the same shape and configuration as the breakers in the KEMA SWGR tests were in place just below the RFAS compartment to provide a similar flow path, cabinet volume and thermal mass as in the electrical arc HEAF tests.

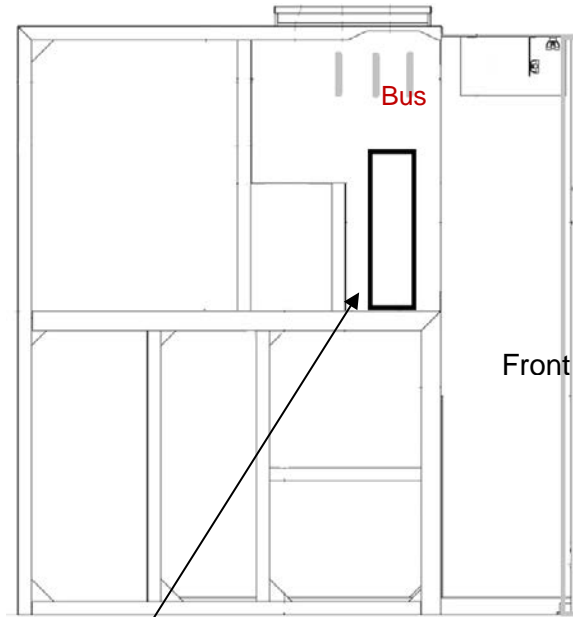


Figure 6.3-2. RFAS Arrangement

6.4 RFAS Test Heat Flux Instrumentation

Heat flux was measured at the NUREG/CR 6850 ZOI locations:

- 0.91 m (3 ft) in front of Cabinets 7 and 8 (locations referred to as Stations 1 and 2, respectively) and approximately 1.98 m (6.5 ft) above the floor;
- 1.5 m (5 ft) above Cabinet 8 (location referred to as Station 3).

The heat flux meters were:

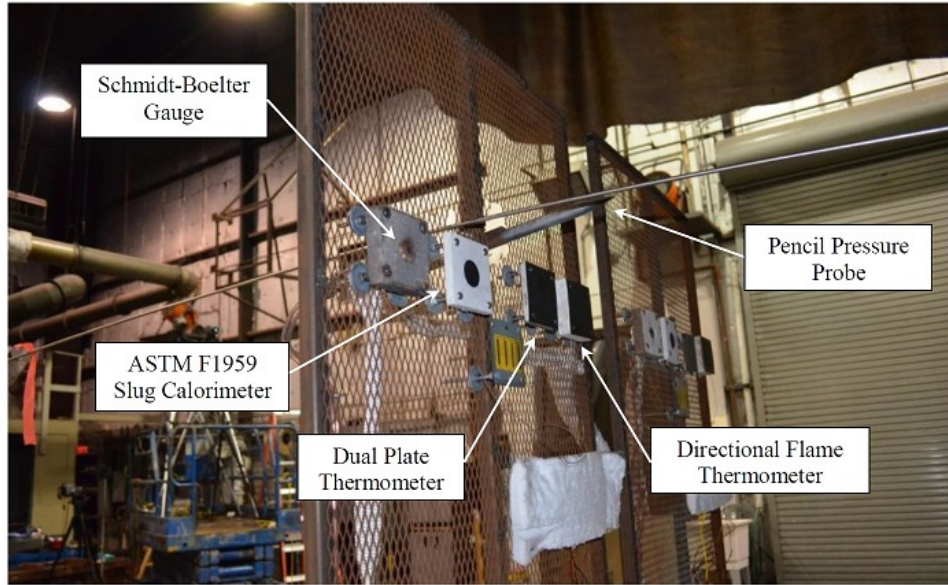
- Schmidt-Boelter (SB) gauge, Medtherm 64-5SB, 50 kW/m² (Station 1 and 2)
- Gardon gauge, Medtherm 64-10, 100 kW/m² (Station 3)
- ASTM F1959 slug calorimeter (like KEMA slug calorimeters)
- Dual Plate Thermometer
- Directional Flame Thermometer

Analyses of the heat flux data indicated that the commercial SB and Gardon gauges had the fastest response times. Consequently, only data from these gauges are presented in this report.

6.5 RFAS Test Temperature Instrumentation

A total of 12, 24-AWG type K thermocouples (TCs) were used to measure the temperatures during each test. Thermocouples 1 through 5 were located on the interior of each cabinet door. The TCs were peened into the door, centered 1.8 m (70 in) from the floor. T6 was centrally located 15.2 cm (6 in) in front of the exterior of the door of Cabinet 8 and TC7 was located 15.2 cm (6 in) in front of the vertical duct near the top. T7 was not attached to the vertical duct to replicate the TC locations for the five cabinet tests performed at KEMA where the TC could not contact the cabinets for safety purposes. T8 to T12 were located in the cable bundle at the top, front portion of each cabinet approximately at the center of the cabinet in order to track the horizontal flame spread along the row of cabinets. The thermocouples were not embedded in the cables.

(a) Station 1 at Cabinet 7 is on the right, Station 2 at Cabinet 8 is on the left



(b) Station 3 at the 1.5 m (5 ft) ZOI above Cabinet 8

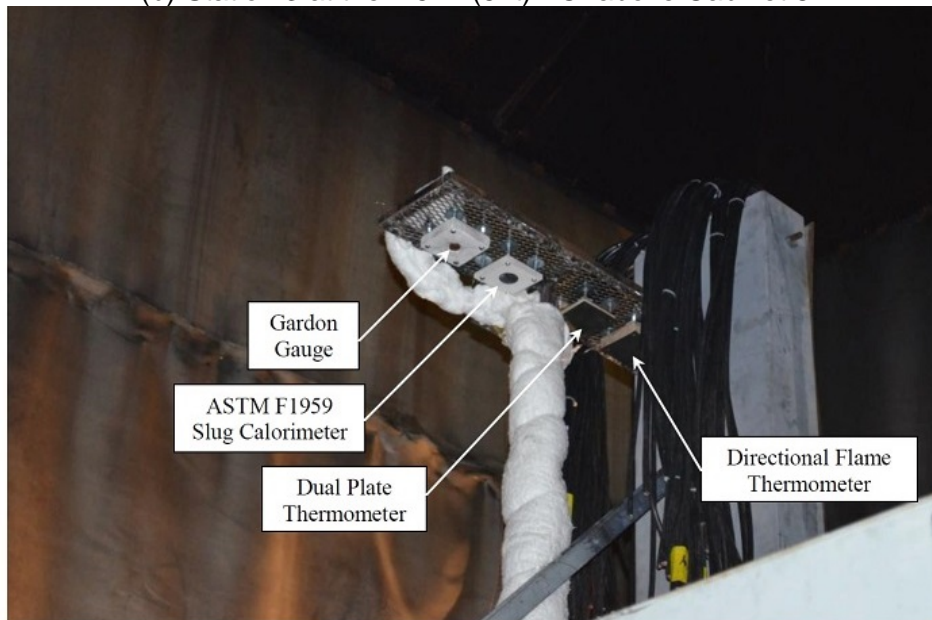


Figure 6.5-1. Heat Flux and Pressure Sensors: Stations 1, 2, and 3

6.6 RFAS Test Pressure Instrumentation

Pressure was measured with a PCB Piezotronic 137B23B “pencil probe”, which is a high speed blast probe with a quartz sensor sampling pressures up to 35 psi (31 kPa) at a rate of 1 kHz. The blast pencil probe was located in front of Cabinet 7 during Test 1 and in front of Cabinet 8 for Test 2 (see Figure 6.5-1, Station 2) because the latter had the larger amount of fuel. There was no useful data from the pencil probe because the pressures were too low and spikes and other transient responses did not make physical sense. No pencil probe data is therefore reported.

A Honeywell Pressure Transducer Model TJE, 50 psi, was used to measure internal cabinet pressure. It was a strain-gauge type pressure transducer, which was connected by 1.83 m (6 ft) of Inconel tube to protect it from heat. There was no useful data from the pressure gauge because the pressures were low and there were apparent temperature effects in the tests. Some data indicate large negative pressures that were not physically possible. No internal pressure data is therefore reported.

6.7 RFAS Test Heat Release Rate and Smoke Production Instrumentation

To measure the HRR during the RFAS event and post-RFAS combustion, the products of combustion and entrained air were collected in a hood and extracted through an exhaust duct by a fan. A gas sample was drawn from the exhaust duct and analyzed for oxygen, carbon dioxide, and carbon monoxide concentrations. The gas temperature and differential pressure across a bi-directional probe were measured for calculating the mass flow rate of the exhaust gases. The HRR measurement generally follows ASTM E2067 [12].

The HRR is usually measured based on oxygen consumption calorimetry. However, the standard method, which relies on the observation for a wide range of fuels that approximately 13.1 MJ of heat is released per kg of oxygen consumed in complete combustion, does not work for the RFAS. This is because rocket fuel combustion is an exothermic reaction that consumes the chemically bound oxygen in the perchlorate molecules (although for the rocket fuel used in the RFAS tests some external oxygen is needed to burn part of the aluminum foil backing and the binder). Therefore, the HRR was calculated two ways, based on oxygen consumption and based on carbon dioxide generation.

The heat of combustion of the rocket fuel as measured in an oxygen bomb calorimeter is 8.72 MJ/kg. Based on the chemical composition of the rocket fuel, 0.24 kg of carbon dioxide is generated per kg of fuel burned. These HRR calculation based on carbon dioxide generation uses these values. That is, 36.3 MJ of heat is released per kg of carbon dioxide generated (8.72 MJ of heat released per kg of fuel consumed divided by 0.24 kg of CO₂ generated per kg of fuel consumed). This measurement assumes that all of the CO₂ evolved from the RFAS, which is reasonable given that there is little or no combustion occurring elsewhere in the test during the RFAS ignition.

The HRR calculation via oxygen consumption is based on the standard method, which assumes that 13.1 MJ ± 5% of heat is released per unit mass of oxygen consumed. As discussed earlier, the standard oxygen consumption technique is not valid for determining the HRR from RFAS combustion and was only used to estimate the post-RFAS HRR from the ensuing cable fire.

The Smoke Production Rate (SPR) is determined by the measured light obscuration in the exhaust duct using a vertically-oriented, white-light extinction photometer located close to the gas sampling port, and the flow rate measured in the exhaust duct.

6.8 RFAS Test Oxygen Measurement

For Test 2, a sampling line was run from the interior of Cabinet 8, through the door, and connected to a paramagnetic oxygen analyzer. This was used to measure the oxygen concentration in the area of the cable bundles throughout the test. The oxygen is a combination of ambient oxygen and any excess oxygen generated as a result of the rocket fuel decomposition.

6.9 RFAS Test 1 Key Observations

The attempt to delay the RFAS2 event during Test 1 was unsuccessful and all four slabs of fuel contained in Cabinets 7 and 8 ignited within 5 seconds. Figure 6.9-1 shows the RFAS event, this test resulted in a total energy release of approximately 140 MJ. A sustained ensuing fire in the cableways was not achieved during Test 1 and the test was terminated at 10 min. Figure 6.9-2 shows the ensuing fire, in which there was only a fire of the bus bar insulation, following the RFAS ignition.

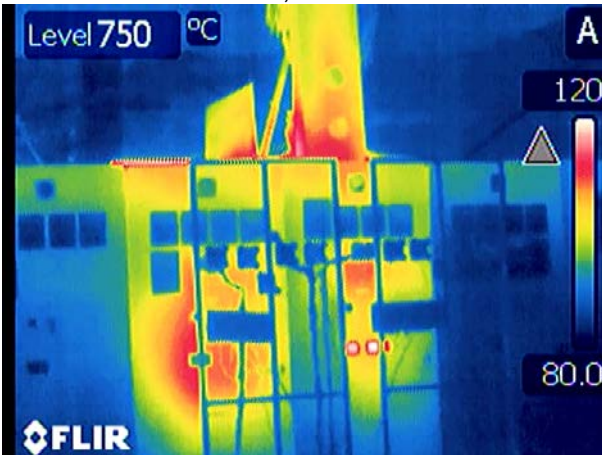


Figure 6.9-1. Test 1: RFAS Event

(a) Small ensuing fire of bus bar insulation



(b) 5 minutes after RFAS1. Note the low maximum temperature- there is residual heat, but no fire



(c) 15 minutes after RFAS1. Note the low maximum temperature- no fire

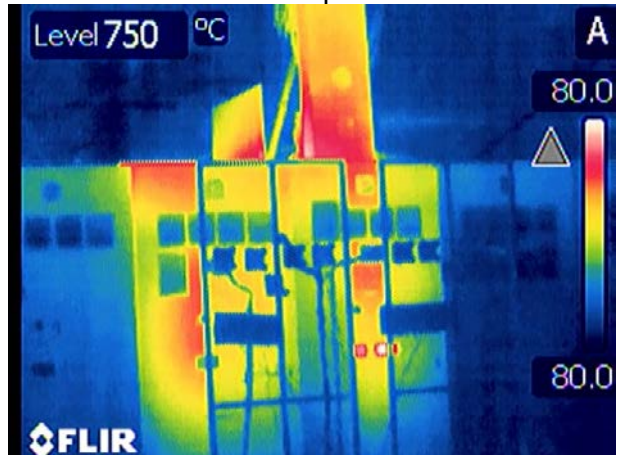


Figure 6.9-2. Test 1 Ensuing Fire

The damage to the exterior of the cabinets was insignificant. Figure 6.9-3 shows the interior damage to each cabinet and Figure 6.9-4 shows the exterior damage.

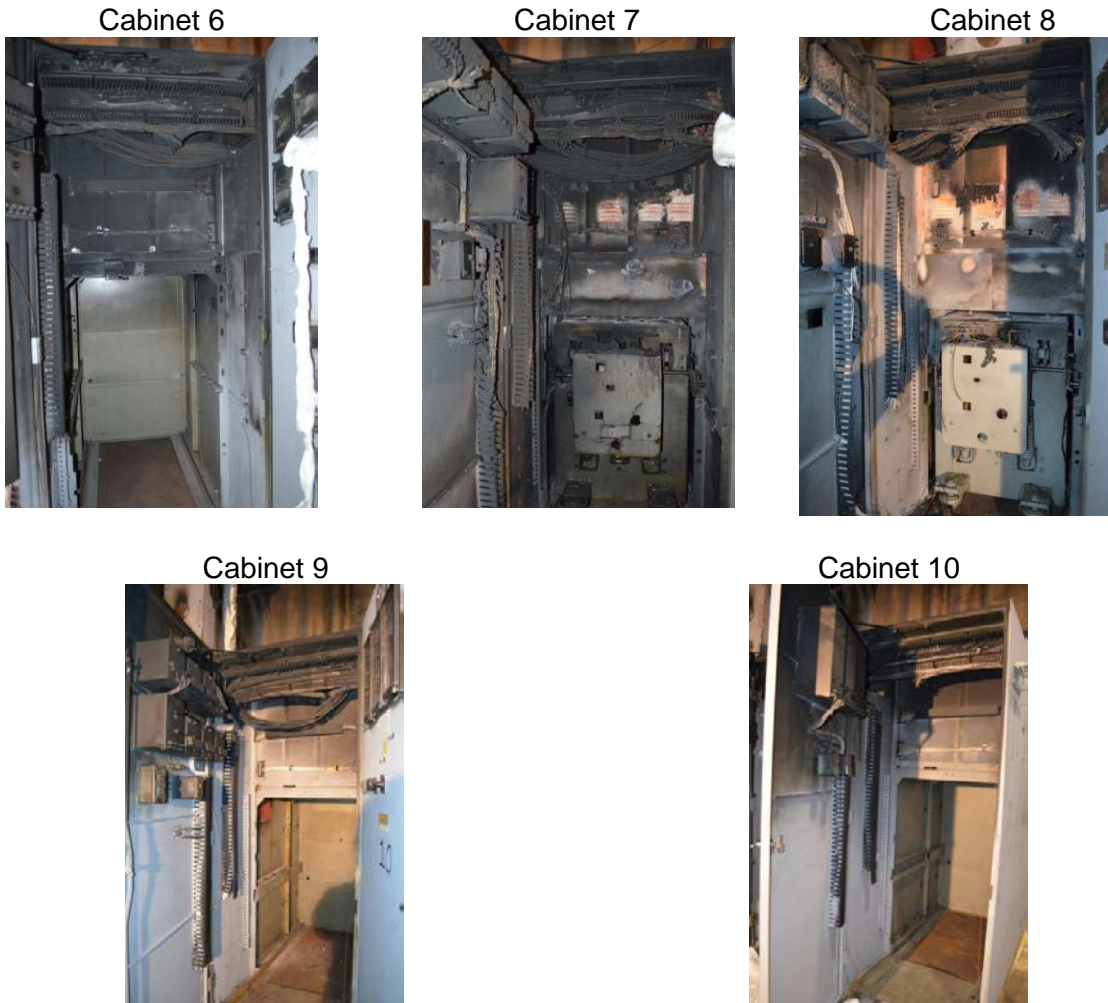


Figure 6.9-3. Test 1 Interior Cabinet Damage



Figure 6.9-4. Test 1 Exterior Cabinet Damage

6.9.1 RFAS Heat Test 1 Flux Data

Figure 6.9-5 shows data from the SB gauge for Stations 1 and 2 and the Gardon gauge for Station 3. The data includes 140 seconds of baseline data at the beginning before the RFAS1 ignition indicated by the spike. The maximum heat flux was at the top of Cabinet 8 where the SB gauge had a view of the flames exiting the top vent spread over the top of the cabinet. The heat fluxes in front of Cabinets 7 and 8 were lower even though the gauges were closer to the cabinet (0.91 m (3 ft) versus 1.5 m (5 ft)) because (1) the heat was transferred through an internal vented wall plus the front door, and (2) these gauges have an oblique view of the flames on top of the cabinet. All heat fluxes were lower than recorded in SWGR Test 2 at KEMA (58 MJ) even though the RFAS released more energy.

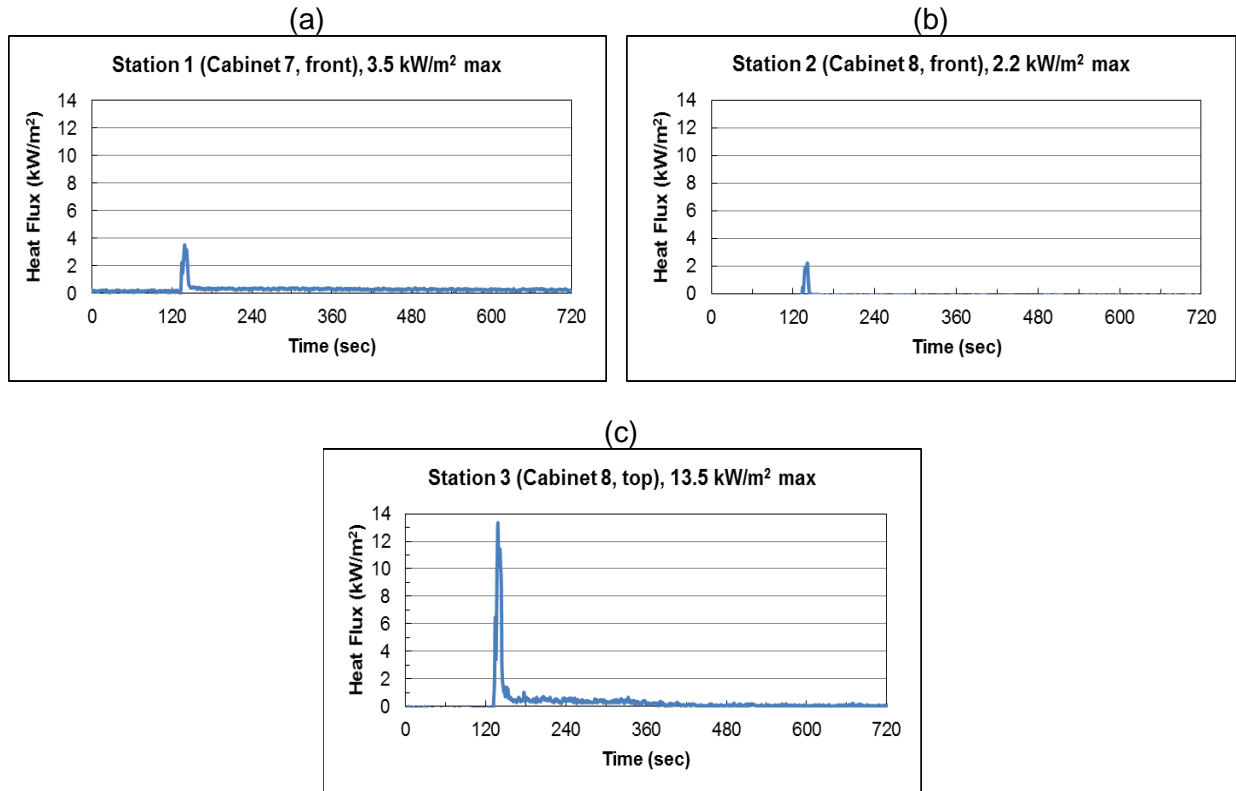


Figure 6.9-5. RFAS Test 1 Heat Flux

6.9.2 Test 1 Temperature Data

Temperature data for Test 1 is shown in Figure 6.9-6. The temperatures quickly peaked at the time of ignition of the RFAS then decreased because there was no major ensuing fire. However, the increasing temperatures on the Cabinet 7 and 8 doors from 3 to 5 minutes indicate some minor combustion. The maximum temperatures were in Cabinet 7 and 8 where the RFAS heat sources were located. The peak external temperature was 98 °C (208 °F) for the Cabinet 7 door and the peak internal cable bundle temperature was 509 °C (948 °F) for Cabinet 7.

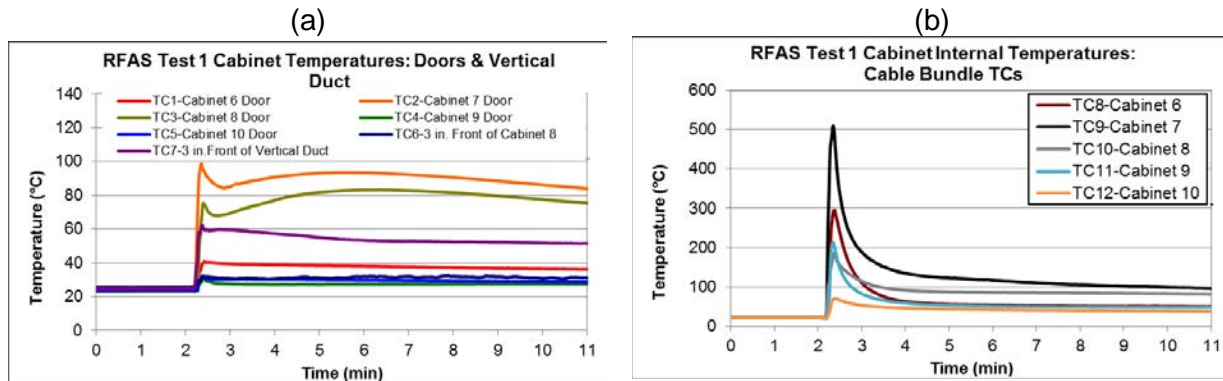


Figure 6.9-6. RFAS Test 1 TC Measurements

6.9.3 RFAS Test 1 Heat Release Rate/Smoke Production Data

During the RFAS ignition, the peak HRR measured in the hood using CO₂ calorimetry was approximately 3.1 MW. The oxygen calorimetry is valid after about 3 minutes and showed very low HRR since there was no ensuing fire. The Total Heat Released (THR) 2 minutes after ignition was 114 MJ, about 82% of the 140 MJ released by the RFAS was actually measured. There were probably some hood losses and the response time of the instrumentation may have been slow to capture the spike of the RFAS HRR.

The peak SPR was about 24.4 m²/sec, which was similar to the Test 2 RFAS SPR discussed in the next section.

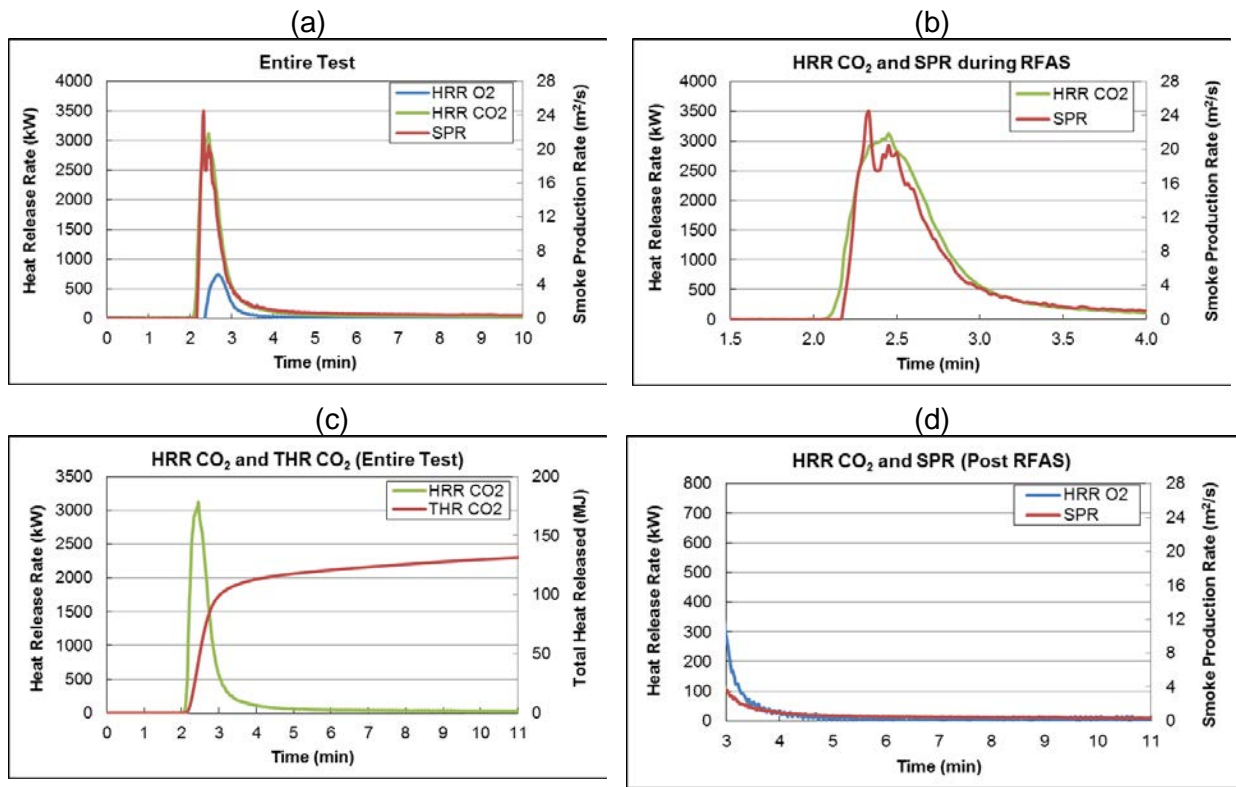


Figure 6.9-7. Test 1 Heat Release Rates and Smoke Production

6.10 RFAS Test 2 Key Observations

The energy released in the first RFAS was 70 MJ, which did not ignite an ensuing fire, but it preheated the cabinets/cables for the next part of the test. The second RFAS released 175 MJ, which resulted in an ensuing fire with an initial intensity and spread similar to that observed in KEMA SWGR Test 2. Figure 6.10-1 shows both RFAS events. The ensuing fire was allowed to burn to completion, which included consumption of the cables inside the vertical duct. The HRR data measured at SwRI is likely representative of the HRR from the fire in KEMA SWGR Test 2.

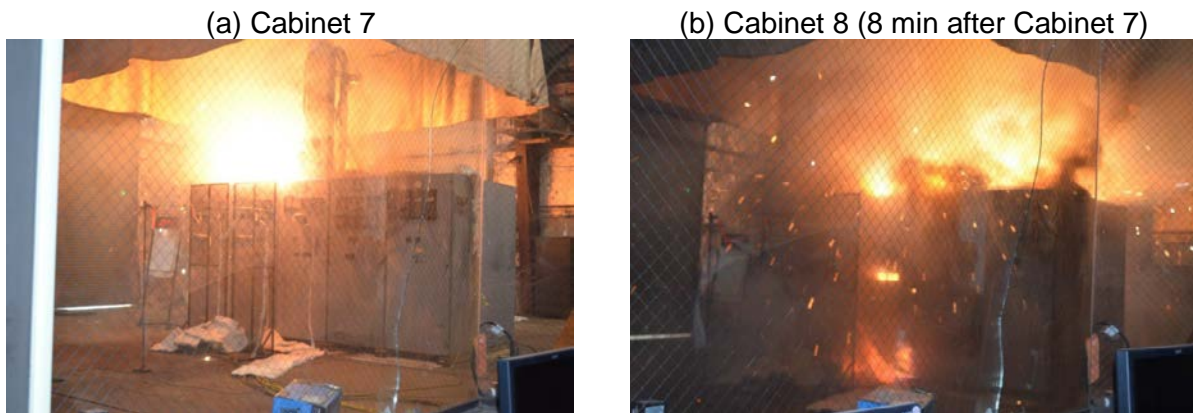


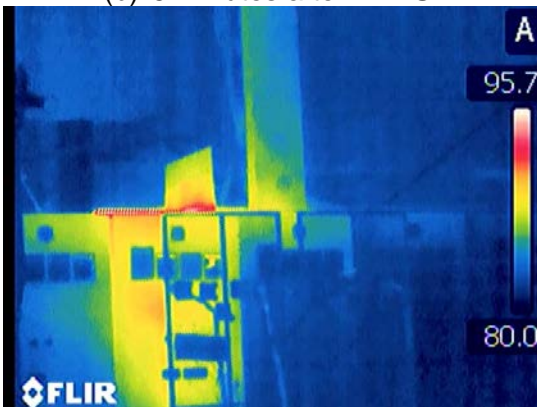
Figure 6.10-1. RFAS Test 2 Events

Figure 6.10-2 shows the ensuing cable fire. A sustained fire of the cables was visible within 1 minute after the second RFAS event, and was allowed to propagate, unimpeded to self-extinguishment. Approximately 8 minutes after the second RFAS event, flames were visible at the top of the vertical duct. The test was continued for 90 minutes, until the burning had slowed to the point that there was virtually no measurable HRR.

(a) 15 minutes after RFAS event



(b) 5 minutes after RFAS1



(c) 15 minutes after RFAS1

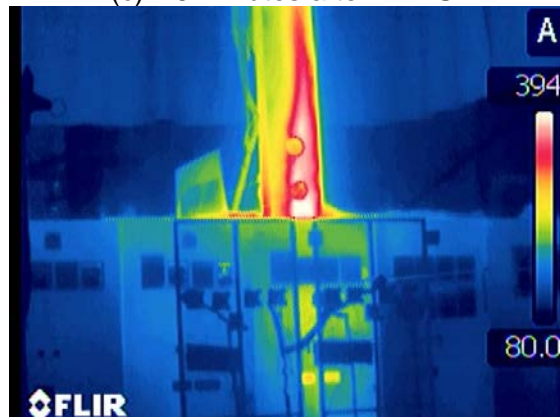


Figure 6.10-2. RFAS Test 2 Ensuing Cable Fire

The RFAS events and ensuing fire resulted in minor internal and exterior damage to the cabinets. The damage to the exterior of the cabinets was greater than in Test 1 due to the long ensuing fire. Figure 6.10-3 shows the internal damage to each cabinet, and Figure 6.10-4 shows the exterior damage. The latter was primarily charring at the top front of the cabinets caused by the internal cable fire, and melting of the instruments on the top front of Cabinet 7. Although the discoloration and charring had a similar pattern to KEMA SWGR Test 2, it was not as severe.



Figure 6.10-3. Test 2 Interior Cabinet Damage



Figure 6.10-4. Test 2 Exterior Cabinets Damage

6.10.1 RFAS Test 2 Flux Data

Data from the SB gauge for Stations 1 and 2 and the Gardon gauge for Station 3 are shown in Figure 6.10-5. The data includes 225 seconds (3 minutes 45 seconds) of baseline data at the beginning before the RFAS1 ignition. The RFAS2 ignition was at 690 seconds (11 minutes 30 seconds).

For the RFAS1, the maximum heat flux was recorded at Station 3 viewing the top of Cabinet 8 as in Test 1. However, the heat flux was lower than in Test 1 (5 versus 14 kW/m²) because the RFAS1 energy in Test 2 was much lower than the combined RFAS1 and RFAS2 energy in Test 1 (70 MJ versus 140 MJ).

Unlike Test 1 and Test 2 RFAS1, the maximum heat flux as a result of Test 2 RFAS2 was not at Station 3 above Cabinet 8; the maximum heat flux was at Station 2 viewing the front of Cabinet 8. Additionally, the heat flux at Station 3 was lower in Test 2 (11 versus 14 kW/m²) even though the RFAS energy was higher (175 versus 140 MJ). This is possibly because in Test 1 both RFAS ignited at the same time and the flame area on the top of the cabinets viewed by the Station 3 heat flux gauge was larger than the flame area in Test 2.

The maximum heat flux of 11.4 kW/m² was measured with an SB at 0.91 m (3 ft) in front of Cabinet 8 (Station 2). The maximum heat flux in Test 1 at the same location was 2.5 kW/m². The increase is consistent with the fact that in Test 1 only 70 MJ was released in Cabinet 8 compared to 175 MJ in Test 2, although the energy ratio (175/70=2.5) is significantly lower than

the heat flux ratio ($11.4/2.5 \approx 4.5$). The discrepancy between the two ratios can be partly explained by the added ceramic fiber insulation which was added between Cabinets 7 and 8 before Test 2, between Cabinets 7 and 8, which may have reduced the heat losses from Cabinet 8 during combustion of RFAS2 in Test 2.

The Test 2 Station 1 results for RFAS1 show a heat flux of 3.5 kW/m^2 that is similar to the 3.3 kW/m^2 in Test 1.

The Test 2 Station 1 results for RFAS2 show a heat flux of 5.6 kW/m^2 that is higher than the 3.3 kW/m^2 in Test 1 by a factor of about 1.7.

The ensuing fire caused a maximum heat flux of about 1.6 kW/m^2 at Station 1 (Cabinet 7) and Station 2 (Cabinet 8) at 1,900 seconds (about 32 minutes). Station 3 at 1.5 m (5 ft) above Cabinet 8 showed negligible heat flux from the ensuing fire.

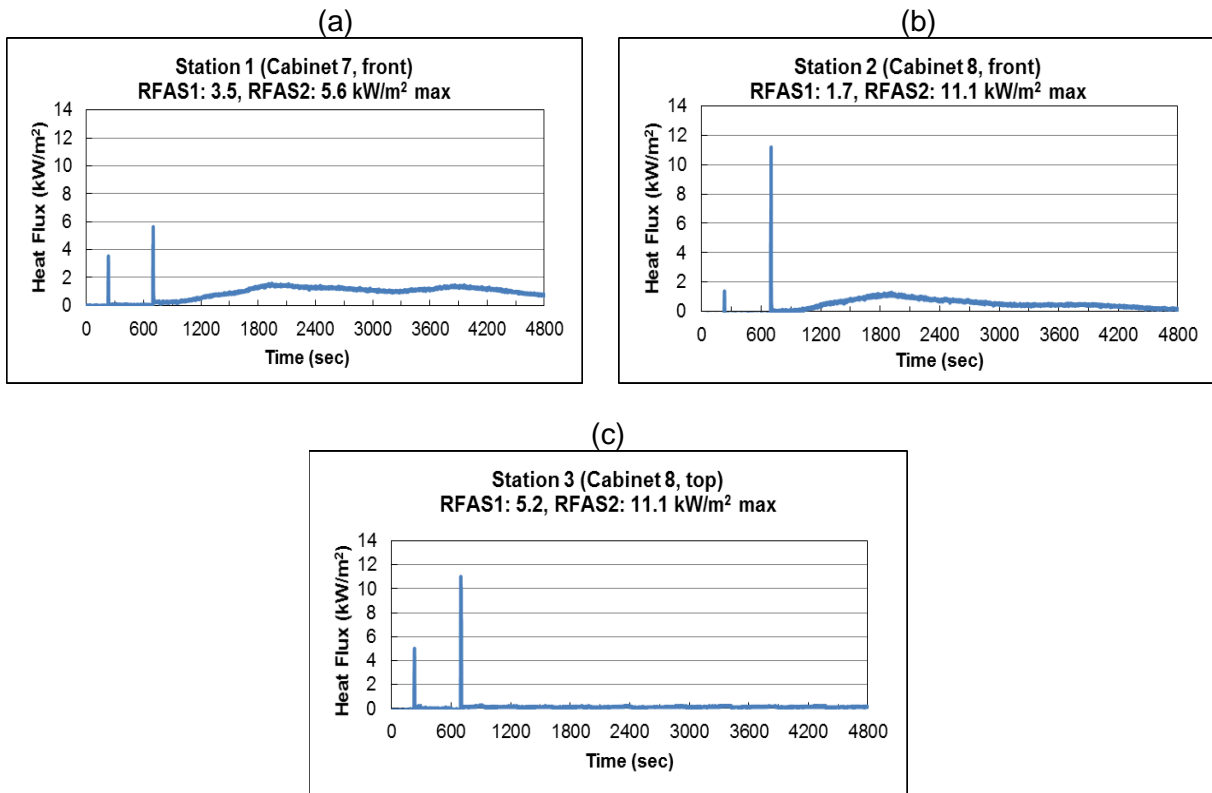


Figure 6.10-5. RFAS Test 2 Heat Flux

6.10.2 RFAS Test 2 Temperature Data

The temperature data for Test 2 are grouped by the time to ignition of the ensuing fire in Figure 6.10-6. In Cabinets 7 and 8 the ensuing fires ignite quickly, and in Cabinets 6, 9, and 10 the ignition is delayed.

The temperatures quickly peaked then recovered at the RFAS1 ignition as in Test 1. However, the peak temperatures were lower than in Test 1 as expected because the RFAS1 energy in Test 2 was lower than the combined RFAS1 and RFAS2 energy in Test 1 by a factor of two. The peak external temperature was 63°C (145 °F) (versus 98°C (208 °F) for Test 1) and the peak internal cable bundle temperature was 371 °C (700 °F) (versus 509°C (948 °F) for Test 1).

In this test, the 70 MJ released from RFAS1 was not adequate to cause an ensuing cable fire in Cabinet 7 or 8. This is inconsistent with the KEMA test results which showed that 50 to 60 MJ of electrical input is adequate ignition energy for an ensuing cable fire. The electrical energy was supplemented by the energy associated with aluminum bus bar oxidation within the cabinet in the KEMA SWGR tests. It is postulated that this additional oxidation energy provided the necessary energy to ignite an ensuing cable fire. This is additional evidence that the aluminum bus bar oxidation in addition to the electrical energy (50 to 60 MJ) in the KEMA tests led to ensuing cable fire ignitions.

The temperatures quickly peaked then decreased after the RFAS2 ignition. The peak external temperatures were higher than in Test 1, as expected, because the cabinets and cables were preheated and the RFAS2 energy in Test 2 was higher than the combined RFAS1 and RFAS2 energy by a factor of 1.75. The peak external temperature was 439 °C (822 °F) (versus 98 °C (208 °F) for Test 1) and the peak internal cable bundle temperature was 812 °C (1494 °F) (versus 509 °C (948 °F) for Test 1).

Cabinets 7 and 8 showed a decrease of the initial high temperature for a few minutes after RFAS2 (about 5 minutes in Cabinet 7 and 6 minutes in Cabinet 8). The ensuing internal cable fire then caused a rapid temperature increase with a peak of about 780 °C (1436 °F). The cabinet exterior temperatures increases lagged in time and reached a maximum temperature of about 680 °C (1256 °F). These temperature behaviors were as expected.

Based on the cable temperatures, a stable cable fire in Cabinet 7 began at minute 17 and steadily persisted for an additional 45 minutes with a slight increase at the end, which is not completely understood but could be attributed to the burning of the instruments mounted in the front door near the cables. The ensuing fire in Cabinet 8 appears to decay between minute 19 and minute 32, and temporarily becomes more intense between minute 32 and minute 40.

As expected for an ensuing cable fire, the cable fires in Cabinets 6 and 9 lagged in time behind the fires in Cabinet 7 and 8. The Cabinet 6 ensuing fire lagged the Cabinet 7 fire by about 6 minutes, resulted in temperatures exceeding 600 °C (1112 °F) from minute 24 to minute 41, and remained relatively steady with temperatures between 400°C (752 °F) and 500°C (752 to 932 °F) from minute 41 to minute 71. The cause for the abrupt change is not known.

The Cabinet 9 ensuing fire lagged the Cabinet 7 internal fire by about 18 minutes during which time, the cable was pre-heated from a temperature of about 70 °C to 140 °C (158 to 284 °F) at minute 32. The Cabinet 9 cables then fluctuated between 215 °C and 465 °C (419 to 869 °F) from minute 32 to minute 65 in a slow burn based on the low temperature.

The Cabinet 10 cable bundle temperature slowly increased to about 143 °C (289 °F) but did not burn as confirmed by post-test observation.

The external vertical duct temperature (TC7) increased similarly to the Cabinet 7 and 8 doors reaching a maximum of 485 °C (905 °F). The TC at this location was not attached to the duct; the temperature was lower than the attached door TCs. The high temperature of TC7 persisted longer than the Cabinet 7 and 8 door temperatures because the cable fire in the vertical duct was the main fire still burning for the last 30 minutes of the test. The unsteady behavior of TC7 at minute 60 was from the cable fire existing the duct and burning down the 0.91 m (3 ft) extra cable dangling outside the duct.

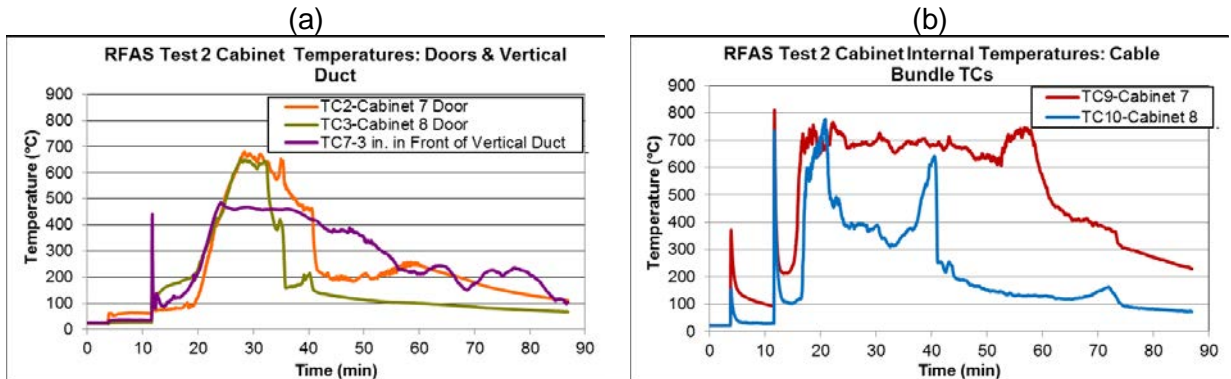


Figure 6.10-6. RFAS Test 1 TC Measurements, Cable Bundles for Cabinets 7 and 8

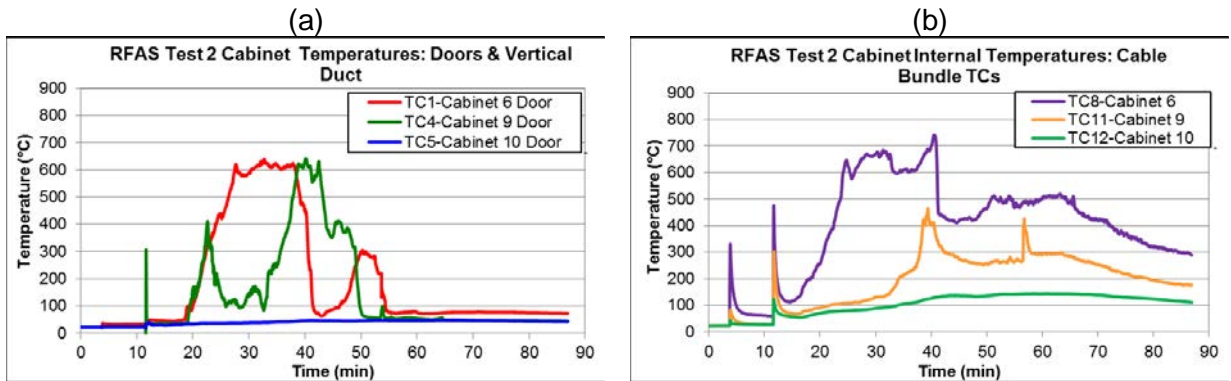


Figure 6.10-7. RFAS Test 1 TC Measurements, Cable Bundles for Cabinets 6, 9 and 10

6.10.3 RFAS Test 2 Heat Release Rate/Smoke Production Rate Data

During the RFAS ignitions, the peak HRRs measured in the hood using CO₂ calorimetry were about 1,634 kW for RFAS1 and 3,512 kW for RFAS2. The HRR quickly decreased to less than one tenth of the peak at about 1.5 minutes after the RFAS ignitions. The measured HRR correlates with the RFAS energy in Test 1:

- RFAS1: HRR was a factor of 0.53 lower than Test 1 (1.63 MW versus 3.12 MW) where the RFAS energy was a factor of 0.50 lower (70 MJ vs. 140 MJ).
- RFAS2: HRR was a factor of 1.12 higher than Test 1 (3.51 MW versus 3.12 MW) where the RFAS energy was a factor of 1.24 higher (175 MJ vs. 140 MJ).

Based on the O₂ calorimetry response, the ensuing fire HRR time evolution was similar to that of the cable bundle temperatures shown previously. The HRR was low (150 to 180 kW) immediately after RFAS2 (this was likely only the bus bar insulation burning plus residual combustion products) and remained low until the steady cable burning HRR reached a peak of 432 kW at 21 minutes. The HRR then steadily decreased as the combustibles were consumed.

The SPR peaks were about 7 m²/sec from RFAS1 and 24.5 m²/sec from RFAS2. The RFAS2 peak SPR was about the same as the Test 1 RFAS SPR even though the energy was 1.24 times higher. Immediately after the RFAS2 the SPR decreased to about 6 m²/sec, and subsequently then increased to 10 to 14 m²/sec from minute 15 to 19. The increase was likely caused by smoldering combustion before the cable fire was established. The Cabinet 7 cabinet fire was established at minute 18 and the SPR decreased to 5 m²/sec. During the steady cable fires after 21 minutes, the SPR correlated to the HRR time evolution, as expected.

The THR 2 minutes after ignition was 57 MJ for RFAS 1 indicating that about 81% of the 70 MJ from the RFAS1 ignition was measured. The THR for RFAS2 increased from 62 MJ to 205 MJ (2 minutes after ignition) for a net increase of 143 MJ from RFAS2 indicating that the hood measured about 81 percent of the 175 MJ from the RFAS2 ignition. As in Test 1, hood losses and slow instrumentation response times probably caused the low measurements versus the RFAS energy. The hood calorimetry losses were surprisingly similar for all RFAS ignitions (Test 1 was 82 percent).

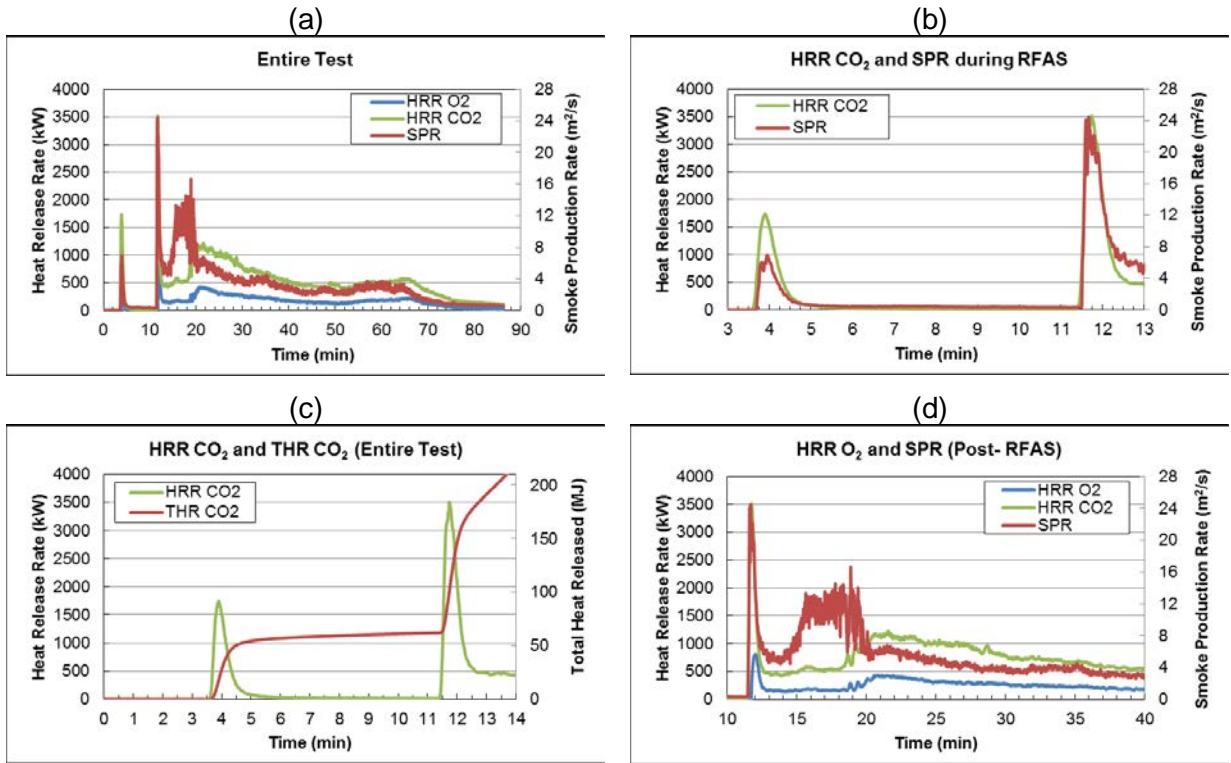


Figure 6.10-8. Test 1 Heat Release Rates and Smoke Production

6.10.4 RFAS Test 2 Oxygen Data

As shown in Figure 6.10-9, there are two spikes of reduced oxygen at the time of the RFAS ignitions that quickly recover. During the ensuing fire, oxygen decreased to 20 percent at about 16 minutes, which indicates the fire was well-ventilated.

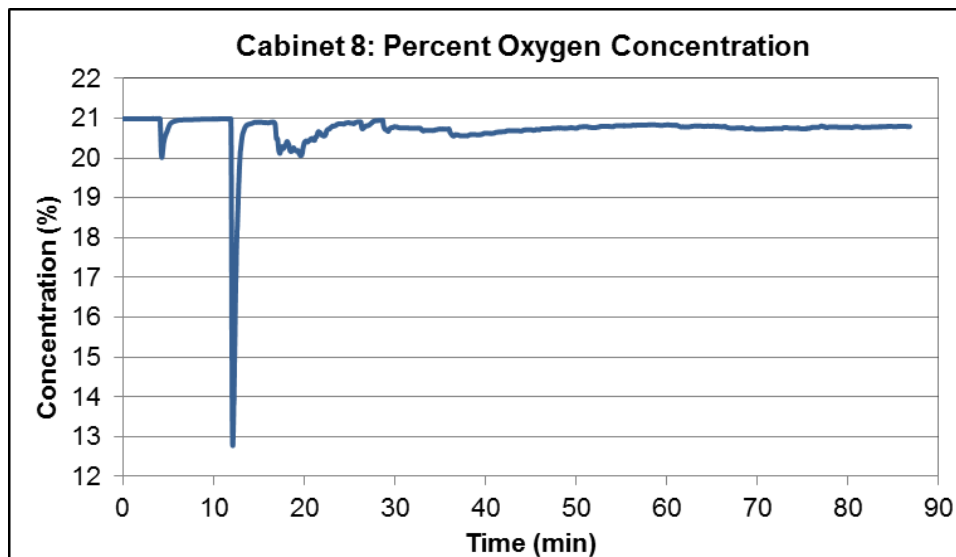


Figure 6.10-9. RFAS Test 2 Oxygen Concentration in Cabinet 8

6.10.5 RFAS Summary

As discussed in Section 6.1, RFAS tests required three to four times more heat energy than the electrical energy in the KEMA electrical arc tests to cause an ensuing fire in similar SWGR configurations. One hypothesis to explain the additional energy required for ignition is that the RFAS oxidation was lowering the oxygen levels in the cabinets, causing under-ventilated combustion conditions. However, the oxygen measurements in Figure 6.10-9 indicate that the oxygen recovered quickly so there was adequate oxygen for combustion. The reason for the higher energy, as discussed in the next chapter was the aluminum bus bar oxidation increased the energy in the KEMA tests.

7 Switchgear Tests Results Discussion

7.1 Onagawa Comparison

7.1.1 Exterior Damage

The results of the KEMA tests are compared with the 2011 Onagawa event conditions in Figure 7.1-1. The Onagawa external charring damage had a V-shape with Cabinet 7 showing the most damage based on the burned paint on the outside of the doors. As shown in the KEMA post-test photos, some paint burning and charring was observed in the KEMA 5-cabinet SWGR Test 2. But the damage and charring was not as severe as Onagawa. The burning and charring was more severe in the KEMA 5-cabinet SWGR Test 4, where there was large aluminum oxidation and large ensuing fire but the damage was still not as severe as Onagawa.

7.1.2 Horizontal Bus Bar Arc

SWGR Test 4, Arc 2 had horizontal bus bar arcing in Cabinet 7 that was like the second arc in the assumed Onagawa event scenario. The initial Arc 2 arc in Cabinet 8 drew high current that caused the horizontal bus bars in Cabinet 7 to bend and touch and the arc in Cabinet 7 became the main arc location at that time. Therefore Arc 8 was very short duration and low energy because the electrical current stopped at the Cabinet 7 arc. The energy and ensuing fire was very large and the damage on the front of Cabinet 7 was similar to Onagawa, as discussed in Section 7.2. This test shows that the aluminum bus bar oxidation was probably a main contributor of such a large fire event at Onagawa.

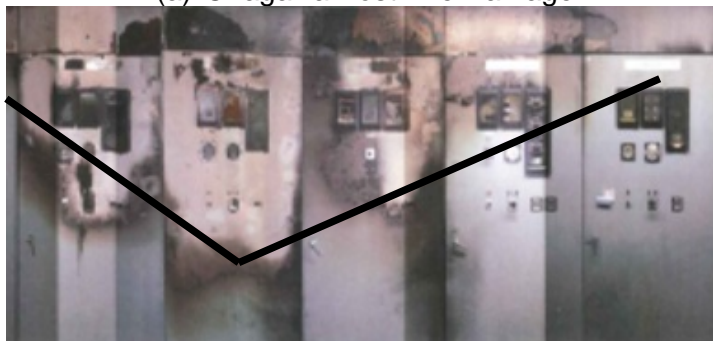
7.1.3 Secondary Side Arc and Damage

In SWGR Test 5, Arc 2, there was a strong arc in the secondary (rear) of Cabinet 8, as planned. However, the damage to the circuit breaker and rear of the cabinet was not as severe as at Onagawa. Perhaps the arc needed to be inside the insulator and travel down into the breaker to cause the severe damage seen at Onagawa. In SWGR Test 5, Arc 2, the hot gas and plasma went up through the roof and out the vent rather than down toward the breaker.

In SWGR Test 6, Arc 2 in the rear of Cabinet 8 traveled along the bus bar, similar to the suspected travel of the second arc at Onagawa. However, the damage in the rear of the cabinet was still much less than observed at Onagawa. In the Onagawa event, the cables were completely burned and the rear part of the breaker was completely destroyed.

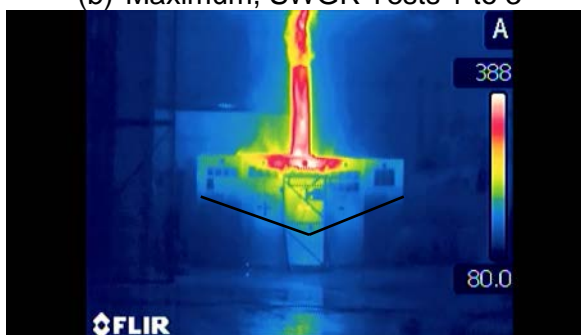
The overall observations are (1) some of the severe conditions at Onagawa like the bus bar oxidation were seen, and (2) the additional energy of aluminum oxidation led to the severe conditions and ensuing fires.

(a) Onagawa Post Fire Damage

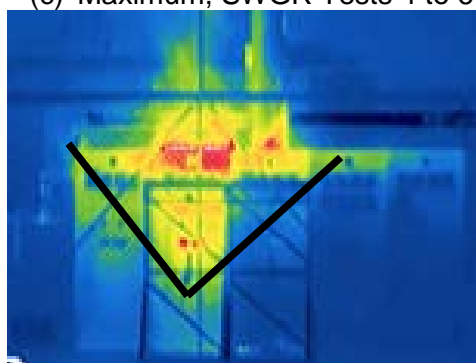


Note: This photo shows the test configuration with Cabinet 6 on the left, the Onagawa configuration is Cabinet 6 on the right.

(b) Maximum, SWGR Tests 1 to 3



(c) Maximum, SWGR Tests 4 to 6



(d) Post-Test Charring

SWGR Test 2



SWGR Test 4



Figure 7.1-1. SWGR Test Comparisons to Onagawa Damage

7.2 Aluminum Bus Bar Oxidation

This section discusses the high energy of oxidation (burning) of the aluminum bus bars at Onagawa and in the SWGR tests. The high energy of aluminum bus bar oxidation is a recognized phenomenon and should be considered in HEAF analyses [9]. The energy is from the aluminum that burns in the arc that forms aluminum oxide (Al_2O_3); the main reaction that occurs is $2\text{Al}(\text{s}) + 3/2\text{O}_2(\text{g}) \rightarrow \text{Al}_2\text{O}_3(\text{s})$. The heat of formation (ΔH_f) for Al_2O_3 is used to determine the amount of energy that is released during this reaction. Using the Born-Haber cycle for the heat of formation of Al_2O_3 , ΔH_f is calculated to be $-1669.79 \text{ kJ/mol (g)}$ (16.37 kJ/g). The oxidation of 1 gram of Al yields 1.89 grams of Al_2O_3 (based on the ratio of molecular weights of Al to Al_2O_3 , 54/102). Thus, 30.9 kJ is released for 1.89 grams of Al_2O_3 , which can also be expressed as 30.9 kJ/g of aluminum burned.

The bus bar oxidation energy during an arc is based on the amount of bus bar destroyed and an energy release of 30.9 kJ/g. Direct measurements of bus bar mass before and after the tests were not recorded; photographic analysis was conducted to determine the length of bus bar that remained after the tests and the associated mass that was lost. The mass loss of the bus bars is therefore an estimate. This is a conservative, bounding analysis because it assumes that all the melted aluminum is converted to Al_2O_3 . Some aluminum may have been ejected as melted aluminum so the actual energy may be lower than reported. Also, in typical situations, aluminum oxidization is limited by condensation of the Al_2O_3 and coating of the aluminum at the reaction point [13] but in the case of the high energy arc, the aluminum and Al_2O_3 are effectively flash melted and vaporized and the coating is probably negligible. That being said, even if only 50% of the aluminum is converted to Al_2O_3 , the Onagawa event would still have had as more than 300 MJ of heat generated from aluminum oxidation based on the results in this section.

Results from Onagawa and the SWGR tests are in the following sections.

7.2.1 Case 1: Onagawa Bus Bar Oxidation in Cabinet 7

The aluminum burned for the three (3) horizontal bus bars in Cabinet 7 is shown in Figure 7.2-1. In this case, the aluminum oxidation is estimated as:

- Bus Bar T: 0 % burned;
- Bus Bar S: 65% burned - a little was left on both sides,
- Bus Bar R: 86% burned, and
- The estimated total horizontal bus bar mass burned was 9.2 kg with a net energy of 284 MJ.

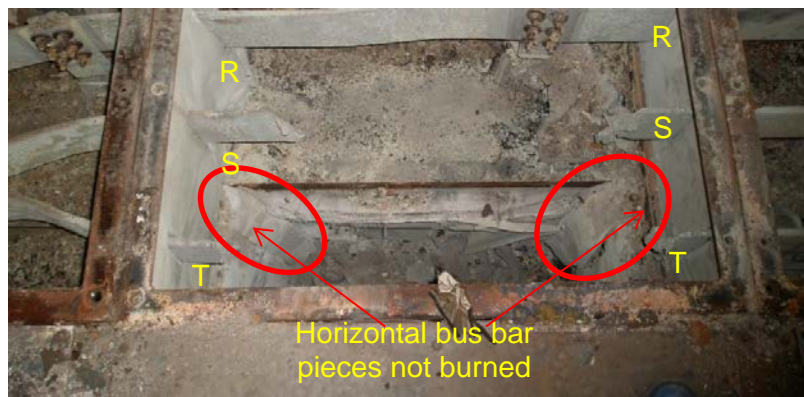


Figure 7.2-1. Onagawa Cabinet 7 Bus Bar Damage

- The vertical bus bars on the primary side of Cabinets 7 and 8 were partially destroyed. Only a small part of the vertical bus bar in Cabinet 8 remained.
 - The estimated total vertical mass burned was 10.8 kg with a net energy of 333 MJ.
 - The total energy from all aluminum bus bars burned at Onagawa was 618 MJ.

7.2.2 Case 2: KEMA 5-Cabinet Lineup June 2013 Test 3

The burned aluminum bus bars are shown in Figure 7.2-2. The estimated total mass burned was 1 kg with an energy of 31 MJ.

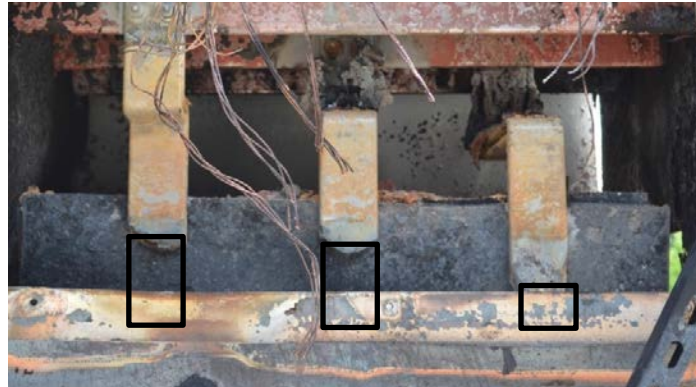


Figure 7.2-2. SWGR Test 3 Bus Bar Damage

7.2.3 Case 3: KEMA 5-Cabinet Lineup March 2014 Test 4

7.2.3.1 Test 4, Arc 1

The burned vertical aluminum bus bars are shown in Figure 7.2-3.

- Arc 1 destroyed the vertical bus bars in Cabinet 7.
- The estimated total mass burned was 5.4 kg with an energy of 167 MJ.

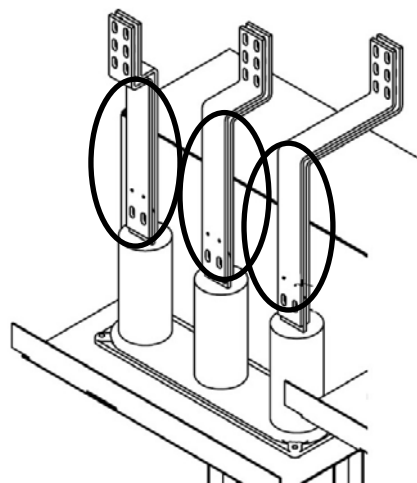


Figure 7.2-3. SWGR Test 4 Arc 1, Cabinet 7 Bus Bar Damage

7.2.3.2 Test 4, Arc 2

The burned horizontal aluminum bus bars in Cabinet 7 are shown in Figure 7.2-4.

- Arc 2 which was initiated about 3.6 minutes after Arc 1, destroyed the front horizontal bus bar in Cabinet 7.
- The estimated total mass burned was 3.7 kg with an energy of 114 MJ.



Figure 7.2-4. SWGR Test 4 Arc 2, Cabinet 7 Bus Bar Damage

7.2.4 Case 4: KEMA 5-Babinet Lineup March 2014 Test 5

7.2.4.1 Test 5, Arc 1

The burned vertical aluminum bus bars are shown Figure 7.2-5.

- Arc 1 destroyed part of the vertical bus bars in Cabinet 7.
- Much less damage than Test 4, Arc 1 so the energy is lower.
- The estimated total mass burned was 1.6 kg with an energy of 49 MJ.

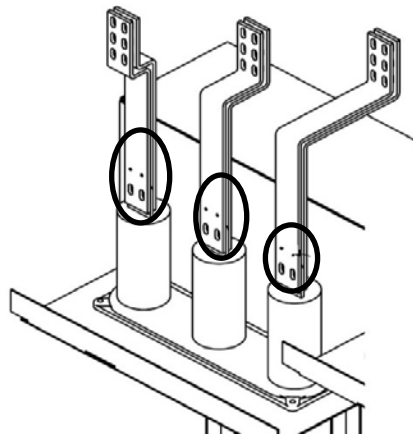
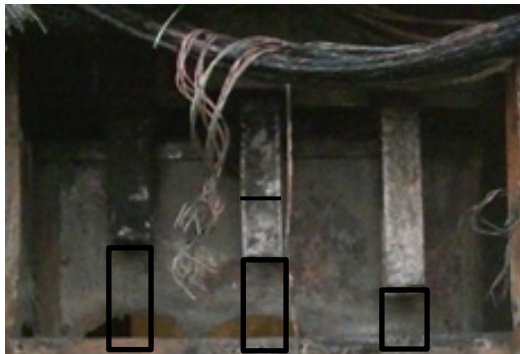


Figure 7.2-5. SWGR Test 5 Arc 1, Cabinet 7 Bus Bar Damage

7.2.4.2 Test 5, Arc 2

The burned vertical aluminum bus bars in the rear of Cabinet 8 are shown in Figure 7.2-6.

- Arc 2 occurred about 2.9 minutes after Arc 1 and destroyed part of the vertical bus bars in Cabinet 8 rear. About 8 cm of each bus bar was lost.
- The estimated total mass burned was 0.5 kg with an energy of 15 MJ.



Figure 7.2-6. SWGR Test 5 Arc 2, Cabinet 8 Rear Bus Bar Damage

7.2.5 Case 5: KEMA 3-Cabinet Lineup March 2015, Test 6

7.2.5.1 Test 6, Arc 1

The burned vertical aluminum bus bars are shown in Figure 7.2-7.

- Arc 1 destroyed part of the vertical bus bars in Cabinet 7.
- The damage was much less than other tests because the arc energy was lower.
- Two bus bars did not burn through; the right bus bar burned through then the connector on top of the insulator fell down.
- The estimated total mass burned was 0.3 kg with an energy of 9 MJ.

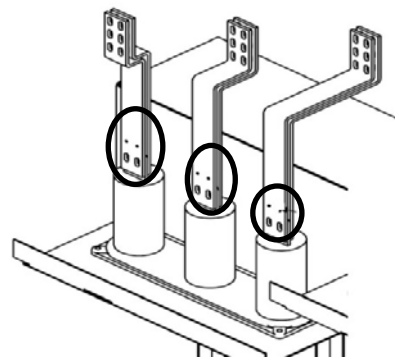


Figure 7.2-7. SWGR Test 6 Arc 1, Cabinet 7 Bus Bar Damage

7.2.5.2 Test 6, Arc 2

The aluminum bus bars in the rear of Cabinet 8 are shown in Figure 7.2-8.

- Arc 2 was about 4 minutes after Arc 1 and the arc was between the top of the bus bar and the roof. About 7 cm at the top of each bus bar was lost. There were two holes in the lost bus bar that reduced the mass lost
- The estimated total mass burned was 0.3 kg with an energy of 9 MJ.

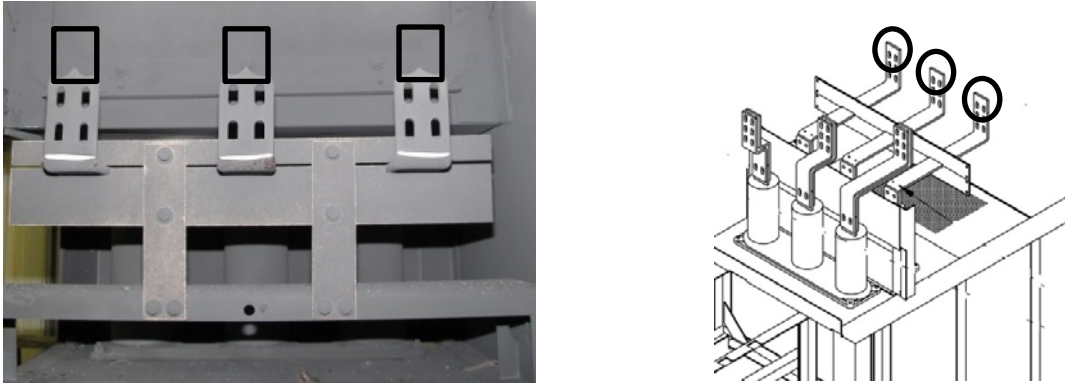


Figure 7.2-8. SWGR Test 6 Arc 2, Cabinet 8 Bus Bar Damage

7.2.6 Aluminum Oxidation Effects Summary

Table 7-1 compares the explosions in the bus bars in the front of the cabinets for various tests. The higher energy explosions have larger fire balls, as expected. Arcs in the horizontal bars located near the top vent have the largest external fireballs.

The aluminum oxidation of vertical and horizontal bus bars at Onagawa resulted in 618 MJ, which was much greater than the 281 MJ resulting from the highest energy KEMA test (167 MJ + 114 MJ in March 2014, Test 4). This is an additional 337 MJ of energy from aluminum oxidation in the Onagawa incident.

The much higher energy for Onagawa could be the reason that the char on the front of the cabinets in the KEMA test is less than Onagawa. The KEMA March 2014 Test 1 total energy including the electrical energy was about 424 MJ (281 MJ + 64.6 MJ + 78.4 MJ). Onagawa was about 658 MJ assuming a minimum of 40 MJ Q_{arc} (the electrical energy at Onagawa is not known) plus 618 MJ for aluminum oxidation. The total energy difference is about 234 MJ and the lower energy resulted in less damage in the KEMA tests as shown, in Figure 7.2-9. If the Onagawa electrical energy was greater than 40 MJ (and it probably was), the difference would be higher.

The higher heat fluxes in the tests with aluminum oxidation indicate that the aluminum oxidation is very important in HEAF events. The large arc explosion and rapid fire in March 2014 Test 4 Arc 1 showed this and the very large arc explosion in March 2014 Test 4 Arc 2 (when the horizontal bus bar burned) are strong proof of the high energy of aluminum oxidation in actual HEAFs.

The energy from the aluminum oxidation was probably the main reason that the SwRI tests using RFAS require more RFAS energy (140 MJ) than the electrical energy at KEMA (nominal 60 MJ) to ignite an ensuing fire. There was no aluminum bus bar oxidation in the SwRI tests.

KEMA March 2014 Test 4



Additional
234 MJ of
Energy










Onagawa



Figure 7.2-9. SWGR Test and Onagawa Front Panel Damage

Table 7.2-1 shows the energies and the fire ball at the time of the arc. Test 4 the arc wire was in the rear but the horizontal bus bars in the front of cabinet 7 arced. The March 2015 tests had much lower total energy and there were no ensuing cable fires.

Table 7-1. Comparison of Arcs in Front Bus Bars of Cabinets.

Tests/Arc	June 2013 Test 3 Vert. Bus Bars	March 2014 Test 4 Arc 1 Vert. Bus Bars	March 2014 Test 4 Arc 2 Hor. Bus Bars	March 2014 Test 5 Arc 1 Vert. Bus Bars	March 2014 Test 5 Arc 2 Rear Bus Bars	March 2015 Test 6 Arc 1 Vert. Bus Bars	March 2015 Test 6 Arc 2 Rear Bus Bars
Electrical Energy (MJ)	64	65	78	57	62	27	21
Aluminum Oxidation (MJ)	31	167	114	49	15	9	9
Total Energy (MJ)	95	232	192	106	77	36	30
Photo							

8 REFERENCES

1. "The Situation of Onagawa Following the Tohoku Region Pacific Ocean Earthquake and Tsunami", Tohoku Electric Power Co., Ltd, May 2011. Japanese only, available at <https://www.nsr.go.jp/archive/nisa/earthquake/files/houkoku230530-2.pdf> (as of 2015-08-19).
2. NUREG/CR-6850 and EPRI 1011989, "EPRI/NRC-RES Fire PRA Methodology for Nuclear Power Facilities," Volume 1: Summary and Overview and Volume 2: Detailed Methodology." Electric Power Research Institute, Palo Alto, CA and U.S. Nuclear Regulatory Commission, Office of Nuclear Regulatory Research (RES) Rockville, MD, September 2005.
3. IEEE C.37.20.7, "IEEE Guide for Testing Metal-Enclosed Switchgear Rated Up to 38 kV for Internal Arcing Faults," 2007 Edition, Institute of Electrical and Electronics Engineers, New York, New York.
4. IEEE 1584, "IEEE Guide for Performing Arc-Flash Hazard Calculations", 2002 Edition, Institute of Electrical and Electronics Engineers, New York, New York.
5. "OECD Fire Project – Topical Report No. 1, Analysis of High Energy Arcing Fault (HEAF) Fire Events", NEA/CSNI/R(2013)6, Organization for Economic Cooperation and Development, June 2013.
6. Lopez, C., Wentz, W.B., Figueroa, V.G., "Evaluation of Select Heat and Pressure Measurement Gauges for Potential Use in the NRC/OECD High Energy Arc Fault (HEAF) Test Program", Sandia National Laboratories, Albuquerque, New Mexico, January 2014.
7. Putorti, A., Melly, N.B., Bareham, S., Praydis Jr, J., "Characterizing the Thermal Effects of High Energy Arc Faults." 23rd International Conference on Structural Mechanics in Reactor Technology (SMiRT 23) – 14th International Post-Conference Seminar on Fire Safety In Nuclear Power Plants and Installations, September, 2015.
8. ASTM F1959, "Standard Test Method for Determining the Arc Rating of Materials for Clothing", 2012 Edition, ASTM International, West Conshohocken, Pennsylvania.
9. ISO 1716, "Reaction to Fire Tests for Products - Determination of the Gross Heat of Combustion (Calorific Value)," 2010 Edition, International Organization for Standardization, Geneva Switzerland.
10. Iwata, M., Anantavanich, K., Pietsch, G.J., "Influence of Current and Electrode Material on Fraction of Electric Arc Energy Leading to Pressure Rise in a Closed Container During Internal Arcing." IEEE Transactions on Power Delivery, Vol. 25, No. 3, July 2010.
11. Ingason, H., Wickstrom, U., "Measuring Incident Radiant Heat Flux Using the Plate Thermometer." Fire Safety Journal, Volume 42, p 161-166, 2007.
12. ASTM E2067, "Standard Practice for Full-Scale Oxygen Consumption Calorimetry Fire Tests", 2008 Edition, ASTM International, West Conshohocken, Pennsylvania.
13. Beckstead, M. W., "A Summary of Aluminum Combustion," in Internal Aerodynamics in Solid Rocket Propulsion. 2004 (Chapter 5). RTO-EN-023.

APPENDIX A. MEASUREMENTS

A.1 Thermocouples and Slug Calorimeter Measurements

Type K thermocouples (TC) were used to measure the temperatures during each test prior to 2015. For safety reasons from possible electrical shorting, the TCs are not in contact with the metal cabinet. The TCs are measuring the air temperature since they are located about 15.2 cm (6 in) from the front of the cabinet, in air. The TCs also detect radiation heat transfer from the cabinet. The temperatures are probably much lower than the actual metal temperature. Therefore, the temperatures are just a qualitative measure of thermal and fire behavior. TCs located in the air were not used in the 2015 tests.

Heat flux is measured using slug calorimeters (slugs) built to ASTM F1959 [8]. ASTM F1959 is used to test protective clothing materials where the arc energy is measured by slug calorimeters that are directly exposed to the arc. The slug calorimeters are placed on metal mesh instrument stands and are placed at the 0.91 m (3 ft) ZOI from NUREG/CR 6850 to measure the heat flux, as seen Figure A.1-1. ASTM F1959 has the procedure to convert the temperature of the slug measurement to a heat flux.

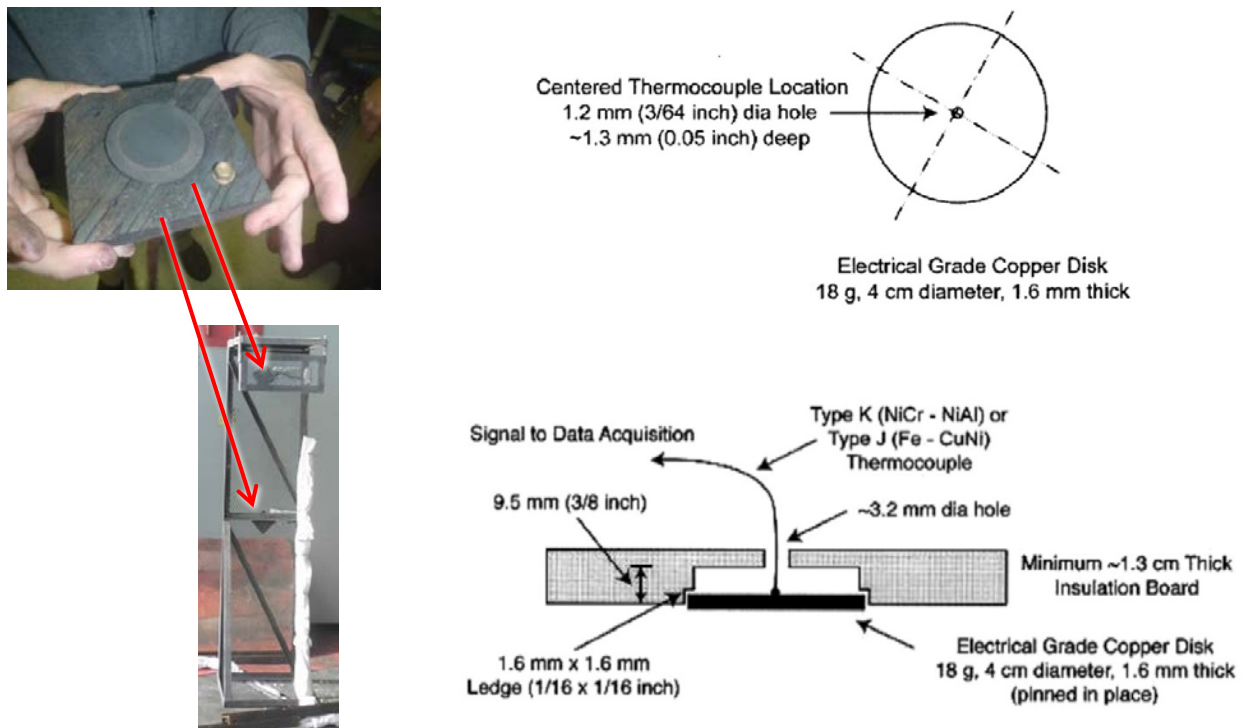


Figure A.1-1. ASTM F1959 Slug Calorimeters³

The method in ASTM F1959, Section 11.10.5 calculates the total energy:

³ Note that ASTM F1959 specifies insulation board however the slug calorimeters in the tests used plywood that should provide suitable insulation to reduce conduction losses.

$$\text{Total heat Energy, } Q = \frac{\text{mass} \times \bar{c}_p \times (\text{Temp}_{\text{final}} - \text{Temp}_{\text{initial}})}{\text{area}} \quad (1)$$

Where:

- Q = Total Heat energy per unit area⁴;
 mass = Mass of the copper slug; listed as “mass” in ASTM F1959, kg (nominal 18 g);
 \bar{c}_p = Specific heat capacity specified in ASTM F1959 (kJ/kg·K)⁵;
 Temp = Temperature (K);
 area = Exposed Area of the slug (12.57 cm²);

ASTM F1959 does not prescribe a method to evaluate heat flux. For the heat flux analysis of the HEAF tests, the energy is divided by the time between Temp_{final} and Temp_{initial}:

$$\dot{Q} = \frac{Q}{\Delta t}$$

- \dot{Q} = heat flux (W/m²);
 Δt = Time associated with ΔT_{slug} (s)

For the analysis of the NRA HEAF tests, the reported flux is the average over the arc duration (Δt is approximately the arc duration) based on the ΔT_{slug} caused by an unknown combination of radiation and convection heat transfer. The flux analysis assumes the flux is predominantly radiation during the arc because the convection would be low during the short time of the arc at the ZOI distances (results where the arcs are impacted by flames and convection may be significant, and are not included in the analysis as discussed in this section). Radiation sources viewed by the slug calorimeters include the flames and plasma that are escaping the cabinet and in some cases, the arc itself if a panel is lost or the arc burns through a cabinet wall. The effects of re-radiation or convection from the back of the slug, conduction to the slug mount and other effects are assumed to be negligible. With the assumption that the dominant flux is via radiation heat transfer, the $1/\varepsilon$ factor is included to account for the emissivity:

$$\dot{Q}_c = \frac{Q}{\Delta t} = \frac{m\bar{c}_p\Delta T_{\text{slug}}}{A\Delta t} \frac{1}{\varepsilon} \quad (2)$$

Where:

- \dot{Q}_c = Incident heat flux (W/m²) corrected for absorptivity;
 m = Mass of the copper slug; listed as “mass” in ASTM F1959, kg (nominal 18 g);
 \bar{c}_p = Specific heat capacity specified in ASTM F1959 (kJ/kg·K);
 ΔT_{slug} = Slug Temperature difference over time (K);
 A = Exposed Area of the slug (12.566 cm²);
 Δt = Time associated with ΔT_{slug} (s);

⁴ This is ASTM F1959 nomenclature; the total heat energy received at the surface of the panel as a direct result of an electric arc.

⁵ This is the average specific heat, c_p , over the temperature range using formula specified by ASTM F1959 that is included in the calculations but the effect is small over the observed temperature ranges in the tests.

ϵ = Emissivity/absorptivity of the coating/paint (~0.9)

An emissivity of 0.9 is assumed in accordance with the paint specified in ASTM F1959. However, the slug calorimeters did not appear to be maintained and re-painted, and the copper surface appeared greyish in some cases and this creates uncertainty in the measurements because the emissivity is not known. The heat energy and the heat flux are indirectly proportional to the emissivity. That is, if the actual emissivity is assumed to be 0.85 to 0.95 the assumption of 0.90 has an uncertainty of $\pm 5.5\%$.

For ASTM F1959 formula (1), the slug calorimeters are 30.5 cm (12 in) from a completely exposed high energy arc, and the slugs are engulfed in flames and convection heat transfer effects are significant and ASTM does not include emissivity explicitly in the formula. Note that for cases where convection is negligible that heat fluxes analyzed using ASTM F1959 formula (1) without the $1/\epsilon$ would be lower by a factor of 1.11 so including the emissivity in (2) above is conservative relative to the ASTM method.

For this method, the $Temp_{final}$ is just after the arc extinguished and the $Temp_{initial}$ was just before the arc initiated. This method is not impacted by electrical noise and temperature spikes during the arc. The results of the slug calorimeter temperature are shown with a straight line that indicates the start and end of the arc and represents the time, Δt , and temperature ΔT used for the flux calculation as shown for DP Test 1 in Figure A.1-2. The ASTM F1959 results are reported for flux in the various results tables in this report. Usually the flux reported is the maximum flux which for Figure A.1-2 was Slug S8.

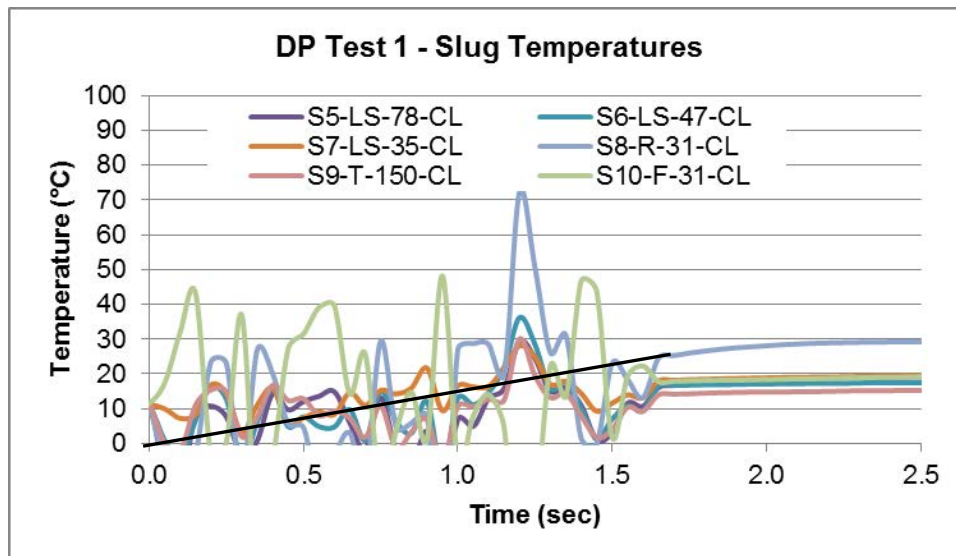


Figure A.1-2. Typical Slug Calorimeter Temperature Results

Most of the results have large variations of the indicated temperature with time. Some of these variations are from EMI/RFI noise that is evident in Figure A.1-2 because negative temperatures are not physically possible. Noise is usually worse if the slug is near the power supply and the noise was usually different for all the slug calorimeters. Other variations are from rapidly varying arc flux or flames escaping the cabinet intermittently through vents or loss of cabinet integrity such as cabinet burn-through, or dislodged and bent cabinet panels that cause the slug to heat and cool.

In some cases, the temperature spikes were very large where the flames contacted the slug calorimeter. If the calorimeter was contacted by flames as indicated by a large spike and review of videos, the data was not used to calculate the flux and this is noted in the results. These cases indicate that radiation may not be the dominant heat transfer mode. Some of the spikes in the calorimeter temperatures are noise but these do no effect the start and end temperatures over the arc interval used for the Formula (2) ASTM F1959 flux calculation because the Δt is between the arc start and arc end.

The flux values that are reported are only for the time during the arc. After the arc quenches, the flux from the arc and residual heat in the cabinet is very small and the decreasing temperature of the slug indicates a negative flux using Formula (2). However, this flux is a measure of the slug calorimeter cooling; not of the cabinet conditions. If an ensuing fire occurs, the slug will eventually heat up, but at this point the slug response is some complicated mix of low radiation heat transfer from the warm cabinet wall the slug is viewing, convective heat transfer from the cabinet to the local air, and the convective heat transfer from the air to the slug. Therefore, it can be assumed that the results are valid during the arc itself because the arc duration is short and the temperature response at the slug is primarily related to heat conditions caused by the arc and the associated escaping flames and plasma.

In cases where the flux measurements using Formula (2) are not valid (for example if there is flame contact), the slug temperature measurements provide a qualitative indication of the temperature that a small metal object at the NUREG/CR 6850 ZOI boundary could attain during the test. The slug's small copper disk with high emissivity provides a conservative estimate of a typical metal object that would typically have much lower thermal inertia and lower emissivity. This is true during the arc, after the arc, and also in cases where the slug calorimeter is contacted by flames. Therefore, the slug temperatures as well as the flux results are presented in this report. For example, an increasing slug temperature response after the arc is a qualitative indicator of an ensuing fire. The reported maximum slug temperatures are immediately after the arc to avoid noise spikes and indicate the maximum temperature a copper object could achieve from the arc heat.

A.2 Pressure Measurements

The Dynisco PT150-50 strain-gauge type Pressure Transducers (PRT) were connected to the cabinets by a reinforced rubber tube and then placed inside a PVC pipe for protection, as shown in various figures in the main text. The PRTs were not attached to the cabinet and moved and flexed the tube during some tests and this may have caused some very small pressure effects in the tubing and electrical effects in the cable. However, such effects were not specifically identified. Since the tubing was not filled with incompressible fluid, the compression of the air may have some effect on the time constant of the pressure response but this is not considered in the analysis.

Figure A.2-1 shows a typical pressure history for SWGR Test 4 in March 2014, Arc 1 where PRT1 was on Cabinet 7 and PRT2 was on Cabinet 8. Moving point averages were used to show the general trend of the response and remove some the noise and pressure effects. The data acquisition frequency was 20 kHz so 50 point averaging covers 0.0025 seconds and is an effective filter. The pressure transducers use strain gauges in bridge circuits that have high frequency response but the frequency response is limited by the mechanical limitations of the internal components and the manufacturer reports a minimum frequency response of 2 kHz but a typical response of 7 kHz depending on the connection to the item being measured. The minimum should allow measurements every 0.0005 seconds and this is adequate to measure the peaks that typically occur in the range of 0.010 to 0.025 seconds. The reported peak pressures were from the un-averaged data because the averaging artificially reduces the amplitudes of the highest peak pressure.

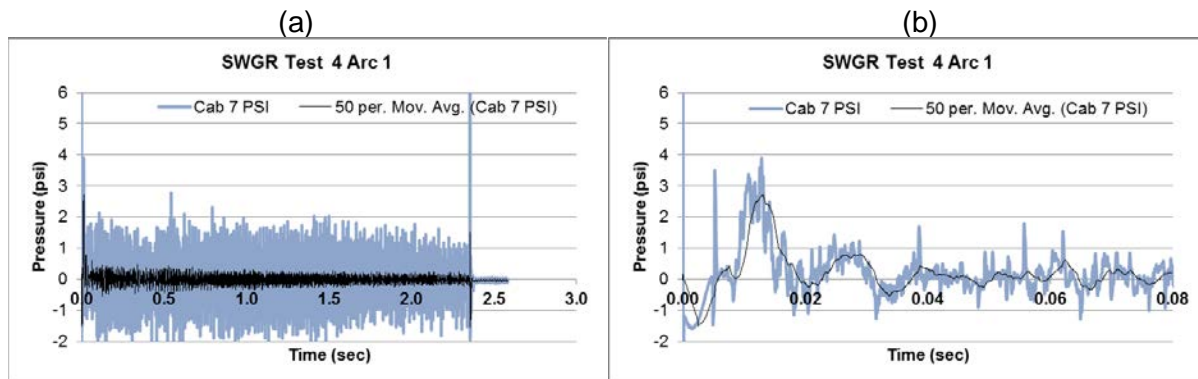


Figure A.2-1. Typical Pressure Results with Noise

The pressure often had spikes as the arc first forms and later quenches. The spikes were probably caused by rapidly changing magnetic field effects as the start and stop of the arc causes unstable and unbalanced current in the 3-phase power in the nearby bus bars and conductors. The maximum pressures for all tests were typically 0.010-0.025 sec after the arc. There were usually one or two noise spikes before the maximum pressure in most tests, as seen in Figure A.2-1. Noise spikes could be distinguished from pressure by expanding the time-scale and observing the response width because noise spikes are extremely narrow as shown in Figure A.2-2 for SWGR Test 4 in March 2014, Arc 1. The noise spike at 0.005 seconds is very narrow compared to the peak pressure at 0.0129 seconds. The initial negative spike down also indicates this is a noise spike. The manufacturer reports that the gauges should not be used to measure negative pressure so any negative pressures are noise.

Note that the pressures are typically very low so electrical noise in the result was estimated and included as a pressure uncertainty. Figure A.2-2 shows a typical pressure analysis to understand the electrical noise in the circuits. The plus/minus (\pm) uncertainty is based on the peak-to-peak un-averaged noise before the arc. The results before the arc initiated were reviewed to manually select the peak to peak noise level including the higher frequency noise that is filtered by the 50-point moving average. This peak-to-peak value was used as a conservative uncertainty.

The high frequency noise is considered when evaluating the maximum pressure as shown in Figure A.2-3. This example shows there is a high frequency noise (around 3.7 kHz) that occurs on many of the pressure results. The origin is not known. The noise is filtered by the 50-point average but the averaging reduces the indicated maximum pressure and delays the time of the maximum pressure as shown in the figure. The maximum pressure that is reported is selected as the mid-point of the peak-to-peak values in the cycle that includes the maximum measured pressure. As shown in the figure, the maximum measured pressure in MCC Test 1 was 4.8 psi but 4.1 psi is reported; this is about a 20% reduction. So, it is important to consider the high frequency noise using this manual method. The maximum pressure and the time are manually recorded directly from the EXCEL[®] chart.

The pressure gauge measurement uncertainty is not included because the only measurements that are reported are the peak pressure relative to the pressure at the start of the arc and the peak pressure that occurs within about 0.025 seconds after the start of the arc. It is assumed that the gauge accuracy that applies to absolute measurements did not change during this short interval and accuracy is not included in the uncertainty. The manufacturer lists the accuracy as $\pm 0.5\%$ of the full scale range which is ± 0.25 psi for the 50 psi full scale range for the PT150-50 and includes linearity, hysteresis, and repeatability. There are other factors that could affect the results such as movement of the PRT and flexing of the tube that connects the PRT to the cabinet but these also occur after the peak pressure and are not considered. The entire pressure data history is shown in the charts for interest, but only the peak pressure is reported.

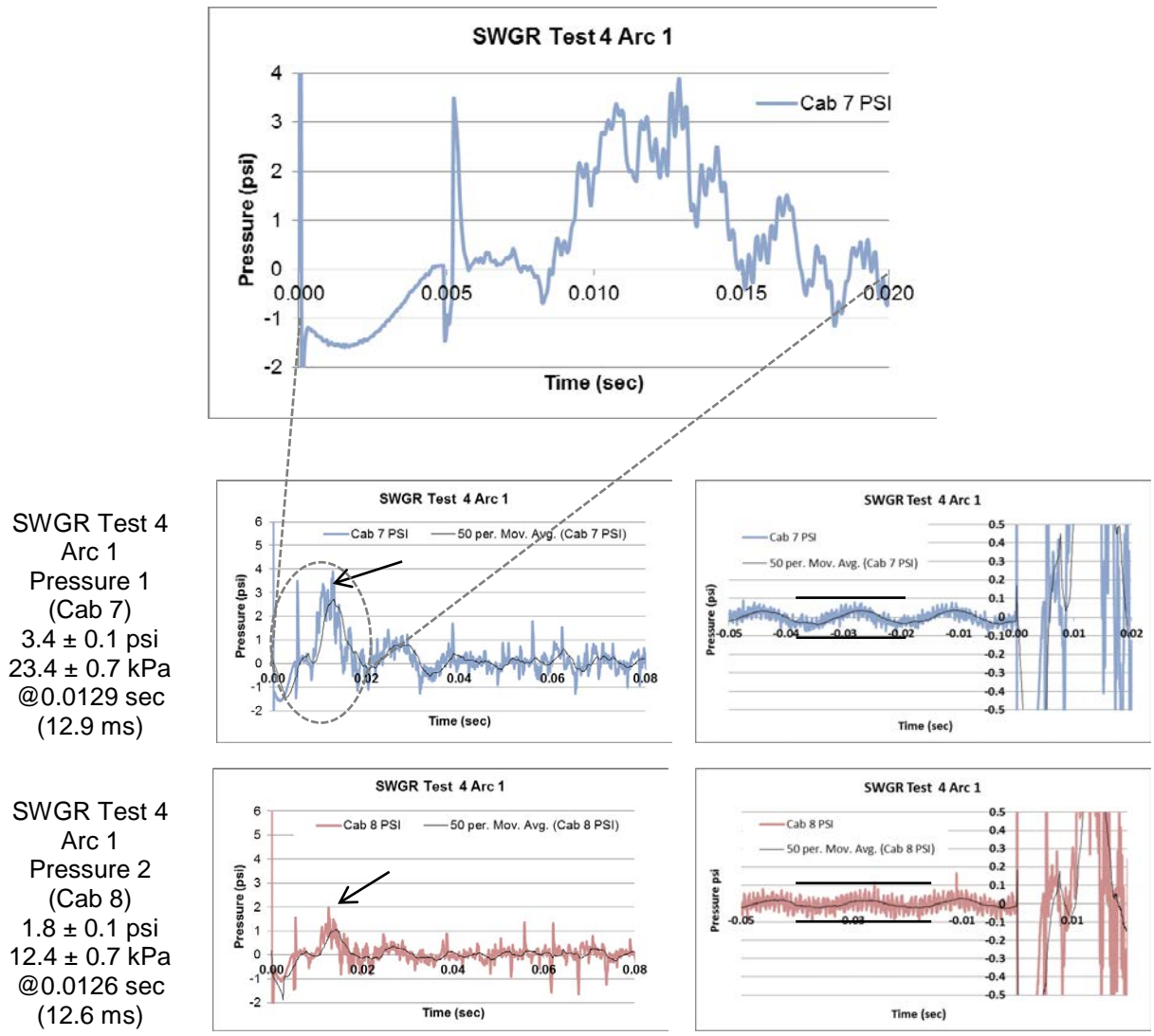


Figure A.2-2. Typical Pressure Results and Uncertainty Estimate

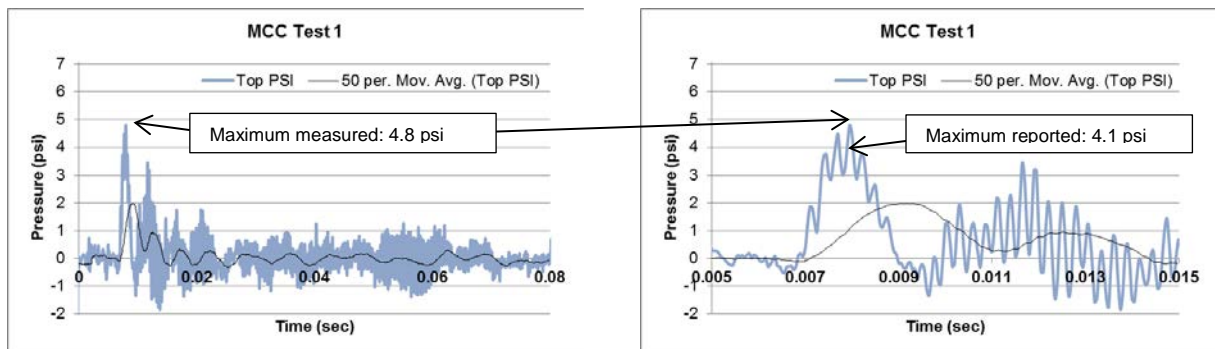


Figure A.2-3. High Frequency Noise Analysis

A.3 Energy Measurements

Total arc energy, Q_{tot} , is a key parameter that characterizes the strength of the arc and the potential for damage and ability to cause an ensuing fire in the cabinet or externally at the ZOI. An EXCEL worksheet is used to calculate the energy for the June 2013 SWGR Test 2, shown in Figure A.3-1. The currents and voltages for each phase, a, b, and c (Columns C-H) are multiplied to give the power in each phase (Columns J-K). The powers from each phase are added and then multiplied by the time step (0.00005 seconds) to give energy in Column M. The energy for each step is added to a cumulative total (referred to as “ Q_{tot} ” or “Energy Total” in this report) in Column N. The resulting graph, as shown in Figure A.3-2, is just for the time of the arc.

The cumulative energy should be a smooth line, linear with time that shows the KEMA power system provided a steady energy for the test. Discontinuities or spikes in the Q_{tot} line indicates the arc was not steady and also could indicate re-strikes. A rise in the Energy or a change in slope of the Energy Total indicate that the electric power is changing and this is observed when the voltage increases as the arc gap increases because the metal at the arc connection points oxidizes or melt and the arc length increases (voltage increase with arc gap).

A	B	C	D	E	F	G	H	I	J	K	L	M	N
time	Time adj	A CURRENT	A-N VOLT.	B CURRENT	B-N VOLT.	C CURRENT	C-N VOLT.		a	b	c	Energy MJ	Energy Cum.
0.0632	0	1992	1002	3828	233.6	2852	-35.94		99.7992	44.71104	-5.12504	0.000139385	0.00017
0.06325	5E-05	-234.4	35.94	39.06	8.984	78.13	35.94		-0.42122	0.017546	0.1404	-2.6327E-07	0.00017
0.0633	1E-04	-117.2	-26.95	0	-8.984	117.2	17.97		0.157927	0	0.105304	2.63231E-07	0.00017
0.06335	0.00015	312.5	-148.2	-78.12	-13.48	585.9	-8.984		-2.31563	0.052653	-0.26319	-2.5262E-06	0.00017
0.0634	0.0002	273.4	-71.87	-1289	-40.43	898.4	8.984		-0.98246	2.605714	0.403561	2.02681E-06	0.00017
0.06345	0.00025	390.6	-17.97	-1641	-40.43	1133	-22.46		-0.35095	3.317282	-1.27236	1.69397E-06	0.00017
0.0635	0.0003	625	-8.984	-2187	17.97	1406	13.48		-0.28075	-1.96502	0.947644	-1.2981E-06	0.00017
0.06355	0.00035	898.4	58.4	-2578	35.94	1719	40.43		2.623328	-4.63267	3.474959	1.46562E-06	0.00017
0.0636	0.0004	1211	-26.95	-3242	-40.43	2031	26.95		-1.63182	6.553703	2.736773	7.65865E-06	0.00018
0.06365	0.00045	1484	26.95	-3828	8.984	2422	-4.492		1.99969	-1.71954	-0.54398	-2.6383E-07	0.00018
0.0637	0.0005	1719	58.4	-4258	35.94	2695	26.95		5.01948	-7.65163	3.631513	9.99367E-07	0.00018
0.06375	0.00055	1953	4.492	-4883	-8.984	2930	0		0.438644	2.193444	0	2.63209E-06	0.00018
0.0638	0.0006	2266	4.492	-5547	13.48	3125	40.43		0.508944	-3.73868	6.317188	3.08745E-06	0.00019
0.06385	0.00065	2539	0	-5977	-8.984	3438	8.984		0	2.684868	1.54435	4.22922E-06	0.00019
0.0639	0.0007	2930	-4.492	-6523	-22.46	3711	71.87		-0.65808	7.325329	13.33548	2.00027E-05	0.00021
0.06395	0.00075	3164	-31.45	-7031	-4.492	3945	53.91		-4.97539	1.579163	10.63375	7.23752E-06	0.00022
0.064	0.0008	3516	31.45	-7656	-13.48	4180	44.92		5.52891	5.160144	9.38828	2.00773E-05	0.00024
0.06405	0.00085	3711	-8.984	-8125	31.45	4492	17.97		-1.66698	-12.7766	4.036062	-1.0407E-05	0.00023
0.0641	0.0009	4063	31.45	-8750	-8.984	4570	-22.46		6.389068	3.9305	-5.13211	5.18746E-06	0.00023
0.06415	0.00095	4336	4.492	-9297	-35.94	5000	44.92		0.973866	16.70671	11.23	2.89106E-05	0.00026
0.0642	0.001	4766	-4.492	-9844	-8.984	5117	62.89		-1.07044	4.421925	16.09041	1.94419E-05	0.00028
0.06425	0.00105	5078	13.48	-10270	17.97	5391	76.37		3.422572	-9.2276	20.58553	1.47805E-05	0.00029
0.0643	0.0011	5391	-13.48	-10820	-35.94	5469	8.984		-3.63353	19.44354	2.456675	1.82667E-05	0.00031
0.06435	0.00115	5703	22.46	-11450	22.46	5625	89.84		6.404469	-12.8584	25.2675	1.88136E-05	0.00033
0.0644	0.0012	6172	40.43	-11950	-17.97	5977	31.45		12.4767	10.73708	9.398833	3.26126E-05	0.00036
0.06445	0.00125	6367	35.94	-12540	-26.95	6016	0		11.4415	16.89765	0	2.83391E-05	0.00039
0.0645	0.0013	6719	-26.95	-12930	-4.492	6055	22.46		-9.05385	2.904078	6.799765	6.49991E-07	0.00039
0.06455	0.00135	7188	31.45	-13590	-40.43	6328	17.97		11.30313	27.47219	5.685708	4.4461E-05	0.00044
0.0646	0.0014	7500	22.46	-14060	-13.48	6563	49.41		8.4225	9.47644	16.21389	3.41128E-05	0.00047
0.06465	0.00145	7969	40.43	-14530	-4.492	6641	22.46		16.10933	3.263438	7.457843	2.68306E-05	0.00050

Figure A.3-1. Test 2 Arc Energy Calculation

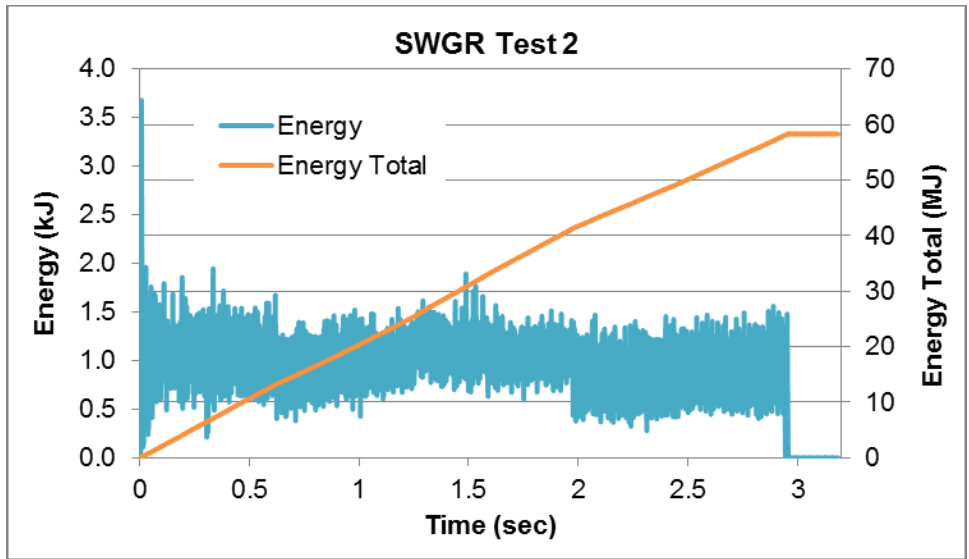


Figure A.3-2. Test 2 Arc Energy Result

APPENDIX B. KEMA TEST LABORATORY

KEMA Laboratories Chalfont (“KEMA”) performed the NRA HEAF tests at their lab facilities in Chalfont, Pennsylvania shown in Figure B.1-1. Both the large KEMA G2 - 2250 MVA, 16 kV, Variable frequency generator and KEMA G1 - 1000 MVA, 16 kV, 60 Hz were used. Note that G1 is fixed at 60 Hz only so the SWGR tests with two arcs were performed at 60 Hz. G2 at 50 Hz was used for all other tests

Test Cell 7 in Figure B.1-2 has a US “Medium Voltage” supply bus for the SWGR 6.9 kV arc (on the left) and a low voltage supply bus for the 480 V DP tests 4 through 6. DP Tests 1 through 3 and MCC Tests 1 through 4 were in Test Cell 1 with a low voltage supply only.

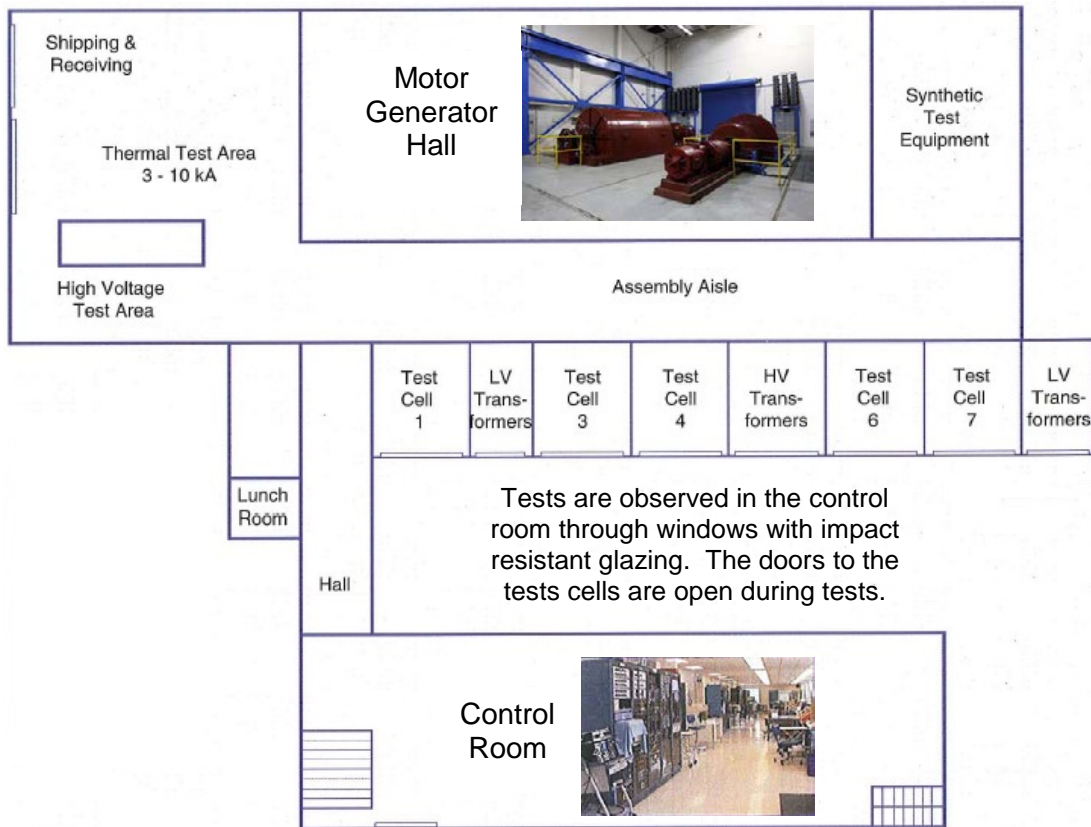
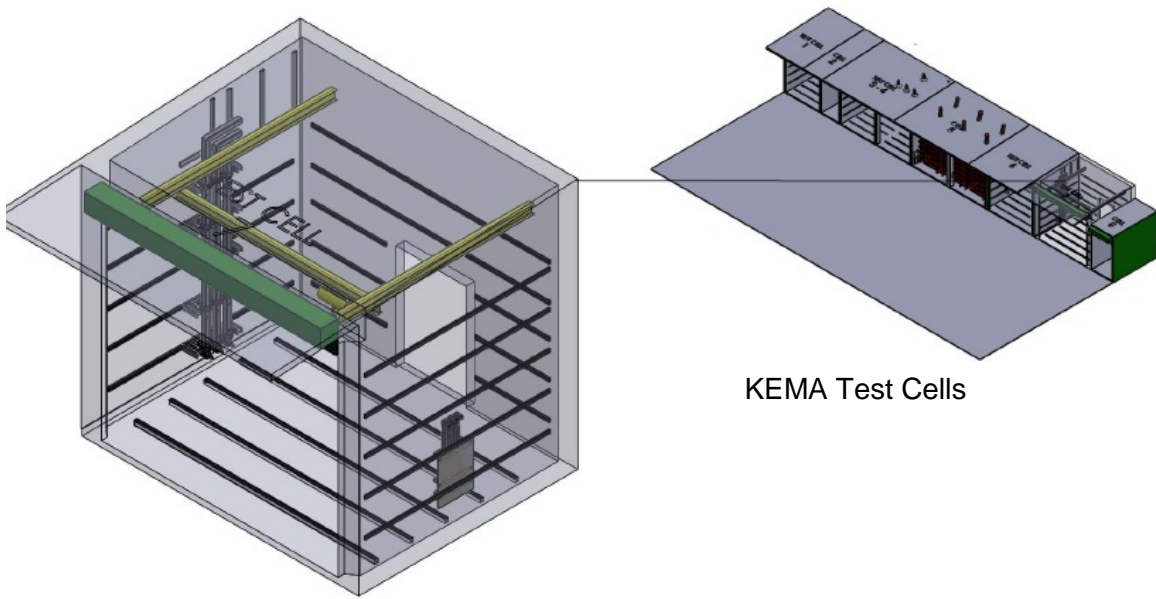


Figure B.1-1. KEMA Powertest Facility



KEMA Test Cells

Figure B.1-2. KEMA Test Cell 7 Arrangement

APPENDIX C. CABLE PROPERTIES

This appendix shows the properties of the cables used as the combustible loads in the NRA tests.

Table C-1. Cable Materials.




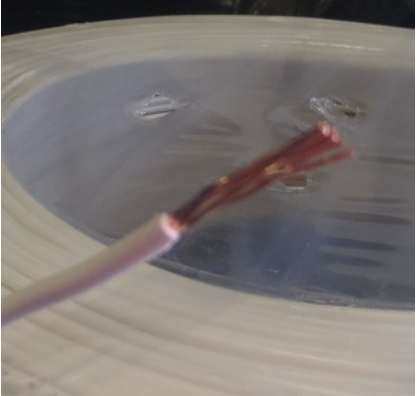
<p style="text-align: center;">CV-4 or CV-2</p> <p>Jacket/Sheath: JIS Flame Retardant Vinyl (Polyvinylchloride PVC) First Wrapping: No Shield: None Fill: Yes Insulation: Cross-Linked Polyethylene (XLPE) Conductor: Stranded</p>	 
<p style="text-align: center;">6KV-CSHVT</p> <p>Sheath: JIS Flame Retardant Vinyl (Polyvinylchloride PVC) First Wrapping: None Shield: None Second Wrapping: None Fill: No, one conductor Insulation: Cross-Linked Polyethylene (XLPE) Conductor: Stranded</p>	
<p style="text-align: center;">HIV</p> <p>Sheath: Fire Retardant Low Hydrochloric Vinyl First Wrapping: None Shield: None Second Wrapping: None Fill: None Insulation: Sheath is insulation</p>	

Table C-2. Cable Properties.

Item	CV-2	CV-4	HIV	6KV-CSHVT
Number of Conductors	2	4	1	1
Conductor area mm ²	2	2	2	250
Outer Diameter mm	10.5	12	3.6	28
Mass per length kg/km	120	180	28	2500
Combustible %	69	61	35	37

APPENDIX D. SHORT CIRCUIT CURRENT CALCULATIONS

As discussed in Section 1.3.1 the bolted fault current that is the maximum feasible fault current for an electric circuit was used as the short circuit current in the tests. The bolted fault current was based on the well-known “infinite bus” short circuit calculation (or “bolted short”) from text books as described below.

D.1. DP and MCC Test Current

The feed circuit in Japan is not specified. The schematic assumed for the DP and MCC in a typical NPP plant is in Figure D.1-1. A 480 V, 3 kA, bus feeds the DP. A 480 V, 600 A, DP MCCB feeds the MCC.

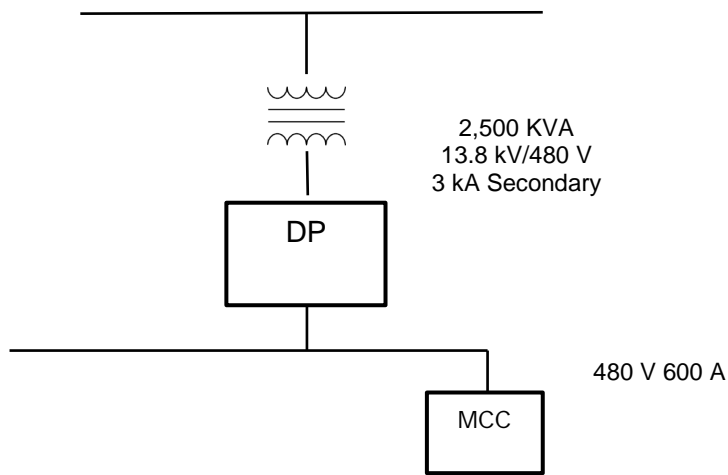


Figure D.1-1. Circuit Assumed for DP and MCC Tests

The calculated maximum, bolted, three phase short circuit current that could occur for a 480 V secondary bus of a 2,500 KVA transformer with a percent impedance of 5.75% is:

$$\begin{aligned} \text{SCA2} &= (\text{FLA2} * 100\%) / Z\% \\ \text{FLA2} &= \text{kVA three-phase} / (\text{Sqrt}(3) * \text{kV}_{\text{LL}}) \\ \text{FLA2} &= 2,500 \text{ kVA} / (1.732 * 0.480 \text{ kV}_{\text{LL}}) \\ \text{FLA2} &= 3,007 \text{ kA} \\ \text{SCA2} &= (3007 * 100\%) / 5.75\% \\ \text{SCA2} &= 52.296 \text{ kA (nominal 53 kA was specified for the tests)} \end{aligned}$$

Where:

SCA2 = bolted short circuit amperes on the secondary bus (short circuit amps)

FLA2 = transformer secondary full load current rating (full load amps)

kV_{LL} = line-to-line voltage in kV

$\text{Sqrt}(3)$ = square root of three which is 1.732

Z% = transformer nameplate percent impedance, 5.75% is a conservative lowest value in typical industrial circuits

Figure D.1-2 shows the basis of determining the available short-circuit current to include the current from the motors that are connected to the MCC. The current includes shorting current from the DP (I_s) and the motors (I_m).

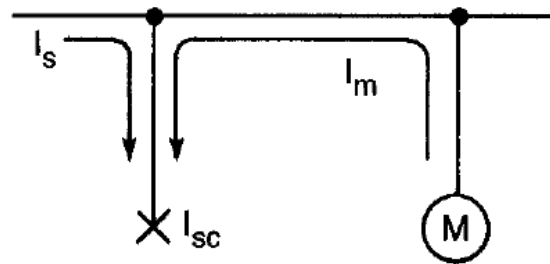


Figure D.1-2. Short Circuit Current for MCC Test

I_s is the short-circuit current available from the system at the point where the MCC is connected in Figure D.1-1. That current (I_s) is nominally 52 kA from the DP above.

I_m is the short circuit current contribution of the motors connected to the MCC. GE and ANSI C37.001 say that if the actual motors are not known, use four times (4X) the continuous-current rating of the main horizontal bus in the MCC. In this case, the continuous rating is 2.8 kA and $I_m = 4 \times 2.8 = 11.2$ kA.

I_{sc} is the available short-circuit current to be used for the test. $I_{sc} = I_s + I_m$. So the test current is $52 + 11.2 = 63.2$ kA. The tests here were conducted at 63 kA.

D.2. SWGR Test Current

The calculated maximum, bolted, three phase short circuit current that could occur at the 6.9 kV secondary bus of a 26 MVA transformer with a percent impedance of 9.5 percent is nominally 23 kA.

$$\begin{aligned} \text{SCA2} &= (\text{FLA2} * 100\%) / Z\% \\ \text{FLA2} &= \text{kVA three-phase} / (\text{Sqrt}(3) * \text{kVLL}) \\ \text{FLA2} &= 26,000 \text{ kVA} / (1.732 * 6.9 \text{ kVLL}) \\ \text{FLA2} &= 2.176 \text{ kA} \\ \text{SCA2} &= (2.176 * 100\%) / 9.5\% \\ \text{SCA2} &= 22.9 \text{ kA; a nominal 23 kA was specified as the symmetric current} \end{aligned}$$

To get higher energy for an ensuing fire the bolted fault current was about 31 kA.

BIBLIOGRAPHIC DATA SHEET

(See instructions on the reverse)

2. TITLE AND SUBTITLE

Nuclear Regulatory Authority Experimental Program to Characterize and Understand High Energy Arcing Fault (HEAF) Phenomena
Volume I

3. DATE REPORT PUBLISHED

MONTH	YEAR
August	2016

4. FIN OR GRANT NUMBER

5. AUTHOR(S)

S. Mehta (NRC), D. Stroup (NRC), N. Melly (NRC), G. Taylor (NRC), F. Gonzalez (NRC), S. Tsuchino, H. Kabashima, (S/NRA/R), S. Turner (Leidos)

6. TYPE OF REPORT

Technical

7. PERIOD COVERED (Inclusive Dates)

8. PERFORMING ORGANIZATION - NAME AND ADDRESS (If NRC, provide Division, Office or Region, U. S. Nuclear Regulatory Commission, and mailing address; if contractor, provide name and mailing address.)

Regulatory Standard and Development Department
Secretariat of Nuclear Regulatory Authority (S/NRA/R)
Tokyo, Japan 106-8450

Leidos, Inc.
301 Laboratory Road
Oak Ridge, TN 37830

9. SPONSORING ORGANIZATION - NAME AND ADDRESS (If NRC, type "Same as above", if contractor, provide NRC Division, Office or Region, U. S. Nuclear Regulatory Commission, and mailing address.)

Division of Risk Analysis
Office of Nuclear Regulatory Research
U.S. Nuclear Regulatory Commission
Washington, DC 20555-0001

10. SUPPLEMENTARY NOTES

M.H. Salley, NRC Project Manager

11. ABSTRACT (200 words or less)

A High Energy Arcing Fault (HEAF) occurred in a high-voltage (6.9 kV) switchgear (SWGR) in Unit 1 of the Onagawa Nuclear Power Plant of the Tohoku Electric Power Company on March 11, 2011 during the Great East Earthquake in Japan. While HEAF events are not common, they have occurred in nuclear power plants (NPP) worldwide and can present a potential threat to the safe operation of NPPs. Thus, the nuclear power industry has placed a new emphasis on understanding and developing evaluation methods for these events. To investigate the HEAF event sequence and to understand the phenomena, the Japan Secretariat of the Nuclear Regulation Authority (NRA) conducted HEAF tests by simulating the design and operating conditions of the SWGR HEAF at Onagawa NPP and using Rocket Fuel Arc Simulator (RFAS) to simulate HEAF energy effects. Tests of 480 V Motor Control Center (MCC) and Distribution Panel (DP) cabinets were also conducted to understand HEAF characteristics. The tests for the MCC and the DP provide insight on HEAF behavior and ensuing fires in low voltage systems. Data such as temperature, heat flux, heat release rates due to HEAF conditions were successfully simulated by the RFAS test.

12. KEY WORDS/DESCRIPTORS (List words or phrases that will assist researchers in locating the report.)

High Energy Arc Faults (HEAF), Fire Safety, Heat Release, Nuclear Power Plant, Zone of Influence, Fire Probabilistic Analysis (PRA), Onagawa, Tohoku, Fire Hazards Analyses (FHA), Fire Protection

13. AVAILABILITY STATEMENT

unlimited

14. SECURITY CLASSIFICATION

(This Page)

unclassified

(This Report)

unclassified

15. NUMBER OF PAGES

16. PRICE



Federal Recycling Program



**UNITED STATES
NUCLEAR REGULATORY COMMISSION**
WASHINGTON, DC 20555-0001

OFFICIAL BUSINESS



**NUREG/IA-0470
Volume 1**

**Nuclear Regulatory Authority Experimental Program to Characterize and
Understand High Energy Arcing Fault (HEAF) Phenomena**

August 2016